2015

November 14

中華民國核醫學學會年會暨學術研討會

Annual Meeting of the Society of Nuclear Medicine, Taiwan, R.O.C.

地　　點：馬偕紀念醫院淡水院區綜合研究大樓

主辦單位：中華民國核醫學學會

行政院原子能委員會核能研究所

馬偕紀念醫院

FUJIFILM

Diagnosis plus Therapy

Nuclear Medicine brings smiles

The 21st century is referred to as the Century of Life.
Expectations for the advancement of both life science and medicine focused on QOL are rising.
Early diagnosis plus therapy that reduces physical burden
We firmly believe nuclear medicine with therapy will play a larger role in the future.
FUJIFILM RI Pharma has contributed to the development of medicine as a supplier
specialized in radiopharmaceuticals essential for nuclear medicine.
We will continue to actively make advances in this field and combine the collective strength
of the group to make better services for medicine and health.

FUJIFILM RI Pharma Co., Ltd.
14-1 KYOBASHI 2-CHOME CHUO-KU TOKYO 104 JAPAN
PHONE 03-5250-2641 FAX 03-5250-2625 home page: http://fri.fujifilm.co.jp

YuanHsin
總代理 元新儀器有限公司
台北市內湖區陽光街365巷37號6樓
電話：(02)8751-3333#530,531,539

目　　錄

吳明哲會長 致詞

蒙學會青睞，馬偕紀念醫院今年首度承辦核醫學年會，並於風光明媚的淡水院區舉行，謹代表院方歡迎各位貴賓與先進蒞臨指導。

淡水曾是臺灣第一大港，有「東方威尼斯」之稱，同時也是北臺灣最早接觸西方文明的窗口。 自 1872 年馬偕牧師在淡水河口登陸後，淡水的歷史更交織著馬偕牧師傳道、醫療、教育的活動與事蹟。各位嘉賓不妨安排半日時間漫遊淡水河畔老街，尋訪馬偕牧師登陸處、滬尾偕醫館、淡水教會禮拜堂、淡江中學八角塔、馬偕博士墓園、淡水女學堂及婦學堂、馬偕故居與牛津學堂等多處腳蹤，實地緬懷前人篳路藍縷，為斯土斯民的犧牲與奉獻。

近年來核醫專業持續受到各醫學領域之發展的試煉洗禮，如何在風起雲湧的醫界戰國中安身立命、因應變局，是核醫界必須積極迎接的挑戰。因此，今年學術研討會內容亦著重在兼具前瞻性及實用性的藥物與診療技術上，期能有助於未來核醫藍海的開拓。

衷心希望，於此富有特殊歷史意義的所在舉辦年度盛會，除了提供專業新知、繼續教育及學術交流外，也能藉由尋幽訪古讓我們得到更清晰的歷史透視與方向感，激發開創新視界的靈感與動力。

竭誠歡迎各位先進同仁踴躍與會，共襄盛舉！

2015 年核醫學學會年會 吳明哲會長

中華民國 104 年 11 月 14 日

核能研究所 馬殷邦所長 賀詞

感謝核醫學會鄭澄意理事長之邀請，讓核能研究所可以參與每年一次的核醫盛會。今年的年會著重在兼具前瞻性及實用性的藥物與診療技術之介紹與分享，這也是核能研究所長久努力之目標，期能在新核醫藥物與醫療器材之研發上能有更多更新產品，有助於核醫界醫療應用之拓展。

核能研究所長期投入核醫藥物之研發，除了申請藥品許可證，供應醫院臨床診療之需求外，近年也開始推動產品之技轉業界。今年，我們已順利將「核研多巴胺轉運體造影」藥品許可證移轉給業界。近期，我們也將推動碘 -123MIBG 注射劑研製技術之移轉，期待有興趣之廠家能承接本項產品，使臨床有新核醫藥物應用於疾病之診斷，並可促進國內核醫產業之生根茁壯。

近年來，核研所也積極投入治療用核醫藥物之研發，「鋂 -188 微脂體」已得衛福部通過，進入第一期人體臨床試驗。「核研鋂必妥【鋂 -188】注射劑」完成製程與毒性試驗及肝癌動物模式之療效試驗，確認產品之安全與有效性，並向台大醫院 IRB 及衛福部申請臨床試驗許可中，相關研發成果將可刺激我國治療性核醫產業發展以及廠商投資意願。

核研所在核醫藥物開發與應用方面，將廣納核醫界與學界之建議，開發臨床俱潛力之新藥，並積極推動新藥技術移轉於業界，促使台灣核醫產業之開拓。最後，感謝諸位先進對本所之支持與協助，預祝大會圓滿成功，並祝福與會大眾身體健康，萬事如意。

核研所所長 馬殷邦所長

中華民國 104 年 11 月 14 日

鄭澄意理事長 致詞

各位嘉賓及核醫先進，大家好：

首先謝謝受邀請的國內外核醫專家蒞臨指導，也感謝核能研究所馬所長及全體同仁多年來的大力支持，使本次大會能順利舉辦，同時也非常感謝吳會長提供馬偕醫院如此良好之環境讓大家齊聚一堂，分享經驗，讓核醫領域的發展能百尺竿頭更進一步，在此也向各位嘉賓及籌備這次大會全體工作人員致最高敬意與感謝。

台灣核醫界目前面對一些嚴峻挑戰，例如在核醫藥物供應的部分，因應衛生福利部最新的 PIC/S GMP 要求，部分核醫藥物在原料藥取得的部分有許多困難，幸而這一部分在核研所先進與魏副理事長的持續努力下，暫時還沒有立即斷藥的危機，但後續仍是需要我們全體會員及相關專家與行政部門長官一起來努力，設法在同時兼顧國民用藥安全及臨床藥物需求的情形下，找出較可行的方案！其次，健保推行至今已滿二十年，核子醫學檢查及治療的成本皆已大幅增加，相關健保給付卻未跟著調整，導致許多檢查目前皆難以執行，此實非國民之福，如何說服健保局在確保健保財務穩定的前提下，適度的調整核子醫學檢查及治療的相關給付，也是目前學會努力的方向！

除了目前面對的嚴峻挑戰，核醫界也有很多新的機會可以把握，例如在許多專家及學者的努力下，許多新的正子同位素持續的發展，在臨床與研究上都有很多新的應用在發展。此外，新一代的 PET/MR 也持續在發展，相信將來一定會是核醫的最重要應用之一。同時，同位素治療也不再僅限於放射碘對甲狀腺癌的治療，在其他許多的疾病也有許多新的發展與應用。因此，本次年會也特別針對新的正子同位素發展與應用，PET/MR 的最新發展，以及同位素治療等相關題目，邀請到相關的學者專家進行經驗分享，相信大家一定可以收穫良多。

最後；再次感謝合辦單位、國內、外專家、學者提供多層次與多面向的交流；馬偕醫院核醫科協助大會籌備及場地安排，以及各位廠商的熱情贊助，並衷心感謝您的參與。

祝大會成功、大家順利平安！

中華民國核醫學學會 理事長 鄭澄意

中華民國 104 年 11 月 14 日

大會平面圖

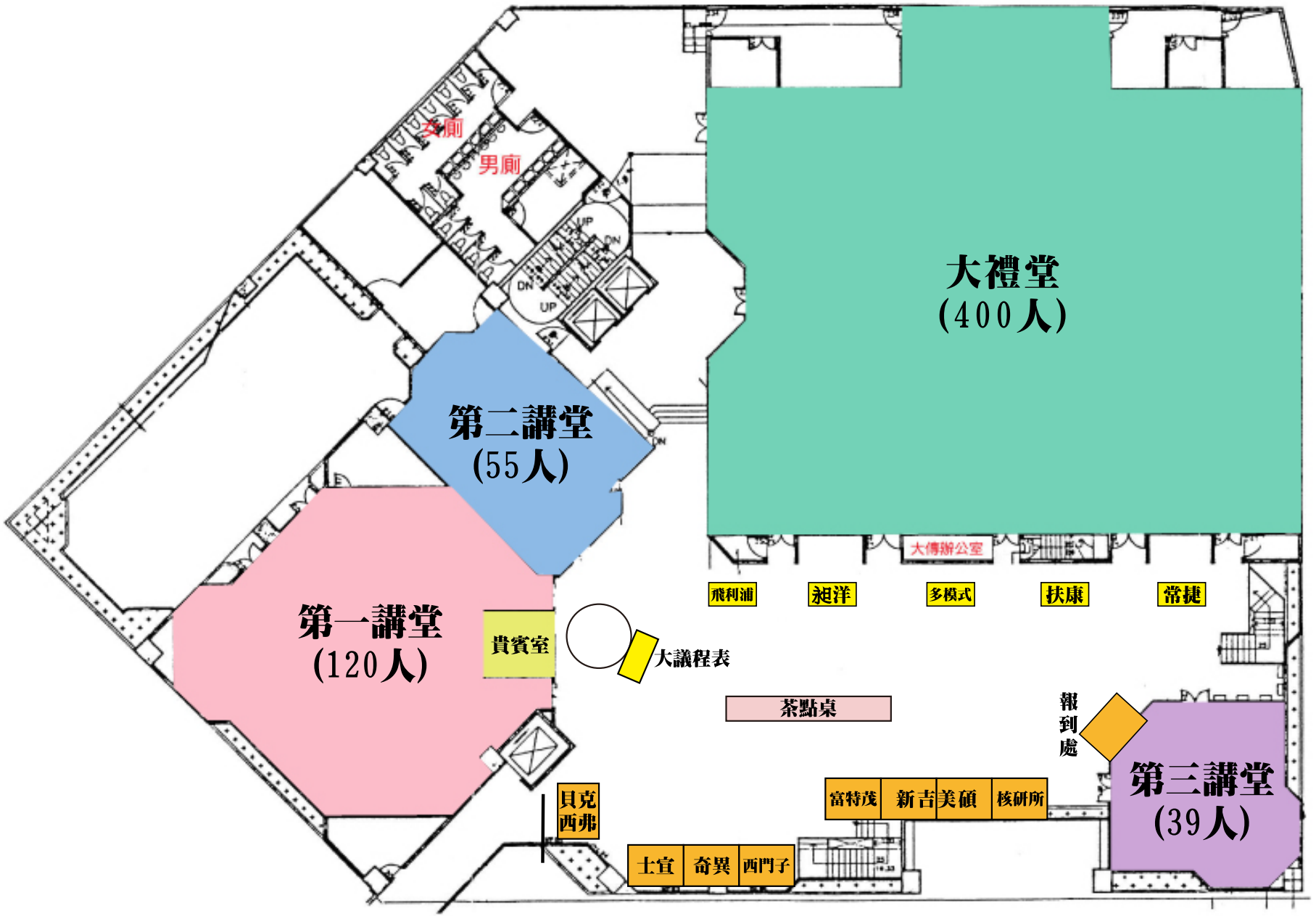
女廁
男廁
UP
DN
DN
UP
大禮堂
(400人)
第二講堂
(55人)
第一講堂
(120人)
大傳辦公室
飛利浦
昶洋
多模式
扶康
常捷
貴賓室
大議程表
茶點桌
報到處
第三講堂
(39人)
貝克西弗
富特茂
新吉
美碩
核研所
士宣
奇異
西門子

中華民國核醫學學會 2015 年會節目表

104 年 11 月 14 日 淡水馬偕

Novel PET tracer: Beyond FDG

時間 / 地點	大講堂（綜合研究大樓）					
08:00~08:50	大會報到					
08:50~09:10	大會開幕（吳明哲會長、鄭澄意理事長）					
	大禮堂				第一講堂	
09:10~09:40	Moving Forward to Precision Medicine 主講：閻紫宸 座長：王世楨、陳遠光				09:10~10:10 非年度電腦斷層品保訓練 -1 主講：杜高瑩 座長：楊邦宏	
09:40~10:10	核醫影像在神經退化疾病臨床運用的現在與未來 主講：徐榮隆 座長：姚維仁、林昆儒					
10:10~10:30	茶點 · 廠商展示				10:10~11:10 非年度電腦斷層品保訓練 -2 主講：王秀珊 座長：杜高瑩	
10:30~11:00	^{18}F-choline PET Scan in Prostate Cancer Application 主講：陳忠信 座長：劉仁賢、顏若芳					
11:00~11:30	PET 在帕金森病早期診斷及鑑別診斷之應用 主講：左傳濤（大陸） 座長：黃文盛、邱南津				11:10~12:10 非年度電腦斷層品保訓練 -3 主講：陳惠萍 座長：楊邦宏	
11:30~12:00	會員大會					
12:00-13:30						
		Lunch Symposium				
時間 / 地點	大禮堂	第一講堂		第二講堂	第三講堂	
12:10~13:00		TOF-PET/MR 同步掃描及衰減校正技術進展介紹 主講：趙周社（大陸） 座長：鄭澄意 友信行		甲狀腺癌放射碘治療 -ATA 2015 指引與新方向 主講：黃玉儀 座長：諶鴻遠 賽諾菲	立足臺灣放眼國際＿從 2007 年貴會與 TAF 簽署備忘錄談核醫影像國際認證 Be a pioneer! 主講：邱曼慈 座長：姚維仁	
13:30~14:00	13:30~14:15 Development of neuro-imaging in dementia -from structural MRI to amyloid and tau PET imaging 主講：松田博史（日本） 座長：杜高瑩、洪光威	13:30-16:20 口頭論文 - 臨床	李將瑄 林昆儒 程紹智 顏若芳	甲狀腺癌案例分享 主講：侯正涵 座長：諶鴻遠、鄭世平	13:30-15:06 口頭論文 - 基礎	王信二 林武智 楊邦宏 鍾相彬
14:00~14:30				鐳 223 於骨轉移治療 主講：林立凡 座長：彭南靖、吳勝堂		
14:30~15:00	14:15~15:00 Dyssynchrony Assessment by Myocardial Perfusion Imaging 主講：陳季（美國） 座長：杜高瑩、洪光威			以碘 -131- 碘化苯甲胍（I-131 MIBG) 治療復發 / 頑固型神經母細胞瘤 主講：王士忠 座長：顏若芳、盧孟佑		
15:00~15:20	Coffee break					
15:20~15:50	MIBI Breast imaging 主講：張賴昇平 座長：楊哲銘、張源清	13:30-16:20 口頭論文 - 臨床	李將瑄 林昆儒 程紹智 顏若芳	RIA 實驗室不符合事件撰寫經驗分享 主講：王安美 座長：鍾相彬	15:50-16:50 住院醫師考試	
15:50~16:20				實驗室認證 (15189 規範）之 NCR 經驗分享 主講：王安美 座長：鍾相彬		
16:20~16:50	核醫前哨淋巴結掃描定位檢查的臨床經驗及觀點 主講：余本隆 座長：曹勤和、劉淑馨			RIA 實驗室緊急應變措施及風險因子之設定經驗分享 主講：王安美 座長：鍾相彬		
16:50-18:30	市區導覽（遊覽車接駁）					
18:30	晚宴（含頒獎）					

Name: 閻紫宸 Tzu-Chen Yen
Title: Prof.
Institution: 長庚醫療財團法人林口長庚紀念醫院
Department: 核子醫學科
Contact: 03-3281200 分機 2744
Address: 桃園市龜山區復興街五號 核子醫學科
Phone: 03-3281200 分機 2744 Fax: 03-2110052
E-mail: Yentc1110@gmail.com

Publications:

1. Wang HM, Cheng NM, Lee LY, Fang YH, Chang TC, Tsan DL, Ng SH, Liao CT, Yang LY, Yen TC*. Heterogeneity of ^{18}F-FDG PET combined with expression of EGFR may improve the prognostic stratification of advanced oropharyngeal carcinoma. *INT J CANCER*. Accepted 2015.08. (SCI = 5.085) correspondence.
2. Peng CH, Liao CT, Ng KP, Tai AS, Peng SC, Yeh JP, Chen SJ, Tsao KC, Yen TC*, Hsieh WP*. Somatic copy number alterations detected by ultra-deep targeted sequencing predict prognosis in oral cavity squamous cell carcinoma. *Oncotarget*. 2015;6:19891-906. (SCI = 6.359) correspondence.
3. Chen SJ, Liu H, Liao CT, Huang PJ, Huang Y, Hsu A, Tang P, Chang YS, Chen HC, Yen TC*. Ultra-deep targeted sequencing of advanced oral squamous cell carcinoma identifies a mutation-based prognostic gene signature. *Oncotarget*. 2015;6:18066-80. (SCI = 6.359) correspondence.

Move Forward to the Era of Precision Medicine

Tzu-Chen Yen

Professor and Director,
Center for Academia and Industrial Collaboration,
Center for Advanced Laboratory Medicine,
Planning Center,
Center for Advanced Molecular Imaging and Translation,
Chang Gung Memorial Hospital and School of Medicine, Chang Gung University Taiwan.

Precision Medicine is a medical model that proposes the customization of healthcare, with medical decisions, practices, and/or products being tailored to the individual patient. In this model, diagnostic testing is often employed for selecting appropriate and optimal therapies based on the context of a patient's genetic content or other molecular or cellular analysis. Tools employed in precision medicine that can create or provide new terminology (such as PheWAS) or taxonomies, diagnostic and treatment strategies that can improve patients' outcomes, including molecular diagnostics, imaging (PET), and analytics/software. Thus, precision medicine is an emerging approach for disease treatment and prevention that takes into account individual variability in genes, environment, and lifestyle for each person. While significant advances in precision medicine have been made for select cancers, the practice is not currently in use for most diseases. Many efforts are underway to help make precision medicine the norm rather than the exception. To accelerate the pace, President Obama unveiled the Precision Medicine Initiative — a bold new enterprise to revolutionize medicine and generate the scientific evidence needed to move the concept of precision medicine into every day clinical practice. The scientific justification of the Precision Medicine Initiative has also been announced by NIH Director Dr. Francis S. Collins and former NCI director Dr. Harold Varmus.

In this talk, I will briefly introduce the current concept of Precision Medicine and also will give you some of our work with the model of Oral Cavity Squamous Cell Carcinoma (OSCC). Most importantly, PET has been choose to be one of the technological considerations in Precision Medicine and I will show you how we integrate this technology to our OSCC model.

Name: 徐隆榮 **Jung Lung Hsu**
Title: Dr., M.D.
Institution: Chang Gung Memorial Hospital
Department: Department of Neurology
Office: Section of Dementia and Cognitive Impairment, Department of Neurology, Chang Gung Memorial Hospital, Linkou, Taiwan
E-mail: tulu@ms36.hinet.net

Present Appointment:
Attending Physician, Section of Dementia and Cognitive Impairment, Department of Neurology, Chang Gung Memorial Hospital, Linkou, Taiwan

Career Highlight:

Affiliation	Units/Departments	Post	Dates
Chang Gung Memorial Hospital	Department of Neurology	Attending	2014/March
Shin Kong WHS Memorial Hospital	Department of Neurology	Attending	1996/July-2014/Feb
University of California San Diego	Swartz Center of Computational Neuroscience	Clinical research fellow	2004/July-2005/June
Taipei Medical University	Institute of Medical Informatics	Assistant Professor	2009/July-now

Academic Background:

School	Country	Department/Major	Degree	Dates
Taipei Medical University	Taiwan	Department of Medicine	M.D.	1987/July-1994/June
Taipei Medical University	Taiwan	Graduate Institute of Medical Informatics	M.S.	2003/July-2006/June
National Taiwan University	Taiwan	Institute of BioMedical Engineering	Ph.D.	2007/July-2014/Jan
Utrecht University	Netherlands	Image science institute	Ph.D.	2008-2013/Nov

Honor and Awards: Educational director in Taiwan Dementia Society

Professional Affiliation / Membership:
Assistant Professor, Graduate Institute of Humanities in Medicine, Taipei Medical University, Taipei, Taiwan

Publications Highlights:

1. Hsu JL, Lee WJ, Liao YC, Lirng JF, Wang SJ, Fuh JL. Posterior Atrophy and Medial Temporal Atrophy Scores Are Associated with Different Symptoms in Patients with Alzheimer's Disease and Mild Cognitive Impairment. PLoS One. 2015 Sep 15;10(9):e0137121.
2. Hsu JL, Chen WH, Bai CH, Leu JG, Hsu CY, Viergever MA, Leemans A. Microstructural white matter tissue characteristics are modulated by homocysteine: a diffusion tensor imaging study. PLoS One. 2015 Feb 18;10(2):e0116330.
3. Keller JJ, Hsu JL, Lin SM, Chou CC, Wang LH, Wang J, Bai CH*, Chiou HY. Increased risk of stroke among patients with ankylosing spondylitis: a population-based matched-cohort study. Rheumatol Int. 2014;34:255-263. (IF

= 2.214, Rheumatology 16/29)

4. Lau CI, Wang HC*, Hsu JL, Liu ME. Does the dopamine hypothesis explain schizophrenia? Rev Neurosci. 2013 Jul 11:1-12. doi: 10.1515/revneuro-2013-0011. (IF = 3.26, Neurosciences 104/251)
5. Chung KH, Huang SH, Wu JY, Chen PH, Hsu JL, Tsai SY*. The Link between High-Sensitivity C-Reactive Protein and Orbitofrontal Cortex in Euthymic Bipolar Disorder. Neuropsychobiology. 2013;68(3):168-73. (IF = 2.371, Psychology 31/75)
6. Wang HC, Hsu JL*, Leemans A. Diffusion Tensor Imaging of Vascular Parkinsonism: Structural Changes in Cerebral White Matter and the Association With Clinical Severity. Arch Neurol. 2012 Jul 23:1-9. (IF = 7.685, Clinical Neurology 9/193)
7. Huang SH, Chung KH, Hsu JL, Wu JY, Huang YL, Tsai SY*. The risk factors for elderly patients with bipolar disorder having cerebral infarction. J Geriatr Psychiatry Neurol. 2012 Mar;25(1):15-9. (IF = 3.525, Clinical Neurology 39/191)
8. Hsu JL, Chen YL, Leu JG, Jaw FS, Lee CH, Tsai YF, Hsu CY, Bai CH*, Leemans A. Microstructural white matter abnormalities in type 2 diabetes mellitus: a diffusion tensor imaging study. Neuroimage. 2012 Jan 16;59(2):1098-105. (IF = 6.252, RADIOLOGY, NUCLEAR MEDICINE & MEDICAL IMAGING 3/120)
9. Wu YY, Cheng IH, Lee CC, Chiu MJ, Lee MJ, Chen TF, Hsu JL*. Clinical Phenotype of G206D Mutation in the Presenilin 1 Gene in Pathologically Confirmed Familial Alzheimer's Disease. J Alzheimers Dis. 2011 Jan;25(1):145-50. (IF = 4.174, Neurosciences 64/251)
10. Huang SH, Tsai SY*, Hsu JL, Huang YL. Volumetric reduction in various cortical regions of elderly patients with early-onset and late-onset mania. Int Psychogeriatr. 2011 Feb;23(1):149-54. (IF = 2.188, Psychology 32/75)
11. Jung-Lung Hsu, Ming H. Hsieh, Yi-Li Tseng, Ming-Jang Chiu, Chih-Min Liu, Fu-Shan Jaw*, Hai-Gwo Hwu. TIME-FREQUENCY ANALYSIS OF MISMATCH NEGATIVITY IN SCHIZOPHRENIA PATIENTS IN TAIWAN. Biomedical Engineering: Applications, Basis and Communications, Vol. 23, No. 4 (2011) 287_293. (IF = 0.233, ENGINEERING, BIOMEDICAL75/79)
12. Hsu JL, Van Hecke W, Bai CH, Lee CH, Tsai YF, Chiu HC, Jaw FS, Hsu CY, Leu JG, Chen WH*, Leemans A. Microstructural white matter changes in normal aging: a diffusion tensor imaging study with higher-order polynomial regression models. Neuroimage. 2010 Jan 1;49(1):32-43. (IF = 6.252, RADIOLOGY, NUCLEAR MEDICINE & MEDICAL IMAGING 3/120)
13. Jung-Lung Hsu, Alexander Leemans, Chyi-Huey Bai, Cheng-Hui Lee, Yuh-Feng Tsai, Hou-Chang Chiu, Wei-Hung Chen*. Gender differences and age-related white matter changes of the human brain: a diffusion tensor imaging study. NeuroImage 2008;39:566-577. (IF = 6.252, RADIOLOGY, NUCLEAR MEDICINE & MEDICAL IMAGING 3/120)
14. Jung Lung Hsu, Tayy-Ping, Jung, Chien-Yeh Hsu, Wei-Chih Hsu, Yen-Kong Chen, Jen-Ren Duann, Han-Cheng Wang*, Scott Makeig. Regional CBF changes in Parkinson's disease: A correlation with motor dysfunction. European Journal of Nuclear Medicine and Molecular Imaging. 2007;Sep;34(9):1458-1466 (IF = 5.114, RADIOLOGY, NUCLEAR MEDICINE & MEDICAL IMAGING 8/120)
15. Fang SC, Hsu JL, Chen WH*. EEG coherence for a patient with Marchiafava-Bignami disease. Clin EEG Neurosci. 2007;38(4):207-12. (IF = 1.818, Neuroimaging 7/14)
16. Light GA*, Jung Lung Hsu, Hsieh MH, Meyer-Gomes K, Sprock J, Swerdlow NR, Braff DL. Gamma Band Oscillations Reveal Neural Network Cortical Coherence Dysfunction in Schizophrenia Patients. Biol Psychiatry 2006;60:1234-1240. (IF = 9.247, Psychiatry 4/135)
17. Jung Lung Hsu, Chien Yeh Hsu, Han Cheng Wang. Developing an automatic classifier for Parkinson's Disease Diagnosis base on statistical analysis of SPECT Data. Journal of Taiwan Association for Medical Informatics.

2006;15:1-4.

18. Jung Lung Hsu, Wei-Chih Hsu, Han-Cheng Wang*. Hyperglycemia-induced unilateral basal ganglion lesions with and without hemichorea—A PET study. Journal of Neurology. 2004;251:1486-1490. (IF = 3.578, Clinical Neurology 36/191)
19. Wang, Han-Cheng , Hsu, Jung Lung*, Shen, Yeh-You. Acute Bilateral Basal Ganglia Lesions in Patients With Diabetic Uremia: An FDG-PET Study. Clinical Nuclear Medicine. 2004; 29(8):475-478. (IF = 2.955, RADIOLOGY, NUCLEAR MEDICINE & MEDICAL IMAGING 26/120)
20. Jung Lung Hsu, Wei-Hung Chen*, Hou-Chang Chiu. Cortical Sensory Loss in a Patient with Posterior Cortical Atrophy: A case report. Neurocase 2004,10:48-51. (IF = 1.05, Psychiatry 99/135)
21. Jung Lung Hsu, Hou Chang Chiu. Fronto-temporal dementia. Formosan J Med. 2001;5:101-4.
22. Jung Lung Hsu. Hou Chang Chiu. Neuropsychological tests in Dementia. Formosan J Med. 2000;4:720-24.

核醫影像在神經退化疾病臨床運用的現在與未來

Jung-Lung Hsu

Section of dementia and cognitive impairment, Department of Neurology
Chang Gung Memorial Hospital, Linkou, Taiwan.

In nuclear medicine, the molecular image provides much clinical relevant information in degenerative disease diagnosis and evaluation. The positron emission tomography (PET) and magnetic resonance imaging (MRI) opened up many new avenues in clinical and research environments, mainly by providing multi-modality images obtained during the examination. In primary neurodegenerative dementia, both PET and MRI provide complementary anatomical and molecular images which help clinician to disclose the spatial correlated, time-dependent pathological process in the brain. Recently, several tracers have been developed to explore the maps of neuronal metabolism, neurotransmitter activity and pathological protein deposition in the brain. The most common molecular image used in neurodegenerative disease is the fluorodeoxyglucose PET (FDG-PET), which assess the resting state cerebral metabolism. This signal intensity is a proxy for neuronal activity and a direct index of synaptic function and density. Various events can contribute to synaptic dysfunction and consequent neurodegeneration, such as altered intracellular signalling cascades and mitochondria bioenergetics, impaired neurotransmitter release, and long-distance disconnection effects that are captured by FDG-PET. Currently, decreased uptake in parieto-temporo region is a neuronal injury biomarker for diagnosis of Alzheimer's disease dementia (AD). In dementia with lewy body (DLB), both the cingulate island sign (CIS) and decreased uptake in occipital region are typical presentation. The frontal-temporal lobar degeneration (FTLD) contains both behavior variant of fronto-temporal dementia (bv-FTD) and primary progressive aphasia (PPA). Decrease frontal and anterior temporal metabolism is characteristic for bv-FTD and the left lateral temporal hypometabolism is typical for semantic dementia. Finally, various new PET tracers had been developed to explore the different pathological biomarker in neurodegenerative disease such as amyloid marker (e.g Pittsburgh compound-B (PiB), florbetapir (AV-45) and florbetaben), tau marker (e.g FDDNP, THK523, THK5105 and THK5117) and monoamine marker (AV-133). These agents, combine with high resolution anatomical image could improve our knowledge related to the pathophysiological process of the different degenerative dementia.

Name: 陳忠信 **Chung-Hsin Chen**
Title: Dr., M.D., Ph.D.
Institution: National Taiwan University
Department: Department of Urology
Position: Attending, Assistant Professor
Address: Dpt of Urology, 11F, 7, Chung-Shan S Road, Taipei, Taiwan
Phone: +886-2-23123456 ext. 65252 Fax: +886-2-23219145
E-mail: mufasachen@gmail.com

Career Highlight:

2013/Jul ~2014/Jun Director, Department of Urology, Yuan-Lin Branch, National Taiwan University Hospital
2014/Nov ~ present Secretary-general, Bladder cancer expert team, Taiwan Cancer Expert committee
2014/Sep ~ present Secretary-general, International Section of Taiwan Urological Association

Academic Background:

School of Medicine, M.D., 1993/Sep to 2000/Jun,
College of Medicine, National Taiwan University (NTU) (台灣大學醫學系)
Graduate Institute of Clinical Medicine, PhD, 2007/Sep to 2012/Dec
College of Medicine, National Taiwan University (NTU) (台灣大學醫學院臨床醫學研究所)

Honor and Awards:

2013 Outstanding Award for the postgraduate students' publications, National Taiwan University College of Medicine (台灣大學醫學院研究生優秀論文獎 傑出獎)
2013 Professor YF Hsieh Memorial Award, Taiwan Urological Association (台灣泌尿科醫學會 紀念謝有福教授優秀論文獎)
2014 Domestic and International Medical Journal Award, Taiwan Urological Association (台灣泌尿科醫學會 國內外醫學雜誌論文獎)

Professional Affiliation / Membership:

Member of Taiwan Urological Association

Publications Highlights:

1. Chung-Hsin Chen, Kathleen G. Dickman, Chao-Yuan Huang, Masaaki Moriya, Chia-Tung Shun, Huai-Ching Tai, Kuo-How Huang, Shuo-Meng Wang, Yuan-Ju Lee, Arthur P. Grollman, and Yeong-Shiau Pu Aristolochic Acid-Induced Upper Tract Urothelial Carcinoma in Taiwan: Clinical Characteristics and Outcomes International Journal of Cancer, 2013 Jul;133(1):14-20 (IF = 5.007; R/C = 34/207; Oncology)
2. M. L. Hoang, Chung-Hsin Chen, V. S. Sidorenko, J. He, K. G. Dickman, B. H. Yun, M. Moriya, N. Niknafs, C. Douville, R. Karchin, R. J. Turesky, Y.-S. Pu, B. Vogelstein, N. Papadopoulos, A. P. Grollman, K. W. Kinzler, T. A. Rosenquist Mutational Signature of Aristolochic Acid Exposure as Revealed by Whole-Exome Sequencing Sci Transl Med 2013 Aug 7;5(197):197ra102 (IF= 14.414 ; R/C = 3/124; MEDICINE, RESEARCH & EXPERIMENTAL)
3. Chung-Hsin Chen, Masaaki Moriya, Kathleen G. Dickman, Jiri Zavadil, Viktoriya S. Sidorenko, Karen L. Edwards, Dmitry Gnatenko, Lin Wu, Robert J. Turesky, Xue-Ru Wu, Yeong-Shiau Pu, and Arthur P. Grollman Aristolochic acid-associated urothelial carcinoma in Taiwan. PNAS 109(21):8241-6, 2012 (IF= 9.809 ; R/C= 4/55; MULTIDISCIPLINARY SCIENCES)

^{18}F-choline PET Scan in Prostate Cancer Application

Chung-Hsin Chen

Department of Urology, National Taiwan University Hospital.

Abstract

Prostate cancer is the fifth leading malignancy in Taiwanese men. About 5,000 prostate cancer patients are diagnosed every year, resulting a heavy health and economy burden in Taiwan. Localized prostate cancers account for about 75%, and the rest (25%) of newly diagnosed ones are metastatic diseases. Compared to western countries, we diagnose the prostate cancer patients later with more advanced stage and older age. The most possible reasons include insufficient alert, lack of symptoms, and no screen program to identify the patients. In contrast, the mortality rate of early stage of prostate cancer is not as high as other major cancers, such as breast, lung and liver cancers, leading to a debate to screen prostate cancer.

In recent decade, a huge advance in diagnosing and treating prostate cancer was achieved. However, the efficiency of diagnostic or staging tools was still not precise to identify the prostate cancer lesions. For example, the accuracy of bone scan used to identify bony metastases was only 18%. Magnetic resonance imaging and ^{18}F-choline positron emission tomography (^{18}F-CH PET) scan significantly increased the sensitivity to diagnose metastatic lesions.

From 2013, we used ^{18}F-CH PET scan to help allocate the status of prostate cancer patients who had ambiguous stages, or recurrent lesions. With the guidance of ^{18}F-PET scan, urologists, radio-oncologists, and medical oncologists can easily get a consensus to treat the given patients. Furthermore, we can perform mastectomy for the patient who was treated with prostate radiotherapy and had single metastatic lesion in pelvis during follow-up.

Among 84 patients, ^{18}F-CH PET showed negative results for 27 patients (age 72.4 $\pm$ 9.0), and positive studies were noted for 63 patients. For those with positive results, 25 patients had been confirmed to have recurrence, and 5 patients had negative pathologic results at the areas with abnormal PET uptake. For the 27 PET negative patients with 30 studies, 2 had recurrence in prostate beds, 4 had negative results from biopsy. At present, the sensitivity, specificity, positive predictive value, negative predictive value and overall accuracy were 96.7%, 85.7%, 92.1%, 93.3%, 92.5% respectively.

For PSA less than 1 ng/ml, only 1 had positive results out of 16 studies (6.3%); PSA between 1-2 ng/ml, 7 had positive results out of out of 9 studies (77.8%); for PSA greater than 2 ng/ml, 55 had positive results out of out of 68 studies (80.9%).

^{18}F-CH PET scan does contribute to identify prostate cancer lesions in the patients with ambiguous stages. It is recommended in clinical practice for prostate cancer management.

Name: 左傳濤 **Chuantao Zuo**
Title: Mr., Prof., M.D.
Institution: Huashan Hospital
Department: Pet Center
Position: Deputy Director
Office: Pet Center, 518 East Wuzhong Road, Shanghai
Address: 518 East Wuzhong Road, Shanghai
Phone: 86-21-64280718 Fax: 86-21-64283265
E-mail: zuoct_cn2000@126.com

Present Appointment:
deputy director of PET centre, Huashan Hospital, Fudan University, China

Career Highlight:
Group leader of committee of PET imaging in neurodegenerative diseases, Chinese Society of Nuclear Medicine.
Vice group leader of committee of translational medicine, Chinese Society of Nuclear Medicine.

Academic Background: Achieved MD from Shanghai Medical College, Fudan University in 2004

Honor and Awards: 2013 HuaYing Academic Award of Huashan Hospital
2013 Scientific Elite Award of Huashan Hospital

Professional Affiliation / Membership: Member of the Chinese Society of Nuclear Medicine

Publications Highlights:

1. Wu P, Yu H, Peng S, Wang J, Ge J, Zhang H, Eidelberg D, Ma Y, Zuo C. Consistent abnormalities in metabolic network activity in idiopathic rapid eye movement sleep behaviour disorder. Brain 2014;137(12):3122-3128. (IF 9.196)
2. Zuo CT, Ma YL, Sun BM, Peng SC, Zhang HW, Eidelberg D, Guan YH. Metabolic imaging of bilateral anterior capsulotomy in refractory obsessive compulsive disorder: an FDG PET study. J Cereb Blood Flow Metab 2013;33(6):880-887. (IF 5.407)
3. Miao Q, Zhang S, Guan YH, Ye HY, Zhang ZY, Zhang QY, Xue RD, Zeng MF, Zuo CT, Li YM. Reversible Changes in Brain Glucose Metabolism Following Thyroid Function Normalization in Hyperthyroidism. Am J Neuroradiol 2011;32(6):1034-1042. (IF 3.589)
4. Wu P, Wang J, Peng S, Ma Y, Zhang H, Guan Y, Zuo C. Metabolic brain network in the Chinese patients with Parkinson's disease based on (18)F-FDG PET imaging. Parkinsonism Relat Disord 2013;19(6):622-627. (IF 3.972)
5. Miao Q, Zhao XL, Zhang QY, Zhang ZY, Guan YH, Ye HY, Zhang S, Zeng MF, Zuo CT, Li YM. Stability in Brain Glucose Metabolism Following Brown Adipose Tissue Inactivation in Chinese Adults. Am J Neuroradiol 2012;33(8):1464-1469. (IF 3.589)

6. Zuo CT, Hua XY, Guan YH, Xu WD, Xu JG, Gu YD. Long-range plasticity between intact hemispheres after contralateral cervical nerve transfer in humans Clinical article. J Neurosurg 2010;113(1):133-140. (IF 3.737)
7. Wang J, Ma YL, Huang ZM, Sun BM, Guan YH, Zuo CT. Modulation of metabolic brain function by bilateral subthalamic nucleus stimulation in the treatment of Parkinson's disease. J Neurol 2010;257(1):72-78. (IF 3.377)
8. Zhang HW, Li DY, Zhao J, Guan YH, Sun BM, Zuo CT. Metabolic imaging of deep brain stimulation in anorexia nervosa: a 18F-FDG PET/CT study. Clin Nucl Med 2013 Dec;38(12):943-948. (IF 3.931)
9. Wang HC, Zuo CT, Hua FC, Huang ZM, Tan HB, Zhao J, Guan YH. Efficacy of conventional whole-body F-18-FDG PET/CT in the incidental findings of parotid masses. Ann Nucl Med 2010;24(8):571-577. (IF 1.41)

PET 在帕金森病早期診斷及鑑別評斷之應用

Chuantao Zuo

摘要：

PET 腦功能成像越來越受到科研及臨床工作者的關注。神經變性病 (Neurodegenerative disease) 是一類慢性、進行性的神經系統疾病，不同類型神經變性疾病的病變部位和病因雖然各不相同，但大腦特定區域的遲發性神經細胞退行性病變、細胞丟失是它們的共同特徵，主要包括帕金森病 (Parkinson's disease, PD)、阿爾茨海默病 (Alzheimer's disease, AD)、亨廷頓病 (Huntington's disease, HD)、肌萎縮側索硬化症 (Amyotrophic Lateral Sclerosis, ALS)、脊髓小腦共濟失調 (spinal cerebellar ataxias) 等疾病。^{18}F-FDG PET/CT 可通過 ^{18}F-FDG 被腦組織所攝取的程度反映腦細胞功能狀態，在此類疾病的早期診斷、鑒別診斷及病情監控中發揮著重要的作用。

MEMO

Name: 松田博史 **Hiroshi Matsuda**
Title: Prof.
Institution: Director General, Integrative Brain Imaging Center

National Center of Neurology and Psychiatry Since 2012

Graduated with a degree in Medicine at Kanazawa University School of Medicine in 1979. Then finished the doctor's course at Graduate School of Kanazawa University School of Medicine in 1983. He specializes in radiology especially in nuclear medicine. He was a Rotary Foundation scholar between 1984 to 1985 at Montreal Neurological Institute. In 1992, he became assistant professor of department of nuclear medicine of Kanazawa University School of Medicine. In 1993, he became head of department of radiology at National Center Hospital of Neurology and Psychiatry. In 2004, he became Professor and Chair, department of nuclear medicine, Saitama Medical University and returned to National Center of Neurology and Psychiatry in 2012. Currently serves as visiting Professor of Saitama Medical University and Tohoku University. He is a board certified specialist of Radiology, Nuclear Medicine, and Dementia research.

Development of Neuroimaging in Dementia -from Structural MRI to Amyloid and Tau PET Imaging-

Hiroshi Matsuda

Integrative Brain Imaging Center, National Center of Neurology and Psychiatry.

Nowhere is the serious social problem of dementia more acute than in Japan, where an estimated one fourth of elderly persons already have or show signs of developing it. The prevalence of dementia has increased over the past few decades, either because of greater awareness and more accurate diagnosis, or because increased longevity has created a larger population of the elderly, the age group most commonly affected. More aging will develop from now on, and so it is predicted that 7 million elderly persons will be demented by 2025 in Japan.

Although the diagnosis of dementia is still largely a clinical one, based on the history and disease course, neuroimaging has dramatically changed our ability to accurately diagnose it. The role of neuroimaging in dementia nowadays extends beyond its traditional role of excluding neurosurgical lesions. Neuroimaging in dementia is recommended by most clinical guidelines. Moreover new neuroimaging methods facilitate diagnosis of most of the neurodegenerative conditions after symptom onset and show promise for diagnosis even in very early or presymptomatic phases of some diseases.

Under these conditions, all clinicians and researchers who are involved in neuroimaging for dementia should decide which patients to scan, when imaging patients is most useful, which modality to use, how to handle imaging data from many institutions, and which analytical tool to use. I would like to give a presentation from structural MRI to the latest modalities such as tau and amyloid PET imaging for the diagnosis of Alzheimer's disease and other dementias, and also provides information on analyzing imaging data.

Name: 陳 季 **Ji Chen**
Title: Prof.
Institution: Emory University
Department: Department of Radiology and Imaging Sciences
Position: Associate Professor
Address: Woodruff Memorial Research Building 1203A, 1364 Clifton Road NE, Atlanta, GA, 30322, USA
Phone: 404-712-4024 Fax: 404-727-3488
E-mail: jchen22@emory.edu

Present Appointment:

1. Associate Professor, Department of Radiology and Imaging Sciences, Emory University
2. Adjunct Professor, Department of Cardiology, Nanjing Medical University, Nanjing, Jiangsu, China

Career Highlight: (in the past 5 years)

1. Assistant Professor of Radiology, Emory University
2. Adjunct Professor, Department of Nuclear Medicine, Chongqing Medical University, Chongqing, China
3. Instructor of Radiology, Emory University, Atlanta, GA, USA
4. Adjunct Instructor of Nuclear and Radiological Engineering Georgia Institute of Technology, Atlanta, GA, USA

Academic Background (please indicate period):

1. 2003-2004 Postdoctoral Fellow in Nuclear Medicine Physics, Supervisor: James R. Galt, PhD and Ernest V. Garcia, PhD, Department of Radiology, Emory University, Atlanta, GA
2. 2002, PhD, Mechanical Engineering, Georgia Institute of Technology, Atlanta, GA
3. 2001, MS, Health Physics, Georgia Institute of Technology, Atlanta, GA
4. 1999 BS Engineering Physics, Tsinghua University, Beijing, China

Honor and Awards:

1. Emory Radiology and Imaging Sciences Outstanding Young Investigator Award, 2011
2. Journal of Nuclear Cardiology Major Achievements Paper, 2011
3. Society of Nuclear Medicine Cardiovascular Council 3rd Best Poster, 2010
4. American Society of Nuclear Cardiology Foundation Research Award, 2006
5. American Society of Nuclear Cardiology Young Investigator Award Finalist, 2005
6. American Society of Nuclear Cardiology Young Investigator Award Finalist, 2002
7. IEEE Medical Imaging Conference Trainee Travel Award, 2001

Professional Affiliation / Membership: (list no more than 10)

1. 2013-2015, Board of Directors, Certification Board of Nuclear Cardiology
2. 2014-present, Member, International Advisory Panel

3. 2005-2012, Member, Quality Assurance Committee
4. 2011, Nominee, Board of Directors, Cardiovascular Council
5. 2012-present, Member, Department of Radiology Awards Committee
6. 2008-present, Member, Department of Radiology Grant Review Committee
7. 2008-present, Co-chair, Radiation Safety Committee III
8. 2008-2009, Member, Radiology Vice Chair for Research Search Committee

Publications Highlights: (list the 10 most recently published or frequently cited)

1. Chen CC, Huang WS, Hung GU, Chen WC, Kao CH, Chen J. Left ventricular dyssynchrony evaluated by Tl-201 gated SPECT myocardial perfusion imaging: a comparison with Tc-99m sestamibi. Nucl Med Commun 2013;34:229-32. [PMID: 23238227]
2. Jacobson AF, Chen J, Verdes L, Folks RD, Manatunga DN, Garcia EV. Impact of age on myocardial uptake of 123I-MIBG in older adult subjects without coronary heart disease. J Nucl Cardiol 2013;20:406-14. [PMID: 23483457]
3. Hsu TH, Huang WS, Chen CC, Hung GU, Chen TC, Chen J. Left ventricular systolic and diastolic dyssynchrony assessed by phase analysis of gated SPECT myocardial perfusion imaging: A comparison with speckle tracking echocardiography. Ann Nucl Med 2013;27:764-71. [PMID: 23775229]
4. Zhou Y, Li D, Feng J, Yuan D, Patel Z, Cao K, Chen J. Left ventricular dyssynchrony parameters measured by phase analysis of post-stress and resting gated SPECT myocardial perfusion imaging. World J Nucl Med 2013;12:3-7. [PMID: 23961248]
5. Hage FG, Aggarwal H, Patel K, Chen J, Jacobson AF, Heo J, Ahmed A, Iskandrian AE. The relationship of left ventricular mechanical dyssynchrony and cardiac sympathetic denervation to potential sudden cardiac deathevents in systolic heart failure. J Nucl Cardiol 2014;21:78-85. [PMID: 24170623]
6. Lin X, Xu H, Zhao X, Chen J. Sites of latest mechanical activation as assessed by SPECT myocardial perfusion imaging in ischemic and dilated cardiomyopathy patients with LBBB. Eur J Nucl Med Mol Imaging 2014. [PMID: 24577952]
7. Hung GU, Huang JL, Wang KY, Lin WY, Tsai SC, Chen SA, Lloyd MS, Chen J. Impact of right ventricular apical pacing on the optimal left ventricular lead positions measured by phase analysis of SPECT myocardial perfusion imaging. Eur J Nucl Med Mol Imaging 2014. [PMID: 24577949]
8. Zhang H, Hou X, Wang Y, Xue S, Liu Q, Chen Z, Wu H, Li W, Cao K, Chen J, Zou J. The acute and chronic effects of right ventricular pacing site on left ventricular mechanical synchrony as assessed by phase analysis of gated SPECT myocardial perfusion imaging. J Nucl Cardiol 2014. (accepted)
9. Zhou Y, Zhou W, Folks RD, Manatunga DN, Jacobson AF, Bax JJ, Garcia EV, Chen J. I-123 mIBG and Tc-99m myocardial SPECT imaging to predict inducibility of ventricular arrhythmia on electrophysiology testing: A retrospective analysis. J Nucl Cardiol 2014. (accepted)
10. Zhou W, Zou J, Piccinelli M, Tang X, Tang L, Cao K, Garcia EV, Chen J. 3D fusion of LV venous anatomy from fluoroscopy venograms with SPECT myocardial perfusion images for guiding CRT LV lead placement. JACC Cardiovasc Imaging 2014. (accepted)

Dyssynchrony Assessment by Myocardial Perfusion Imaging

Ji Chen

Abstract:

Phase analysis of myocardial perfusion imaging has been established for the assessment of left-ventricular (LV) dyssynchrony. This lecture will introduce several clinical applications of the LV dyssynchrony assessment, and provide some technical aspects of using the phase analysis technique. The technical aspects involve the image acquisition, quality control and processing, and result interpretation, which are critical to achieve high-quality phase analysis for those clinical applications.

MEMO

Name: 張 賴 昇 平 **Sheng-Pin Changlai**
Title: MD., Ph.D., CCD., CDT
Institution: LIN- SHIN Medical Corporation LIN-SHIN Hospital
Department: Nuclear Medicine & Radiology Department
Position: Director
Address: No. 36 Sec. 3 Hwei Chung Rd. Nantun District, Taichung, Taiwan
E-mail: spchanglai@yahoo.com.tw

Brief Autobiography (up to 150 words):
A very unique and dedicated medical doctor who is a board certificated member and specialist in nuclear medicine, radiology and osteoporosis fields for more than 30 years, here in Taiwan. He who also devoted himself to the educational career at the medical school and teaching hospital for almost 30 years. For the past 12 years, a new task for osteoporosis continue education in Taiwan, under the ISCD accreditation, is a big successful program and keep going on without stop by me.
2006-Now Director of Medical Imaging Department
2004-2006 Post-Doctor Program, UCLA Medical School Pharmacology Department, Los Angles, USA
2000- 2003 Ph.D. Degree, Chung-Shan Medical University, Taichung, Taiwan.
1998 Research Fellowship, UCLA Medical Center, Los Angles, USA.
1997 Research Fellowship, Tokyo University Hospital, Tokyo, Japan
1991 Research Fellowship, Tokyo Keio University, Tokyo, Japan
1988 Research Fellowship, Tokyo University Hospital, Tokyo, Japan
1984 Resident of National Taiwan University Hospital
Director of Nuclear Medicine, Radiology and Radiotherapy at Chung-Shan Medical University
Associate Professor of The Chung-Shan Medical University, The Central Taichung University

Present Appointment:
1. Director of Nuclear Medicine & Radiology Department, Lin Shin Hospital
2. Associate professor of The Central Taichung University
3. International Faculty of ISCD

Career Highlight: (in the past 5 years)
1. Set up at least five unit of nuclear medicine department, three unit of CT, MRI imaging center and one unit of osteoporosis center in Taiwan hospital.
2. Board of Taiwan SNM (Society of Nuclear Medicine)
3. Board of TOA (Taiwan Osteoporosis Association)
4. Board of RSROC (Radiology Society of Republic of China)

Academic Background (please indicate period):

1. 2004-2006, Post-Doctor Program, UCLA Medical School Pharmacology Department, Los Angles, USA
2. 1998-1999, PET/CT program of UCLA Amhanson Biological Imaging Clinic, Los Angelos, USA
3. 1984-1991, Resident, the National Taiwan University Hospital

Honor and Awards:

1. SNM Highlight 1999
2. Winner of The Phi Tau Phi Scholastic Honor Society 2003
3. Lecture of the Osteoporosis Round Table Forum in LIN-SHIN Hospital

Professional Affiliation / Membership: (list no more than 10)

1. The Radiology Society of R.O.C.
2. The Society of Nuclear Medicine, Taiwan (R.O.C.)
3. The Taiwanese Osteoporosis Association
4. International Faculty of ISCD (International Society of Clinical Densitometry)
5. The Radiology Society of North America

Publications Highlights: (list the 10 most recently published or frequently cited)

1. Consensus of Official Position of IOF/ISCD FRAX Initiatives in Asia-Pacific Region. J Clin Densitometry 2013
2. Updates in understanding and management of thyroid cancer ISBN 978-953-51-0299-1 2012
3. DXA examination and interpretation: the principal and case analysis ISBN 978986129924 2014
4. ....over 200 publications

核醫乳房攝影摘要

Sheng-Pin Changlai

Nuclear medicine breast imaging (also called scintimammography) is a supplemental breast exam that may be used in some patients to investigate a breast abnormality. A nuclear medicine test is not a primary investigative tool for breast cancer but can be helpful in selected cases after diagnostic mammography has been performed. Nuclear medicine breast imaging involves injecting a radioactive tracer (dye) into the patient. Since the dye accumulates differently in cancerous and non-cancerous tissues, scintimammography can help physicians determine whether cancer is present.

Currently, only the Miraluma Tc-99m sestamibi compound, manufactured by DuPont Pharmaceuticals, is approved by the Food and Drug Administration (FDA) for breast imaging in the United States. Therefore, the nuclear medicine breast imaging test may be referred to as a "Miraluma." Nuclear medicine may be appropriate in patients who have dense breast tissue that makes their mammograms difficult to interpret or in patients with palpable abnormalities (i.e., those able to be physically felt) but whose mammograms do not reveal any abnormalities.

MEMO

Name: 余本隆 **Ben-Long Yu**
Title: M.D.
Institution: Koo Foundation Sun Yat-Sen Cancer Center
Department: Division of General Surgery
Office: 886-2-2897-0011 ext. 1609
Address: 125 Lih-Der Road, Pei-Tou District, Taipei 11259, Taiwan
E-mail: benlong@kfsyscc.org

Academic Background:

1. Residence, Department of General Surgery, National Taiwan University Hospital, Taipei, Taiwan, 1993.07-1998.06.
2. Chief Residence, Department of General Surgery, National Taiwan University Hospital, Taipei, Taiwan, 1997.07~1998.06.
3. Deputy Physician, Department of General Surgery, National Taiwan University Hospital, Taipei, Taiwan, 1998.07~2000.06.
4. Attending Physician, Department of General Surgery, Koo Foundation Sun Yat-Sen Cancer Center, Taipei, Taiwan, 1998.07~2003.12.31.
5. Senior Member, Department of General Surgery, Koo Foundation Sun Yat-Sen Cancer Center, Taipei, Taiwan., 2004.01~present.
6. Clinical Research Associate, Dana-Farber Cancer Institute & Brigham and Women's Hospital. 2006.09~2007.08.
7. Chief of Cancer Screening Program, 2009.12~present.

Professional Affiliation / Membership:

- Taipei Medical Assciation
- Taiwan Surgical Association
- Taiwan Surgical Society of Gastroenterology
- The Breast Cancer Society of Taiwan
- Taiwan Society of Ultrasound Medicine
- Taiwan Association for Endoscopic Surgery

乳癌前哨淋巴結核醫掃描定位檢查的臨床經驗
Experience of Sentinel Lymph Nodes Biopsy of Breast Cancer Patients in KFSYSCC

Ben-Long Yu

Axillary lymph nodes dissection (ALND) has been an important part of traditional radical breast cancer surgery since about 120 years ago. It has the therapeutic effect and also as prognostic index. However, there are a lots of short-term and long-term side effects and morbidity after ALND such as lymphedema and paraesthesia. Sentinel lymph node biopsy (SLNB) for clinical node negative breast cancer patients is probably the most important advancement in breast cancer surgery in the recent 20 years. The use of SLNB could spare ALND in SLN (-) and some selected SLN (+) patients with same local recurrence and survival rate. We started SLNB in our hospital at May 2002. There are 5173 cases of SLNB (including 174 bilateral breast cancer patients) done till the end of 2014 at Koo-foundation Sun Yat-Sen Cancer Center (KFSYSCC). With the dual mapping methods of isotope (Tc99m labeled sulfur colloid or Phytate) and dye methods (methylene blue dye), there are 83 mapping failure cases. For the 5090 patients with successful SLN identification, 3737 patients (73.4%) were spared of further ALND after SLNB. As we changed our Tc99m isotope drug from sulfur colloid to Phytate at 2008, the mapping failure rate by isotope method increased. However, as we change the injection method from subdermal to intradermal injection, the mapping failure rate declined dramatically. Under this improvement, some of our surgeons now use only single mapping method with Tc99m-Phytate with same excellent results. We carefully followed up our patients without ALND after SLNB. The disease free survival is similar to those with same cancer stage with ALND.

Name: 杜 高 瑩 Tu Kao Yin
Title: Mr.
Institution: 馬偕紀念醫院
Department: 核子醫學科
Office: 台北中山北路二段 92 號 4F 核子醫學科
Phone: 25433535#2925
E-mail: kenny@mmh.org.tw

非年度電腦斷層品保訓練 -1

Present Appointment:

馬偕紀念醫院核子醫學科 醫事放射師

Career Highlight:

1992.6~1996.6 馬偕紀念醫院核子醫學科 醫事放射師
1996.7~2001.6 馬偕紀念醫院核子醫學科 組長
2001.7~2013.6 馬偕紀念醫院核子醫學科 技術主任

Academic Background:

1985.6 元培醫專 放射技術科
1992.6 中原大學 醫學工程系畢業
2001.1 陽明大學 放射醫學科學研究所 碩士

Honor and Awards:

2002.2~2004.7 中台醫護技術大學 放射技術系 講師
2003.8~ 迄今 陽明大學 生物醫學暨放射科學系 講師

Professional Affiliation / Membership:

2010.11~ 迄今 中華民國放射師公會全國聯合會 理事
2010.11~2014.10 中華民國核醫學學會 副理事長
2014.11~2018.10 中華民國核醫學學會 理事
2007~ 迄今 醫院評鑑暨醫療品質策進會 教學補助計畫審查委員
2010~ 迄今 醫院評鑑暨醫療品質策進會 教學醫院評鑑委員

Publications Highlights:

專書 (年)	專書名稱
2010.7	跨領域團隊合作照護教案

期刊 (年)	期刊發表名稱	期刊發表篇名
2013.1	醫療品質雜誌	醫事放射學校教育與職場的無縫接軌
2012	Annals of Nuclear Medicine and Molecular Imaging	核子醫學醫技現況與未來發展
2010.12	核醫技術雜誌	核子醫學資訊系統的設計與開發

Name: 王 秀 珊 **Hsiu-Shan Wang**
Title: Ms.
Institution: Tri-Service General Hospital
Department: Dep, Nuclear Medicine & PET Center
Address: 104 台北市內湖區成功路二段 325 號
Phone: 02-87923311#17558 Fax: 02-87922681
E-mail: susanwang@office365.ndmctsgh.edu.tw

非年度電腦斷層品保訓練 -2

Present Appointment:
三軍總醫院正子中心放射化學室代理主任

Career Highlight:
台中市醫事放射師公會會員代表
中華民國核醫學會醫技委員會執行秘書

Academic Background:
國立清華大學原子科學系碩士班畢業

Honor and Awards:
三軍總醫院醫事人員進階臨床教師

Professional Affiliation / Membership:
正子造影、電腦斷層品保、輻射防護 / 核醫學會會員編號 911

Publications Highlights:

(A) REFEREED PAPER:

1. Hsiu-Shan Wang, Ching-Han Hsu. A Multiresolution Deconvolution Technique for Quantitative Renogram *Department of Nuclear Science, National Tsing-Hua University, Hsinchu, Taiwan* Ann Nucl Med Sci 2004;17:87-92.

(B) Poster:

1. Hsiu-Shan Wang, Ta-Wei Tseng , Cheng-Yi Cheng, Wen-Sheng Huang. False-positive focal oral uptake due to dental prosthesis seen on PET/CT. The 8th Terry Fox and Chang Gung Memorial Hospital International Cancer Symposium on PET/CT in Oncology.
2. En-Shih Chen, Hsiu-Shan Wang, Ta-Wei Tzeng, Li-Fan Lin, Cheng-Yi Cheng, Hueng-Yuan Shen. Study of the factors influencing cardiac uptake on FDG PET/CT scans. *Department of Nuclear Medicine / PET Imaging Center, Tri-Service General Hospital, Taiwan*. The 51th Annual Scientific Meeting of the Japanese Society of Nuclear Medicune.

Name: 陳 惠 萍 Chen Hui Ping
Title: Mrs.
Institution: LIN-SHIN Hospital
Department: Nuclear Medicine department
Address: 40867 台中市南屯區惠中路三段 36 號
Phone: 04-22586688#1778 Fax: 04-22586688#1768
E-mail: rebecca_0625@yahoo.com.tw

非年度電腦斷層品保訓練 -3

Present Appointment:
林新醫院核子醫學科 放射組長

Career Highlight:
台中縣醫事放射師公會第一、二屆理事長
中華民國醫事放射師全聯會第二、三屆理事

Academic Background:
中台科技大學放射科學研究所碩士畢業

Honor and Awards:
中華民國醫事放射師全聯會專家委員

Professional Affiliation / Membership:
核醫造影、正子造影、電腦斷層品保、輻射防護 / 核醫學會會員編號 462

Publications Highlights:
人類纖維母細胞株受低劑量輻射照射後之基因表現 (核醫學會期刊發表)
自製假體進行正子電腦斷層檢查之體內劑量評估 (研究計畫)
核子醫學科環境劑量分佈評估 (研究計畫)

非年度電腦斷層品保訓練

根據“輻射醫療曝露品質保證組織與專業人員設置及委託相關機構管理辦法”規定，電腦斷層掃描儀品保測試項目又可分爲非年度及年度品保人員。人員資格分爲：(一) 非年度品保人員：參加主管機關、相關學（協、公）會或醫療院所舉辦之電腦斷層掃描儀醫療曝露品保訓練課程 3 小時以上。取得資格後，每年應接受 3 小時以上相關繼續教育訓練。(二) 年度品保人員：參加主管機關或相關學（協、公）會舉辦之電腦斷層掃描儀醫療曝露品保實作訓練課程 8 小時以上。取得資格後，每年應接受 3 小時以上相關繼續教育訓練，且每年應獨立完成 1 次年度品保作業。

本次年會假馬偕醫院場地舉行，爲協助核醫放射師會員取得電腦斷層掃描儀非年度品保人員資格，特由馬偕醫院核醫科主辦本會協辦舉辦此次非年度品保人員訓練，課程內容包括核醫用電腦斷層掃描儀品保項目及法規介紹等。

Name: 趙周社 Zhou She Zhao
Title: M.D., Ph.D.
Institution: GE Healthcare China
Department: MR/PET Advanced Application
Address: Rm 1201 Building A, e-Town International Center, No. 10 Ronghua Road, Beijing Economic & Technology Development Area, Beijing 100176, China
E-mail: Zhoushe.zhao@ge.com

Present Appointment:
MR/PET Advanced Application Manager of GE Healthcare China

Career Highlight:
趙博士在 1993 年取得北京協和醫院核醫學與分子影像博士學位後，在各大國際醫療設備廠擔任核子醫學產品經理，現任 GE 公司的 PET/MR 高級臨床應用經理；主要的研究領域爲分子探針與分子影像技術，包含探針製備、標記方法和影像處理，以及轉化醫學研究。2001 年開始從事 PET 藥物開發；2012 年開始，專注於水通道蛋白成像技術研究和應用。從 2015 年 6 月開始專注 PET/MR 的臨床應用和科研專案。

Academic Background:
- 1990-1993 年：中國醫學科學院北京協和醫院　核醫學與分子影像博士研究生；研究方向：SPECT 影像處理技術
- 1987-1990 年：西安醫科大學第一醫院　核醫學科　在職核醫學碩士研究生；研究方向：肝臟血流量測量及臨床意
- 1980-1985 年：西安醫科大學醫療系　本科生

Publications Highlights:
- 郭啓勇，辛軍，張新，趙周社等。MRI 水擴散加權成像分子機理研究進展，中國臨床醫學影像雜誌 [J]. 2013,24(07):496-500。
- 李加慧，李秋菊，於兵，張新，趙周社，石喻，辛軍，郭啓勇。DWI-MRI 多 b 值水通道蛋白分子成像機理和方法學研究，中國臨床醫學影像雜誌 2014;25 (3):186-189。
- 韓婷婷，杜名，張新，曹禮，李紅，趙周社，辛軍，郭啓勇。13N-NH3 H2O PET/CT 在大鼠肝纖維化模型成像的定量研究。2014 年；25(4):243-247。
- 曹禮，杜名，張新，韓婷婷，李宏利，趙周社，郭啓勇，辛軍，[11C] 標記水通道蛋白抑制顯象劑全自動合成方法，中國臨床醫學影像雜誌 2014 年；25(5):344-346。
- Li QJ, Li JH, Yu B, Zhang X, Shi Y, Xin J, and Gou QY. Assessment of aquaporins function in stages of liver fibrosis using multi-b diffusion weighted magnetic resonance imaging. 2014 ISMRM
- Ling XY, Zhao ZS, Zhang ZP, Huang Li. Characterization of water transportation via aquaporin via aquaporin using tri-exponential model in cerebral infarction and Parkinson's disease. 2014 ISMRM
- Ma Quanmei, Xin Jun, Zhao Zhoushe, et al. Value of ^{18}F-FDG PET/CT in the diagnosis of primary gastric cancer via stomach distension. Eur J Radiol 2013 Jun 22;82(6):302-6.
- Zhu Zhaohui, Miao Weibing, Li Qianwei, et al. 99mTc-3PRGD2 for integrin receptor imaging of lung cancer: a multicenter study. J Nucl Med 2012 May 12;53(5):716-22.
- Tian Jiahe, Yang Xiaofeng. et al. A multicenter clinical trial on the diagnostic value of dual-tracer PET/CT in pulmonary lesions using 3'-deoxy-3'-18F-fluorothymidine and 18F-FDG. J Nucl Med 2008;49(2):186-94.
- 徐浩，淩雪英，趙周社，黃力，腦血流量測量方法進展，現代生物醫學進展 2014 年待發表。

TOF-PET/MR 同步掃描及衰減校正技術進展介紹

趙周社

GE Healthcare China MRI Modality.

摘要：

PET 的飛行時間技術 (Time of Flight, TOF) 除在 PET 和 PET/CT 設備中發揮提高 PET 圖像對比度的作用外，在一體化、同步掃描 PET/MR (TOF-PET/MR) 設備中還發揮著更爲重要的作用。TOF 技術能夠消除來自 MR 的靜態磁場、梯度線圈和射頻系統等產生的噪音引起的星狀僞影 (Star Artifact)（又被稱爲“熱器官”徵象），並且能夠顯著降低 MR 靜態磁場引起正電子核素在空腔臟器發生的穿透效應 (Shine-Through in PET/MR) 所致的僞影，從而提高 PET 與 MR 同步掃描獲得 PET 圖像品質和採用 MR 資訊對正電子發生湮滅輻射作用後 γ 射線在組織細胞的衰減進行衰減校正 (MR Based Attenuation Correction, MRAC)。MRAC 技術的基礎是獲得水、脂分離的圖像資訊，採用 MRAC 時不但要關注水、脂圖像品質，是否存在反相，而且需要特別注意對全身不同部位 MRAC 圖集 (Atlas- Based Methods) 的正確選擇。最近推出的 MRI 零回波 (Zero Echo Time, ZTE) 技術能夠準確獲得骨骼皮質結構，從而提高 MRAC 精准度。

我們初步臨床使用的經驗表明 TOF-PET/MR 同步掃描在神經系統（腦血管病、頸動脈斑塊、脊髓動靜脈瘺和癲癇）疾病，腫瘤（頭頸部、腹部）早期診斷、精准分期和療效評估，以及對心肌存活性檢測均具有重要的臨床價值。

Name: 黃玉儀 Yu-Yi Huang
Institution: 和信醫院
Department: 核子醫學科
Address: 112 台北市北投區立德路 125 號
E-mail: yuyi@kfsyscc.org

學歷：
陽明大學醫學系 學士，1994/9-2001/6

專長：
核醫診斷，核醫治療，核醫腫瘤學

證書：
畢業證書、考試及格證書、專科醫師證書、聘書、執業執照…等。

學會會員：
中華民國核醫學學會 (編號 A199)

著作（依發表年序列舉）

A. 有審查論文 (REFERRED PAPER)

1. YY Huang, JSH Tsung: Alpha-fetoprotein Producing Gastric Cancer: A Case Report. J Biomed Lab Sci, 2002;14:25-28.
2. YY Huang, DL You, YM Lin, TCL Soong, VP Chuang, PS Yang: Radionuclide Hepatobiliary Imaging in Evaluation of Reserved Hepatic Function in Patients with Hepatocellular Carcinoma before Transcatheter Arterial Embolization. Ann Nucl Med Sci 2004;17:1-6.
3. YY Huang, DL You, BL Yu, MH Tsou: Radionuclide Sentinel Lymph Node Scan and Biopsy in Breast Cancer: The Experience in a Cancer Center. Ann Nucl Med Sci 2004;17:185-190.
4. Yu-Yi Huang, Dong-Ling You, Mei-Hwa Tsou, Chia-Chuan Liu, Pei-Ing Lee. Primary Pulmonary Pleomorphic Adenoma with High Uptake of FDG - A Case Report. Eur J Radiology Ex 2007;62:73-76.
5. YL Lin, Dl You, BL Yu, AY Chuang, NC Shih, MH Tsou, PI Lee, YY Huang. Radiation Safety with Breast Sentinel Lymph Node Lymphoscintigraphy. Ann Nucl Med Sci. 2007;20:15-19.
6. Yu-Yi Huang, Dong-Ling You, Mei-Ching Liu[2], Tran-Der Tan[2], Pei-Ing Lee[1], Ming-Yuan Lee[3]. Under performance of Gallium-67 Scan vs. FDG-PET is greater in relapse than in initial staging. Clin Nucl Med 2011;36: 867-871.
7. Yu-Yi Huang, M. D., Pei-Ing Lee, M. D., Mei-Ching Liu, M. D., Chien-Chih Chen, M. D., Kuo-Cheng Huang, M. D., Andrew T. Huang, M. D.. A general cut-off level combined with personalized dynamic change of serum

carcinoembryonic antigen can suggest timely use of FDG-PET for early detection of recurrent colorectal cancer. Clin Nucl Med; accepted in May, 2015.

B. 學會發表論文 (CONFERENCE PAPER)

1. Quantitative Hepatobiliary Imaging in Evaluation of Reserved Hepatic Function in Patients with Hepatocellular Carcinoma before Transcatheter Arterial Embolization. July, 20th, 2002 於台北榮總舉行之中華民國核醫學學會 2002 年學術研討大會發表口頭報告。
2. Using FDG PET-CT in Sraging of Esophageal Cancer: The Experience of SYSCC. Oct. 25th, 2003 於三軍總醫院舉行之中華民國核醫學學會 2003 年學術研討大會會發表口頭報告。
3. Radionuclide Sentinel Lymph Node Biopsy in Predicting Axillary Lymph Node Metastases in Early Stage Breast Cancer. Oct. 25th, 2003 於三軍總醫院舉行之中華民國核醫學學會 2003 年學術研討大會發表口頭報告。
4. The Role of FDG PET-CT in Detection of Recurrent Hepatocellular Carcinoma Suspected by Increasing Serum Alpha-fetoprotein. Nov. 20th, 2004 於台北榮總舉行之中華民國核醫學學會 2004 年學術研討大會發表口頭報告。
5. When to Use FDG PET to Detect Recurrent Colorectal Cancer in Patients With Elevated Serum CEA Level. Oct. 27th, 2007 於台北醫學院附設醫院舉行之中華民國核醫學學會 2007 年學術研討大會發表口頭報告 Clinical Impact of FDG PET in Stage pN3 Breast Cancer. Nov. 15th, 2008 於高雄醫學院附設醫院舉行之中華民國核醫學學會 2008 年學術研討大會發表口頭報告。
7. Yu-Yi Huang, Dong-Ling You, Huei-Wen Lai, Pei-Ing Lee, and Po-Shen Yang. Clinical value of radionuclide hepatic arterial infusion pump perfusion scan in detecting extrahepatic perfusion of hepatic arterial infusion pump. J. NUCL. Med. MEETING ABSTRACTS, May 2006;47:481P. Poster presentation. 2006 SNM Annual Meeting.
8. Huei-Wen Lai, Dong-Ling You, Yu-Yi Huang, and Ming-Shen Kao. The influence of concentrations of oral contrast agent in artifact in PET-CT study. J. NUCL. Med. MEETING ABSTRACTS, May 2006;47:541P. Poster presentation. 2006 SNM Annual Meeting.
9. Yu-Yi Huang, Do-Ling You, Mei-Ching Liu, Chien-Chih Chen, and Pei-Ing Lee. Optimize the detection rate of FDG PET in patients suspicious for recurrent colorectal cancer presenting with elevated serum CEA level. J. NUCL. Med. MEETING ABSTRACTS, May 2007;48:391P. Poster presentation. 2007 SNM Annual Meeting.
10. Yu-Yi Huang, Dong-Ling You, Mei-Jean Liu, Pei-Ing Lee, Ming-Yuan Lee. 2008 June. Larger difference of performance between FDG-PET and Ga-67 scan in detecting recurrence than in initial staging of lymphoma. Poster presentation. 2008 SNM Annual Meeting. J. NUCL. Med. MEETING ABSTRACTS;49:259P.
11. Lee Pei-Ing, You Dong-Ling, Yu Ben-Long, Tsou Mei-Hua, Huang Yu-Yi. 2008 June. Pathologic significance of sentinel lymph node mapping failure in breast cancer. Poster presentation. 2008 SNM Annual Meeting. J. NUCL. Med. MEETING ABSTRACTS;49:257P.
12. Yu-Yi Huang, Dong-Ling You, Ming-Yuan Lee, Tran-Der Tan, Pei-Ing Lee. 2009 June. Correlation between FLIPI score and the uptake of FDG PET in patients with low grade follicular lymphoma Poster presentation. 2009 SNM Annual Meeting. J. NUCL. Med. MEETING ABSTRACTS;50:1677.
13. Yu-Yi Huang[1], Pei-Ing Lee[1], Mei-Ching Liu[2], Chien-Chih Chen[3], Kuo-Chen Huang[2], Andrew T. Huang. A general cut-off level or a personalized dynamic change of serum CEA can suggest timely use of FDG-PET for early detection of recurrent colorectal cancer. Accepted by 2014 SNM Annual Meeting.

甲狀腺癌放射碘治療 -ATA 2015 指引與新方向

黃玉儀

ATA 2015 guidelines for thyroid cancer 甫於 10 月中旬發布，將甲狀腺癌的治療帶入以實證醫學爲依據的新領域，同時也帶入了部分的新觀念。

重點在於根據病人在診斷、復發、追蹤等不同時期的風險評估 (Risk stratification) 來指引治療的方式，包含放射碘治療的使用時機與方式。本次報告將統整此份指引中對於放射碘治療的建議，提供各位做爲未來執行甲狀腺癌放射碘治療的參考。

Outline:

1. The role of RAI therapy
   - Initial therapy
     Ablation/Adjuvant
     Persistent disease
     Incomplete response to initial therapy
     Advanced/metastatic disease
2. RAI refractory

MEMO

Name: 侯正涵 **Cheng-Han Hou**
Title: M.D.
Institution: Tri-Service General Hospital, National Defense Medical Center
Department: Department of Nuclear Medicine
Office: Nuclear Medicine Department, Tri-Service General Hospital (3F)
Address: No. 325, Sec. 2, Chenggong Rd., Neihu Dist., Taipei City 114, Taiwan (R.O.C.)
E-mail: davidhou@mail.ndmctsgh.edu.tw / davidhou0617@gmail.com

Present Appointment:

Aug. 2015 — present Medical Officer, Medical Battalion, 3rd Regional Support Command, Army Logistics Command, Taoyuan, Taiwan

Career Highlight:

Aug. 2014 — July 2015 Fellow, Nuclear Medicine and PET, Tri-Service General Hospital, National Defense Medical Center (NDMC), Taipei, Taiwan

Aug. 2013 — July 2014 Chief Resident, Nuclear Medicine and PET, Tri-Service General Hospital, NDMC, Taipei, Taiwan

Jan. 2013 — Jan. 2015 Problem-Based Learning (PBL) Tutor, School of Medicine, NDMC, Taipei, Taiwan

Jan. 2013 — July 2013 Acting Chief Resident, Nuclear Medicine and PET, Tri-Service General Hospital, NDMC, Taipei, Taiwan

Feb. 2011 — July 2011 Post-Graduate Year Resident, General Medicine, Tri-Service General Hospital, NDMC, Taipei, Taiwan

July 2010 — July 2015 Clinical Instructor, School of Medicine, NDMC, Taipei, Taiwan

July 2010 — Dec. 2012 Resident, Nuclear Medicine and PET, Tri-Service General Hospital, NDMC, Taipei, Taiwan

Aug. 2008 — July 2010 Medical Officer, Southern Ammunition Depot, 4th Regional Support Command, CLC, Kaohsiung, Taiwan

Academic Background:

Aug. 2001 — July 2008 Doctor of Medicine (M.D.), School of Medicine, NDMC, Taipei, Taiwan

Professional Affiliation / Membership:

Nov. 2014 — present Executive Secretary, Society of Nuclear Medicine, Taiwan (R.O.C.)

Nov. 2014 — present Committee Member, Radioiodine and Radioisotope Therapy Committee, Society of Nuclear Medicine, Taiwan (R.O.C.)

Oct. 2014 — present Member, Taiwan Association of Medical Education

Nov. 2010 — present Member, Society of Nuclear Medicine, Taiwan (R.O.C.)

PROFESSIONAL INTERESTS

Nuclear Medicine, Molecular Imaging, Radioisotope Therapy, Medical Curriculum Design

甲狀腺癌案例分享

侯正涵 Cheng-Han Hou　諶鴻遠 Daniel HY Shen

Department of Nuclear Medicine, Tri-Service General hospital, National Defense Medical Center.

Abstract

Approximately 90% of thyroid cancers arise from follicular epithelium and correspond to differentiated thyroid carcinomas (DTC) including papillary (PTC) and follicular (FTC) thyroid carcinomas. Despite more than 90% of DTC patients diagnosed in early stages has normal life expectancy, 5% of patients with distant metastasis at the diagnosis and 10%-15% patients presenting recurrent disease during the follow-up show a reduction of survival. In the last decades, radioactive iodine treatment (RAI) plays a major role in the management of patients with DTC. However, RAI may become refractory and is associated with molecular biology and pathway (e.g. RET/PTC rearrangement, RAS/RAF/MAPK mutation, activation and dysregulation of the intracellular signaling cascade PI3K/Akt/mTOR). As the tumor (DTC) progresses to RAI-refractory DTC and is known as dedifferentiation, target therapy must be considered. Sorafenib is now the first approved by the FDA for DTC refractory to RAI.

As a multikinase inhibitor, sorafenib involves in the development and progression of DTC, including the RAF, VEGF (VEGFR-2, VEGFR-3), PDGF (PDGFR), c-KIT and RET kinases. The most frequently reported adverse events include hand-foot skin reaction, diarrhea, anorexia, fatigue, and rash or desquamation. Most adverse events were graded 1 or 2. In this session, we would like to present 3 cases of FTC with unique clinical features and results to share our preliminary practical experience with sorafenib.

Name: 林立凡 **Li-Fan Lin**
Title: Dr.
Institution: Tri-Service General Hospital
Department: Nuclear Medicine
Office: 02-89832233-16717
Address: 325 Cheng-Kung Road, Nei-Hu, Taipei 114, R.O.C
E-mail: fanlin2@gmail.com

Academic Background: M.D., Medical School, National Defense Medical Center, Taipei, R.O.C.

Professional Affiliation / Membership: Membership of Society of Nuclear Medicine, Taiwan, R.O.C.

Selected Publications:

1. Chen YY, Huang TW, Tsai WC, Lin LF, Cheng JB, Lee SC, Chang H. Lymphovascular space invasion and tumor differentiation are predictors for postoperative recurrence in patients with pathological stage I nonsmall cell lung cancer. J Chin Med Assoc. 2014 Aug;77(8):416-21. (SCI)
2. Lin LF, Cheng CY, Hou CH, Tseng NC, Shen DH. Experience of low-dose aminophylline use to relieve minor adverse effects of dipyridamole in patients undergoing stress myocardial perfusion imaging. J Nucl Cardiol. 2014 Jun;21(3):563-9. (SCI)
3. Chen YY, Huang TW, Tsai WC, Lin LF, Cheng JB, Chang H, Lee SC. Risk factors of postoperative recurrences in patients with clinical stage I NSCLC. World J Surg Oncol. 2014 Jan 10;12:10. (SCI)
4. Huang TW, Lin LF, Hsieh CM, Cheng YL, Chang H, Tzao C, Lee SC. Positron emission tomography in bronchioloalveolar carcinoma of the lung. Eur J Surg Oncol. 2012 Dec;38(12):1156-60. (SCI)
5. Hou CH, Shen DH, Lin LF, Gao HW, Hsu YC, Cheng CY. Aggressive Right Atrial Tumor with Extensive FDG-avid Metastases in a Case of Cardiac Angiosarcoma. Ann Nucl Med Sci 2012;25(4):201-205.
6. Lin LF, Shen DH, Tsai WC, Hou CH, Cheng CY, Chen CY. "Quasi-Symmetric" FDG Avidity of Bilateral Salivary Glands in Mikulicz Disease Yielding False-Positive Staging in Lung Cancer. Clin Nucl Med. 2012 Nov;37(11):1102-4. (SCI)
7. Lin LF, Chang CY, Hou CH, Shen DH. Unusual Tc-99m methylene diphosphonate uptake by clinically suspected adrenal metastases from hepatocellular carcinoma. Clin Nucl Med. 2011 Dec;36(12):e207-e208. (SCI)
8. Shen DH, Chang CY, Lin LF, Gao HW, Cheng YL, Chen CY. Conversion from FDG-negative to -positive during follow-up in a rare case of pulmonary lymphoepithelioma-like carcinoma. Clin Nucl Med. 2011. (SCI)
9. Lin LF, Chang CY, Cherng SC. Advanced squamous cell carcinoma of the bulbar conjunctiva seen on PET/CT. Clin Nucl Med. 2008 Dec;33(12):929-30. (SCI)
10. Chang CY, Cheng CY, Shen DH, Bai CY, Lin LF, Huang WS. Tumoral calcinosis demonstrated on Tc-99m sestamibi scintigraphy. Clin Nucl Med. 2008 Dec;33(12):920-1. (SCI)
11. Lin LF, Chang CY, Tsai, CJ, Cheng CY, Lee MS, Chen MR, Yung SP, Huang WS. Changes of Cardiac Functions in Athyreotic Patients With and Without Suppressive Thyroxine Treatment. Ann Nucl Med Sci 2008;21:65-71.
12. Tsai WC, Jin JS, Chang WK, Chan DC, Yeh MK, Cherng SC, Lin LF, Sheu LF, Chao YC. Association of cortactin and fascin-1 expression in gastric adenocarcinoma: correlation with clinicopathological parameters. J Histochem Cytochem. 2007 Sep;55(9):955-62. Epub 2007 May 17. (SCI)
13. Chang CY, Lin LF, Lin YS, Peng YJ, Huang WS, Cherng SC. Laryngeal giant cell tumor mimicking thyroid cancer demonstrated by PET/CT. Clin Nucl Med. 2007 May;32(5):390-2. (SCI)
14. Huang WS, Lin LF, Wu Elizabeth, Ho Eugene, Chang CY, Wu SY. Nuclear Medicine in Treating Differentiated Thyroid Carcinoma J Med Sci 2006;26(3):083-092.
15. Lin LF, Tsai CS, Ho Eugene, Wu SY, Lin JC, Cheng CY, Huang WS. PET in Vascular Diseases: Applications of FDG PET/CT in Vasculitis and Therapeutic Response Ann Nucl Med Sci 2006;19:91-98.

Ra-223 Treatment in Bone Metastasis of CRPC: TSGH Preliminary Experience

Li-Fan Lin, C-H Ho, YF Chen, S-T Wu, T-L Cha, C-Y Cheng, H-Y Shen*

Radium-223 Dichloride (Ra-223) is the first agent to extend overall survival by targeting bone metastases in CRPC. Ra-223 binds with minerals in the bone to deliver radiation directly to bone tumors, limiting the damage to the surrounding normal tissues. In the US double-blinded, randomized trial - ALSYMPCA trial, Ra-223 treatment has the benefit of 3.6 months increase in median overall survival while there were no apparent differences in hematological toxicity for patients receiving post-study chemotherapy, irrespective of whether they had received Ra-223 treatment. Ra-223 has a majority in alpha emission (> 97%), however, there is still some beta and gamma emission. The radiation protection issue of the procedure still has some debate about adapting to Taiwan's regulation rules. Herein we represent the preliminary experience of Ra-223 treatment in a tertiary medical center.

Name: 王士忠 **Shih-Chung Wang**
Title: Prof.
Institution: 彰化基督教兒童醫院
Department: 兒童血液腫瘤科
Address: 500 彰化縣彰化市南校街 135 號
E-mail: 68122@cch.org.tw

學歷：

1. 私立長榮大學醫學研究所在職碩士班碩士　2005/9~2009/7
2. 私立中國醫藥大學中醫學系學士　1988/7~1995/6

證書：

1. 中華民國醫師證書 醫字第 026361 號　1996/6~
2. 中華民國小兒科專科醫師證書 兒專醫字第 002471 號 2001/2~
3. 中華民國血液病專科醫師證書 中血專醫字 93210 號　2003/1~
4. 中華民國血液及骨髓移植專科醫師證書 中血移專醫字 96068 號　2008/1~
5. 中華民國教育部部定講師 講字第 104098 號　2011/8/1

現職：

1. 彰化基督教兒童醫院 兒童血液腫瘤科 主任　2007/7~
2. 彰化基督教醫院 教學部 實習暨聯合訓練中心 主任　2011/8/1~

經歷：

1. 彰化基督教醫院 兒科部 住院醫師　1997/7~2000/6
2. 彰化基督教醫院 兒科部 總醫師　2000/7~2001/7
3. 國立台大醫院 兒童血液腫瘤科 研究醫師　2001/8~2003/7
4. 彰化基督教醫院 兒童血液腫瘤科 主治醫師　2004/1~2007/6
5. 彰化基督教醫院 教學部 醫學教育中心 主任　2006/6~2010/6/30
6. 彰化基督教醫院 教學部 醫師教育中心 協同主任　2010/7/1~2011/7/31
7. University Hospitals Rainbow Babies & Children Hospital Cleveland, OH U.S.A. Visiting Scholar　2012.9.1~2013.2.28

I-131-MIBG Therapy in Patients with Relapsed/refractory Neuroblastoma---Two Case Report

Shih-Chung Wang[1], Lien-Yen Wang[2], Kai-Yuan Tzen[3], Meng-Yao Lu[4], Yen-Lin Liu[5], Hsiu-Ju Yen[6]

[1]Division of Pediatric Hematology and Oncology, Department of Pediatrics, Changhua Christian Children Hospital, Changhua, Taiwan;
[2]Department of Nuclear Medicine, Changhua Christian Hospital, Changhua, Taiwan;
[3]Department of Nuclear Medicine, National Taiwan University Hospital, Taipei, Taiwan;
[4]Division of Pediatric Hematology and Oncology, Department of Pediatrics, National Taiwan University Children Hospital, Taipei, Taiwan;
[5]Division of Pediatric Hematology and Oncology, Department of Pediatrics, Taipei University Hospital, Taipei, Taiwan;
[6]Division of Pediatric Hematology and Oncology, Department of Pediatrics, Taipei Veterans General Hospital, Taipei, Taiwan.

Introduction: Neuroblastoma, which derives from neural crest, is the most common extracranial solid cancer in childhood. More than half of patients have metastases at diagnosis. Main metastatic sites are regional lymph nodes, liver, bone and bone marrow. High-risk patients (Age greater than 1 year at diagnosis, advanced primary lesion or metastases, and MYCN amplification) have poor prognosis in spite of forcible multimodality therapies. Ninety-percent of neuroblastoma express the norepinephrine (NE) transporters on their cell membrane and take in MIBG via a NE transporter. I-131-Metaiodobenzylguanidine (I-131-MIBG) therapy for neuroblastoma was firstly reported in 1986. Since then, many trials of I-131 MIBG therapy in patients with neuroblastoma have been done. Monotherapy with a low dose of I-131 MIBG could achieve high-probability pain reduction. The combination therapy with I-131 MIBG and other modalities such as chemotherapy and myeloablative chemotherapy with hematopoietic stem cell transplantation improved the therapeutic response in patients with refractory or relapsed neuroblastoma. We have performed I-131 MIBG therapy for two patients with relapsed/refractory neuroblastoma. This is the firstly reported experience in Taiwan.

Methods: I-131 MIBG, 150-300 mCi (3.5-5 mCi/Kg body weight) diluted in 50-100 ml saline was administered by slow intravenous infusion for 2 hours via an indwelling cannula using a lead-shielded infusion system. Vital signs were closely monitored.

Results: No major side effects except mild nausea was noted in these two patients. Patients were discharged on 2nd and 3rd hospital day, respectively. The treatment course was smoothly and patients tolerated well.

Conclusions: I-131 MIBG therapy can be safely administered for patients with relapsed/refractory neuroblastoma. Optimal administered activity per treatment cycle, total number of treatments and treatment interval by tumour type and the role of I-131 MIBG in early neuroblastoma need further study.

Name: 王安美 **An-mei Wang**
Title: Director
Institution: MacKay Memorial Hospital
Department: Nuclear Medicine
Address: No. 92 , Zhongshan N Road, sec. 2, Zhongshan District, Taipei City
Phone: 02-25433535 ext. 3386
E-mail: **cliff@ms1.mmh.org.tw**

Brief Autobiography:

After graduating from Tatung University then services in Mackay Memorial hospital, Nuclear Medicine department, Radioimmunoassay Laboratory, shortly promoted as technical leader and to be technical director in 2013. As TAF Assessor in medical laboratory, I am willing to share ideas and experiences in RIA laboratory accreditation with you in order to improve the quality and efficiency of laboratory and reach for the benefit of the public health.

RIA 實驗室不符合事件撰寫、風險因子之辨識經驗分享

王安美

摘要：

在 ISO-15189 醫學實驗室 – 品質與能力特定要求中，已明訂實驗室應具備調查程序，以鑑別品質管理系統中不符合實驗室所訂程序或先前預定要求之各類問題。ISO-15189 也明確規定此調查程序應與矯正措施及預防措施相連結。除此之外，ISO-15189 亦指明實驗室管理階層應審查實驗室品質管理系統與支援病人照護之所有活動的適切性及有效性，並導入必要的改變。實驗室若要做到上述要求，必須全盤考量每個程序中每一個步驟所存在的潛在風險並且仔細完成風險因子的辨識。

RIA 實驗室認證多年，對於實驗室不符合事件的撰寫，仍多停留於事件說明、預防再發生的對應，卻對發生不符合事件時，事件不影響其流程是否可立即處理之措施，甚至一些比較嚴重事件後續之處理審查或鑑別等等似乎未能切入重點撰寫。因此學會藉由此次機會，經由討論分享，指引各實驗室同仁對於不符合事件撰寫，將實驗室中的不符合事物、錯誤與異常事件作分類，以期助於達成實驗室品質監控的目的。

Name: 邱曼慈 **Man Tzu Chiu**
Organisation: 財團法人全國認證基金會 / 實驗室認證處
Position within Organisation (including field): 認證專員 (生醫組)
Email Address: mandychiu@taftw.org.tw

Education Background:

2007-2009 中國醫藥大學醫學檢驗暨生物技術所碩士班
2003-2006 中國醫藥大學醫學檢驗暨生物技術所學士班

Training Record:

- July/ 2012 ISO 15189 Training course
- Sep/ 2012 GLP Inspector Training course
- Sep/ 2012 ISO/IEC 17025 Laboratory Assessor Training course
- Nov/ 2012 Training Course on Statistics and External Quality Assessment Programme (EQAP) for Medical Laboratories, HKAS
- Jul/ 2013 APLAC ISO 15189 Training course, Thailand
- Feb/ 2014 TAF speaker Initial Training course
- Sep/ 2014 APLAC ISO 15189 Training course, HKAS
- Jan/ 2015 Training course on ISO/IEC 17011, HKAS
- Jun/ 2015 Insight into the new ISO 9001:2015
- Oct/ 2015 APEC workshop on capacity building for providing medical EQA programme

Accreditation Experience:

- 2012-2015 生醫組認證專員

Other Professional Experience:

- 2015 疾病管制署高防護實驗室導入「實驗室生物風險管理系統」提升預防能力及降低感染風險研究 / 研究人員
- 2014 勞動部勞工體格及健康檢查指定醫療機構檢驗品質改善計畫 / 計畫主持人
- 2013 前勞工委員會勞工體格及健康檢查指定醫療機構檢驗品質改善計畫 / 研究人員
- 2011-2012 華廣生技股份有限公司 / 法規專員
- 2009-2011 台灣尖端先進生技醫藥股份有限公司 / 副研究員
- 國家考試院合格醫事檢驗師

摘要

財團法人全國認證基金會 (簡稱 TAF) 爲符合 ISO/IEC 17011 的國際認證組織，其實驗室認證處依據 ISO/IEC 17025 與 ISO 15189 提供實驗室認證服務，亦代表台灣於國際簽署國際實驗室認證聯盟與亞太實驗室認證聯盟的相互承認協議。TAF 於 2007 年與核醫學會簽署合作備忘錄，以期後續能攜手致力於醫學檢查與提升相關技術交流，促進醫病福祉與雙方推廣合作。本次將介紹本會工作現況、核子醫學影像認證相關事務與技術規範等資訊，提供與會者參考。

OB001

Synthesis and Characterization of a Novel Radioiodinated Phenylacetamide and its Homologue as Theranostic Agents for Malignant Melanoma

Chih-Chao Chang[1], Chih-Hsien Chang[1,2], Chih-Chieh Shen[3], Chuan-Lin Chen[1], Ren-Shyan Liu[1,4,5], Ming-Hsien Lin[6*] Hsin-Ell Wang[1*]

[1]Department of Biomedical Imaging and Radiological Sciences, National Yang-Ming University, Taipei, Taiwan;
[2]Isotope Application Division, Institute of Nuclear Energy Research, Taoyuan, Taiwan;
[3]Department of Nuclear Medicine, Cheng Hsin General Hospital, Taipei, Taiwan;
[4]Molecular and Genetic Imaging Core/Taiwan Mouse Clinic, National Comprehensive Mouse Phenotyping and Drug Testing Center, Taipei, Taiwan;
[5]National PET/Cyclotron Center and Department of Nuclear Medicine, Taipei Veterans General Hospital, Taipei, Taiwan;
[6]Department of Nuclear Medicine, Taipei City Hospital, Zhongxiao Branch, Taipei, Taiwan.

Background & Aims: Malignant melanoma has become a global public health problem and its incidence keeps increasing. Melanin is an attractive target for the diagnosis and treatment of malignant melanoma. This study reports the preparation and biological characterizations of N-(2-(diethylamino)ethyl)-2-(3-$^{123/131}$I-iodo-4-hydroxyphenyl)acetamide and N-(2-(diethylamino)ethyl)-3-(3-$^{123/131}$I-iodo-4-hydroxyphenyl)propanamide ($^{123/131}$I-IHPA and $^{123/131}$I-IHPP) as novel melanin-specific theranostic agents.

Methods: $^{123/131}$I-IHPA and $^{123/131}$I-IHPP were developed from self-synthesized precursors via a one-step electrophilic radioiodination followed by solid phase extraction (SPE) cartridge purification. $^{123/131}$I-IHPA and $^{123/131}$I-IHPP can both be prepared in 30 min with a high radiochemical yield of > 80% and radiochemical purity of > 95%. The specific uptake of ^{131}I-IHPA and ^{131}I-IHPP in pigmented B16F0 melanoma cells was studied and compared with that in A375 amelanotic melanoma cells. The biological characterizations of $^{123/131}$I-IHPA and $^{123/131}$I-IHPP, including biodistribution study and microSPECT imaging, were performed in two mouse models, e.g., the C57BL/6 mice bearing B16F0 melanoma, and the BALB/c nude mice bearing A375 amelanotic melanoma. The OLINDA/EXM program was utilized for estimating the radiation dosimetry.

Results: These two tracers were hydrophilic, exhibited good serum stability and high binding affinity to melanin. In vitro and in vivo studies revealed rapid, high and tenacious uptakes of both ^{131}I-IHPA and ^{131}I-IHPP in melanotic B16F0 cell line and in C57BL/6 mice bearing B16F0 melanoma, but not in amelanonic A375 cell line and tumors. Small-animal SPECT imaging also clearly delineate B16F0 melanoma since 1 h postinjection of ^{123}I-IHPA and ^{123}I-IHPP in tumor-bearing mice. Owing to the favorable biodistribution of ^{131}I-IHPA and ^{131}I-IHPP after intravenous administration, the estimated absorption dose was low in most normal organs and relatively high in melanotic tumor.

Conclusions: Our studies demonstrated that both $^{123/131}$I-IHPA and $^{123/131}$I-IHPP were excellent SPECT probes for targeting melanin both in vitro and in vivo. The melanin-specific binding ability, sustained tumor retention, fast normal tissues clearance and acceptable projected human dosimetry supported that ^{131}I-IHPA and ^{131}I-IHPP are promising theranostic agents for melanin-positive melanoma.

OB002

A Successful Experience in Performing Repeated Quantitative Small Animal PET Studies

Hsiao-Ming Wu[1], Chun-Hu Wu[2], Ya-Yao Huang[3], Miao-Ling Tsai[1], Szu-Fu Chen[2], Kai-Yuan Tzen[3]

[1]*School of Medicine, Fu-Jen Catholic University, Taiwan;*
[2]*Graduate Institute of Life Sciences, National Defense Medical Center, Taipei, Taiwan;*
[3]*Department of Nuclear Medicine, National Taiwan University Hospital, Taiwan.*

Introduction: Performing quantitative small animal PET study with arterial input function was technically challenging. In this study, we show that performing longitudinal, quantitative FDG PET studies with arterial input functions in rats is routinely feasible.

Methods: Two rats underwent microsurgical procedures for repeated arterial blood sampling and FDG bolus injections. A week after surgery, each rat had two FDG PET studies (i.e. 15 serial blood samples followed by a 20 minutes dynamic brain PET scan) performed on two consecutive days, one study with and one study without the influence of 2% isoflurane anesthesia. Blood samples were taken with an automated microfluidic device allowing take small samples (either < 1 μl for deriving input function or > 50μl for calculating plasma/whole blood FDG ratio). Tissue FDG uptakes were sampled by drawing ROIs on the parietal lobes of brain PET images. Cerebral metabolic rates of glucose (CMRG; in unit of μmol/100min/g) were calculated using a modified version of Operational Equation, where a k4 microparameter was included to account for phosphatase activities and tissue heterogeneities in ROI (Yu et al., 2009).

Results: All 12 PET studies (6 morning sessions; 2 studies per session) were performed successfully. Both rats remained in good health (30% of weight increase during the month of studies) after 6 PET studies with blood samples taken. The CMRG obtained from the two rats with (i.e. unconscious state) or without anesthesia (i.e. conscious state) were listed in the following table. Results showed that the CMRG of both rats were suppressed more than 50% under the isoflurane anesthesia.

		Right Parietal region			Left Parietal region		
		CMRG (μmol/100min/g)			CMRG (μmol/100min/g)		
		Consious	Unconscious	% Suppression	Consious	Unconscious	% Suppression
Rat 1	week 1	97.7	34.9	64%	100.6	34.3	66%
	week 2	104.6	45.4	57%	108.5	49.9	54%
	week 3	85.3	39.5	54%	84.6	39.4	53%
Rat 2	week 1	92.2	35.3	62%	92.1	33.7	63%
	week 2	114.5	32.4	72%	115.5	31.7	73%
	week 3	103.2	29.7	71%	105.2	29.8	72%

Conclusions: For the first time, CMRG of a rat were monitored over time using indwelling catheters and FDG PET imaging. Our studies suggest that similar PET studies can be performed in rats routinely using other radiotracers where plasma separation and metabolites correction are required for input function derivation.

OB003

Quantitation of ^{99m}Tc-Trodate-1 (TRODAT) with LEHR Collimation and Quantitative SPECT Reconstruction: A Comparative Phantom Study with Fan-beam Collimation

Chih-Hsing Wan[1], Wen-Wen Cheng[1], Ing-Jou Chen[2], Chih-Yuan Lin[2], Wen-Sheng Huang[3], Ming-Che Wu[1], Bailing Hsu[2,4]

[1]Department of Nuclear Medicine, Mackay Memorial Hospital Tamshui Branch, Taipei, Taiwan;
[2]Department of Medical Physics Research, Bailing Cloud Biomedical Technologies Innovation, Taipei, Taiwan;
[3]Department of Nuclear Medicine, Changhua Christian Hospital, Changhua, Taiwan;
[4]Nuclear Science and Engineering Institute, University of Missouri-Columbia, Missouri, USA.

Introduction: In Taiwan, fan-beam (FB) collimation for TRODAT SPECT has been validated in the historical development pathway. Although LEHR collimation becomes widely utilized, in fact, it can be more challenging to correctly quantify functional parameters due to factors of high physical interference, low count statistics and small striatal object size.

Methods: A standard striatal phantom (RSD Inc, USA) was filled with various levels of ^{99m}Tc activity concentration in caudate (C), putamen and (P) occipital (O) areas (P&C = 2.0-8.0 uCi/ml; O = 2.0 uCi/ml) to create specific binding ratio (SBR) and caudate-to-putamen ratio (CPR) in the range of 1.0-4.0. FB TRODAT SPECT was performed on a GE Infinia SPECT scanner with vendor recommended parameters. LEHR TRODAT SPECT was acquired with 256 × 256 matrix, dual-energy windows (125-154, 109-125 keV), 2.21 mm pixel size, 120 angels within 360° arc and 30 sec/angel, and separated CT scans on Toshiba Aquilion-640 CT scanner for attenuation correction and striatum localization. LEHR TRODAT SPECT images were reconstructed with FBP and full physical corrections (QSRS). Values of SBR and CPR were calculated with precise striatal ROI defined by fused SPECT-CT images and compared with true values. The impact of incorrect striatal localization was verified by systematically shifting SPECT images with 1-4 pixels (2.21-8.84 mm).

Results: Count statistics in LEHR SPECT was significantly lower than that of FB SPECT (0.19, p = 0.0056). Linear correlations for SBR and CPR with true values were overall excellent (Table 1). Compared with FB, LEHR-QSRS significantly enhanced SBR measurement (p = 0.004) with comparable CPR (p = 0.089). ROI misallocation in only 1 pixel off (4.42 mm) resulted in 8.6% error in SBR and 13.8% error in CPR calculations, and further increased to 44.5% and 84.1% for 4 pixels off (8.84 mm).

	Linear Regression (y = ax + b)	
	SBR	CPR
FB	a = 0.53, b = –0.28, R^2 = 0.92	a = 0.32, b = 0.72 , R^2 = 0.83
LEHR-FBP	a = 0.40, b = –2.02 , R^2 = 0.97	a = 0.30, b = 0.63 , R^2 = 0.97
LEHR-QSRS	a = 0.54, b = 0.95, R^2 = 0.96	a = 0.48, b = 0.44, R^2 = 0.98

Conclusions: In ^{99m}Tc-TRODAT-1 SPECT, precise striatal localization is extremely important in quantifying functional parameters. LEHR collimation with full physical corrections can outperform FB collimation to measure specific binding ratio even with considerably inferior imaging condition.

OB004

阿茲海默症早期診斷藥物 F-18-HDACi-INERi1577 之初步研發成果

李銘忻[1] 薛晴彥[2] 朱漢祥[1] 張瀚之[1]

[1] 行政院原子能委員會核能研究所
[2] 台大正子中心

前言：

茲海默症 (AD) 是老年癡呆症中最常見的形式之一，過往的研究指出，澱粉蛋白級聯假說 (Amyloid cascade hypothesis) 中描述因 Aβ 的堆積導致致病，如認知缺陷、記憶障礙、神經元缺失等，而目前越來越多證據顯示 HDAC 蛋白有可能參與此過程：HDAC 蛋白質可以調控組蛋白 (Histone) 被乙攜化 (Acetylation) 的量，進而改變某些參與了 AD 症中有關於認知、記憶等重要基因的表達。HDAC 抑制劑 (HDACi) 在動物模組中可能能夠改善認知功能障礙與記憶障礙，其能夠逆轉 Aβ 所誘發的神經毒性可能在於：(1) HDAC 抑制劑抑制了 tau 蛋白質因 Aβ 所誘發的過度磷酸化；(2) HDAC 抑制劑可能調控了有關記憶與學習的重要基因表達，因此有越來越多單位積極投入 HDACi 的相關研究。

方法：

本研究之實驗流程如圖一所示：以 Seo (2014) 文獻中一種 HDAC 抑制劑 HDACi-INER-1557 做爲結構模型，修飾結構上的取代基，產生一系列以 benzamide 爲骨架的類似物，其結構如圖二所示；經 HPLC 分離純化後進行 in vitro 細胞抑制實驗，篩選出最具抑制效果的化合物後，在其結構上特定位置標誌上放射性核種 F-18，進行大鼠 in vivo 實驗，並觀察化合物是否有穿過大鼠之 BBB，最終進行動物模組的實驗，以觀察藥物是否能藉由抑制 HDAC 蛋白質，進而對 AD 症產生療效。

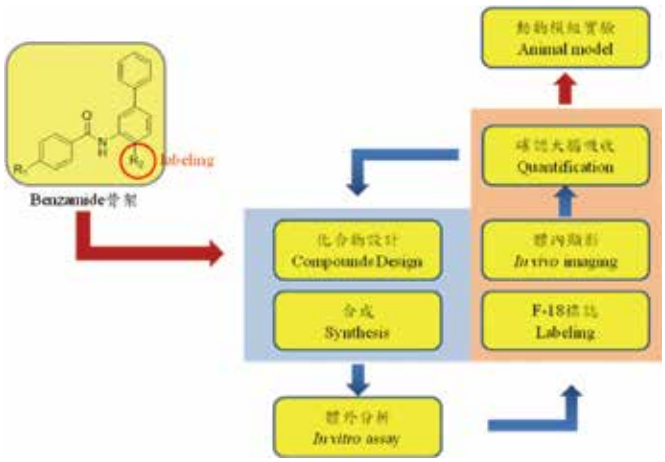

圖一、實驗總體流程

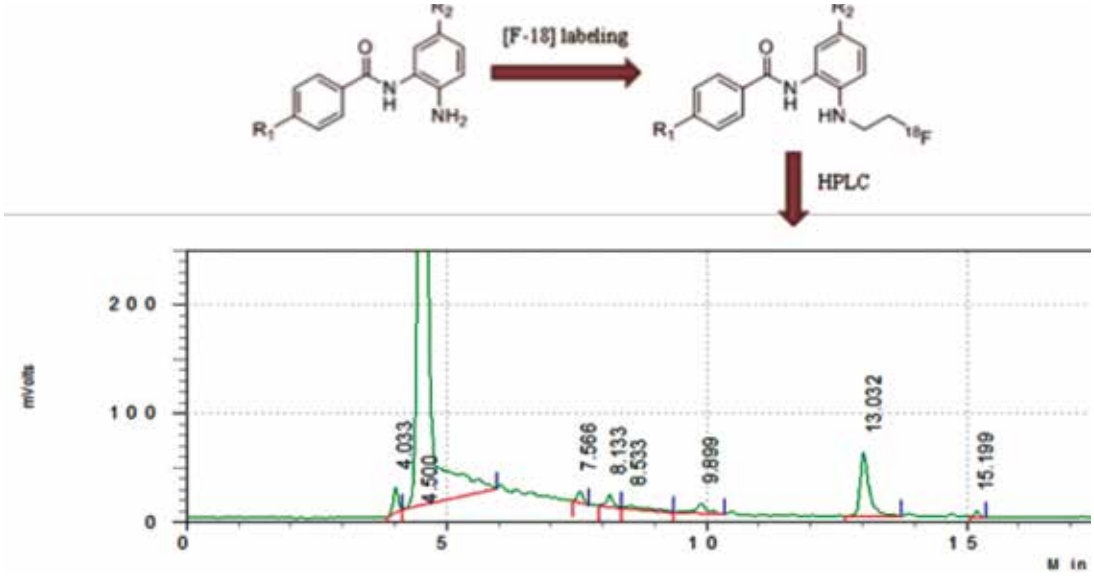

圖二、HDACi-INER-1577 之結構與標誌完 [F-18] 後進行 HPLC 分離之圖譜

結果：

1. in vitro 細胞抑制實驗中，我們以不同來源之乳癌細胞株 4T1 與 MCF 進行實驗，結果如圖三與表一所示，HDACi-INER-1577 對於這四種細胞株所誘發的 HDAC 皆有抑制效果，其中又以 069MCF 細胞株的效果最佳 (～ 70%)。

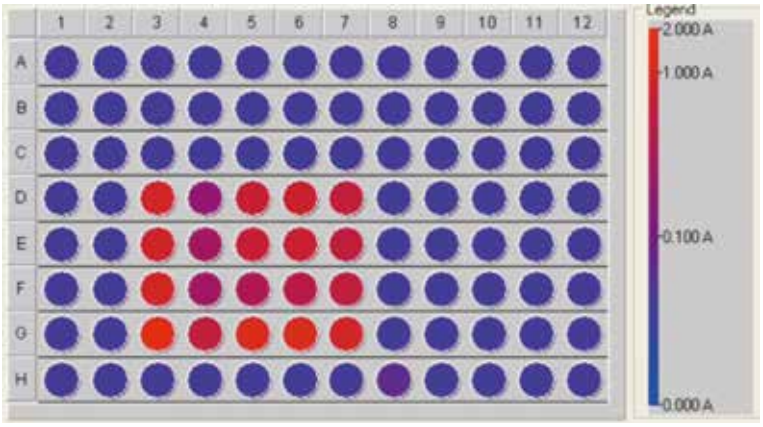

圖三、細胞抑制實驗之圖示

表一、細胞抑制實驗之結果

	正調控	負調控	s1	s2	s3	S 平均值	標準差	抑制率
052 MCF	0.914	0.197	0.705	0.812	0.618	0.711667	0.097172	28.3%
052 4T1	0.849	0.291	0.701	0.715	0.582	0.666	0.073082	32.8%
069 MCF	0.951	0.276	0.395	0.475	0.588	0.486	0.096969	68.9%
069 4T1	1.423	0.592	1.21	1.141	0.945	1.098667	0.137478	39.1%

2. 根據 in vivo 大鼠的腦部顯影結果，可以得知 [F-18] HDACi-INER-1577 穿過 BBB，在腦內形成放射性影像，其吸收百分比大於 1%，如圖四所示。

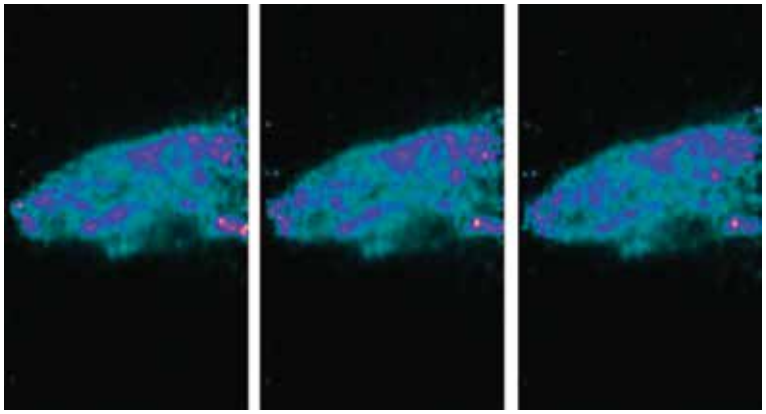

圖四、大鼠腦內的藥物放射影像，可以得知藥物能夠穿透血腦障壁

結論：

透過 in vivo 大鼠體內實驗，[F-18] HDAC-INER-1577 穿過血腦障壁的結果是顯而易見的，因此之後要進行腦中藥物的 nano-PET/CT 或 micro-PET/MRI 定量分析，以測量藥物在腦中的吸收程度；最後進行動物模組實驗：將患有 AD 症的大鼠注入藥物，以觀察藥物是能對 AD 症具有療效；除此之外，我們也同時在發展其他候選藥物。

OB005

A Study of Liposomal Doxorubicin in Combination of Liposomal Vinorelbine for Treating Colon Carcinoma in a Mouse Model

Chun-Yi Wu[1], Jo-Hsin Tang[2], Sheng-Husn Wang[1], Ming-Hsien Lin[3], Hsin-Ell Wang[2]

[1]Department of Biomedical Imaging and Radiological Science, China Medical University, Taichung,Taiwan ;
[2]Department of Biomedical Imaging and Radiological Sciences, National Yang-Ming University, Taipei, Taiwan;
[3]Taipei City Hospital Zhongxiao Branch, Taipei, Taiwan.

Objective: Colorectal cancer is the most common type of gastrointestinal cancer. The incidence of colorectal cancer ranked second in Taiwan, and is the third leading cause of cancer death including men and women. Surgical resection is the standard treatment for localized colorectal cancer. However, over 40% cases are diagnosed metastasized and apparently inoperable. Systemic chemotherapy provides an alternative to these patients. Liposomal doxorubicin and vinorelbine own longer biological half-life and circulation time than their parent drug and have been used against a variety of cancers. This study aims to evaluate the therapeutic efficacy of liposomal doxorubicin (lipoDox) and liposomal vinorelbine (lipoVNB) combined treatment in a CT-26 colon carcinoma-bearing mouse model.

Materials and methods: The *in vitro* cytotoxicity of doxorubicin and vinorelbine on CT-26 cancer cells was determined by MTT and colony formation assay. The morphological change in different dosing regimen-treated cells was assessed by fluorescent microscopy. The pharmacokinetics, including microSPECT/CT and biodistribution studies, was investigated by using radioactive ^{111}In-labeled lipoDox and lipoVNB. Male BALB/c mice were inoculated with CT-26 cells in the right flank. When tumor size reached 200 ± 50 mm^3, mice were treated following different protocols. Tumor burden, body weight and survival were recorded. Immunohistochemical staining and ^{18}F-FLT microPET scanning were performed coordinately to survey the therapeutic efficacy.

Results: Based on the results of pharmacokinetic study, co-administration of lipoDox and lipoVNB did not affect their individual systemic distribution *in vivo*, while lipoDox retained longer in blood than lipoVNB did. Maximal tolerated dose (MTD) was determined for finding the optimal therapeutic dose regimen. The dosage without apparent toxicity was then used in the therapeutic efficacy studies. Superior tumor growth retardation was observed in the group receiving lipoDox/lipoVNB administration (both 1 mg/kg each, namely D1V1) than those injected with lipoDox/VNB (both 1 mg/kg each, namely D1fV1). No severe side effects were detected in each group. In terms of tumor volume, a significant difference between the treatment of D1V1 and control ($p < 0.05$) was observed on day 4. The tumor-to-muscle ratio (T/M) derived from ^{18}F-FLT microPET images of D1V1-, D1fV1-treated mice and the control on day 7 was 6.88 ± 0.54, 7.5 ± 0.84, and 9.87 ± 0.73, respectively, indicated that D1V1 is a more efficacious regimen in cancer treatment. The result of PCNA immunohistochemical staining was consistent to the findings of ^{18}F-FLT microPET images.

Conclusion: This study demonstrated that the combination of lipoDox/lipoVNB was more efficacious than lipoDox/VNB for treating colon carcinoma, and ^{18}F-FLT PET is a promising approach in predicting the treatment outcome.

OB006

GMP-compliant Automatic Production of [^{18}F]T807 and its Comparative Biodistribution in Mice and Monkeys

Ya-Yao Huang[1], Chia-Ling Tsai[1], Hao-Yu Hsieh[2], Ta-Kai Chou[3], Ling-Wei Hsin[2,4], Kai-Yuan Tzen[1,4], Ruoh-Fang Yen[1,4], Chyng-Yann Shiue[1,3-4]

[1]*PET Center, Department of Nuclear Medicine, National Taiwan University Hospital, Taipei, Taiwan;*
[2]*School of Pharmacy, College of Medicine, National Taiwan University, Taipei, Taiwan;*
[3]*PET Center, Department of Nuclear Medicine, Tri-Service General Hospital, Taipei, Taiwan;*
[4]*Molecular Imaging Center, National Taiwan University, Taipei, Taiwan.*

Introduction: [^{18}F]T807 has been proved to be a promising PHF-tau tracer for studying AD in humans. However, the reported methods for [^{18}F]T807 production were somewhat complicated. In this study, we presented the improved production and quality control tests of [^{18}F]T807 in conditions that meet good manufacturing practice (GMP) requirements for clinic study. Additionally, for the optimal strategy of molecular PET imaging for pre-clinic and clinic study in the future, we also presented the whole-body biodistribution of [^{18}F]T807 in the mice and monkey.

Method: The [^{18}F]T807 was synthesized in a FxFN module as reported previously with some modifications [3]. Briefly, fluorination of N-t-Boc protected precursor (1) with K[^{18}F]/K2.2.2 in DMSO was carried out to gave the intermediate (2). A solution of HCl was added to (2) and the mixture was heated for deprotection. Following neutralizion with NaOAc and buffer, the crude product was purified with a semi-preparative HPLC to give [^{18}F]T807 (Scheme 1). For animal study, male ICR mice (n = 4) and male Formosa rock monkeys (n = 2) were injected with a bolus of about 0.2 and 2.6 mCi of [^{18}F]T807, respectively. VOIs were defined on co-registrated PET/CT images according to evident tracer accumulation in the area of the liver and data was expressed as standard uptake value (SUV).

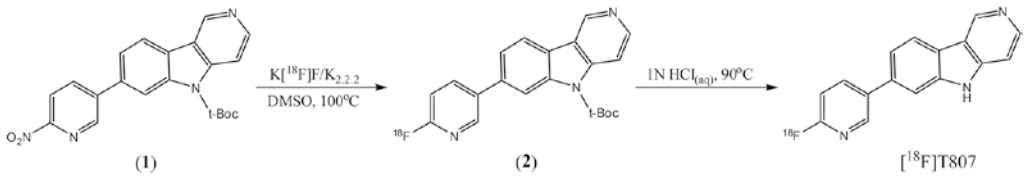

Scheme 1. Synthesis of [18F]T807

Results: The radiochemical yield of [^{18}F]T807 synthesized by our method was 13 ± 4% (EOS, n = 15) in a synthesis time of ~ 70 min from EOB. Both the chemical and radiochemical purity were > 95% with a specific activity of 151 ± 52 GBq/μmol. PET imaging in mice showed that the uptake of [^{18}F]T807 in GB and LLI were high and increased with time. PET imaging in monkeys showed that the initial uptake of [^{18}F]T807 in lung, liver and kidneys were high but decreased with time. In contrast to mice, the uptake of [^{18}F]T807 in monkeys only GB was high and increased with time.

Conclusions: In this study, [^{18}F]T807 could be reliably produced for preclinical and clinical studies with the USP quality and certified as GMP. Additionally, the whole-body biodistribution of [^{18}F]T807 in mice and monkeys reveal similarities and differences.

Acknowledgement: We are grateful to Mr. Pei-Yao Lin and Mr. Chi-Han Wu of Molecular Imaging Center of National Taiwan University for their technical assistances.

OB007

A Two-centre Study for the Quality Control of [^{18}F]FDG using FASTlab Phosphate Cassette

Ya-Yao Huang[1], Stephen Taylor[2], Koziorowski Jacek[3], Yu-Ning Chang[4], Wei-Hua Kao[1], Chyng-Yann Shiue[1,4,5], Kai-Yuan Tzen[1,4], Ruoh-Fang Yen[1,4]

[1]PET Center, Department of Nuclear Medicine, National Taiwan University Hospital, Taipei, Taiwan;
[2]Department of Nuclear Medicine, Royal Brisbane and Women's Hospital, Herston QLD, Australia;
[3]Universitetssjukhuset, Linköping, Sweden;
[4]Molecular Imaging Center, National Taiwan University, Taipei, Taiwan;
[5]PET Center, Department of Nuclear Medicine, Tri-Service General Hospital, Taipei, Taiwan.

Introduction: FASTlab has been used for routin [^{18}F]FDG production using phosphate cassette. However, the intermittent appearance of a white precipitate in the product vial post synthesis prompted us to re-examine the quality of [^{18}F]FDG products that included the analysis of Al^{3+} in final products.

Method: [^{18}F]FDG was synthesized using the FASTlab with phosphate cassette at both RBWH of Australia and NTUH of Taiwan. At RBWH, the appearance of 12 batches of [^{18}F]FDG were visually observed at different time points and tested the impact of alumina cartridge for such precipitation. At NTUH, several batches of [^{18}F]FDG products were performed complete QC procedures 24 hrs post synthesis except for the analyses related to radioactivity. The concentration of Al^{3+} in [^{18}F]FDG products were analyzed using ICP-MS at RBWH and with ICP-OES as well as using three semi-quantitative methods at NTUH, respectively.

Results: At RBWH and NTUH, the precipitates appeared in [^{18}F]FDG products after 4 and 24 hrs post synthesis, respectively. Rinsing the alumina cartridge prior to radiosynthesis could not prevent the precipitation to occur and the precipitation probability was varied with different batches of FASTlab cassette or different sterile vials (38-100%). Some batches of FASTlab [^{18}F]FDG products were found to contain 10-15 ppm of Al^{3+} from ICP-MS or ICP-OES analyses.

Conclusion: All pharmacopoeias demand that the final product solution should be clear and particulate-free within the given shelf-life/expiration time, which may extend to 16 hours. In order to avoid the potential QC problems, the FASTlab citrate buffer cassettes may be a option for [^{18}F]FDG.

Acknowledgement: We are grateful to Mr. Wei-Ting Chen of Agilent Technologies for the technical assistance in ICP-OES analysis.

OB008

Five Years Production Experience of [^{18}F]FDOPA with a TracerLab Fx$_{FE}$ Module

Ching-Hung Chiu[1], Ya-Yao Huang[1], Kai-Yuan Tzen[1,2], Chyng-Yann Shiue[1,2], Ruoh-Fang Yen[1,2]

[1]PET Center, Department of Nuclear Medicine, National Taiwan University Hospital;
[2]Molecular Imaging Center, National Taiwan University, Taipei, Taiwan.

Introduction: [^{18}F]FDOPA (1) is a useful imaging agent for studying dopamine synthesis and has been synthesized either by nucleophilic or electrophilic fluorination of the appropriate precursors. For the last five years, we have synthesized (1) through electrophilic fluorination route using a TracerLab Fx$_{FE}$ module (Fig. 1). We reported herein our experience on the production of this imaging agent.

Method: The carrier-added [^{18}F]fluorine was produced from the ^{20}Ne(d,α)^{18}F reaction in a neon (99.999%) target containing 1% carrier fluorine (99.9%). The target gas was bombarded with deuteron beam (8.4 MeV, 40 μA) for 120 min. and the resulting [^{18}F]F$_2$ (8 ± 2 GBq) was delivered into a reaction vessel (TRACERlab FX$_{FE}$, GE Healthcare, Milwaukee, WI) containing 60 mg of precursor in 10 mL of Freon-11 (99.9%) at –20°C. The reaction mixture was kept at 310°C for 4 min and the solvent was evaporated. HBr (48%, 2mL) was added, heated at 130°C for 10 min and then cooled to 40°C. The resulting mixture was neutralized with NH_4OH (37%, 1.4 mL) and loaded onto a semi-preparative HPLC column for purification. The peak containing [^{18}F]FDOPA was collected, sodium ascorbate (30 mg in 0.2 mL of H2O) was added and the solution was subsequently filtered through a 0.22 sterile filter into an injection vial (Scheme 1). The QC tests of [^{18}F]FDOPA were performed based on USP monograph and the residual [^{18}F]Fluoride level was measured by radio-TLC method.

Results: In our five years (from 6/1/2010 to 6/1/2015) production experience, [^{18}F]FDOPA was reliably produced with a radiochemical yield of 22 ± 5% (EOS, based on trapped [^{18}F]F$_2$ in reaction vessel) in a synthesis time of 46 ± 8 min from EOB. The quality of [^{18}F]FDOPA was found to be suitable for clinical applications. During these five years, we have 341 productions with 8 failed and 7 low RCY (< 5% syntheses. Additionally, residual [^{18}F]Fluoride in [^{18}F]FDOPA injection ranged from 0.0% to 21.6%. However, by monitoring residual ^{18}F-Fluoride levels and keeping stringent restraint procedures after 7/30/2011, low ^{18}F-Fluoride content was achieved in most batches of [^{18}F]FDOPA production.

Conclusion: [^{18}F]FDOPA can be reliably produced through electrophilic fluorination route using a TracerLab Fx$_{FE}$ moduler with a radiochemical yield of 22 ± 5% (EOS, n = 341) in a synthesis time of 46 ± 8 min from EOB. For optimal patient imaging, residual [^{18}F]Fluoride in [^{18}F]FDOPA product was routinely monitored and can be kept below 4%.

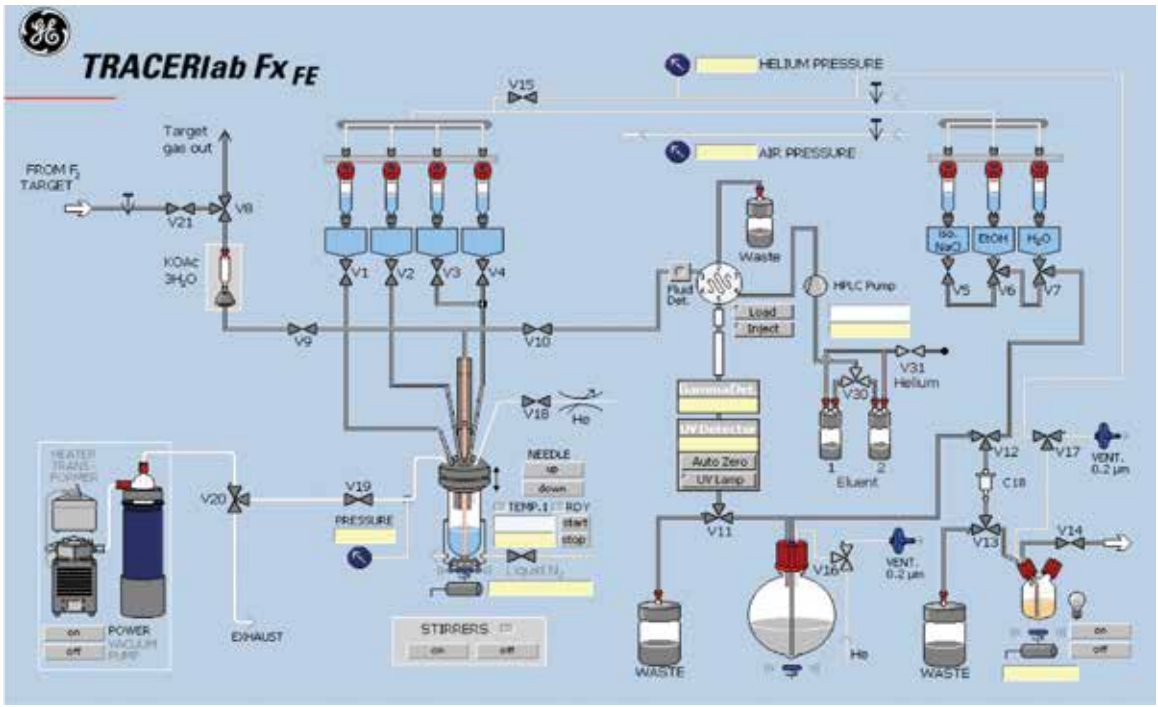

Fig. 1 Commercial module Tracer Lab™ FxFE for the automated radiosynthesis of [^{18}F]FDOPA in NTUH.

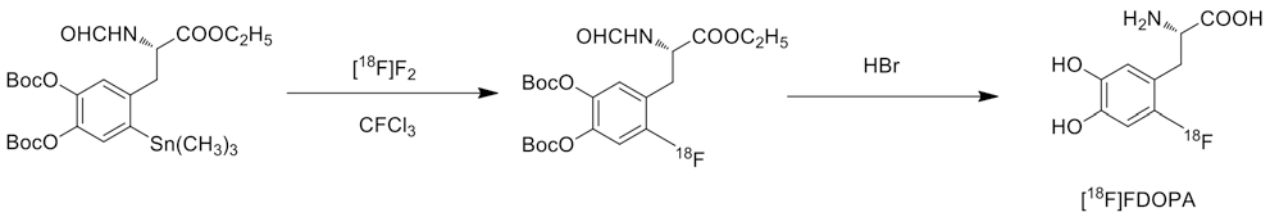

Scheme. 1 Radiosynthesis scheme of [^{18}F]FDOPA.

OC001

Predictive Value of Vascular Invasion by ^{18}F-FDG PET/CT in Hepatocellular Carcinoma

Chiung-Wei Liao[1,2], Lu-Yen Chu[1,2], Te-Chun Hsieh[1,3], Kuo-Yang Yen[1,3], Long-Bin Jeng[4,5], Chia-Hung Kao[1,5]

[1]Department of Nuclear Medicine and PET Center, China Medical University Hospital, Taichung City, Taiwan; [2]China Medical University, Taichung City, Taiwan; [3]Department of Biomedical Imaging and Radiological Science, China Medical University, Taichung City, Taiwan; [4]Department of Surgery, Organ Transplantation Center, China Medical University Hospital, Taichung, Taiwan; [5]Graduate Institute of Clinical Medical Science and School of Medicine, College of Medicine, China Medical University, Taichung, Taiwan.

Introduction: ^{18}F-FDG PET/CT has been widely used in oncology; however, its usefulness in hepatocellular carcinoma (HCC) is limited due to low sensitivity. We perform a retrospective study to determine the value of pre-transplantation ^{18}F-FDG PET/CT to predict vascular invasion in patients with HCC.

Methods: This retrospective study enrolled 65 candidates (54 males and 11 females; mean age = 56.25 years, ranging from 30 to 74 years) of liver transplantations for HCCs. All candidates underwent ^{18}F-FDG PET/CT before operations. Volumes of interest (VOIs) were drawn for the tumors and normal liver tissues, and standardized uptake value (SUV) in each VOI was measured. We calculated the SUV_{max} of tumor, the ratio of tumor SUV_{max} to normal-liver SUV_{max} (T_{SUVmax}/L_{SUVmax}), and the ratio of tumor SUV_{max} to normal-liver SUV_{mean} ($T_{SUVmax}/L_{SUVmean}$). The predictive value among metabolic parameters and conventional prognostic factors was analyzed.

Results: Vascular invasions were pathologically proven in 15 (23.08%) of 65 patients. Comparison analysis showed more advanced T stage ($p = 0.003$), higher serum AFP ($p = 0.000$), greater tumor number ($p = 0.017$), larger tumor size ($p = 0.001$), higher SUV_{max} ($p = 0.008$), greater T_{SUVmax}/L_{SUVmax} ($p = 0.002$), and greater $T_{SUVmax}/L_{SUVmean}$ ($p = 0.006$) in the vascular invasion group. In the multivariate regression analysis, serum AFP ($p = 0.004$) and tumor size ($p = 0.011$) were determined to be significant. Of three metabolic parameters, only the $T_{SUVmax}/L_{SUVmean}$ revealed a modest predictive value ($p = 0.051$), and showed accredited discrimination (0.736 of area under curve) with a cutoff of 1.65.

Conclusions: In this study, high pre-operative $T_{SUVmax}/L_{SUVmean}$ demonstrated a trend towards vascular invasion found during transplantation in a patient with HCC.

OC002

Radiation Safety of Cotton Ball Covered on the Injection Site of Sentinel Lymph Node Imaging

Shu-Fen Chen, Dung-Ling Yu

Department of Nuclear Medicine, Mennonite Christian Hospital, Hualien, Taiwan.

Introduction: The injection site of breast sentinel lymph node (SLN) imaging is covered with a cotton ball (CB) to prevent leakage of tracer through the needle puncture site. This study is to evaluate if the CB covered on the injection site of SLN imaging will cause hazard of radiation safety.

Methods: There were 32 CBs collected from 16 patients with breast cancer for study. All of patients were injected subdermally with two injection sites at periareolar and peritumor areas with 0.5 mCi of Tc-99m Phytate. Gentle finger massage was performed at each injection site to promote uptake of the tracer into lymphatic flow. All of CBs were counted using ATOMLAB r-Counter (Biodex). The radioactivity more than 10 times the count of background (BG) was defined as contaminated CB.

Results: The average count of BG was 2048 cpm. All of CBs have radioactivity more than 10 times the count of BG. The minimal count of CB is 173390 cpm (84 times the count of BG), and the maximal count of CB is 532118 cpm (259 times the count of BG). The average count of CBs are 412576 cpm (201 times the count of BG).

Conclusions: Our study shows the radioactivity of CBs covered on the injection site is more than 10 times the count of BG. We suggest the CBs covered on the injection site of SLN imaging should be treated as a radioactivity-contaminated waste.

OC003

Evaluation of Lymphoma with Bone Marrow Involvement by ^{18}F-FDGPET/CT

Yu-Chieh Chang[1,2], Lu-Yen Chu[1,2], Te-Chun Hsieh[1,3], Kuo-Yang Yen[1,3], Chia-Hung Kao[1,4]

[1]Department of Nuclear Medicine and PET Center, China Medical University Hospital, Taichung City, Taiwan;
[2]China Medical University, Taichung City, Taiwan;
[3]Department of Biomedical Imaging and Radiological Science, China Medical University, Taichung City, Taiwan;
[4]Graduate Institute of Clinical Medical Science and School of Medicine, College of Medicine, China Medical University, Taichung, Taiwan.

Introduction: The aim of this study was to compare metabolic parameters with bone marrow biopsy (BMB) in the detection of bone marrow involvement (BMI) in patients with Hodgkin's lymphoma (HL) and diffuse large B-cell lymphoma (DLBCL).

Methods: This retrospective study enrolled 58 patients (32 males and 26 females; mean age = 53.2 ± 17.5 years) with aggressive type lymphomas (11 with HL and 47 with DLBCL). Every patient eligible underwent both FDG PET/CT and BMB. PET/CT-assessed bone marrow was characterized as uptake pattern (diffuse vs. unifocal vs. multifocal) and Deauville score. In patients without focal lesions, Deauville score of diffuse marrow uptake was recorded. The final diagnosis of bone marrow status was defined by BMB result or image-guided biopsy finding or clinical follow-up.

Results: Of total 58 patients, 9 (15.5%) had focal lesions (unifocal, 4; multifocal, 5) and 49 (84.5%) had diffuse marrow uptake; otherwise, 36 (62.1%) showed Deauville score 2, 11 (19.0%) showed score 3, 5 (8.6%) showed score 4, and 6 (10.3%) showed score 5 in marrows and focal lesions. BMIs were finally diagnosed in 12 (20.69%) patients. Statistical analysis revealed Deauville score being the most accurate tool to detect BMI (area under curve = 0.919, vs. 0.827 of uptake pattern and 0.667 of BMB). With a cutoff level of 4, Deauville score identified positive and negative BMIs with a sensitivity, specificity, positive predictive value, and negative predictive value of 75%, 96%, 82%, and 94%, respectively. The negative likelihood ratio of Deauville score for BMI was 0.261.

Conclusions: In patients with HL and DLBCL, Deauville score of bone marrow provides better diagnostic performance for bone marrow status. A high Deauville score indicates bone marrow involvement despite uptake pattern. Bone marrow biopsy is still necessary in the PET negative group due to the relatively weaker negative likelihood ratio.

OC004

Application of Puffed-Cheek F-18 FDG PET/CT on Oral Cancer Patients

Chih-Yung Chang[1,2,3], Bang-Hung Yang[1,3], Ko-Han Lin[1], Ren-Shyan Liu, MD[1,2,3], Shyh-Jen Wang[1], Cheng-Yi Cheng[2,4], Daniel Hueng-Yuan Shen[2,4], Wen-Sheng Huang[2,5]

[1]Dpartment of Nuclear Medicine, Taipei Veterans General Hospital and National Yang-Ming University, Taipei, Taiwan;
[2]School of Medicine, National Defense Medical Center, Taipei, Taiwan;
[3]Department of Biomedical Imaging and Radiological Sciences, National Yang-Ming University, Taipei, Taiwan;
[4]Department of Nuclear Medicine, Tri-Service General Hospital, Taipei, Taiwan;
[5]Department of Nuclear Medicine and Medical research, Changhua Christian Hospital, Changhua.

Introduction: The complexity of small oral cavity and intimate apposition of the oral cavity mucosal surfaces make computed tomography (CT) identification of obvious masses difficult. Puffed-cheek CT improves the evaluation of oral cavity lesions. We used the puffed-cheek maneuver with F-18 FDG PET/CT scans to determine the feasibility and accuracy in clinical practice and to identify any benefits.

Methods: Twenty-two patients with oral cancer were included. They were instructed to perform the puffed-cheek maneuver after a conventional F-18 FDG PET/CT scan. Two physicians reviewed the puffed-cheek and conventional F-18 FDG PET/CT images and achieved consensus about the cancer extent, location, and dental artifacts before classifying and grading the oral cancers. Dichotomous results of localized or extended cancer, and artifact grading scores from the puffed-cheek and conventional F-18 FDG PET/CT methods were compared using McNemar's test and the Wilcoxon signed-rank test. A p value < 0 .05 was considered significant.

Results: The puffed-cheek maneuver with F-18 FDG PET/CT was practical and had incremental benefits. The conventional F-18 FDG PET/CT classified 12 patients correctly as having localized or extended cancer, and the puffed-cheek F-18 FDG PET/CT classified 21 patients correctly. Puffed-cheek F-18 FDG PET/CT found a synchronous skip cancer and provided detailed cancer delineation. This method might reduce the effects of dental artifacts without undesirable muscular FDG uptake.

Conclusions: Puffed-cheek PET/CT is feasible in the current clinical setting and can improve the delineation of oral cancer extent and location, with a potential benefit of reducing dental artifacts.

OC005

Clinical Impact of F-18 FDG PET/CT Imaging in Patients with Cancer of Unknown Primary Site

Yung-Yueh Su[1], Chia-Hsun Hsieh[2], Chun-Ta Liao[3], Chien-Yu Lin[4], Chung-Jan Kang[3], Tzu-Chen Yen[1,5]

Departments of [1]Nuclear Medicine, [2]Medical Oncology, [3]Head and Neck Surgical Oncology, [4]Radiation Oncology, [5]Molecular Imaging Center, Chang Gung Memorial Hospital at Linkou, Taoyuan, Taiwan.

Purpose: We sought to investigate the clinical utility of FDG PET/CT for the detection of primary tumors and/or distant metastases (DM) in patients with cancer of unknown primary site (CUPs). We also determined the priority of definitive treatment in CUPs patients who had negative FDG PET/CT results.

Materials and Methods: Between September 2006 and June 2014, a total of 62 CUPs patients were retrospectively identified. All of the study participants underwent FDG PET/CT imaging aimed at identifying the occult primary tumor and/or DM. Clinicopathological risk factors and PET parameters were analyzed in relation to 5-year overall survival (OS) rates using the Kaplan-Meier method and Cox regression analyses.

Results: Of the 62 patients, 16 (25.8%) had their primary tumors detected by FDG PET/CT. In six of them, FDG PET/CT identified both the primary malignancy and the presence of DM. An additional twelve patients had their DM diagnosed by FDG PET/CT. Among the 27 patients in whom FDG PET/CT failed to identify both the primary tumor and DM, the maximum standardized uptake value (SUV_{max}) of cervical nodes was the only significant predictor of 5-year OS ($p = 0.036$, 95% confidence interval [CI] = 0.014–0.871). Specifically, patients with a cervical node $SUV_{max} \geq 13.8$ showed a significantly lower 5-year OS than those with $SUV_{max} < 13.8$ (13.3% versus 66.4%, respectively; hazard ratio = 7.619, 95% CI = 2.192–26.485, $p < 0.001$). Approximately one third of the study participants had their treatment modified by FDG PET/CT findings.

Conclusion: FDG PET/CT is clinically useful for predicting OS and modifying treatment approaches in CUPs patients.

OC006

Clinical Usefulness of ^{18}F-FDG PET/CT for the Detection of Infections of Unknown Origin in Patients Undergoing Maintenance Hemodialysis

Jing-Ren Tseng[1], Chieh-Wei Lin[1], Shih-Hsin Chen[1], Tzung-Hai Yen[2], Pei-Ying Lin[3], Ming-Hsun Lee[4], Tzu-Chen Yen[1]

[1]*Nuclear Medicine and Molecular Imaging Center, Chang Gung Memorial Hospital at Linkou, Taoyuan, Taiwan;*
[2]*Department of Nephrology, Chang Gung Memorial Hospital at Linkou, Taoyuan, Taiwan;*
[3]*Center for Traditional Chinese Medicine, Chang Gung Memorial Hospital at Linkou, Taoyuan, Taiwan;*
[4]*Division of Infectious Diseases, Department of Internal Medicine, Chang Gung Memorial Hospital at Linkou, Taoyuan, Taiwan.*

Introduction: Patients with end-stage renal disease undergoing maintenance hemodialysis (MHD) are highly prone to infections. The potential clinical usefulness of ^{18}F-FDG PET/CT for the detection of infections of unknown origin in this patient population remains unclear. This study was designed to investigate this issue.

Methods: Between October 2011 and July 2014, a total of 104 adult MHD patients with sepsis underwent ^{18}F-FDG PET/CT for the detection of unknown in- fection foci. Follow-up was continued until October 2014. Positive ^{18}F- FDG PET/CT findings and mortality served as the main outcome measures.

Results: Of the 104 study patients, 73 (70.2%) had positive ^{18}F-FDG PET/CT findings, and a total of 95 major infection foci were identified. Eighteen patients (24.6%) had at least 2 infection foci on ^{18}F-FDG PET/CT scans. Seven (53.8%) of the 13 patients with primary vascular access–related infections had concurrent metastatic foci. Twenty-eight patients (26.9%) had their treatments modified by ^{18}F- FDG PET/CT results. Multivariate logistic regression analysis demon- strated that low hemoglobin and high C-reactive protein levels at di- agnosis were the independent predictors of positive ^{18}F-FDG PET/CT results. Twenty-seven patients (26.0%) died during their hospital stay, and 24 of them had positive ^{18}F-FDG PET/CT findings (*P* 5 0.014). Positive ^{18}F-FDG PET/CT results were an independent predictor of mortality (hazard ratio, 3.896; 95% confidence interval, 1.039–14.613; *P* 5 0.044).

Conclusion: Our results suggest that ^{18}F-FDG PET/CT may be clinically useful for detecting occult infection foci in end-stage renal disease patients undergoing MHD. In this population, positive ^{18}F-FDG PET/CT findings may lead to a significant change in clinical management and independently predict mortality.

OC007

Prediction of Territorial Perfusion Defects on Myocardial Perfusion Imaging with Multi-detector Computed Tomography Angiography

Hsi-Huei Lu[1], Pei-Shan Wu[1], Yi-Shan Tsai[2]

[1]*Department of Nuclear Medicine;*
[2]*Department of Radiology, National Cheng Kung University Hospital, Tainan, Taiwan.*

Introduction: The role of radionuclide myocardial perfusion imaging (MPI) in the diagnosis, assessment of myocardial viability, and management of coronary artery disease (CAD) treatment is firmly established. Novel alternative imaging studies, such as multi-detector computed tomography angiography (CTA), have also been reported to successfully predict CAD events and stratify CAD risk. We evaluated the ability of CTA in predicting MPI abnormalities in a cohort of patients with clinically suspected or confirmed CAD.

Methods: We retrospectively included 61 patients who underwent MPI and CTA within 3 months. We defined the territorial summed stress score (tSSS) for each major coronary artery territory by calculating the sum of semi-quantitatively scored index according to 17-segment model. Two CTA parameters of territorial ejection fraction (tEF) and territorial coronary artery calcium score (tCAC) of each major coronary artery were calculated. Receiver-operator curve (ROC) analysis was employed to obtain the optimal cut-off point of the CTA parameters to predict absence (tSSS < 4) or presence (tSSS $\geqq 4$) of perfusion defects in each coronary artery territory.

Results: There were 28 territorial perfusion defects in a total of 183 MPI coronary artery territories. We found a significant difference in tEF ($p < 0.001$) and tCAC ($p = 0.001$) between territories with and without perfusion defects. Using the cutoff- defined abnormality by ROC analysis, the sensitivity, specificity, and accuracy of tEF and tCAC to predict territorial perfusion defects were 89.3%, 72.9%, 75.4%, and 39.3%, 93.6%, 85.2%, respectively. Ten of 10 (100%) coronary artery territories with abnormal tEF and abnormal tCAC were presence of territorial perfusion defects, and 103 of 105 (98.1%) coronary artery territories with normal tEF and normal tCAC were absence of territorial perfusion defects.

Conclusion: Territorial ejection fraction predicts MPI territorial perfusion defects with a higher sensitivity, while territorial calcium score has a higher specificity. Both tEF and tCAC are abnormal strongly indicating territorial perfusion defects. Normal two CTA parameters are good for screening and provide support to avoid further exams in patients with clinically suspected CAD. MPI or cardiac catheterization is still warranted in the condition of only one CTA parameter is abnormal.

OC008

The Clinical Value of Radionuclide Shuntography in Hydrocephalic Patients with Suspected Ventriculo-peritoneal Shunt Malfunction

Szu-Ying Tsai[1], Shan-Ying Wang[1,2], Yen-Wen Wu[1,2,3,4]

[1]*Department of Nuclear Medicine, Far Eastern Memorial Hospital, New Taipei City, Taiwan;*
[2]*Department of Biomedical Imaging and Radiological Sciences, National Yang-Ming University, Taipei, Taiwan;*
[3]*National Yang-Ming University School of Medicine, Taipei, Taiwan;*
[4]*Department of Nuclear Medicine, National Taiwan University Hospital and National Taiwan University College of Medicine, Taipei, Taiwan.*

Introduction: Cerebrospinal fluid ventriculoperitoneal (V-P) shunts are often used in the treatment of hydrocephalus. Complications from shunts are not uncommon and can present with a variety of signs and symptoms, which could be evaluated by clinical examination and neuro-imaging. The radionuclide cerebrospinal fluid (CSF) shunt study provides a simple, effective, and low-radiation-dose method of assessing CSF shunt patency. When a discrepancy between neurological examination and imaging, additional radionuclide shuntography can be helpful. The purpose of our study was to analyze in the imaging findings and clinical interpretation of a variety of shuntography results and to determine the applicability of shuntography in patients with suspected shunt malfunction.

Methods and Results: In our department, 90 radionuclide shuntographic tests using (99m) technetium-pertechnetate (DTPA) was performed in 66 patients between August 2005 and September 2015. No complications or discomfort were noted in the examinations. The results of shuntography were evaluated visually and qualitatively, and correlated with clinical follow-up. Of them, 30 tests were interpreted as normal examination; and the other 60 tests were interpreted as abnormal, including complete distal obstruction (n = 24, 40%) partial distal obstruction (n = 33, 55%) or miscellaneous (n = 3, 5%). Clinical outcomes within 30 days were defined based on subsequent need for revision, re-implantation or adjustment of shunt pressure. The sensitivity (Se) and specificity (Sp) were 82.4% and 53.8%, respectively; positive predictive value (PPV), negative predictive value (NPV) and overall accuracy were 70%. In patients undergoing surgery (28 tests from 25 patients), highly concordant results were noted based on the imaging interpretations and surgical findings (Se = 100%, Sp = 91.7%, PPV = 100%, NPV = 66.7%, overall accuracy = 92.9%).

Conclusions: The radionuclide shuntography is a simple, useful and safe tool with low radiation in the evaluation of hydrocephalic patients suspected shunt malfunction not elucidated by conventional examinations. Besides, it is a reliable test procedure to guide further surgical intervention.

OC009

The Characterization and Prognostic Values of ^{18}F-fluorodeoxyglucose Positron Emission Tomography in Patients With Ischemic Cardiomyopathy

Wan-Ling Lin[1], Shan-Ying Wang[1,2], Yu-Chien Shiau[1], Yen-Wen Wu[1,3]

[1]Department of Nuclear Medicine, Far Eastern Memorial Hospital, New Taipei City, Taiwan;
[2]Department of Biomedical Imaging and Radiological Sciences, National Yang-Ming University, Taiwan;
[3]National Yang-Ming University School of Medicine, Taipei, Taiwan

Introduction: ^{18}F-fluorodeoxyglucose positron emission tomography (^{18}F-FDG PET) has been used to evaluate hibernating myocardium in patients with suspect myocardial scar detected by the myocardial perfusion imaging (MPI). The aim of the study is to evaluate the clinical usefulness of ^{18}F-FDG PET in patients with ischemic cardiomyopathy (ICMP).

Methods: A total of consecutive 63 patients with coronary artery disease (CAD), impaired left ventricular ejection fraction (LVEF ≤ 40%) and myocardial scar on ^{201}Tl MPI who underwent ^{18}F-FDG PET between March 2012 and September 2015 were reviewed. Only one patient was excluded for sequent analysis due to high blood sugar and poor image quality. The amounts of hibernating myocardium and scar were quantified in visual assessment. Regional values of perfusion-metabolism mismatch were analyzed quantitatively and qualitatively using a 17 segment model from 0-4 degree (4 = preserved perfusion/metabolism, to 0 = absent perfusion/preserved metabolism). Patients were divided into 3 groups representing "≥ 3 segments" (group 1), "1-2 segments" (group 2) and "none" (group 3) of mismatched myocardium. Clinical course according to the type of therapy (medical therapy with/out revascularization) provided after imaging and mismatched patterns were analyzed.

Results: Among 62 patients, 26 patients with significant amount perfusion-metabolic mismatched myocardium (group 1), 6 in group 2, and 29 patients without any mismatched myocardium (group 3) were noted. The severity scores were 9.73 ± 4.6, 3.83 ± 0.75 and 2.2 ± 1.97, respectively. In group 1, 15 (58%) received revascularization therapy. One patient expired in early post-operative stage and two patients died of non-cardiac related condition. Two of four patients (50%) showed improving LVEF > 5 % after one year follow up. On the other hand, 1 (17%) of group 2, and 12 (41%) of group 3 received revascularization therapy after the imaging. 3 patents followed after one year and showed deterioration of LVEF (> 5%). In patents who did not undergo revascularization procedures, 1 died of acute myocardial infarction and 2 died of non-cardiac related condition. In all patients groups, 7 patients were transferred to other hospitals and 13 patients lost follow-up.

Conclusion: In patients with ICMP, hibernating myocardium assessed using ^{201}Tl MPI and ^{18}F-FDG PET provides an improved approach for the identification of patients most likely to benefit from revascularization therapy, even with poor LVEF.

Table 1: Patient Characteristics

Parameter	Group 1 (n = 26)	Group 2 (n = 6)	Group 3 (n = 30)
Age (year)	62.6 ± 12.1	67.3 ± 14.4	57.6 ± 11.9
Male (%)	24 (92%)	4 (67%)	26 (87%)
Diabetes Mellitus	18 (69%)	2 (33%)	21 (70%)
Glucose level before FDG injection	131.0 ± 27.3	145.7 ± 62.8	140.6 ± 53.3
Visual assessment	Perfusion-metabolic mismatch ≥ 3 segments	Perfusion-metabolic mismatch in 1-2 segments	No perfusion-metabolic mismatch
17-segment severity score	9.73 ± 4.6	3.83 ± 0.75	2.2 ± 1.97
Revascularization	15 (58%)	1 (17%)	12 (40%)

OC010

Automatic Localization of Blood-pool Sampling to Warrant the Quality and Accuracy of SPECT Myocardial Blood Flow Quantitation

Ing-Jou Chen[1], Chih-Yuan Lin[1], Gunag-Uei Hung[2], Tau-Chen Wu[3], Bailing Hsu[1,4]

[1]*Department of Medical Physics Research, Bailing Cloud Biomedical Technologies Innovation, Taipei, Taiwan;*
[2]*Department of Nuclear Medicine, Changhua Schowchwan Memorial Hospital, Changhua, Taiwan;*
[3]*Section of Cardiology, Department of Internal Medicine, Taipei Veterans General Hospital, Taipei, Taiwan;*
[4]*Nuclear Science and Engineering Institute, University of Missouri-Columbia, Missouri, USA.*

Introduction: In myocardial blood flow (MBF) quantitation, proper arterial input function is essential to determine the quality of kinetic modeling and the accuracy of flow calculation. This study was aimed to investigate the performance of an automated blood-pool (BP) sampling approach to obtain consistent arterial input time-activity curve (TAC) for MBF quantitation.

Methods: Twenty-five consecutive subjects who received dynamic SPECT (DySPECT) scan on a dual-head SPECT/CT scanner (Siemens Symbia SPECT/CT) were included in this study. DySPECT data acquisition consisted of 10 × 10 + 5 × 20 + 4 × 60 + 1 × 280 sec (12 min) frames. DySPECT images were reconstructed with full physical corrections (QSRS). Myocardial (Myo) regions were fully sampled to create dynamic polar maps for Myo TAC. A dedicated manual (DM) approach was performed to preciously position the BP box (10 × 10 × 40 mm) between left ventricle and atrium for BP TAC by two well-trained operators. One-tissue-compartment flow model was utilized to calculate kinetic parameters for rest/stress flow (RMBF & SMBF) and reserve (MFR). An automatic approach (AT) by using ellipsoid-guided geometry information was then executed to generate new BP TAC and then triggered new flow calculation. The performance of AT was accessed by quality of kinetic modeling and the accuracy of flow values. Linear regression and Bland-Altman analyses were performed using DM as the reference standard.

Results: The quality of kinetic modeling indicated by R^2 was slightly higher in AT (0.82) than in DM (0.80) ($p = 0.009$). Correlations of flow parameters between the two approaches were excellent with a slope close to 1.0 (Table 1). Bland-Altman analysis revealed only small difference for RMBF ($\Delta = -0.082$ ml/min/g, 95% CI = –0.22-0.57), SMBF ($\Delta =$ –0.32 ml/min/g, 95% CI = –1.16-0.53) and MFR ($\Delta = 0.03$, 95% CI = –0.9-0.96) between AT and DM.

Linear regression (y = ax), All $p < 0.05$				
Rest K1 (ml/min/g)	RMBF (ml/min/g)	Stress K1 (ml/min/g)	SMBF (ml/min/g)	MFR (ml/min/g)
a = 0.85, R2 = 0.87	a = 0.89, R2 = 0.94	a = 0.86, R2 = 0.79	a = 0.89, R2 = 0.87	a = 0.99, R2 = 0.72

Conclusion: A geometry-guided automatic approach can perform consistently to provide proper arterial input function. With this approach, minimization in potential user variability to preserve the accuracy of SPECT myocardial blood flow quantitation can be warranted.

OC011

Alleviate the Impact of Extra-cardiac Uptake in SPECT Myocardial Blood Flow (MBF) Quantitation Using Priori Information and B-spline Curve Fitting Technique

Chih-Yuan Lin[1], Chi-Tai Ku[2], Ing-Jou Chen[1], Tau-Chen Wu[3], Yen-Kung Chen[2], Bailing Hsu[1,4]

[1]Department of Medical Physics Research, Bailing Cloud Biomedical Technologies Innovation, Taipei, Taiwan;
[2]Department of Nuclear Medicine, Shin Kong Wu-Ho Su Memorial Hospital, Taipei, Taiwan;
[3]Section of Cardiology, Department of Internal Medicine, Taipei Veterans General Hospital, Taipei, Taiwan;
[4]Nuclear Science and Engineering Institute, University of Missouri-Columbia, Missouri, USA.

Introduction: In SPECT MBF quantitation, it is challenging to properly determine myocardial boundary (MB) in inferior segments due to rapid liver uptake adjacent to myocardium (Myo). This study was aimed to alleviate the impact by improving boundary detection between inferior and liver regions.

Methods: Twenty patients who underwent 99mTc-sestamibi (MIBI) dynamic SPECT (DySPECT) scan on dual-head SPECT (Siemens ECAM) and showed high liver uptake adjacent to myocardium (Myo) were included in this study. DySPECT images were acquired with 10 × 10 + 5 × 20 + 4 × 60 + 1 × 280 sec (12 min) frames and reconstructed with full physical corrections (QSRS). Transformed into spherical coordinate, MB was determined by the max MIBI uptake points within wall segments to create polargram recording radius (r) as a function of sampling angles (θ, ϕ). Over extended MB to liver region was corrected by priori MB information and fitted with B-spline to join discrete MB. Flow was quantified from arterial input and dynamic polar map (PM) with and w/o MB corrections, and then compared with each other to assess the effectiveness of MB correction.

Results: With MB correction, r in inferior wall was reduced 51.1% ($p < 0.0001$) to relieve overestimation of MIBI uptake in 38.5% ($p < 0.0001$). Bland-Altman analysis revealed decreased rest flow (Δ =–0.14 ml/min/g, 95% CI =–0.99-0.7), increased stress flow (Δ = 0.2 ml/min/g, 95% CI = –0.25-0.29) and increased reserve (Δ = 1.7, 95% CI = –4.68.0) in right coronary artery territory (RCA) while flow values in regions of left anterior descending (LAD) and left circumflex (LCX) were unaffected.

Conclusion: In SPECT MBF quantitation, rapid high liver uptake can impact to degrade the accuracy of flow measurement in RCA territory. A proposed corrective method using priori information and B-spline fitting can effectively alleviate the impact while preserving the accuracy in other territories.

OC012

F-18 FDG PET/CT and Gallium-67 Inflammation Scan with SPECT/CT in Patients with Mycotic Aneurysm

Chien-Hsin Ting[1], Cheng-Pei Chang[1]

[1]*Department of Nuclear Medicine, Taipei Veterans General Hospital.*

Introduction: Mycotic aneurysms are localized, irreversible vascular dilatations caused by weakening and destruction of the vessel wall by an invasive organism establishing an infective arteritis. CT, MRI, and ultrasound have been used as a complementary imaging approach for the assessment of mycotic aneurysm. However, hematomas and seromas in the aneurysm appear anatomically similar to an abscess, thus making it sometimes difficult to distinguish between non-infected and infected aneurysm on these images. PET/CT and Gallium scan have the potential to further improve diagnosis and correct localization of disease processes, including infection and inflammation.

Materials and Methods: Patients with clinical and/or by image suspicious mycotic aneurysm were referred for PET/CT an Gallium inflammation scan with SPECT/CT before treatment. The PET/CT whole-body imaging was obtained from head to upper portion of thigh at 60 to 90 minutes after injection of 7.9 –11.0 mCi of FDG intravenously. After the PET/CT was done, all patients received 5 mCi of Gallium-67 citrate intravenously and the image was obtained 48 hours later.

Results: Our total population comprised of 12 patients (9 men and 3 women), with a mean age of 75.8 years (range: 62–93 years).

No.	Y/G	B/C	SUVmax	Ga	Location	WBC	CRP
1	71/M	-	5.71	+	TAA	10700	10.71
2	74/F	-	5.61	+	AAA	7200	6.46
3	77/M	Salmonella	10.35	+	TAA	11800	20.28
4	92/M	S.epidermidis	10.38	+	TAA	11700	10.07
5	77/F	-	6.2	-	TAA	7800	0.15
6	72/F	-	8.2	+	TAA	11700	11.69
7	67/M	-	3.5	+	AAA	3700	12.83
8	64/M	-	8.28	+	TAA	9200	12.72
9	93/M	-	-	-	I. iliac	4900	0.23
10	62/M	S. aureus	6.86	+	TAA	16400	10.17
11	84/M	-	7.14	+	AAA	6200	13.92
12	77/M	-	20.13	+	AAA	7000	9.34

Conclusions: In conclusion, this study involved a small number of patients, but it highlights the potential usefulness of FDG-PET/CT in the diagnosis of infected aortic aneurysms. In cases where CT imaging, physical findings, and inflammatory findings suggest the presence of an infected aortic aneurysm, FDG-PET/CT examination may be used to inform the operative strategy. Gallium-67 inflammation scan has low spatial resolution, however, in combination with SPECT/CT, it can also be a good tool for diagnosis of mycotic aneurysm.

OC013

The Role of F-18 FDG PET/CT in a Dilemma of Postoperative Colorectal Cancer Patients: High CEA Level with Negative Conventional Imaging Result

黃俊穎[1] 陳輝墉[2]

[1] 義大醫療財團法人義大醫院核子醫學科

ABSTRACT

Background: Serum carcinoembryonic antigen (CEA) level is commonly followed up in population with postoperative colorectal cancer to detect early recurrence. Although elevated CEA level is sensitive in response to recurrent disease, conventional imaging may show negative results at the time. We evaluate the value of F-18 FDG PET/CT in this commonly situation as an aid to clinical decision making.

Methods: From February 2005 to September 2014, sixty-eight consecutive patients were retrospectively identified from E-Da hospital who met the criteria: (1) postoperative colorectal cancer patients with elevated CEA level (> 5 ng/ml), (2) less than 6 weeks before PET/CT, it showed negative findings on CT, colonoscopy, ultrasound or MRI, (3) with histopathological results or a minimum of 12 months of clinical follow-up. Results of histopathology or a series of conventional imaging combined with clinical manifestations during follow-up after PET/CT provided conclusive evidence.

Results: The prevalence rates of recurrent disease were 50% (34/68) and 54.5% (37/68) when follow-up period set as 6 months and 12 months respectively. During 6 months follow-up, the sensitivity, specificity, positive predictive value (PPV) and negative predictive value (NPV) for recurrence were 88% (30/34, 95% CI 73-97), 88% (30/34, 95% CI 73-97), 0.88 and 0.88. During 12 months follow-up, the sensitivity, specificity, PPV and NPV for recurrence were 84% (31/37, 95% CI 68-94), 90% (28/31, 95% CI 74-98), 0.91 and 0.82. In subgroups of CEA level (CEA 5-7, 7-13 and >13 ng/ml), the sensitivity were 75%, 88% and 82%. During 12 months follow-up, liver was the most recurrent site (17/37, 46%). With positive PET/CT findings, 7 out of 37 relapsed patients (19%) received excision surgery and 3 out of 37 patients (8.1%) received radiofrequency ablation for curative intent.

Conclusion: F-18 FDG PET/CT provides superior sensitivity and specificity regarding elevated CEA level with negative findings of conventional imaging in postoperative colorectal cancer patients. In those, about 27% relapsed patients underwent PET/CT can gain the opportunity of curative treatment. Thus, F-18 FDG PET/CT should be used in this clinical situation.

MEMO

PB001

^{188}Re-labeled Antibodies for EGFR-targeted SPECT/CT Imaging in Human Lung Carcinoma Model

Cheng-Fu Chao, Po-Yen Liu, Cheng-Hui Chuang, Liang-Cheng Chen, Chih-Hsien Chang

Institute of Nuclear Energy Research, Taoyuan, Taiwan

Introduction:

^{188}Re is a high energy beta-emitting radioisotope which emits 2.2 MeV beta photons and 155 KeV gamma photons. Panitumumab (Pan) is a fully human monoclonal antibody specific to the epidermal growth factor receptor (EGFR). Panitumumab fragment antigen-binding domain (PanFab), which is composed of one constant and one variable domain of each of the heavy and the light chain of Pan that binds to EGFR. In this study, we investigate the in vivo NanoSPECT/CT imaging of radiolabeled ^{188}Re-Pan and ^{188}Re-PanFab in a NCI-H292 human lung carcinoma model. The anti-EGFR effect of ^{188}Re-Panab and ^{188}Re-PanabFab displays site-specific tumor image.

Methods:

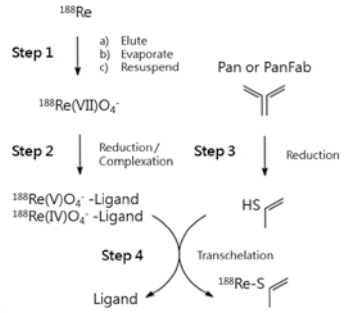

Figure 1. Radiolabeling process of ^{188}Re-Pan and ^{188}Re-PanFab. In step 2, the reducing agent is stannous chloride or stannous fluoride or stannous tartrate. In step 3, the reducing agents are tris (2-carboxyethyl) phosphine (TCEP), 2 mercaptoethanol (2-ME), dithiothreitol (DTT), stannous tartrate

Results:

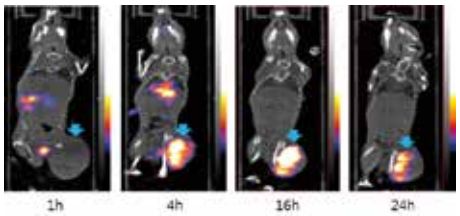

Figure 2. NanoSPECT/CT images of NCI-H292 solid tumor-bearing mice via intravenous (i.v.) injection of ^{188}Re-Pan (50 μCi/70 μL). The sections of images are shown for 1, 4, 16 and 24 h after i.v. injection. The NCI-H292 bearing mice were treated at average tumor (arrow) volume 850-900 mm^3.

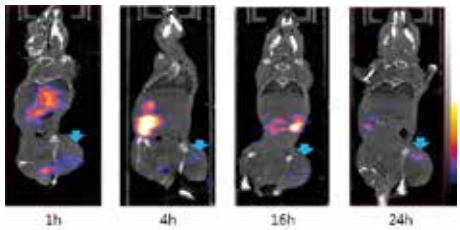

Figure 3. NanoSPECT/CT images of NCI-H292 solid tumor-bearing mice via intravenous (i.v.) injection of ^{188}Re-PanFab (50 μCi/70 μL). The sections of images are shown for 1, 4, 16 and 24 h after i.v. injection. The NCI-H292 bearing mice were treated at average tumor (arrow) volume 650-700 mm^3.

Conclusions:

The results of *in vivo* nuclear images studies reveal the potential advantages and benefits of ^{188}Re-Pan for site tumor imaging and therapeutics. According to nuclear images studies and the tumor/organ ratio of images comparing with ^{188}Re-Pan and ^{188}Re-PanFab, ^{188}Re-Pan has better site tumor imaging and therapeutics abilities than ^{188}Re-PanFab.

PB002

核子醫學部門之醫療廢棄物輻射防護管理－以中部某地區醫院爲例

林仁祥[1] 鍾承諺[2]

[1] 大千綜合醫院核子醫學科
[2] 大千綜合醫院放射科

背景介紹：

依我國行政院原子能委員會公佈之「一定活度或比活度以下放射性廢棄物外釋計畫導則」，醫療院所之核子醫學科應備有放射性固體廢棄物外釋處理程序。許多文獻指出應嚴謹管理具放射性之生醫廢棄物，確保因此對民眾與工作人員造成之輻射暴露不超過法規限值。

方法：

本科自 2015 年 2 月 12 日起始營運，住院病人接受核醫診療後，本科人員給予護理人員或看護人員一張「住院病人尿布與尿袋處理通知單」，提醒將病人產生之生醫廢棄物（尿布、汙衣、墊巾等）。爲提升接受核醫診療住院病人產生之生醫廢棄物回收儲放率及降低管理錯失，自 2015 年 8 月 1 日起，修改「住院病人尿布與尿袋處理通知單」，並黏貼於生物醫療廢棄物專用垃圾袋，每遇需使用尿布或尿袋住院病人，給予 3 個，並通知主責護理人員自核醫藥物注射後至出院所收集之生醫廢棄物皆需收集至核醫科專區儲放。

結果：

我們分別統計兩區間之廢棄物產量。2015 年 2 月 12 日至 7 月 31 日間產生 19 件生醫廢棄物，以接受核醫診療住院病人數爲變項進行校正（174 人），計算出住院人均產生廢棄物數爲 0.11。2015 年 8 月 1 日至 8 月 31 日共產生 7 件生醫廢棄物，平均每位接受核醫診療住院病人產生 0.21 件廢棄物。兩相比較，後者之人均產生生醫廢棄物比前者高 90%。

結論：

此介入措施對加強合醫科住院病人之生醫廢棄物收集具有效果。本研究護理人員本身不具輻射背景知識，此爲資訊不對等；再者提供黏有提醒通知之垃圾袋予病房護理人員即輻射防護之目的所設，屬合理。依不同檢查所注射藥物具有不一之生物半衰期，須提供幾個收集袋爲合理量須待進一步研究。

PB003

ReO-MN-16-acid 合成研究

盧桂林　蔡嘉東　張瑜　徐成芳

核能研究所化學組

背景介紹：

近年來由本所同位素組發展一種具有治療肝癌潛力之新藥「銖必妥」，^{188}ReO-MN-16-ET/Lipiodol。此藥物是以 H_3-MN-16-ET (4A) 爲配位子，與放射性 ^{188}Re 反應形成 ^{188}ReO-MN-16-ET，之後再將其溶於 Lipiodol 中，即可獲得兼具有診斷與治療雙功能特性之 ^{188}ReO-MN-16-ET/Lipiodol 核醫藥物。我們已掌握 ReO-MN-16-Et (6A) 之合成核心技術，並可供應所內做非放射性 ^{188}ReO-MN-16-Et 標準品之 HPLC 及動物放大劑量測試之用。由於在動物體內 ReO-MN-16-Et (6A) 有可能會水解成 ReO-MN-16-acid (7)，因此我們計畫要合成出 ReO-MN-16-acid (7) 以提供比對。

方法：

一方面將 PPh_3 和 NH_4ReO_4 反應生成 $ReO(PPh_3)_2Cl_3$ (1)，並以 $Br(CH2)_{15}COOH$ 酯化後生成新取代基 $Br(CH_2)_{15}COOEt$(2A) 及 $Br(CH2)_{15}COOBn$(2B)。另一方面以 CPh_3OH 將 2-mercaptoethyl hydrochloride 上保護後，可得 Tr-Cystramine (2)。化合物 2 與 chloroacetyl chloride 反應後得到 [Tr-Cystramine] N-chloroacetamide (3)。再將化合物 2 與化合物 3 偶合得到 N-[2-((Triphenylmethyl)thio)-ethyl] [2-((triphenylmethyl)thio)- ethylamino] acetamide (4)。將分別化合物 2A 及化合物 2B 與化合物 4 偶合後可生成 H_3-MN-16-ET (5A) 及 H_3-MN-16-ET (5B)。分別將化合物 5A 及 5B 去保護後與化合物 1 反應，可得化合物 ReO-MN-16-ET (6A) 及 ReO-MN-16-Bn (6B)。分別將化合物 6A 與 6B 和 iodotrimethylsilane 反應合成出 [N-(2-thioethyl)-3-aza-19-hydroxycarbonyl- 3-(2-thioethyl) octadecan amido]oxorhenium (ReO-MN-16-acid, 7)。

結果：

使用「三甲基碘矽烷」後確實可將 ReO-MN-16-Et(6A) 及 ReO-MN-16-Bn(6B) 去酯化，而得到 ReO-MN-16-acid(7)。其中 ReO-MN-16-Et(6A) 之去酯化雖然需要六小時的反應時間，但後續純化步驟較 ReO-MN-16-Bn(6B) 去酯化簡易。

結論：

「三甲基碘矽烷」確實可將 ReO-MN-16-Et(6A) 及 ReO-MN-16-Bn(6B) 去保護，可得最終產物化合物 7 (產率約 35%)。

PB004

[^{18}F]FCH Production with an Automated TracerLab FxFN Module: A 2.5 Year Experience

Chia-Ling Tsai[1], Ya-Yao Huang[1], Hsiang-Ping Wen[1], Kai-Yuan Tzen[1,2], Chyng-Yann Shiue[1-3], Ruoh-Fang Yen[1,2]

[1]PET Center, Department of Nuclear Medicine, National Taiwan University Hospital, Taipei, Taiwan;
[2]Molecular Imaging Center, National Taiwan University, Taipei, Taiwan;
[3]PET Center, Department of Nuclear Medicine, Tri-Service General Hospital, Taipei, Taiwan.

Introduction: [^{18}F]Fluoromethylcholine ([^{18}F]FCH) is a potent tumors imaging agent. In order to fulfill the demand of clinical studies, we have developed a high yield one-pot synthesis of this potent tumors imaging agent using a TracerLab FxFN module. The aim of this study was to summarize our 2.5 years, 88 syntheses experience of [^{18}F]FCH production with this improved method.

Methods: The reaction sequence used for our original [^{18}F]FCH production with TracerLab FX_{FN} module was a two-step procedure (Figure 1 and Scheme 1) as reported by Iwata *et al*. and DeGrado *et al*. Briefly, fluorination of CH_2Br_2 with ^{18}F-KF/$K_{2.2.2}$ in MeCN at 65-120°C followed by purification with Silica cartridges gave ^{18}F-FCH_2Br. ^{18}F-FCH_2Br was then transferred on line to react with dimethylaminoethanol (DMAE) which was pre-loaded on a reversed phase Sep-Pak, followed by SPE purifications to give [^{18}F]FCH. Quality control tests of [^{18}F]FCH were carried out according to USP criteria and the specifications (radio TLC) established by our site.

Results: A total of 88 [^{18}F]FCH syntheses were performed between November 2013 and May 2015 with 9 failures. The radiochemical yield (RCY) of [^{18}F]FCH was 12 ± 4% with a synthesis time of about 50 min. The radiochemical purity (RCP) was 96 ± 2%. The content of residual DMAE level was 20 ± 5 ppm.

Conclusions: Our study showed that the improved ^{18}F-FCH automated synthesis method was reliable with a relatively low incident of failures and with high RCY and RCP. Moreover, there was minimal operator intervention and radiation exposure, as well as low acceptable running costs.

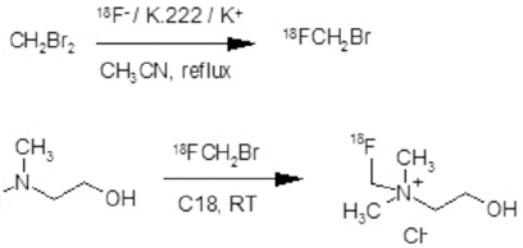

Scheme 1. Radiosynthesis of ^{18}F-FCH.

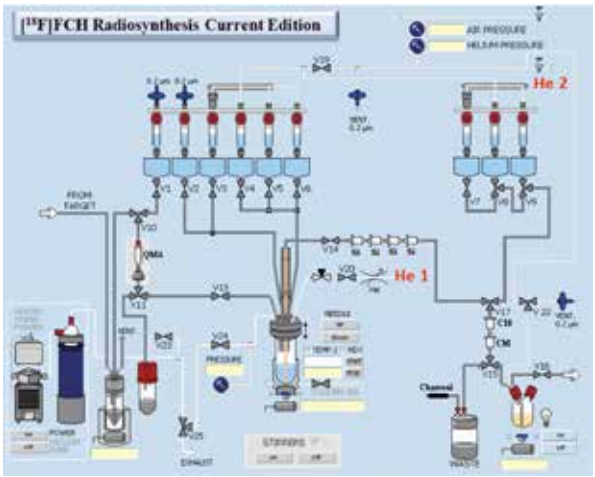

Figure 1. Modified TracerLab FxFN module for ^{18}F-FCH production.

PB005

GMP-compliant Radiosynthesis of [^{18}F]FMISO and Its Whole-Body Biodistribution via Whole-Body PET imaging of Mice

Ya-Yao Huang[1], Yu-Ning Chang[1], Pei-Yao Lin[2], Hsiang-Ping Wen[1], Kai-Yuan Tzen[1,2], Ruoh-Fang Yen[1,2]

[1]PET Center, Department of Nuclear Medicine, National Taiwan University Hospital;
[2]Molecular Imaging Center, National Taiwan University.

Introduction: [^{18}F]Fluoromisonidazole ([^{18}F]FMISO), is the most widely applied nitroimidazole for PET imaging of hypoxia. In this study, we presented the production and quality control (QC) tests of [^{18}F]FMISO in conditions that meet good manufacturing practice (GMP) requirements for clinic study. Furthermore, we also presented the whole-body biodistribution of [^{18}F]FMISO via microPET imaging

Method: The automated production of [^{18}F]FMISO is based on reported procedures from Oh *et al*. and Lim *et al*. Briefly, [^{18}F]FMISO was produced by nucleophilic fluorination of NITTP precursor, acidic hydrolysis and SPE purification via Tracerlab MxFDG module (Scheme 1). The QC tests were performed based on EP monograph of [^{18}F]FMISO. For animal study, male ICR mice (20–30g) were used with free access to water 12 hours prior to experiment and then injected with a bolus of about ~ 250 μCi (n = 3). By using small-animal Argus PET/CT scanner, dynamic sinograms were produced for 90 min with 2 x 10 sec, 2 x 20 sec, 4 x 60 sec, 2 x 240 sec, 2 x 600 sec, 1 x 720 sec frames. VOIs were defined on co-registrated PET/CT images according to evident tracer accumulation in the area of the liver and data was expressed as standard uptake value (SUV).

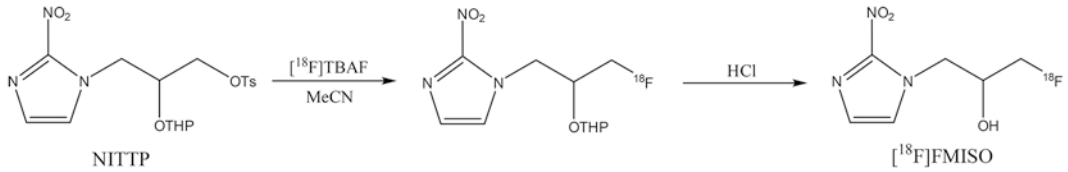

Scheme 1. Radiosynthesis of [^{18}F]FMISO

Results: The synthesis of [^{18}F]FMISO was successfully validated under GMP conditions, resulting in radiochemical yield of 19 ± 5% (EOS) within 54 ± 1 min (n = 6). Radiochemical purity of each batch was > 95%. MicroPET studies revealed [^{18}F]FMISO was highly taken up by the mice bladder and was gradually increased until the end of scanning (78 min).

Conclusion: In this study, we tried to produce [^{18}F]FMISO with the EP quality and certified as GMP. The use of disposable cassette and cartridge purification simplifies the handling and shortens the synthesis time. It is convenient to produce qualified [^{18}F]FMISO for clinical and pre-clinical use based on current module for [^{18}F]FDG.

PB006

Practical Experience with the Improved Specific Activity of [^{11}C]PiB in NTUH

Ya-Yao Huang[1], Chia-Ling Tsai[1], Ching-Hong Chiu[1], Kai-Yuan Tzen[1,2], Ruoh-Fang Yen[1,2]

[1]PET Center, Department of Nuclear Medicine, National Taiwan University Hospital;
[2]Molecular Imaging Center, , National Taiwan University.

Introduction: Alzheimer's disease is the most common cause of dementia in the world. In 2010, we have successfully synthesize [^{11}C]PiB with TracerLab F_{Xc} (GE Medical System). However, the specific activity (SA) of [^{11}C]PiB seems be an issue for clinical or pre-clinical use. The purpose of this study was to summarize our experience in the SA improvement of [^{11}C]PiB since May 2014.

Method: [^{11}C]CO_2 was produced by ^{14}N(p,α)^{11}C reaction in a PETtrace cyclotron and was transferred into TracerLab F_{Xc} module for producing [^{11}C]CH_4 via H_2(g)/Ni reduction. Activity of [^{11}C]CH_4 produced ranged from 110 ± 30 GBq (n = 41) with 71 ± 10 min of irradiation time and 50 μA of beam current. Target gas was N_2 (6.0) spiked with 1.0% or 0.5% O_2 (5.5). Followed by gas halogenations of [^{11}C]CH_4, [^{11}C]CH_3I was obtained and then reacted with AgOTf to prepare [^{11}C]CH_3OTf. The [^{11}C]CH_3OTf was trapped in a vessel containing the precursor, 6-OH-BTA-0. After labeling, semi-preparative HPLC was performed to purify the labeled product. Afterward a series of quality control tests were performed for [^{11}C]PiB product. Five consecutive test periods were carried out with different configurations including: 1) Variant O_2 content in target gas. 2) Flushing of transfer line from target to the module. 3) Pre-irradiation of target. 4) Additional purifiers for all gases.

Results: We have routinely produced [^{11}C]PiB in a radiochemical yield (RCY) of 19 ± 6% (based on radioactivity of [^{11}C]CH_3OTf, n = 41) with synthesis time 28 ± 3 min and radiochemical purity > 90% from May 2014 to June 2015. Starting with an initial SA of [^{11}C]PiB about 25 GBq/umol, before applying the described improvements. With the implementation of different configurations, SA of [^{11}C]PiB could reached a range between 100-200 GBq/umol.

Conclusions: Based on our long-term observation, target conditioning process (flushing and pre-irradiation) as well as gas purifiers were critical parameters that enable to achieve [^{11}C]PiB with improved specific activity.

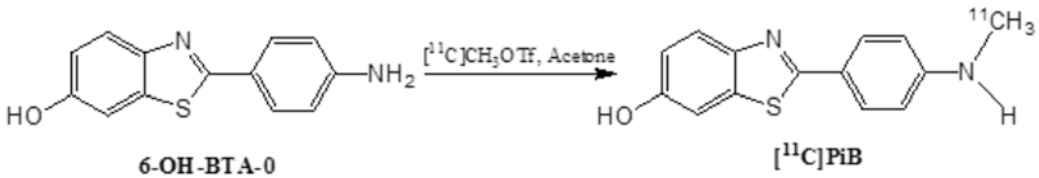

Scheme 1. Radiosynthesis of [^{11}C]PiB

PB007

人員生物劑量統計方法之應用—不同年度反應曲線之合併

趙晟富　葉冠毅　張翠容　莊程惠　張志賢

行政院原子能委員會核能研究所

背景介紹：

在臺灣約有 44,000 位輻射工作人員，包含在核能電廠、工業及醫院等領域。爲因應輻射意外曝露事件之發生，我國有必要建置一個生物劑量實驗室。當人員受到輻射意外曝露時，可利用染色體雙中節分析做爲曝露劑量評估，並做爲後續醫療照護的參考依據。

方法：

國際目前於人員生物劑量相關效應的研究，一致認爲雙中節分析乃爲一快速簡單且符合效益之黃金標準。本計畫以 0、0.5、1、2、3、4 和 5 Gy 之鈷 –60 加馬射線在室溫下照射正常受試者之血液樣本，再進一步培養血液中淋巴球。將培養後的淋巴球染色體經由顯微鏡照像後，再進行染色體雙中節分析。將分析後的數值以 DoseEstimate 軟體計算後可得一檢驗劑量 - 效應二次方程式 ($Y = C + \alpha D + \beta D^2$) 曲線。

結果：

本實驗室在 101 年、102 年及 104 年分別完成了四條檢驗劑量 - 效應曲線，並利用 *F-test* 以及 *p-value* 的計算得知此四條反應曲線無明顯差異，故可將此四條反應曲線合併成一標準曲線。

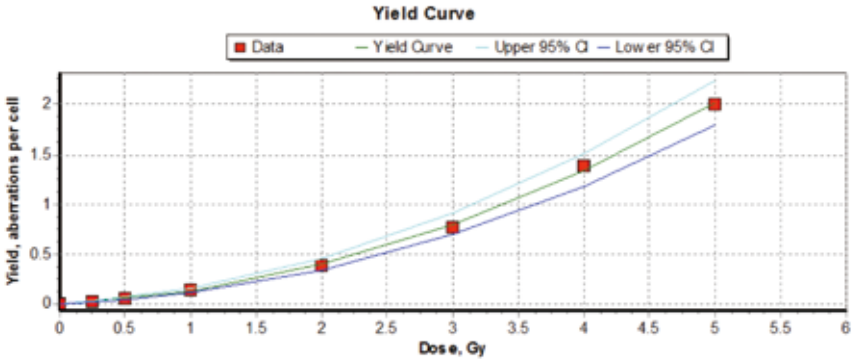

$$Y = 0.0022\ (\pm\ 0.0015\ ) + 0.0623\ (\pm\ 0.0093\ ) \times D + 0.0682\ (\pm\ 0.0028\ ) \times D^2$$

結論：

本實驗室已建立鈷 –60 加馬射線的檢驗劑量 - 效應標準曲線，未來實驗室測量未知劑量樣品時，即可將分析後所得之 yield 值代入標準曲線公式，即可計算得知該樣品的估計劑量，以及 95% 信賴區間之估計劑量。此有助於臺灣對輻射意外曝露事件之緊急應變作爲。

PB008

DOTA-tris(^{t}Bu ester) 之製備方法

李青雲　盧桂林　張瑜　徐成芳

核能研究所化學組

背景介紹：

提供一種可標幟 Ga 的 DOTA 衍生物有機配位子 DOTA- tris(^{t}Bu ester) 之方法改良。透過螯合劑 DOTA 大環衍生物的使用，可使放射性標幟與胜　類物質快速且有效地結合，縮短整個標誌流程所需的時間，且具有很高的比活度，讓放射性核種的使用更有效率。雖然化合物 DOTA-tris(^{t}Bu ester) 是可商購的，但成本高嚴重地限制了它的廣泛利用 (250 mg, 售價 12,000 元)，因此本研究開發合成技術。

方法：

將 起 始 物 1,4,7,10-tetraazacyclododecane (1) 與 tert-butyl bromoacetate 反 應 生 成 1,4,7,10-tris(tert-butoxycarbonylmethyl)-1,4,7,10-tetraazacyclododecane (2)。化合物 2 與 benzyl bromoacetate 偶合得到 1-(benzyl acetate)-4,7,10-tris- (tert-butoxy-carbonylmethyl)- 1,4,7,10-tetraazacyclododecane(3) 。將化合物 3 氫化還原可得最終產物 DOTA-tris(^{t}Bu ester) (4)。所有化合物皆以核磁共振光譜及紅外吸收光譜確認其分子結構。

結果與討論：

採用本方法合成 DOTA 大環結構 DOTA-tris(tBu ester)，共須三個步驟，參考文獻的作法並加以改良與文獻具有相同之核磁共振光譜及質譜數據，且最終步驟產率可達 89%。已成功的將 DOTA 結構衍生化，以利其與後續生化分子之結合，成爲具有潛力之核醫藥物。本研究開發合成的 DOTA-tris(^{t}Bu ester) 具有經濟競爭力，相較市售產品約降低 81% 成本 (250 mg，售價 2,233 元)。此配位子將可與 6-(2-nitro-1*H*-imi-dazol-1-yl) hexan-1-amine 偶合，以製作新型缺氧組織造影劑 DOTA-Ni。此配位子亦可與含長烷基偶合的 Oleic acid 與 Lipiodol 分別形成 DOTA-Oleic acid 與 DOTA-Lipiodol 配位子之標幟前驅物供標幟 Re-188，以應用爲肝癌之核醫治療領域的用途。

PB009

評估中草藥對於細胞因子、葡萄糖攝取與腦部血流差異性作用分析

張剛瑋[1] 陳輝墉[2] 林明佳[2]

[1] 行政院原子能委員會核能研究所同位素組
[2] 義大醫院核子醫學科

背景介紹：

中國傳統醫學 (Traditional Chinese Medicine, TCM) 至今已超過 4000 年的歷史，被廣泛應用於中國、日本、韓國、新加坡等世界各地。中藥 (TCM) 常被用來在滋補氣血，促進血液循環等。但由於其作用機制之複雜，雖可得到許多病理情況的治療，但其作用機制與原理仍是不明。

本研究擬以將試驗動物餵食萃取後之 TCM，用以評估 TCM 於試驗動物中腦部之葡萄糖代謝、腦血流及腦部多巴胺受體之影像醫學分析工作。

方法：

本試驗之中草藥是源至於生物原料 (植物) 提煉、萃取而成的天然物質。該試驗將試驗動物 (小鼠) 區分爲三個劑量組別 (高劑量組：0.25 g/ml、低劑量組：0.125 g/ml 與對照組)。每天以胃管方式餵食二次，持續二週。試驗方式利用小型動物 ^{18}F-FDG/PET 進行葡萄糖代謝分析、Tc-99m-HMPAO/SPECT 進行腦部血流分析和 ^{123}I -Epidepride/SPECT 進行腦部多巴胺 D2 受體影像分析工作。

結果：

於腦部葡萄糖代謝與腦部血流分析結果顯示，在給予不同劑量之中草藥後於腦部各區域之攝取劑量均有顯著降低。於腦部多巴胺 D2 受體結合試驗中，於特定區域之多巴胺 D2 結合 I-123-Epidepride 也有明顯之差異性。

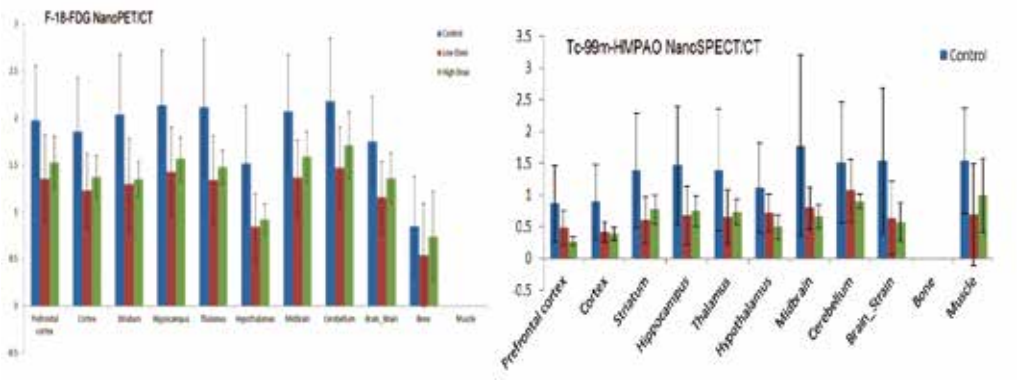

結論：

於此試驗中，利用之 TCM 藥理特性在於減重方面，故於此研究結果中，我們可發現 TCM 降低腦部活性 (代謝能力) 與血流部分，並有少量將透過多巴胺之調節方式，達到基礎藥理特性。未來我們將持續利用 PET，SPECT 和放射性藥物的體內成像原理和作用於人體的療效之解釋。

PB010

腫瘤增生衍生物 5-Nitro-CdR-$(Ac)_3$ 之合成研究

蔡嘉東　張瑜　徐成芳

核能研究所化學組

背景介紹：

癌症在全國已成爲十大死因的第一名。放射性標幟之腫瘤增生 (Tumor Proliferation) 藥物結合正子斷層造影或單光子斷層掃描，可協助臨床偵測腫瘤病灶與腫瘤治療效果之評估用途。近年來由核能研究所同位素組發展一種新穎的腫瘤增生探針，此藥物是以脫氧胞苷作爲主體，與放射性 ^{131}I 反應形成 [^{131}I]ICdR，作爲顯影劑，因此，本實驗開發新型的單光子斷層腫瘤造影的標誌前驅物 5-Nitro-CdR-$(Ac)_3$，希望未來能有助於核子醫學造影於腫瘤偵測或治療預後評估之發展。

方法：

本研究關於腫瘤增生衍生物 5-Nitro-2'-deoxycytidine-triacetate (5-Nitro-CdR-$(Ac)_3$) 之合成方法及特性描述。首先將起始反應物 2'-deoxycytidine 在醋酸酐與 pyridine 進行取代反應，可獲得化合物 2'-Deoxycytidine-triacetate (CdR-$(Ac)_3$)，並與 Nitrosonium tetrafluoroborate ($NOBF_4$) 於無水 DMF 下進行硝化反應而生成最終產物 5-Nitro-CdR-$(Ac)_3$。

結果：

就核子醫學而言，正子斷層造影在臨床使用上並沒有像單光子斷層造影普遍，主因爲單光子斷層造影應用的核種取得相對容易、示蹤劑製備較爲簡單，以及費用較低廉等。然而，[^{18}F]FDG 做爲正子造影腫瘤示蹤劑的造影結果已被臨床接受並廣泛使用，反之 SPECT 卻仍無具代表性的造影藥物。目前核苷類腫瘤增生造影劑被視爲可直接與增生相關，主要是利用不受控制的腫瘤細胞處於 S phase 時會大量表現 thymidine kinase (TK1)，而磷酸化核苷類似物提供 DNA 序列合成以達增生的目的，許多核苷酸類似物如 [^{18}F]FLT、[^{18}F]FMAU、[$^{124/131}I$]IUdR 等都被證實其積聚量確能當作細胞增生速率的指標。本研究所述之標幟前驅物 5-Nitro-CdR-$(Ac)_3$ 之合成方法，步驟少且容易操作，產率良好，其 IR，NMR 與質譜之分析數據均與 5-Nitro-CdR-$(Ac)_3$ 之構造吻合。

結論：

本研究已成功建立多步驟合成 5-Nitro-CdR-$(Ac)_3$ 的方法，並由光譜確定與結構吻合。

PB011

NOTA 衍生物合成應用研究

劉哲宇　張瑜　徐成芳

核能研究所化學組

背景介紹：

「血管新生」（angiogenesis）是人體一種正常的生理現象。當組織中需要血管時，有些促使血管新生的因子的分泌量會增加，以造就血管新生來供應氧氣和養分，讓傷口的細胞得以存活。腫瘤內新生的血管系統和正常組織大不相同，整合素 αvβ3 是一種與腫瘤血管新生及腫瘤轉移相關的細胞黏著受器 (cell adhesion receptor)，整合素 αvβ3 腫瘤新生血管內皮細胞表面和部分腫瘤細胞表面。由於整合素 αvβ3 與具 Arg-Gly-Asp (RGD) 序列之胜肽具有高度的專一結合性，利用放射性標誌 RGD 胜肽可發展成爲有效且具專一性的腫瘤造影劑。近年來由本所同位素組發展正子腫瘤造影劑 Ga-68-NOTA-RGD-EGFx 及新穎正子多巴胺轉運體造影劑 TRODAT-2，因此，本實驗開發新型腫瘤造影劑前驅物 Bis-t-butyl NOTA，希望未來能有助於核子醫學造影於腫瘤偵測或治療預後評估之發展。

方法：

首先將起始反應物一方面以 Tosyl chloride 將 Ethylene glycol 接上保護基後，可得 1,2-bis(p-toluenesulfonyl)-1,2-ethanediol (1)。另一方面亦以 tosyl chloride 將 Diethylenetriamine 接上保護基後，可得 N, N', N"-tris-(p-toluenesulfonyl)-diethylenetriamine (2)，以碳酸銫當作鹼的條件下進行反應生成 1,4,7-tris(p-toluenesulfonyl)-1,4,7-triazacyclononane (3)。將化合物 3 再以濃硫酸去除 Ts 保護基，濃鹽酸處理後生成之 HCl 鹽類再以氫氧化鈉中和，可得 1,4,7-triazacyclononane (TACN)。TACN 與 tert-butyl bromoacetate 進行結合，利用 pH 的變化進行萃取純化，生成 di-tert-butyl 2,2'-(1,4,7-triazonane-1,4-diyl)diacetate (4)；再將化合物 4 以 benzyl-2-bromoacetate 進行取代反應，再利用 pH 的變化進行萃取純化，生成 di-tert-butyl 2,2'-(7-(2-(benzyloxy)-2-oxoethyl)-1,4,7-triazonane-1,4-diyl)diacetate (5)；最後，將化合物 5 進行氫化還原反應，得最終產物 2-(4,7-bis(2-(tert-butoxy)-2-oxoethyl)-1,4,7-triazonan-1-yl)acetic acid(Bis-t-butyl NOTA)。

結果：

往常合成化合物 (4) 及化合物 (5) 時，必須使用矽膠管柱來進行純化，純化過程耗時，並容易損失產率。本研究改良純化方法，利用 pH 的變化進行萃取純化，改善先前繁瑣的純化步驟，與先前純化方式比較，發現產率有明顯提升。

結論：

本研究所述之標幟前驅物 Bis-t-butyl NOTA 之合成方法，容易操作，產率良好，可做爲未來大量生產的實驗依據，其 IR，NMR 與質譜之分析數據均與 Bis-t-butyl NOTA 之構造吻合。

PB012

I-131 病房之建構與使用經驗

陸建華[1] 吳志順[1] 李將瑄[2]

[1] 奇美醫療財團法人柳營奇美醫院核子醫學科
[2] 奇美醫療財團法人奇美醫院核子醫學科

前言：

I-131 病房之設置是爲了醫治甲狀腺癌之病人，但因爲有輻射劑量問題，以至於在建構及治療病人過程中有很多部分需詳加考慮及解決，對此就本院十年來治療病人之經驗，提供建置建議及問題改善方式，提供同儕醫院參考。

方法：

(1) 本院廢水槽爲四槽加一預備槽之設計，其排水方式爲各槽排入預備槽後再排入醫院廢水系統，其不理想處爲，如預備槽被污染則其他四槽之廢水將無法排出，會影響病人收入院治療作業，改善方法爲每槽均應設置獨立排放出口，則將不會影響每槽廢水之排放。(2) 病人住院期間不愼將免洗褲丟入馬桶，或遇停電時廢水槽電動閥開關被關閉，以致產生管路阻塞現象，改善方式前者爲加強病人衛教教育，馬桶旁放置夾子及公告並於管路中段裝設管路阻塞報警及自動通報系統，當阻塞液面淹到警報器時，系統將主動以簡訊告知輻防及工務人員前往立即處理，後者於 I-131 電動閥開關處加裝不斷電系統，可避免排泄物因電動閥被關閉或阻塞，而外溢至病房區造成輻射污染事件。(3) 本院 I-131 病房爲兩床設計，中間隔鉛板，旁邊擺放飲水機、冰箱及書櫃，如遇內床病人需急救要將推床推往加護中心時，病床無法順利推出，改善方式爲將飲水機、冰箱內縮成上下層置放，移除書櫃如此才能使動線順暢。(4) 病房前室空間狹小，遇病人急救時，醫護人員防護衣穿脫不便，改善方式爲將病房推門改成拉門，如此可以加大內部空間。(5) I-131 病人產生之廚餘及固態廢棄物有輻射劑量問題，除加強病人廚餘及廢棄物分類教育並可於病房放置小型冰箱存放輻射廚餘，固態廢棄物則於病人出院後由輻防人員至病房偵測後將超標廢棄物回收至核醫科熱核室存放靜置 .

結果：

(1) 目前本院雖未發生預備槽被污染事件，但該項錯誤之設計可提供爲同儕醫院新增或增建廢水槽時之參考經驗。(2) 自從裝設管路阻塞報警及自動通報系統後，雖遇到過幾次報警及停電事件，該二項裝置均能發揮功效，並無排泄物外溢情事發生。(3) 及 (4) 兩項經過本院輻射意外事件演練實際測試結果，均能符合需求及發揮功效。(5) 針對廚餘及廢棄物處理問題，已檢討改善並訂出「碘 -131 病室垃圾 (含廚餘) 處理流程」供同仁遵循管制，且均已無輻射廚餘及廢棄物外釋事件發生。

結論：

以上所列，均可爲設置 I-131 病房之醫院需考量及可能會遭遇之問題，各醫院均有其不同之問題及解決方式，本文就本院設置十年來，就病房建置使用及已遭遇問題，提供改善方案，供同儕醫院參考。

PB013

腦神經受體在熱潮紅模式的調適機制與療效評估

林俊龍[1] 林婉琪[1] 吳鴻明[2] 鄭澄意[3] 薛晴彥[3,4] 黃文盛[2,3] 李德偉[1]

[1] 行政院原子能委員會
[2] 彰化基督教醫院
[3] 國防醫學院
[4] 台大醫院

背景：

約 75% 停經後婦女有熱潮紅現象 (Hot flash)，多發於停經初期，造成生活上的困擾。Risperidone 是一種多巴胺拮抗劑，可結合於腦部紋狀體，文獻顯示 e 它可有效緩解熱潮紅模式大鼠 (OVX) 之症狀。本研究擬針對 OVX 動物模式與腦部血清素 (Serotonin)、多巴胺 (Dopamine) 系統作相關性分析，藉由 Risperione 給予後腦分子影像及生化試驗等方式瞭解其紓緩停經徵狀之機制。

方法：

於建立完成之 OVX 動物模式中給予 0.005 與 0.05 mg/kg 的 Risperidone (Intraperitoneal inj.)，試驗期間量測其體溫變異性、I-123-Epidepride 和 F-18-Altanserin 影像分析並在試驗結束後檢測其子宮重量、生化差異性等。

結果：

生化試驗與體溫變異性結果均顯示 Risperione 可促使 OVX 大鼠之體溫、子宮重量、血中 NOx 與雌性激素濃度的恢復。F-18-Alterserin 於 OVX 與對照組比較，出現 F-18-Alterserin 與 HTR2A 受體的結合量下降 ($p < 0.05$, student t-test)；給予 Risperidone 後可見其 HTR2A 受體結合量有恢復的趨勢。於 I-123-Epidepride 試驗中，OVX 會導致 I-123-Epidepride 與多巴胺 D2 受體的結合量下降。在給予 Risperidone 後則出現紋狀體之多巴胺 D2 受體結合量明顯抑制。

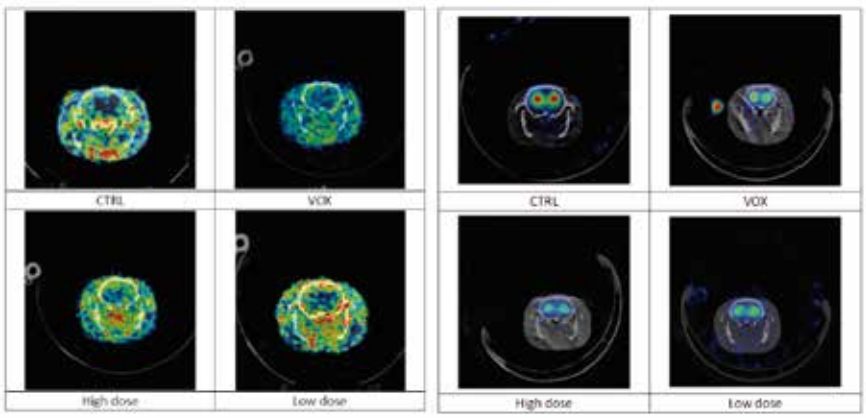

F-18-Alterserin 大鼠 PET/ CT 成像　　I-123-Epidepride 大鼠 SPECT/ CT 成像

結論：

本研究建立 OVX (卵巢切除) 動物及其腦受體造影模式，結果佐證 Risperidone 治療機制並提供未來停經後婦女熱潮紅藥物篩選平台。

PB014

Determination of Impurities in the PET Imaging Agent FEONM using Liquid Chromatography Tandem Mass Spectrometry

Yu-Chieh Hsiao[1], Wei-Hsi Chen[1], Pei-Cheng Wang[1], Jenn-Tzong Chen[2]

[1]*Chemistry Division, Institute of Nuclear Energy Research, Taoyuan, Taiwan;*
[2]*Isotope Application Division, Institute of Nuclear Energy Research, Taoyuan, Taiwan.*

Introduction: Currently the diagnosis of Alzheimer's disease scientific method is used of Positron Emission Tomography (PET) to observe the formation of Aβ plaque. FEONM is one of the new radioactive drug which could be labeled with radionuclide 18F as an imaging agent to monitor specific binding to Aβ plaque. Herein, the quality and impurities of homemade FEONM was determined using LC-UV-MS/MS to resolve the impurities.

Methods: Prepared of 10 mg/L synthesized standard (3 μL) were analyzed using HPLC on an Eclipse XDB-C18 column (4.6 mm ID x 50 mm, 1.8 μm, Agilent) and gradiently eluted with mobile phase composed of 10 mM ammonium acetate dissolved in D.D. water and acetonitrile. Analyte was simultaneously detected by UV 250 nm and MS in positive ion mode with Q1, product ion and multiple reaction monitoring (MRM) scan mode with turnaround time 25 min.

Results: The peak at retention time 10.86 min in the UV chromatography was composed of the target FEONM and synthetic intermediate. Nevertheless, mass spectrometry could resolve the co-eluate components using m/z respectively. The results showed that chromatographic purity of FEONM was only below 18.45% and there were seven process impurities with abundance more than 1%. Most of the impurities were identified based on tandem mass spectra.

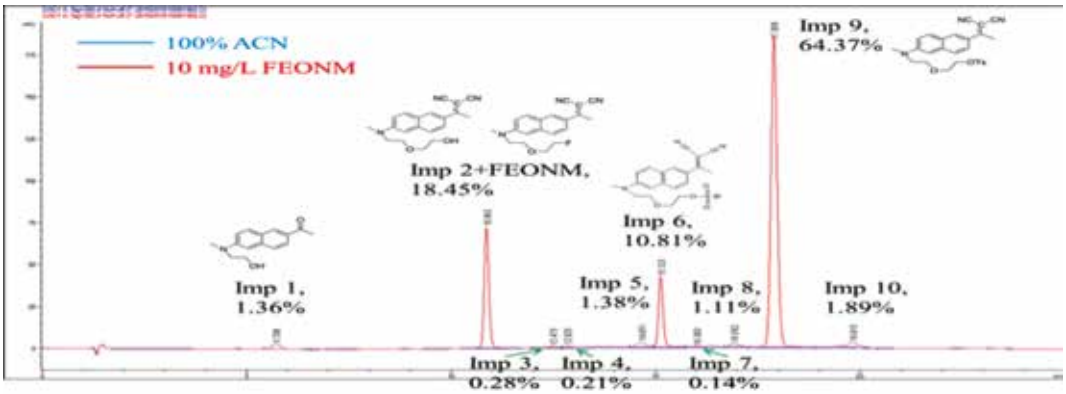

Conclusions: There were several impurities residual in the material which came from improperly purified processes. The study offered the directions to improve drug material quality for the Lab which prepare of FEONM.

PB015

Parameter Optimization in the Synthesis of FLT、FDDNP、FET

Li-Yuan Huang, Yean-Hung Tu, Jenn-Tzong Chen, Wuu-Jyh Lin

Division of Isotope Application, Institute of Nuclear Energy Research, Taoyuan, Taiwan.

Abstract

Purpose: The study is mainly focused on the optimized parameters on the synthesis of [F-18] radiopharmaceuticals. The present parameters have not been efficient on the yields and radiochemical purities, it is to help improving the protocol for a better yield and purity. There are four variables affecting, fluorination temperature, fluorination time, hydrolysis temperature, and hydrolysis time.

Methods: For the experimental design, Taguchi method has been applied. The parameters usually used are collected and set to start with in experiment of each drug. The four variables are tested one after another. Each of the parameters is changed and tested according to the structures of the drug while the rest three are fixed, then the results are compared. There are three [F-18] radiopharmaceuticals to be studied, [F-18] FLT. [F-18] FET, and [F-18] FDDNP. All three drugs will come up with the parameters that suit each of them by the end of the work.

Results: The results obtained are that 110°C for 5min is needed for [F-18] FLT fluorination temperature and time with 85°C 5min for hydrolysis to obtain 50~60% yield and 98% radiochemical purity, [F-18] FET needed 87°C 3 min as fluorination temperature and time, with 133°C 3 min as hydrolysis temperature and time for 48% and 99.7% yield and radiochemical purity, respectively, and [F-18] FDDNP would need fluorination at 95°C for 15 min to get a 36~50% yield with 95% radiochemical purity.

Conclusion: These data showed that drugs have different structures which give them different physical and chemical properties. Such differences mainly accorded to 1. Leaving groups, 2. Degree of the compound (primary, secondary or tertiary). These two factors must be observed first before the experiments begin in order to be efficient.

Keywords: [F-18] Radiopharmaceutical, Taguchi method

PB016

PET/CT Evaluation of Tumor Imaging with ^{18}F-FCdR, ^{18}F-FUdR, ^{18}F-FLT and ^{18}F-FDG in A Mouse Xenograft Model

Jyun-Hong Chen[1], Hung-Wen Yu[1], Ya-Yao Huang[2], Ching-Hong Chiu[2], Wei-Ting Chen[1], Wuu-Jyh Lin[1], Kai-Yuan Tzen[2,3], Chyng-Yann Shiue[1-3]

1 Isotope Application Division, Institute of Nuclear Energy Research; 2 PET Center, Department of Nuclear Medicine, National Taiwan University Hospital; 3 Molecular Imaging Center, National Taiwan University, Taipei, Taiwan

Introduction: [^{18}F]FDG has been the most widely used radiotracer for PET studies in neuroscience, cardiology, and oncology. Positron-emitter labeled nucleosides also have been synthesized and used for measuring cell proliferation and monitoring the responses of cancer therapy. The aim of this study was to compare [^{18}F]FDG, [^{18}F]FLT, 5-[^{18}F]FCdR and 5-[^{18}F]FUdR as tumor imaging agents in LL/2-tumor bearing mice.

Methods: [^{18}F]FDG and [^{18}F]FLT were synthesized by nucleophilic fluorination of the appropriate precursors with K[^{18}F]/K2.2.2 followed by de-protection, purifications and formulations. 5-[^{18}F]FUdR and 5-[^{18}F]FCdR were synthesized by electrophilic fluorination of the appropriate precursor with [^{18}F]F_2 or [^{18}F]AcOF followed by hydrolytic cleavage of the protecting groups with NaOH or NH_4OH and purification with HPLC. C57BL/6 mice were implanted subcutaneously into the right leg with LL/2 cells. Seven days after implantation, the tumor uptake and whole-body biodistribution of all tracers in LL/2-tumor bearing mice were performed for 1.5 hr using an Argus PET/CT scanner. Volumes of interest were defined on co-registrated PET/CT images using PMOD, and the time-activity curves of these tracers in various organs were expressed as SUV.

Results: The RCYs of [^{18}F]FDG, [^{18}F]FLT, 5-[^{18}F]FCdR and 5-[^{18}F]FUdR were 80 $\pm$ 4, 10 $\pm$ 2%, 4 $\pm$ 1, 8 $\pm$ 4% (EOS, n $>$ 5), respectively, with a radiochemical purity of $>$ 90% in a synthesis time of 30~70 min from EOB. In contrast to [^{18}F]FDG which has high accumulation of radioactivity in bladder, PET studies in LL/2-tumor bearing mice showed that the radioactivity of these three ^{18}F-labelled nucleosides accumulated mainly in the kidney and bladder. The tumor-to-muscle ratios of [^{18}F]FDG, [^{18}F]FLT, 5-[^{18}F]FUdR and 5-[^{18}F]FCdR in LL/2-tumor bearing mice were 8.6 $\pm$ 0.4, 1.8 $\pm$ 0.3, 4.5 $\pm$ 0.5 and 4.7 $\pm$ 0.5 (n $>$ 3), respectively.

Conclusions: In addition to [^{18}F]FDG, PET studies in mice showed that 5-[^{18}F]FUdR and 5-[^{18}F]FCdR were superior to [^{18}F]FLT for visualization of LL/2-tumor in mice. The utility of these tracers for imaging other tumors are under investigations.

PB017

Study of ^{188}Re Radiation Effects on Protected-H_3MN-16ET and ReMN-16ET using Liquid Chromatography Tandem Mass Spectrometry

Pei-Cheng Wang[1], Wei-Hsi Chen[1], Yu-Chieh Hsiao[1], Tsai-Yueh Luo[2], Yu Chang[1]

[1]*Division of Chemistry, Institute of Nuclear Energy Research, Taoyuan City, 32546, Taiwan;*
[2]*Division of Isotope Application, Institute of Nuclear Energy Research, Taoyuan City, 32546, Taiwan.*

Introduction: Protected-H_3MN-16ET was labeled with radioactive ^{188}Re to prepare of ^{188}Re-MN-16ET which is a potential candidate for hepatoma treatment under preclinical trial. It is a great concerned issue whether the raw material, protected- H_3MN-16ET and product, ^{188}Re-MN-16ET would be decomposed arising from ^{188}Re radio effects. In this study, the stabilities of protected-H_3MN-16ET and non-radio Re-MN-16ET were evaluated under radionuclide ^{188}Re coexisting. The tested solutions were analyzed by liquid chromatography-tandem mass spectrometry (LC-MS/MS) to identify of degradation products of protected-MN-16ET and Re-MN-16ET.

Methods: After mixing the tested solutions of protected-H_3MN-16ET (1000 mg mL^{-1})/^{188}Re and Re-MN-16ET (1000 mg mL^{-1})/^{188}Re (with radiation activity 50 mCi, 150 mCi) respectively then waiting for 7 days, the solutions were analyzed using LC-MS/MS (Agilent 1100 coupled with Sciex 4000 QTrap) in positive enhance MS and enhanced product ion detection mode.

Results: The results demonstrated that ^{188}Re radiation could not significantly affect on protected-H_3MN-16ET. However, abundance of Re-MN-16ET reduced obviously and depended on 188Re radioactivity. It was found that there are four degradation products present in chromatogram and were identified via tandem mass spectra.

Conclusions: The force degradation of Re-MN-16ET and protected- H_3MN-16ET study via ^{188}Re radiation were investigated using liquid chromatography tandem mass spectrometry. There are four degradation products were founded which were H_3MN16ET (m/z = 477) and its derivates (m/z = 465, m/z = 411 and m/z = 362).

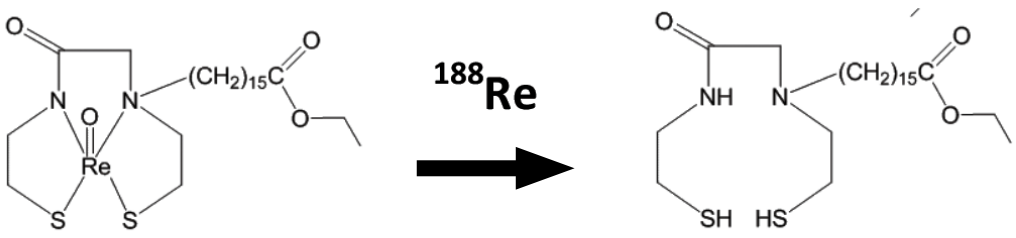

deprotected H_3MN-16ET
MW = 476.3

PB018

使用 ACR 認證假體在台灣地區進行多中心核醫影像品保之初步研究

羅浚哲[1] 李國威[2] 詹美齡[2] 高潘福[1,3]

[1] 中山醫學大學 核子醫學科
[2] 行政院原子能委員會核能研究所
[3] 中山醫學大學 醫學系

背景介紹：

相較於歐美地區之核醫儀器品保規範，台灣地區尚未有明確規定。本研究使用 Jaszczak Deluxe Flangeless ECT 假體進行台灣地區核子醫學儀器 (9 台 SPECT-CT 和 8 台 PET-CT) 之影像品質評估並且希冀將來更進一步的研究能以本實驗結果作爲基石制定出符合台灣之核醫品保標準。

方法：

研究團隊以固定比例之放射線藥物填充 Jaszczak Deluxe Flangeless ECT 假體，隨後進行八個不同單位之核醫儀器 (3 台 SPECT,5 台 SPECT-CT 和 8 台 PET-CT) 進行實驗，本研究採用臨床常規檢查之掃描參數進行影像擷取。最後，9 位年資達 15 年以上之核醫專科醫師進行影像評分，該評分項目包含：空間解析度 (Resolution)、核醫影像和電腦斷層影像對位情形 (Alignment)、變形程度 (Deformity)，以及整體影像評分 (Overall satisfaction)；在影像對位以記錄實際移動多少距離 (mm)、在解析度評分爲可視數目。變形程度以及整體影像等地爲：5 ＝最優，4 ＝優，3 ＝可接受，2 ＝差，1 ＝最差。

結果：

PET-CT 和 SPECT-CT 的對位結果在 x,y,z 軸向分別爲 0.19 ± 0.42 mm，0.51 ± 0.87 mm，1.41 ± 3.61 mm 和 0.37 ± 0.60 mm，0.97 ± 1.46 mm，0.23 ± 0.58 mm；在空間解析度分別 3.40 ± 0.81 和 2.20 ± 1.11；影像變形程度爲 3.80 ± 1.20 和 2.62 ± 0.91；整體影像評分爲 3.68 ± 1.68 和 2.68 ± 0.77。

結論：

從初步研究的實驗結果可使我們更有信心去推廣全面性的核醫儀器品保規範。該研究仍持續進行至全台灣具指標性的核子醫學中心，盼望能在將來爲台灣核醫儀器品保標準貢獻微薄之力。

PB019

Multicenter Phantom Program for Image Quality Evaluation in Taiwan

Ming-Yuan Shih[1], Kuo-Wei Lee[1]

[1]*Health Physics Division, Institute of Nuclear Energy Research, Longtan, Taoyuan, Taiwan.*

Introduction: The aim of this study is to evaluate the image quality for routine usage of single photon emission computed tomography (SPECT) and positron emission tomography (PET) scanner by standard phantoms in Taiwan.

Methods: There are nine SPECT scanners and eight PET scanners belonged to 8 hospitals included in this study. Each hospital performed SPECT and PET imaging on the cardiac phantom, ACR's phantom, and our home-made spherical phantom. The scanning protocols were the same with the hospitals' clinical setting but the radioisotope activities were adjusted by phantom weight. Cardiac phantom with defects was used to simulate human diseased heart. ACR phantom has four sizes of cylinders for hot lesions on the top, six sizes of spheres for cold regions in the middle and six dimensions for evaluating resolution at the bottom. Six equal-size spheres (8 cc in volume) filled with radioactive liquid as hot lesions were placed circularly in spherical phantom. Image quality results were evaluated by both computer algorithms and human observer.

Results: Owing to the scanning protocols and reconstructing setting, it showed obviously different results in image quality among eight hospitals. Overall recommendations, such as minimum hot lesion size and alignment between CT and nuclear medicine image, have been made. Routine quality assurance items were also suggested.

Conclusions: Due to differences of instruments and built-in imaging parameters, variations in the image quality are ordinary. Proper quality assurance processes can provide intense progress in the future.

PB020

Extended Acute Toxicity Study of ^{188}Re-Human Serum Albumin Microsphere in Male Rats

Hsiao-Chiang Ni, I-Shu Huang, Ya-Jane Chang, Chung-Li Ho, Po-Yen Liu, Wan-Chi Lee, Hsiang-Lin Yu, Sheng-Nan Lo, Kuan-Yi Yeh, Cheng-Fu Chao, Liang-Cheng Chen, Su-Jung Chen, Chih-Hsien Chang, Te-Wei Lee

Institute of Nuclear Energy Research, Taoyuan, Taiwan

Abstract

Objectives: The objective of the present study was to investigate extended acute radiotoxicity of ^{188}Re-human serum albumin microsphere (^{188}Re-HSAM) in the SD male rat model.

Methods: Human serum albumin microspheres bought from Pharmalucence company. HSAM was labelled with ^{188}Re-BMEDA. Rats were intra-arterially administrated with ^{188}Re-HSAM (6.5, 4.5, 2.25 mCi), normal saline as a blank control and non-radioactive HSAM as a vehicle control. Mortality, clinical signs, food consumption, body weights, urinary, biochemical and hematological analyzes were examined for 28 days. In addition, gross necropsy and histopathological examinations were also performed at the end of the follow-up period.

Results: No clinical sign was observed in all the other rats. In the 6.5 and 4.5 mCi groups, the body weight increasing rate was significant lower to compare with the two control groups. There was the same trend in food consumption. The aspartate aminotransferase (AST/GPT) value of the 6.5 mCi groups was higher than the two control groups. There were no significant differences in urinary analyzes and hematology parameters. In histopathological assessments, the interlobular fibrosis, infarcted necrosis, bile duct hyperplasia and peripheral vascular inflammation of liver were dose-dependent.

Conclusions: The present study on extended acute toxicity of ^{188}Re-HSAM implied that the toxicity response was dose-dependent in SD rat model via intra-arterial route.

PB021

The In Vitro and In Vivo Evaluation of Radiolabeled-Human Serum Albumin Nanospheres in MDA-MB-231 Breast Cancer Model

Yuan-Ruei Huang, Ming-Syuan Lin, Chang-An Chen, Liang-Cheng Chen, Chih-Hsien Chang, Te-Wei Lee

Institute of Nuclear Energy Research, Taoyuan, Taiwan.

Introduction: The aims of this study were to explore the cytotoxicity of radiolabeled -human serum albumin nanospheres (HSANP) in MDA-MB-231 human breast cancer cell line, and demonstrated radiolabeled-HSANP may offer images for tumor.

Methods: Human serum albumin nanospheres were synthesized and labelled with ^{188}Re in Institute of Nuclear Energy Research (INER). Cytotoxicity assay was performed using 96-well plates. Each well was inoculated with 1×10^4 cells and incubated for 24 h to achieve 60–70% confluency. The serial dilutions of ^{188}Re-HSANP from 0 to 2 mCi were added to each well of 96-well plates, respectively. After 24 hours incubation with ^{188}Re-HSANP at 37°C, cells were washed twice with PBS and then added DMEM for another 24-hours incubation. We evaluated the viabilities of cells by alamarBlue assay. Tumor xenografts were produced in 6-wk-old female BALB/c nude mice by subcutaneous injection of 1×10^7 MDA-MB-231 cells, and used for ^{99m}Tc-HSANP nanoSPECT/CT imaging.

Results: The labeling efficiency of ^{188}Re-HSANP was more than 90%. The viabilities of MDA-MB-231 cells incubated with ^{188}Re-HSANP were 108.4 ± 3.9%, 115.2 ± 4.5%, 110.6 ± 3.4%, 112.0 ± 18.6%, 76.4 ± 5.3% and 40.47 ± 7.6% in 0.0625, 0.125, 0.25, 0.5, 1 and 2 mCi, respectively. NanoSPECT/CT imaging showed a ^{99m}Tc-HSANP accumulation in the MDA-MB-231 tumor.

Conclusions: This study showed that ^{188}Re-HSANP could suppress cell growth of MDA-MB-231 human breast cancer cell line and nanoSPECT/CT imaging showed ^{99m}Tc-HSANP was accumulated in the tumor. We are going to prove ^{188}Re-HSANP has the capability as radiotherapy drug for breast cancer in the future.

PB022

The Predictive Role of [^{18}F]FDG/PET/CT in Estimating the Fraction of Cancer Stem Cells in Thyroid Cancer Patients

Ya-Ju Hsieh[1], Fu-Sheng Teng[1], Lin-Rou Yu[1], Yaoh-Shiang Lin[2], Shiuh-Inn Liu[3], Ren-Shyan Liu[4], Nan-Jing Peng[5]

[1]Department of Medical Imaging and Radiological Sciences, Kaohsiung Medical University;
[2]Department of Otolaryngology, Kaohsiung Veterans General Hospital, Kaohsiung;
[3]Department of General Surgery, Kaohsiung Veterans General Hospital;
[4]Department of Biomedical Imaging and Radiological Sciences, National Yang-Ming University;
[5]Department of Nuclear Medicine, Kaohsiung Veterans General Hospital.

Abstract

Introduction: Thyroid cancer is the most common endocrine cancer and causes more deaths than all other endocrine cancers combined. Many evidences suggest that cancer stem cells (CSCs), which are highly resistant to standard chemotherapeutic agents and radiation, is a major driving force governing tumor recurrence and metastasis after cancer therapy. They display properties characteristic of stem cells and are in an undifferentiated status. As high uptake of FDG has been shown to be associated with poor differentiation and unfavorable prognosis, we hypothesize that tumor with higher proportion of CSC population would show higher glucose uptake and stem-cell specific gene expression than that with lower proportion of CSC population.

Materials and methods: [^{18}F]FDG/PET/CT scans were performed on patients with thyroid cancer and the maximum SUV values of tumors (SUV_{max}) were calculated. The tumor and normal thyroid tissue were obtained from each patient and prepared for total RNA extraction. The mRNA expressions of the CSCs marker (CD133) and stem cell marker (Oct4, Nanog) were measured via real-time PCR. The protein expression levels of different markers on tumor or normal tissue sections were evaluated by Immunohistochemistry (IHC).

Results: In all cases, the mRNA expressions of CD133, Oct4, Nanog were higher in thyroid cancer than that in normal thyroid tissue, whereas normal thyroid tissue showed higher expression of thyroid-specific gene. After IHC staining, CD133, Oct4, and Nanog positive signals were only observed in tumor but not in normal thyroid tissue, demonstrating the existence of CSCs in thyroid cancer. Moreover, [^{18}F]FDG/PET/CT imaging showed that thyroid tumor with higher mRNA expressions of CSC and stem cell-related genes would have higher SUV_{max}.

Conclusions: Our findings suggest that the proportion of CSCs in tumor may be associated with the ability of tumor FDG uptake. Therefore, the pre-therapeutic tumor SUV_{max} obtained from [^{18}F]FDG/PET/CT imaging may be a potential predictor for evaluating the proportion of CSC population in individual cancer patient.

PB023

An Automatic Synthesizer for Gallium-68-DOTATATE PET Radiopharmaceuticals

Ming-Hsin Li[1], Hsin-Han Hsieh[1], Han-Hsiang Chu[1]

[1]*Institute of Nuclear Energy Research.*

Introduction: Fast implementation of Ga-68-DOTATATE PET into clinical studies and research has resulted in high demands in the automated modules for the preparation of Ga-68-DOTATATE PET radiopharmaceuticals in a safe and reproducible process

Methods: The purpose of this study is to develop a fully automated controlled system for the synthesis of Ga-68-DOTATATE, with a compact synthesizer module. Main procedures of the process include: (1)absorption of Ga-68 cation; (2)reaction with DOTATATE ligand; (3) condition with C18 cartridge; (4)raw Ga-68-DOTATATE separation by C18 cartridge; (5) separation; (6)through 0.22um filter; and (7) collected in collection vial.

Results: The advantages of this fabricated synthesizer module are illustrated as follows. Firstly, the whole processes are operated in a closed system with a liquid nitrogen trapper used to condense the release gases of leaked radioactive material and organic solvent that can reduce the environmental radiation. Secondly, the assembly of the module is made as small as possible. Thirdly, this module is functioned with a fully automated control for synthesis of making Ga-68-DOTATATE. The process time is about 50mins.

Conclusions: The products obtained with purity of greater than 95% is sufficient to meet the requirements of the specifications for Ga-68-DOTATATE PET in nuclear medicine applications. Other than the previous statements, the software designed can be used to execute the process step by step precisely under the command to be called. During the process performance, the temperature, pressure and variation of radiation dose can be monitored and recorded simultaneously to reflect the reaction situation at that time and compliant with the regulation of GMP.

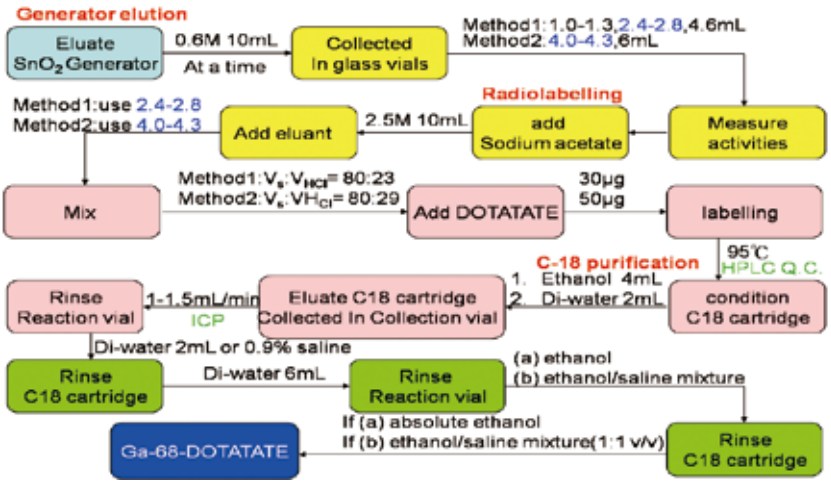

Automatic process

PB024

The Uptake Kinetic of [F-18]FEONM in Glioma Tumor-Bearing Mice

Jenn-Tzong Chen[1], Shu-Huang Lin[1], Kang-Wei Chang[1], Li-Yuan Huang[1], Yean-Hung Tu[1], Yin-Cheng Huang[2], Shiou-Shiow Farn[1], Wuu-Jyh Lin[1], Chyng-Yann Shiue[1,3,4]

[1]*Institute of Nuclear Energy Research, Taoyuan, Taiwan;*
[2]*Department of Neurosurgery, Chang Gung Memorial Hospital at Linkou, Chang Gung University, Taoyuan, Taiwan;*
[3]*National Taiwan University Hospital, Taipei, Taiwan;*
[4]*Tri-Service General Hospital, Taipei, Taiwan.*

Abstract

Objective: 2-(1-{6-[(2-[18F]fluoroethyl)(methyl)amino]-2-naphthyl}ethylidene)-malononitrile ([^{18}F]FDDNP) is a potent TauT and ABeta imaging agent in brain (Liu et al., 2007). In order to improve its lipophilicity and selectivity, we have synthesized 2-(1-{6-[(2-2'-[^{18}F]Fluoroethoxyethyl)(methyl)amino]-2-naphthyl}ethylidene)malononitrile ([^{18}F]FEONM) as a new Tau protein imaging agent (Chen et al., 2014). In addition to neurodegenative diseases, Tau protein also has been shown to be a potential predictive marker in cancer chemotherapy (Smoter et al., 2013) and was considered to be a target in cancer chemotherapy (Bhat and Setaluri, 2007). The objective of this study was to analyze the uptake kinetic of [^{18}F]FEONM in human brain tumor-bearing mice in comparison with normal mouse.

Method: [F-18]FEONM was synthesized as reported previously (Chen et al., 2014). The animals used in this study were two human U87 cell-bearing mice and one normal mouse. The PET scanner used for this study was NanoPET/CT (Bioscan, USA). The uptake of [^{18}F]FEONM in human U87 cell-bearing mice and normal mouse were performed for 1 hr post-injection. Regions of interest were defined on co-registrated PET/CT images using PMOD.

Results: The average uptake rate of [F-18]FEONM in human U87 cell-bearing mice was about 50% faster than that in normal mouse.

Discussion: The uptake kinetic of [F-18]FEONM on both human U87 cell-bearing mice and control were zero order within one hour PET imaging. Besides, the coefficients of determination of brain tumor mice were 0.9988 and 0.9997 respectively. The uptake kinetic rate echo our preliminary finding that [F-18]FEONM had higher uptake in glioma tumor of human U87 cell-bearing mice (Chen et al., 2014). The degree of [F-18]FEONM uptake in tumor may reflect the concentration of tau protein within the tumor and the aggressiveness of tumor. The uptake of other tau protein imaging agents in different tumors are under investigations.

Keyword: FEONM, Brain tumor, Tau protein, Uptake kinetic, PET.

References:

1. Bhat KMR and Setaluri V. 2007. Microtubule-associated proteins as targets in cancer chemotherapy. Clin Cancer Res. 13(10): 2849-2854.
2. Chen J.T., Lin S.H., Chang K.W., Huang L.Y., Tu Y.H., Huang Y.C., Farn S.S., Lin W.J., Shiue C.Y., 2014. Synthesis of 2-(1-{6-[(2-2'-[18F]Fluoroethoxyethyl)(methyl)amino]-2-naphthyl} ethylidene)malononitrile (FEONM) as a potential Tau protein imaging agent. Annual meeting of Taiwanese Society for Molecular Imaging, 42.
3. Liu J., Kepe V., Zabjek A., Petric A., Padgett H.C., Satyamurthy N., Barrio J.R., 2007. High-yield, automated radiosynthesis of 2-(1-{6-[(2-[18F]fluoroethyl)(methyl)amino]-2-naphthyl}ethylidene)malononitrile [18F]FDDNP) ready for animal or human administration. Mol. Imaging Biol. 9, 6-16.
4. Smoter M., Bodnar L., Grala B., Stec R., Zieniuk K., Kozlowski W., Szczylik C., 2013. Tau protein as a potential predictive marker in epithelial ovarian cancer patients treated with paclitaxel/platinum first-line chemotherapy. Journal of Experimental & Clinical Cancer Research 32:25. (OA).

PB025

The Antiproliferation Evaluation of ^{188}Re-human Serum Albumin (HSA) Microspheres in GP7TB Hepatoma Cell Line

Chung-Li Ho, Wan-Chi Lee, Su-Jung Chen, Chung-Yen Li, Te-Wei Lee

Institute of Nuclear Energy Research, Taoyuan, Taiwan.

Purpose: The aim of this study was to perform the antiproliferation study of ^{188}Re-human serum albumin microspheres (^{188}Re-HSAM) in GP7TB hepatoma cell line. The study was confirmed the inhibition effect of ^{188}Re-HSAM in GP7TB hepatoma cell line.

Methods: Human serum albumin microspheres bought from Pharmalucence company. HSAM was labelled with ^{188}Re by microwave method in Institute of Nuclear Energy Research (INER). Antiproliferative assay was performed using 6-well plates. Individual assay of 6-well plate was inoculated with 2 ml DMEM medium and 10% FBS containing 5×10^5 cells. All plates were incubated for 24 h to achieve 60–70% confluency. The serial dilutions of ^{188}Re-HSAM and ^{188}Re were added to each well of 6-well plates, respectively. The doses of ^{188}Re-HSAM and ^{188}Re were 0.1, 1, 10, 100 and 1000 μCi per assay. GP7TB cells were incubated with ^{188}Re-HSAM and ^{188}Re for 24 hour at 37°C. For 24 hours later, the cells were washed twice with PBS, and detached by 0.25% trypsin. The numbers of the alive cells were calculated.

Results: The size of HSA microspheres was distributed between 10~40 μm. The labeling efficiency of ^{188}Re -HSAM was more than 90%. The viabilities of GP7TB cells incubated with ^{188}Re-HSAM were 121.9 ± 2.3%, 93.8 ± 9.4%, 75.0 ± 2.3%, 49.9 ± 4.7% and 19.9 ± 2.0% in 0.1, 1, 10, 100 and 1000 μCi/ml, respectively. The viabilities of GP7TB cells incubated with ^{188}Re were 112.5 ± 0%, 114.8 ± 4.7%, 75.0 ± 13.0%, 67.7 ± 1.6% and 21.3 ± 0.5% in 0.1, 1, 10, 100 and 1000 μCi/ml, respectively. The viability of GP7TB cells incubated with HSAM was 103.1 ± 6.2%.

Conclusions: This study showed that ^{188}Re-HSAM could improve the antiproliferation in GP7TB hepatoma cell line and had the capability as radiotherapy drug for liver cancer.

PB026

Quantitative Distribution Study of Brown Adipose Tissue by ^{18}F-FDG

Po-Fan Chen, Ping-Yen Wang, Jyun-Yan Huang, Chung-Hsien Ho, Mei-Hui Wang

Division of Isotope Applications, Institute of Nuclear Energy Research, Atomic Energy Council, Taoyuan, Taiwan.

Introduction: More and more researches are interested in increasing brown adipose tissue amounts because brown adipose tissue functions to generate body heat and may be possibly relative to weight loss. In this study, we aim to setup a platform for molecular monitoring of brown adipose tissue in vivo by ^{18}F-FDG PET/CT imaging.

Methods: PET/CT scanning was performed for 20 min in male and female mice with cold exposure after 1 h intravenous injection of ^{18}F-FDG (150 u Ci) by tail vein. The π- pmod (3.5 version) was used to quantitate the amount of brown adipose tissue in the upper paravertebral region.

Results: The ^{18}F-FDG uptake and distribution is different between male and female. The total amounts was higher in female than in male, and the distribution was more at interscapular region in female, but more at supraclavicular region in male. The perirenal area was observed with more ^{18}F-FDG uptake in female than in male also.

Conclusion and Discussion: The ^{18}F-FDG uptake to the certain extent in brown adipose tissue using PET / CT has gender difference. The gender difference in ^{18}F-FDG molecular imaging demonstrated the activation in brown adipose tissue of female mouse was distinguished than male, which indicates female is a better model for further investigation of drug screening for weight loss. To be a platform for molecular monitoring of brown adipose tissue in vivo by ^{18}F-FDG PET/CT imaging, we will establish further the normal range of ^{18}F-FDG molecular imaging in female mice with cold exposure to provide the reference for strategy of weight loss and such drug screening.

PB027

Strategy on Rat Preparation for Pharmacokinetic Analysis of New Radiotracers

Hsiao-Ming Wu[1], Miao-Ling Tsai[1], Yu-Sha Hsueh[1]

[1]*School of Medicine, Fu-Jen Catholic University, Taiwan;*
FDG PET Studies Were Performed at Taipei Veterans General Hospital and Supported by Taiwan Mouse Clinic.

Introduction: New radiotracer developments for nuclear medicine imaging require analysis of blood as a function of time in small animals. Here, we report a procedure how we engineered a rat to ease radiotracer injection and blood sampling. The preparations allowed us perform pharmacokinetic studies on the same animal repeatedly.

Methods: Four rats were studied. Each rat underwent one aseptic microsurgery. We cannulated the right femoral artery and left femoral vein of the animal with subcutaneous indwelling catheters for blood samples and radiotracer injections, respectively. The blood patency of cannula was maintained by replacing flesh heparin in glycerol (500 IU/ml) once a week. Every week, a blood sampling procedure (18 < 1 μl samples in one hour or 24 in 2 hours) was performed on each animal. The animal was either under conscious or unconscious (i.e. under 2% isoflurane anesthesia) condition. The animal was euthanized by the end of two months. Body weight, blood pressure and blood glucose of the animals were recorded over time. In three rats, pharmacokinetic studies using FDG were performed. FDG was bolus-injected through the venous catheter; multiple blood samples (18 < 1 μl samples in one hour or 24 in 2 hours) were then taken from the arterial catheter using an automated microfluidic blood sampler. Eight additional large (~80 μl taken in 4 seconds) blood samples were also taken from a rat to derive plasma FDG curve. Pharmacokinetic analysis uses compartmental model analysis.

Results: The successful rate for FDG injections reached 100%. The blood sampling procedure was successful if only systolic blood pressure measured > 90 mmHg at the cannula. The total blood loss was < 250 μl for an 18-blood-sample, one-hour study. If large (e.g. eight ~80 μl blood samples) were also taken, the total blood loss was ~1 ml. The rats remained in good health (e.g. body weight double in two months) before being euthanized. Three-exponential decay fitted significantly better than two-exponential decay for blood FDG clearance. This result is comparable with those reported in the literature.

Conclusions: Our method of implanting indwelling catheters in rats was proven useful in performing pharmacokinetic analysis for a new radiotracer. The preparations in rat make bolus-injection easy and longitudinal studies possible. Similar blood-sampling technique can be used if metabolite-correction is necessary for a new radiotracer.

PB028

探討不同濃度射源強度對 SPECT 每日品質管制均勻度的影響

朱麗蓉[1] 鄭如金[1] 王淑芳[1] 李冠瑩[1] 詹勝傑[1]

[1] 基隆長庚紀念醫院 核子醫學科

前言：

目前，均勻度爲 SPECT 每日必要的品管項目，而內在均勻度可以直接測試閃爍晶體〈Crystal〉和電子元件的功能，由於 Tc-99m 射源每日取得方便，因此爲最常用來做品質管制 (Quality Control, QC) 的射源。Siemens E-CAM 爲國內常用的 SPECT 機型，根據 E-CAM 的操作手冊，QC 時射源強度不宜過高 (20-30 μCi)，但配置此濃度射源不易，造成操作上的困難；爲兼顧臨床實務的時效性，若可將 QC 的射源強度放寬，如此一來不用花太多時間調整劑量強度，就可達到品質管制的目的。

材料與方法：

此次所使用的伽瑪照相機爲 2007 年購入西門子公司 E-CAM。E-CAM 每日均勻度造影方式是採用內在均勻度，須在無準直儀的情況下將 Tc-99m 點射源放置在兩個偵測頭的中間，計數值收集至 30 * 10^6 counts。收集完成後，透過內建軟體的處理分析便可得到均勻度數值。爲了確認射源強度對於均勻度的影響，2015 年 1 月到 6 月間，我們實作 QC 時調配不同射源劑量，由於射源強度 73 μCi 時達到機器飽和計數的狀況，因此我們調配 20-60 μCi 濃度射源，並以每隔 10 μCi 當作間距，記錄均勻度的變化。

結果：

下表爲 2015 年 1 月到 6 月均勻度之平均值 ± 標準差，從中可觀察出 QC 射源強度 20-60 μCi，E-CAM 的內在均勻度數值均符合儀器操作手冊上的均勻度容許值標準，不同濃度射源所得到的均勻度統計上均無差異。（根據西門子的儀器操作手冊上的均勻度容許值爲 Center FOV Integral ＜ 2.94%、Center FOV Differential ＜ 2.54%，而 Useful FOV Integral ＜ 3.74%、Useful FOV Differential ＜ 2.74%。）

濃度	Detector 1 Central FOV intergral	Detector 1 Central FOV differential	Detector 1 Useful FOV intergral	Detector 1 Useful FOV differential	Detector 2 Central FOV intergral	Detector 2 Central FOV differential	Detector 2 Useful FOV intergral	Detector 2 Useful FOV differential
20	2.02±0.17	1.28±0.13	2.27±0.22	1.49±0.14	1.97±0.14	1.31±0.14	2.29±0.19	1.54±0.16
30	1.98±0.19	1.22±0.13	2.28±0.25	1.48±0.14	1.95±0.20	1.27±0.10	2.28±0.25	1.44±0.12
40	1.94±0.21	1.20±0.11	2.30±0.31	1.44±0.14	1.93±0.20	1.26±0.16	2.27±0.26	1.51±0.17
50	1.99±0.28	1.24±0.16	2.31±0.32	1.52±0.15	1.96±0.14	1.23±0.13	2.34±0.35	1.47±0.22
60	2.06±0.18	1.19±0.08	2.24±0.19	1.48±0.18	2.04±0.14	1.26±0.10	2.36±0.28	1.53±0.12

討論與結論：

透過此次的分析，可以發現即使射源劑量高達 60 μCi，E-CAM detector 均勻度的平均值仍與使用 20-30 μCi 差不多。因此爲兼顧臨床實務的時效方便性，可將 QC 的射源強度放寬，如此一來不用花太多時間調配劑量強度，便可監測儀器均勻度，提供正確影像的品質保證。

PB029

Analysis of Inter-Detector Scattering in PET with Various Energy Window Settings

Zih-Jie Wei[1], Hsin-Hon Lin[1], Keh-Shih Chuang[1]

[1]*Department of Biomedical Engineering and Environmental Sciences, National Tsing-Hua University, Taiwan.*

Introduction: In conventional small animal PET, an energy window of [350 650] keV is commonly used. The partial deposited energy of the annihilation gamma in the detector generates a so-called inter-detector scattering (IDS) triple events in PET. These events that contain useful information are often discarded since they are outside the conventional energy window. For enhancing the sensitivity, methods proposed for recovering such events usually rely on the chosen of maximum energy or are based on Compton-scatter kinematics with a wider window settings. In this work, the distribution of scattered IDS event using different identification techniques were investigated under various energy window settings.

Methods: GATE/GEANT4 simulation platform is used to study the research. The Monte Carlo (MC) model of Inveon preclinical PET scanner is developed. A ^{18}F uniformly filled cylinder phantom with activity levels of 0.01, 0.1 and 1.0 mCi are used to evaluate the true IDS to true double ratio and the scattered IDS to scattered double ratio with various energy window settings. For evaluating the distribution of scattered IDS and comparing it with the scattered double, a shifted line source of 0.25 mCi ^{18}F inside a cylinder phantom is simulated.

Results: The true IDS/true double ratio and scattered IDS/scattered double ratio are independent of activity. Besides, NECR increased with the increase of the lower limit of energy window. The scattered IDS distribution identified by ME method was similar to scattered double. By contrast, the scattered IDS distribution identified by KNS method differed from scattered double.

Conclusion: In this work, we found that the selection rule is effective to eliminate scattered IDS events, while including most of true IDS events. The accuracy of the identification techniques not only affects the distribution of true IDS events but also the scattered IDS events. Hence, the inclusion of the wrongly recovered IDS into double coincidence may introduce additional error when scatter correction method, such as single scatter simulation, is performed. The quantification of the errors on reconstructed image needs further investigation.

PB030

導入風險管理觀念的人員體外輻射劑量監測紀錄評估研究 —以南部某醫院核子醫學科爲例

陳素英[1] 卓世傑[2] 蕭莉茹[1] 林秋美[1] 陳怡如[1] 陳宜伶[1] 古琴鳳[1] 鍾相彬[1]

[1] 高雄醫學大學附設中和紀念醫院核子醫學科
[2] 永康奇美醫院核子醫學科

背景介紹：

2012 年 ISO-15189 提出風險管理 (Risk Management)，嘗試將此風險管理的觀念，導入人員體外輻射劑量監測紀錄的評估。研究發現，可提供改善輻射工作人員接受職業曝露時之輻射安全問題。

方法：

本研究爲收集南部某醫院核子醫學科 102 年 1 月～ 104 年 8 月造影室放射師之 (1) 深部劑量、(2) 淺部劑量、(3) 肢端劑量，將其資料整理，並將整理出之資料以 EXCEL 畫出柱狀圖。另，評估其資料相關輻射安全問題。

結果：

(1) 102 年 5 月起，指環劑量計更換爲晶片。更換後數據明顯不同，即顯示原本之指環劑量計功能可能失效。(2) 放射師 E 與 H 之肢端輻射劑量高於其他放射師，顯示手部之作業程序可能有異常，導致其肢端劑量均偏高。(3) 放射師 H 於 104 年度因懷孕狀態，深部、淺部與肢端均顯示背景輻射劑量。(4) 放射師 G 之深部、淺部輻射劑量均較高於其他人，其工作性質爲核醫藥物接收與調配，故其接受之輻射曝露最高。

結論：

藉由監測人員體外輻射劑量紀錄評估，研究發現：(1) 指環劑量計功能可能失效問題，影響輻射工作人員的輻射安全至鉅，持續監控劑量紀錄是必要的。(2) 檢討放射師 E、H 之手部作業流程可能異常，如有錯誤或缺失必須進行矯正並改善。(3) 依游離輻射防護法之精神，放射師 H 因懷孕略做工作調整，所以深部、淺部與肢端均顯示爲背景輻射劑量。(4) 放射師 G 之工作性質爲核醫藥物接收與調配，其接受之輻射曝露最高。依游離輻射防護安全標準規定，其劑量在限值之下，故不需調整其工作內容或工作量。由以上研究顯示如能以風險管理的觀念進行評估，將有助於醫學品質程序的落實與改進，並從根本上減少問題的產生。

BP031

探討不同稀釋液對高濃度 CEA 測定的影響

盧永承　杜東峻

戴德森醫療財團法人嘉義基督教醫院 核子醫學科

目的：

Cisbio Bioassays CEA-RIACT 試劑套組有提供專用的稀釋液，成分是由 Human plasma、sodium azide 及 EDTA 所組成，稀釋後的數據依其原廠說明書應做結果的校正 探討原廠稀釋液、蒸餾水及生理食鹽水對高濃度 CEA 測定的影響，以及改良原廠公式後的應用。

方法：

收集 20 例高濃度 CEA 檢體，濃度分布在線性範圍內約 100~200 ng/ml 之間的檢體，分別用原廠稀釋液、蒸餾水及生理食鹽水稀釋 10 倍後測定，並同時與原血清檢體測定結果相比較。而稀釋液濃度原廠認定爲 2 ng/ml CEA，因此所得之結果需以公式 (value read off-(9/10 * 2)) * 10 ng/mL 進行校正。同批次實驗會同時測定稀釋液的濃度，以取代公式中 2 的濃度，做爲改良的公式用。所有回乘 10 倍的結果，與原檢體測定結果相比，計算其 Bias%，計算方式爲：(回乘 10 倍的結果 - 原檢體測定結果) / 原檢體測定結果 *100%。

結果：

實驗室自行求得稀釋液的濃度爲 0.7 ng/ml，因此改良後的公式爲 (value read off-(9/10 * 0.7)) * 10 ng/mL。兩個公式校正後與各回乘的結果與原檢體測定的差距結果如下：

	平均值 ng/ml	平均 Bias%	最大 Bias%	最小 Bias%
原檢體測定結果	140.08	--	--	--
原廠稀釋液	118.41	-16.9%	-21.4%	5.2%
原廠改良公式	130.11	-6.8%	-10.7%	2.7%
蒸餾水	161.56	16.7%	28.1%	10.0%
生理食鹽水	147.19	5.7%	12.4%	2.9%

結論：

CEA 是使用最普遍的癌症指標，可用來監測癌症的病情進展及治療後的復發。在平常 Cisbio CEA 試劑操作中，發現稀釋後的數據有偏低的情況，於是此次來探討不同稀釋液對高濃度 CEA 測定的影響，經研究發現，依原廠稀釋液產生的結果確實有明顯偏低情況，而以蒸餾水稀釋後的結果則明顯偏高，雖然研究樣本太少、稀釋倍數太高以及單管操作等可能造成研究的誤差，但依此結果，認爲最好的稀釋方式則是使用由 Human plasma 等所組成的稀釋液來做稀釋，並依實驗室自己求得稀釋液中 CEA 的濃度來做校正，才是最理想的。

PB032

乳房專用正子攝影儀之隨機與散射特性研究

倪于晴[1] 詹美齡[2] 林志崑[1] 黃莉婷[1] 王士彥[1]

[1] 核能研究所 保健物理組
[2] 長庚大學放射醫學研究院

背景介紹：

核研所乳房專用正子攝影儀可近距離掃描乳房，具有高靈敏與高解析度之特色。然而隨機計數與散射計數仍有可能影響影像品質。本研究透過擬人假體模擬乳房掃描實驗，分析來自造影範圍 (FOV) 內外各器官對乳房造影之隨機計數與散射計數貢獻，做爲後續校正方法研究的參考。

方法：

造影系統爲兩相對 180 度之平面偵檢器 (196.8×98.4 mm^2)，由 1.64×1.64×10 mm^3 的 LYSO 晶體組成，以下實驗兩偵檢器間距皆爲 120 mm。利用 XCAT 擬人假體模擬上半身軀幹，乳房附近器官之 F-18-FDG 活度設定爲乳房 2.5 kBq/ml、心臟 22.7 kBq/ml、肝臟 7.9 kBq/ml、肺臟 3 kBq/ml、肌肉 2.58 kBq/ml (參考法國里昂大學的 oncoPET_DB 資料庫)。趴式造影受測乳房下垂位於 FOV 內，身體其他器官位於 FOV 外。另側乳房被撐住緊貼身體，本研究忽略不計。左右乳房分別造影，造影時間各爲 300 秒，能量窗設定爲 350~650 keV。本文實驗數據皆透過 GATE 蒙地卡羅模擬環境執行、記錄發射自各器官被偵檢器接收的計數值，並分析其貢獻比率。

結果：

左乳 (右乳) 掃描實驗中有 29.9% (25.6%) 隨機分率及 34.1% (33.3%) 的散射分率，FOV 外身體的隨機分率總貢獻爲 27.7% (23.4%)，而散射分率總貢獻爲 5% (4.2%)。

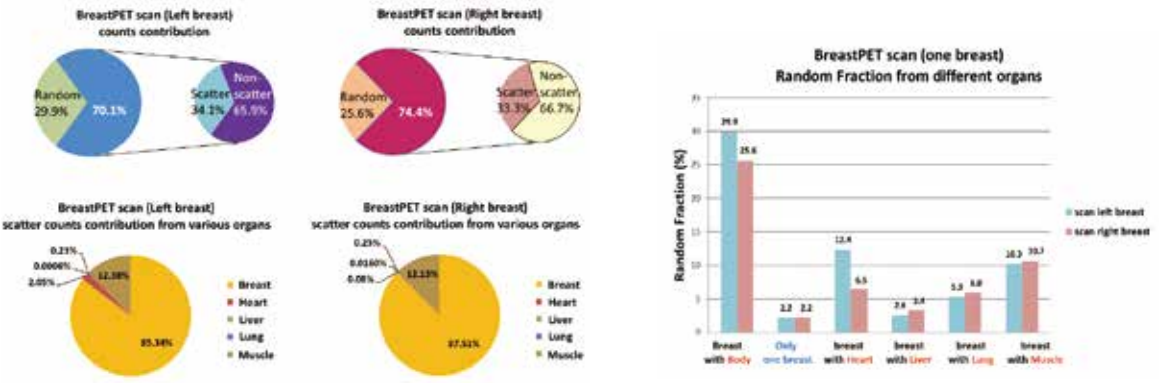

結論：

利用擬人假體模擬乳房專用正子攝影儀掃描實驗，可獲得 FOV 內外各器官之隨機計數與散射計數光子貢獻。系統可利用 delay circuit 濾除隨機計數，降低心臟及肌肉造成的隨機計數干擾；散射計數主要貢獻來自受測乳房，FOV 外其他器官貢獻可忽略。後續乳房專用正子攝影儀的散射校正方法設計將聚焦於受測乳房本身，以提高乳房影像 TNR(tumor-to-normal tissue ratio) 定量精確度。

PC001

Colon Cancer with Solitary Spermatic Cord Metastasis: A Case Report

Bor-Tau Hung, Pei-Wen Wang, Chien-Chin Hsu,
Yung-Cheng Huang, Yen-Hsiang Chang, Shu-Hua Huang

Department of Nuclear Medicine, Kaohsiung Chang Gung Memorial Hospital and Chang Gung University College of Medicine, Kaohsiung, Taiwan.

Abstract

Malignant lesions of the spermatic cord are very rare, and metastatic carcinoma of the spermatic cord is extremely unusual. We herein report a rare case of solitary metastasis to the spermatic cord from colon cancer. A 72-year-old male who had undergone a right hemicolectomy for stage II colon cancer 4 years ago had abnormal CEA (10.9 ng/ml) during regular follow-up. Positron Emission Tomography (PET) was performed and disclosed a hypermetabolic lesion in right inguinal region. Three months after PET scan, right inguinal palpable mass was found and the patient underwent surgical intervention. The histological examination of right spermatic cord revealed adenocarcinoma, consistent with metastasis from colon cancer. Although unusual, it is important to include metastatic lesion in the spermatic cord arising from colon cancer in the differential diagnosis, as resection of such lesions might improve patient survival.

PC002

Normal Variations of ^{18}F-FDG-PET SUVmax of Bilateral Postcricoid Regions between Healthy People and Head and Neck Cancer Patients

Bo-Ming Tzeng[1], Yi-Ting Shih[2], Shu-Chane Shen[1], Chao-Yang Men[1], Chien-Chang Lu[1]

[1]Department of Nuclear Medicine, St. Martin De Porres Hospital, Chiayi; Taiwan;
[2]Department of Radiation Oncology, St. Martin De Porres Hospital, Chiayi.

Purpose: To evaluate the normal variations of ^{18}F-FDG-PET maximum standardized uptake value (SUVmax) of bilateral postcricoid regions which consists of bilateral posterior cricoarytenoid muscle and inferior constrictor muscle between healthy people and head and neck cancer patients.

Materials and Methods: A total of 100 people, composed with 53 people for healthy examination and 47 patients for head and neck cancer study received ^{18}F-FDG-PET/CT examination between October 2012 and May 2014. Patients with hypopharyngeal or laryngeal malignancy were excluded. SUVmax of bilateral postcricoid region at 60 minutes after injection of ^{18}F-FDG were collected. We investigated normal variations of SUVmax of bilateral postcricoid regions between healthy people and patients with head and neck cancer. The optimal cutoff value of SUVmax was determined by receiver-operating-characteristic method.

Results: The SUVmax of bilateral postcricoid regions is from 1.61 to 5.51 in right side and 0.02 to 6.03 in left side. Fifteen healthy people had SUVmax of right postcricoid region ≧ 2.3 and 38 healthy people < 2.3. Thirty-four head and neck cancer patients had SUVmax of right postcricoid region ≧ 2.3 and 13 patients < 2.3. Similarly, 16 healthy people had SUVmax of left postcricoid region ≧ 2.3 and 37 healthy people < 2.3. Thirty head and neck cancer patients had SUVmax of left postcricoid region ≧ 2.3 and 17 patients < 2.3. The distribution of normal SUVmax of bilateral postcricoid regions is different in healthy people and head and neck patients ($p < 0.001$ in right side and $p = 0.002$ in left side by Yates's correction for continuity).

Conclusion: Most patients with head and neck cancer had higher normal values of SUVmax of bilateral postcricoid regions compared with healthy people.

PC003

PET/CT 檢查床升降之病人安全問題

曾柏銘[1] 呂建璋[2] 沈淑禎[2] 門朝陽[1] 林雅婷[1] 薛欣宜[3] 葉聿謙[4]

[1] 財團法人天主教聖馬爾定醫院正子造影中心
[2] 財團法人天主教聖馬爾定醫院核子醫學科
[3] 樹人醫護管理專科學校
[4] 財團法人亞東紀念醫院

前言：

隨著國人生活條件愈來愈好，資訊傳遞也愈來愈發達，對於醫療安全層面也日漸重視，但由於正子中心爲特殊輻射單位，注射高能量的 F-18 FDG，該單位之高輻射量常常令醫事放射師憂心其輻射傷害，故請病患上檢查台時，常會使用小樓梯請病患自行走上去以減少醫事放射師曝露的時間。在檢查台在不降下來的情況下請病患自行走上去難保不會發生意外，且自行上樓梯也未必會提升病患躺床之速度。故本實驗將收集 40 位病患，將檢查台升起至檢查高度 (H128, Early phase)，以及檢查台下降至最低位置 (H500, Delay phase) 去研究，看所花費的時間是不是相鉅甚大。

方法：

本實驗使用 40 位健保病患，每一病患 (不能行走之病患除外) 在 Early Phase 時皆以小梯子之方式上下檢查台 (H:128)，在 Delay Phase 時則改將檢查台降至最低 (H:500)，再由醫事放射師將檢查台升起，以碼錶按壓方式從病患進攝影室至檢完畢出攝影室，去估算病患在上下床時所花費之時間。

討論：

醫事放射師爲了降低病患注射 F-18 FDG 所帶來的曝露，請病人上檢查台的方式也跟著有所變化，其中又以請病患自行上檢查台的方式爲最多。一般認知認爲病患自已上檢查台能有效的降低與病患接觸的時間，但實際上請病患自行上檢查台既緩慢，又有跌倒之風險，而將檢查台降低則可大大免除此問題。實驗結果其 P > 0.05，確實有顯著之差異

	成對變數差異					顯著性 (雙尾)
	平均數	標準差	平均數的標準誤	差異的 95% 信賴區間		
				下界	上界	
成對 1 H:128 上床 - H:500 上床	9.425	14.151	2.237	4.899	13.951	.000
成對 2 H:128 下床 - H:500 下床	9.050	10.089	1.595	5.823	12.277	.000

結論：

自行上檢查台與放射師親自將檢查台升起所耗的時間延長許多，推論可能因檢查台較高且較小，病患得使用更久的時間才能躺平，另一個原因則是病患不熟悉檢查床的臥躺方法。但，將檢查台降低，表面上醫事放射師會接受更多的輻射劑量，但實際上卻能以差異不大的時間，獲得更多的病人安全。

PC004

單光子電腦斷層掃描於骨骼掃描之應用：判讀淋巴結鈣化而非骨轉移

劉芝庭　莊雅雯　朱秀蘭　蔡亦欣　許玉春

高雄醫學大學附設中和紀念醫院核醫科

背景介紹

核醫骨骼掃描是目前唯一可以進行全身骨骼癌症轉移的篩檢工具，其敏感度比 X- 光高 30-40%，且發現病灶的時間可以比 X- 光提早 3-6 個月，更由於具有高敏感度及早期偵測骨骼病灶的能力。優點是描繪器官功能狀態，但缺乏解剖上精確定位過去一直是其極限之一，雖其靈敏度極高，看到許多功能性「熱點」，有時候這些熱點是在骨骼上、在內臟裡、在淋巴結，但因身體前後器官重疊，在平面影像上無法區分病灶位置，若進一步搭配使用單光子電腦斷層掃描 (Single Photon Emission Computed Tomography, SPECT/CT)，結合功能性與解剖性兩種造影，將兩組影像融合可精確定位功能代謝異常的病灶，還可以廣泛用在特定檢查的衰減校正，以達到更符合眞實的影像品質與診斷結果。

病歷報告

一位 40 歲男性，在 2012 年確診爲左大腿的骨骼系統之外間質軟骨肉瘤，定期於本科進行骨骼掃描。在 2015 年 2 月的骨骼掃描中，呈現正常的影像。在 2015 年 7 月的骨頭掃描中，發現在正面影像的右邊第二對胸肋軟骨接合處上有熱點，在側面影像卻是在靠近第三根肋骨上有熱點，疑似骨轉移。因在平面影像上無法確認病灶位置，便進一步搭配使用單光子電腦斷層掃描，藉由 SPECT/CT 的影像中可以確認並不是在骨頭的位置上，而是在右肺門中的淋巴結鈣化處，而非骨轉移。

結論

骨骼掃描是針對全身骨骼癌症轉移之篩檢相當重要且最常用的工具，但因身體前後器官重疊，在平面影像上無法區分病灶位置。隨著近年來核醫儀器的進展，傳統閃爍造影機可與單光子電腦斷層掃描進行影像結合，提供解剖定位更精確之融合影像，提高骨骼掃描判讀的正確性及臨床價值。

PC005

利用 ^{123}I-MIBG 鑑別帕金森氏症和多發性系統退化症

陳沛穎[1] 林虔睦[1,2] 楊哲銘[1,2,3]

[1] 臺北醫學大學部立雙和醫院核子醫學科
[2] 臺北醫學大學醫學系放射線學科
[3] 臺北醫學大學醫務管理學系暨研究所

背景介紹：

帕金森氏症 (Parkinson's disease, PD) 是一種中樞神經系統退化性疾病，多發性系統退化症 (Multiple system atrophy, MSA) 以呈現兩種以上神經系統退化症狀而得名。因兩者臨床表現類似，需較有臨床經驗醫師方能做出準確判斷，故本病例利用 ^{123}I-MIBG 照影胸部以鑑別診斷 PD 與 MSA。

方法：

受檢者從檢查前一天至檢查後一天，連續三天服用 Lugol's，一天三次、每次 3 c.c，藥物注射前請受檢者平躺 30 分鐘後，將 3 mCi ^{123}I-MIBG 注入生理食鹽點滴瓶 (100 ml) 內，於靜脈緩慢注射 5 ～ 10 分鐘，注射 20 分鐘後，掃描早期 (Early) 胸部前位靜態平面像 (Static view) 5 分鐘；注射 3 ～ 4 小時後，掃描晚期 (Delay) 胸部前位靜態影像 5 分鐘。圈選心臟與縱膈腔之 ROI，將兩者所得 counts/pixel 數相除，得一 H/M (Heart to mediastinum) 值。

結果：

影像無心臟顯影，Early H/M 值爲 1.18、Delay H/M 值爲 1.32，影像判讀偏向 PD。

討論：

Braune, S. 等人研究中，PD 群組病患相較於 MSA 病患 H/M 值相對較低 ($p < 0.002$)，PD H/M 值平均 1.08、標準差 0.13；MSA H/M 值平均 2.03、標準差 0.39。

結論：

此一檢查方式只需一般 SPECT 儀器及簡易的分析程序，價格相較於 ^{18}F-FDG PET/CT 低廉、也比 ^{18}F-DOPA PET/CT 較易鑑別 PD 及 MSA。

PC006

Malignant Sarcomatous Transformation from Osteochondroma Showed Low- metabolism on ^{18}F-FDG PET/CT

Po-Yin Chen[1], Nan-Jing Peng[1,2], Gin Hu[1]

[1]Department of Nuclear Medicine, Kahsiung Veterans General Hospital, Kaohsiung, Taiwan;
[2]National Yang-Ming University, School of Medicine, Taipei, Taiwan.

Abstract:

A 44-year-old man has the history of osteochondromatosis (familial exostosis) s/p excision of bony tumor lesions over left distal femur and proximal tibia. After 7 years, he suffered form right hip pain and ^{18}F-FDG PET/CT was performed to survey. Multiple sessile or pedunculated exostoses was noted, and the largest one (> 10 cm in size) is arising from right iliac ala with much soft tissue component, which shows uneven mild FDG uptake (SUVmax: early 2.1, delayed 2.0). Then he accepted the surgery of tumor removal and chondrosarcoma (grade 1) was diagnosed histologically.

Osteochondroma accounts for nearly 40% of benign bone tumors and 10% of all primary skeletal tumors. A rapid increase in size of the lump and/or pain in a previously asymptomatic osteochondroma arouses the suspicion of malignant transformation. Plain radiography, CT scan, and MRI have been widely used for the initial evaluation and for confirming the clinical suspicion of a malignant transformation of osteochondromas.

In some studies shows the higher histological type of chondrosarcoma may have higher glucose metabolism and it explains why this case have no glucose hypermetabolism.

PC007

Asymmetry of Thyroid Gland on I-131 Scan Might Imply Thyroid Cancer

Li-Fang Lin[1], Shu-Hsing Cheng[2]

[1]Department of Nuclear Medicine, Taoyuan General Hospital, Ministry of Health and Welfare, Taoyuan , Taiwan;
[2]Department of Internal Medicine, Taoyuan General Hospital, Ministry of Health and Welfare, Taoyuan, Taiwan.

Introduction: Thyroid cancer typically appeared as cold nodule on I-131 thyroid. But thyroid cancer could be massed if the cold nodule is located at poles.

Case Report: A 35-year-old woman received chest CT for survey of fever source. An incidental nodule with calcification at right upper pole of thyroid was suspected to be thyroid cancer. Then I-131 thyroid scan reveal complete absence of right upper pole, which looks just like asymmetry in the bilateral lobes. The pathology of the cold nodule is papillary thyroid cancer.

Conclusion: The incidence of malignancy in a cold nodule is 10%. When a cold nodule is surrounded by normal thyroid tissue, the identification is not difficult. But it could be misleading if the cold nodule is exactly located at the poles. In most people, the right lobe is slightly longer than the left one1, or the bilateral lobes are symmetry. To interpret I-131 thyroid scan appropriately, correlation with anatomical studies is warranted.

PC008

Scintigraphic Findings of Incidental Muscle Metastases: 2 Case Reports

Li-fang Lin[1], Tzu-Yi Chuang[2], Wei-Jie Wang[2]

[1]*Department of Nuclear Medicine, Taoyuan General Hospital, Ministry of Health and Welfare, Taoyuan , Taiwan;*
[2]*Department of Internal Medicine, Taoyuan General Hospital, Ministry of Health and Welfare, Taoyuan , Taiwan.*

Introduction: Although muscle accounts 50% of body mass, muscular metastases is not commonly detected and prone to be ignored. In the literature, muscular metastases could happen in cancers of head and neck, thyroid, lung, GI tract and prostate, whereas lung cancer is the most prevalent.

Case report 1: The 63-year-old man had squamous cell lung cancer (cT3N2M1), with metastases to lung, brain, muscle, nerve and bone. He once received radiotherapy for neoplastic lumbosacral plexopathy involving right sciatic nerve and bone metastases in the left shoulder and right pelvis. He was hospitalized for fever and dizziness. Ga-67 scan revealed concurrent intense Ga-67 uptake in the right pelvic wall, right proximal thigh. Correlated to CT, these Ga-67 avid lesions were muscular metastases.

Case report 2: The 67-year-ld man has prostate cancer with bone metastases. He was suffering from left thigh swelling for 1 month, so he received Tc-99m RBC venography for suspected deep vein thrombosis. Huge hyperemic masses in the left hip and left buttock were noted on both arterial and venous phase. These mass was proved to be muscular metastases by following CT.

Conclusion: Muscular metastasis is related to poor prognosis but tends to be under-diagnosed, because patients may not feel pain or are even asymptomatic. Awareness of abnormal soft tissue tracer uptake is very important.

PC009

Subacute Thyroiditis Manifests as Fever of Known Origin in A Young Man

Li-Fang Lin[1], Chien-Yu Cheng[2]

[1]*Department of Nuclear Medicine, Taoyuan General Hospital, Ministry of Health and Welfare, Taoyuan , Taiwan;*
[2]*Department of Internal Medicine, Taoyuan General Hospital, Ministry of Health and Welfare, Taoyuan , Taiwan.*

Introduction: Subacute thyroiditis is less common in young men and seldom presented as fever of unknown origin (FUO). Ga-67 scan plays a role to seek the etiology.

Case repot: The 30-year-old man without underlying disease and had been hospitalized twice for intermittent fever. He denied history of animal contact, travel abroad, and unprotected sexual behaviors. Laboratory studies such as microorganism culture, factors of autoimmune and rheumatoid disease were negative. Because his fever didn't resolve, he underwent Ga-67 scan. Intense Ga-67 uptake in the neck was revealed. Subacute thyroiditis was diagnosed with following thyroid echography and a suppressed TSH level (0.008 mIU/L).

Conclusion: Subacute thyroiditis more commonly occurs in young woman and causes typical symptoms like weight loss, heat intolerance, or occasional neck pain. Though rarely, subacute thyroiditis could manifest as fever of known origin (FUO) and leads to confusion with infectious diseases. Different from infectious diseases, subacute thyroiditis is mostly self-limited. Ga-67 scan helps to investigate the focus of fever and avoid unnecessary antimicrobial medication.

PC010

Poor Correlation between Estimated GFR by Equations and Tc-99m DTPA Renogram in Spinal Cord Injury Patients: Experience in A Regional Hospital

Li-Fang Lin[1], Wai-Keung Lee[2], Sheng-Ping Lee[3], Jung-Hsing Li[1]

[1]Department of Nuclear Medicine, Taoyuan General Hospital, Ministry of Health and Welfare, Taoyuan , Taiwan;
[2]Department of Physical Medicine and Rehabilitation, Taoyuan General Hospital, Ministry of Health and Welfare, Taoyuan, Taiwan;
[3]Department of Urology, Taoyuan General Hospital, Ministry of Health and Welfare, Taoyuan, Taiwan.

Introduction: Estimated GFR (eGFR) via serum creatinine and equations like Modification of Diet in Renal Disease (MDRD) had been found to be less reliable to spinal cord injury (SCI) patients. Chronic Kidney Disease Epidemiology Collaboration (CKD-EPI), which had take account into parameters such as age and race, is considered to the more accurate to objects without SCI (non-SCI). In a veterans cohort study, addition of a correction factor of 0.7 for MDRD (MDRD-SCI/D) is proposed to prevent overestimation. Our retrospective study aims to determine the correlations between GFR measured by Tc-99m DTPA renogram (mGFR) and eGFR in SCI and non-SCI patients.

Methods: Demographic data, mGFR and eGFR of 30 SCI and 13 non-SCI patients were analyzed. Correlations between mGFR and eGFR by MDRD, by CKD-EPI and by MDRD-SCI/D were verified.

Results: Poor correlation between mGFR and eGFR by MDRD, by CKD-EPI and by MDRD-SCI/D is observed in SCI patients. Conversely, good correlation is seen in non-SCI patients (MDRD-SCI/D is not applicable and thus not performed.)

Pearson correlations tests between mGFR and eGFR			
Group	MDRD	CKD-EPI	MDRD-SCI/D
SCI	0.232	0.272	0.230
Non-SCI	0.883	0.874	N/A

Conclusion: GFR measured by Tc-99m DTPA renogram is considered to be the gold standard but rarely applied in clinical practice due to more inconvenience than estimated GFR by equations. Although there is good correlation in non-SCI patients, overestimation of eGFR in SCI patients may delay the diagnosis of renal function insufficiency.

PC011

Diffuse Large B-cell Lymphoma Presents as A Huge Paraspinal Mass on A Ga-67 Scan

Li-Fang Lin[1], Jung-Hsing Li[1]

[1]*Department of Nuclear Medicine, Taoyuan General hospital, Ministry of Health and Welfare, Taoyuan , Taiwan.*

Introduction: Diffuse large B-cell lymphoma (DLBCL) is a great mimicker with variable imaging manifestations. But new diagnosed DLBCL with bone destruction is rare.

Case Report: The 89-year-old man was a nursing home resident and going to be transferred to medical center due a huge incidental right paraspinal mass on MRI. On the day he was prepared for transferal, he suddenly lost his consciousness, and was sent to our hospital. Results of laboratory studies and chest X-ray suggested septic shock, so he was admitted to ICU. Tc-99m MDP bone scan shows small hot spots in bilateral ribs, intense liver uptake and a suspicious osteolytic lesion having a photopenic center with heterogeneous peripheral tracer uptake. Ga-67 inflammation scan shows intense Ga-67 uptake in the lower lobe of left lung, liver, and notably, a huge mass at right pelvis. But there are no lymphadenopathies in the neck, chest and abdomen on CT. The pathology of surgical biopsy of the right paraspinal mass is DLBCL, while bone marrow biopsy revealed no lymphoma involvement.

Conclusion: Ga-67 is a traditional tumor agent to lymphoma and more commonly used to detect infection focus in the age of FDG PET/CT. Nevertheless, lymphoma must be the included in the differential diagnosis of tumor with intense Ga-67 uptake.

PC012

Intense [^{18}F] Fluorodeoxyglucose Uptake In a Bronchial Artery Aneurysm, Mimicking Malignancy – A Case Report

Jei-Yie Huang[1], Hsien-Li Kao[2], Ching-Yao Yang[3], Yeun-Chung Chang[4], Rouh-Fang Yen[1], Kai-Yuan Tzen[1], Mei-Fang Cheng[1]

[1]Department of Nuclear Medicine, [2]Internal Medicine, [3]Surgery, and [4]Medical Imaging and Radiology, National Taiwan University Hospital and National Taiwan University College of Medicine, Taipei, Taiwan.

Abstract

FDG PET/CT provides functional data on tumor metabolism and has been widely used in evaluation of malignancy. However, it is well known that non-neoplastic tissues can uptake FDG and mimic neoplasm. Aneurysm with FDG uptake is mostly reported in abdominal aortic aneurysm (AAA), with increased FDG distribution in the vascular wall, representing inflammation.

Bronchial artery aneurysm (BAA) is a rare but potentially fatal entity, caused by weakening of vessel wall and increased blood flow to the bronchial arteries. Diagnosis of BAA is by identifying a vascular origin on chest CT and selective bronchial arteriography.

We represent a patient with history of gastric gastrointestinal stromal tumor status post laparoscopic wedge resection. [^{18}F] Fluorodeoxyglucose PET/CT showed moderate hypermetabolism at upper stomach and local tumor recurrence was suspected. Another round area of intense hypermetabolism was found at aorto-pulmonary window (SUVmax = 20.4). Secondary primary of malignancy, was highly suspected. However, contrast-enhanced chest CT revealed the CT density of the mass (2.8 cm) was identical to blood in the aorta. This finding was interpreted to be more consistent with an aneurysm, rather than a metastatic tumor. Subsequently, angiography was performed and supported the diagnosis of a BAA.Coil embolization was performed afterward.

This case emphasizes the importance of careful evaluation of clinical history and other imaging studies when an atypical site of metastasis was demonstrated by FDG PET/CT.

PC013

Gallium Scan: A Case with PJP Infection and Behcet's Colitis

Tzyy-Ling Chuang[1], Yuh-Feng Wang[1,2]

[1]*Department of Nuclear Medicine, Buddhist Dalin Tzu Chi Hospital, Chia Yi, Taiwan;*
[2]*School of Medicine, Tzu Chi University, Hualien, Taiwan.*

Introduction: We present a case with coexistence of pulmonary PJP infection and Behcet's colitis shown in gallium scan.

Case report: A 21-year-old female had a history of Behcet's disease diagnosed in 2009, and juvenile rheumatoid arthritis diagnosed in 2010. She presented with chills, high fever, and general soreness. Laboratory tests showed WBC: 18,440/ul (seg. 90.5%). Urinalysis showed no pyuria. Blood and stool cultures showed no growth. Gallium scan showed diffusely intense uptake of bilateral lungs, typical pattern of PJP infection, and a fixed focal uptake at RLQ abdomen since 6 hours images. Chest radiography showed bilateral increased infiltration. CT showed R/O Behcet's colitis at RLQ abdomen, and interlobular septal thickening with areas of ground-glass opacity and interstitial change in bilateral lungs. Bronchoscopic transbronchial lung biopsy showed only few neutrophils and lymphocytes, but there are GMS(+) microorganisms with intracystic dots found within the fibrinoid foamy exudate; a pneumocystis pneumonia should be firstly considered.

Discussion: PJP is one of the most common causes of infection in patients with immunocompromised condition, including HIV infection or other diseases with immunosuppressive drugs, such as ulcerative colitis, rheumatoid arthritis, systemic lupus erythematosus, bone marrow transplantation and Behcet syndrome. The case of PJP infection in Behcet syndrome had been reported on the literatures; however, the coexistence of pulmonary PJP infection and Behcet colitis found at the gallium scan is first reported. Indeed, the gallium scan is a powerful infection hunter even in such an immunocompromised patient without other evidence of infection source.

PC014

Unusual Lymphedema: A Case of Lymphoma

Tzyy-Ling Chuang[1], Yuh-Feng Wang[1,2]

[1]*Department of Nuclear Medicine, Buddhist Dalin Tzu Chi Hospital, Chia Yi, Taiwan;*
[2]*School of Medicine, Tzu Chi University, Hualien, Taiwan.*

Introduction: We present a case of recurrent diffuse large B cell lymphoma, who initially presented as left lower leg lymphedema.

Case Report: A 64-year-old male had diffuse large B cell lymphoma of right testis (stage IEA, IPI 0) and received right orchiectomy in 2009. Subsequently , he received CHOP, rituximab and radiotherapy with complete remission. Recently, he had redness and skin rashes with left lower extremity swelling for two weeks. Cellulitis was suspected and antibiotics was failed. Deep vein thrombosis (DVT) or lymph node obstruction was suspected. A sonogram showed subcutaneous edema without DVT evidence. Tc-99m phytate lymphoscintigraphy showed left lower leg dermal backflow consistent with left lower extremity lymphedema. A FDG PET/CT study showed left external iliac and left inguinal lymph nodes, multiple subcutaneous lesions at the left thigh and especially at the left lower leg which were highly suspicious for malignant lesions. A skin excisional biopsy showed diffuse large B-cell lymphoma. The skin lesions subsided after chemotherapy.

Discussion: Lymphedema, also known as lymphatic obstruction, is a condition of localized fluid retention and tissue swelling caused by a compromised lymphatic system. Tissues with lymphedema are at risk of infection. Dermal backflow in lymphscintigraphy is a feature of lymphedema. Lymphoma and its treatments put patients at risk for secondary lymphedema (as opposed to primary lymphedema which is hereditary), even after the lymphoma goes into remission. In our case, his skin lesions and swelling subsided after chemotherapy, suggestive that correct diagnosis with FDG PET/CT and lymphscintigraphy as useful tools.

PC015

放射免疫分析實驗室內外部品管表現之分析及探討

廖建國[1] 張素雲[1] 薛予婕[1] 莊紫翎[1] 王昱豐[1,2]

[1] 佛教大林慈濟醫院核子醫學科
[2] 慈濟大學醫學系

背景：

內部及外部品管作業，爲醫學實驗室重要的流程，攸關檢驗數據的正確性，因此大多數實驗室會將內部品管及外部品管之表現訂定相關指標，以定期監控檢驗品質。本研究目的即爲分析本科近三年之內外部品管表現，以作爲持續改進之參考。

方法：

回溯性收集 2013 年至 2015 年 (1-6 月) 之內外部品管指標監測值及其相關異常資訊，分別依不同年度及項目異常情形進行分析，並比較不同年度之品管表現，以了解實驗室檢驗品質是否有所進步。

結果：

在外部品管方面，2013 年外部品管異常率 (2.5%) 最高，其次爲 2014 年 (1.8%) 及 2015 年 (0.6%)，顯示外部品管異常比率有明顯的改善 (圖 1)。其中異常件數以 AFP 及 TSH (各 2 件) 佔最多，其次爲 cortisol、ferritin、prolactin、T4 (各 1 件) (圖 2)。而在內部品管方面，各年度之異常率排序分別爲 2013 年 (0.36%)、2014 年 (0.2%) 及 2015 年 (0.15%)，顯示內部品管異常率亦有逐年下降之趨勢 (圖 1)。其中異常件數以 CA 15-3 (3 件) 及 thyroglobulin (2 件) 佔最多，而 CA 19-9、AFP、PSA、cortisol、TSH、prolactin 及 T3 等項目則各佔 1 件。由異常項目來看，近三年內部及外部品管都曾出現異常之項目包括 AFP、cortisol、TSH、prolactin 等 4 項，其中較值得注意的是 AFP 之外部品管曾因試劑運送溫度問題於同年度 (2013 年) 發生 2 次異常，此異常在改善試劑溫度後至今未再發生結果超出可接受範圍之情事。此外，cortisol、ferritin 及 prolactin 等 3 項 2014 年至 2015 年 (1-6 月) 出現外部品管異常，但 2013 年卻未發生異常，此部份值得再繼續監控品管表現。

結論：

分析結果顯示，本科實驗室近三年之內部及外部品管表現，均有逐年的進步。其中外部品管呈現大幅的改善，但 cortisol、ferritin 及 prolactin 等 3 項近兩年曾出現外部品管異常，應繼續監控其品管表現，以持續提升檢驗品質。

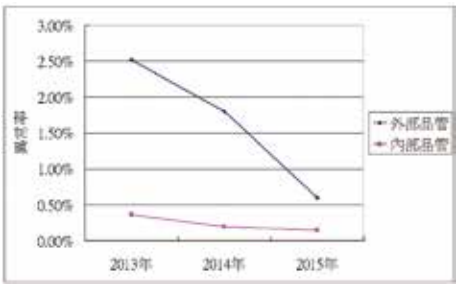

圖 1. 2013-2015 年 (1-6 月) 外部品管異常率

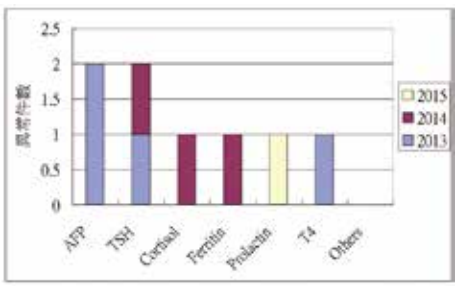

圖 2. 2013-2015 年 (1-6 月) 外部品管異常項目

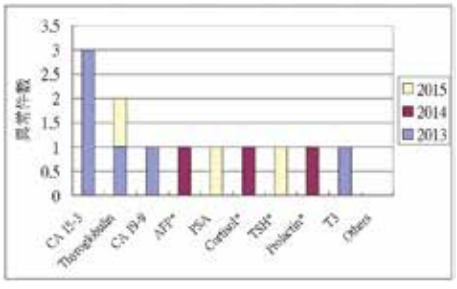

圖 3. 2013-2015 年 (1-6 月) 內部品管異常項目
(*：內部及外部品管都曾出現異常)

PC016

運用 HFMEA 改善核醫造影品質之初步成效分析

廖建國[1] 許幼青[1] 蘇淨儀[1] 莊紫翎[1] 王昱豐[1,2]

[1] 佛教大林慈濟醫院核子醫學科
[2] 慈濟大學醫學系

背景：

醫療照護失效模式與效應分析 (HFMEA) 爲醫療界使用的一種預防性的系統風險分析工具，廣泛應用於改善醫療作業流程。本科已於 2013 年以 HFMEA 手法評估核醫造影作業流程之失效模式及可能原因，本研究目的即爲分析導入 HFMEA 後之初步成效，以作爲改善策略之參考。

方法：

依 HFMEA 危害分析方法，針對之前決定之優先改善流程 (表 1)，進行發生頻率 (表 2) 與嚴重度 (表 3) 之評估，危害指數以發生頻率與嚴重度之乘積計算，比較改善前後之危害指數，以探討導入 HFMEA 兩年後之初步改善成效。

表 1. 優先改善項目風險評估結果

潛在失效模式(結果)	潛在失效模式(原因)	改善前危害分析			決策樹分析(Y/N)				決策類
		發生率	嚴重度	危害指數	單個弱點	現有控制	可明顯察覺失效	是否繼續	排除/控制/接受
排程疏失	疏忽排錯	4	4	16	→	N	N	Y	控制
藥物疏失	訂藥疏漏	4	4	16	→	N	N	Y	控制
造影前準備不當	金屬異物未清除	4	4	16	→	N	N	Y	控制
	病人未排尿	4	4	16	→	N	N	Y	控制
	病人排尿不乾淨	4	4	16	→	N	N	Y	控制
	病人未配合要求(禁食或停藥)	4	4	16	→	N	N	Y	控制

表2. HFMEA發生頻率分類

分 類	分 數	定 義
經常 (frequent)	4	預期很短時間內會再發生或1年內發生數次
偶而 (occasional)	3	很可能再次發生或1-2年內發生幾次
不常 (uncomnon)	2	某些情況下可能再次發生或2-5年內發生1次
很少 (remote)	1	很少發生，只在特定情況下發生或5-30年內發生1次

表3. HFMEA嚴重度分級

分　類	分　數	定　義
嚴重	4	病人因非疾病因素死亡或永久性功能喪失
重度	3	病人因非疾病因素造成永久性功能減低
中度	2	病人因非疾病因素造成短期功能障礙
輕度	1	病人雖發生意外，但未造成任何傷害也無需額外的醫療照護

註：嚴重度之判定以可能發生或造成影響之最嚴重情況判定

結果：

改善前各項目之危害指數均爲 16，改善後危害指數有明顯改善者，分別爲疏忽排錯 (8)、訂藥疏漏 (8)、金屬異物未清除 (8)、病人未排尿 (8)、病人未禁食或停藥 (8)，而病人排尿不乾淨 (16) 則因少數病人不願意接受導尿，而無法完全排除 (圖 1)。回顧檢討本科以 HFMEA 評估造影作業流程，找出 8 項潛在的失效模式 (包括檢查單開立不常、排程疏失、衛教不當、候檢時間過長、藥物疏失、造影前準備不當、造影條件不正確、未注意病人移動安全、未注意檢查結束之病人安全、影像品質不佳、報告疏失)，並分析其根本原因，再由找出的 32 項原因中選定 8 項優先改善之項目，此爲系統性的檢視整個作業流程，並透過品保會議的全員參與及討論而達成，其中也運用到 RCA 及 TRM 的品質改善工具，初步改善成效值得肯定。

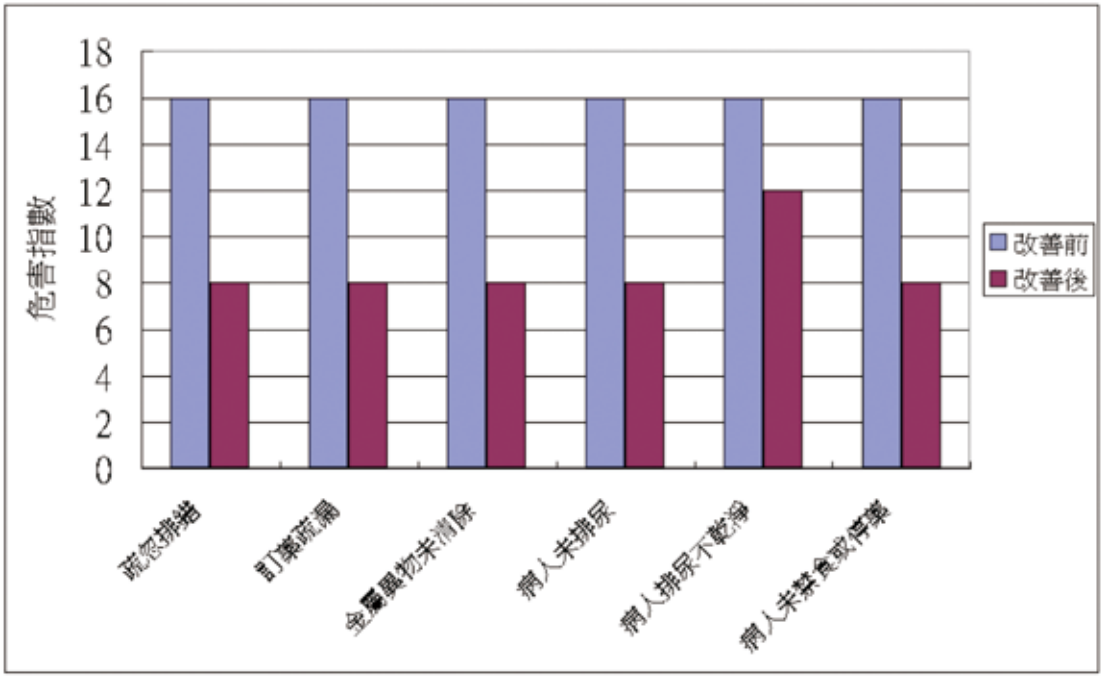

圖 1. 改善前後危害指數比較

結論：

本科以 HFMEA 改善造影作業流程之初步成效顯著，有助於持續改善造影品質。管理階層可適當運用 HFMEA 工具，找出作業流程中潛在的失效模式及原因，並加以改善。

PC017

醫造影報告異常通報分析及探討

廖建國[1] 許幼青[1] 莊紫翎[1] 王昱豐[1,2]

[1] 佛教大林慈濟醫院核子醫學科
[2] 慈濟大學醫學系

背景：

當影像檢查結果出現危急值或重要異常值時，由核醫醫師即時通知臨床醫師處置，這樣的通報機制對於提升診療品質及病人安全有很大的幫助。近年來，本科例行以電話進行通報作業，而未建立電子通報機制。本研究目的即爲分析近三年之通報結果，並探討電話通報方式的優劣，以作爲持續改善之參考。

方法：

收集 2013 年 1 月至 2015 年 6 月間，影像檢查有特殊發現或重要異常結果，核醫醫師通報臨床醫師之個案。如：臨床上診斷爲良性疾病，檢查結果懷疑有潛在惡性可能；心臟檢查卻發現肺部有問題等。依不同月份計算件數，並分析比較不同年度之通報件數以及各項目之分佈情形。

結果：

總計收集 75 件通報個案，平均每月通報件數爲 3.3 件，其中通報件數最多爲 2013 年 2 月 (13 件)，其次爲 2014 年 12 月及 2015 年 4 月 (各 7 件)，而件數最少的爲 2014 年 10 月 (0 件)，各月份之通報情形，並無明顯的規則性，顯示通報件數不會因爲季節不同而呈現不同的變化 (圖 1)。另外，比較不同年度之通報件數，發現雖然 2015 年較 2014 年略有成長，不過各年度之變化不大。在通報項目方面，發現心肌灌注掃描佔最多 (37%)、其次爲骨骼掃描 (35%) 以及 shunt (8%)，這樣的分佈應和作業量有關，其中心肌灌注掃描多於骨骼掃描和其他檢查，可能由於心肌缺血等心臟異常問題較須立即通報臨床醫師知悉。此外，以電話通報的方式，由於可以線上與臨床醫師溝通，並解答其疑問，對於接受通知的醫師而言，是較理想且滿意的通報方式。不過，其缺點爲核醫醫師必須於通報後完成記錄，增加額外的工作，另外這樣的通報方式可能並不適用於作業量非常大的醫院。

結論：

分析結果顯示，近三年平均月通報件數均不超過 10 件，各年度間變化不大，也無季節性的影響。本院以電話進行通報作業，深受臨床醫師肯定，也無通報後須檢討回覆率的問題，較電子通報理想，應可繼續維持作業。

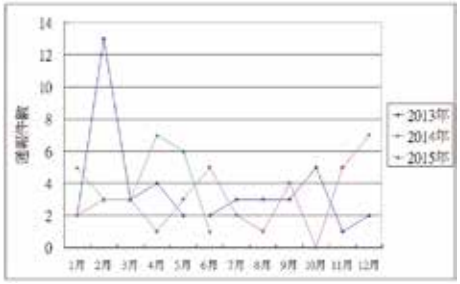

圖 1. 不同月份核醫造影異常通報件數變化

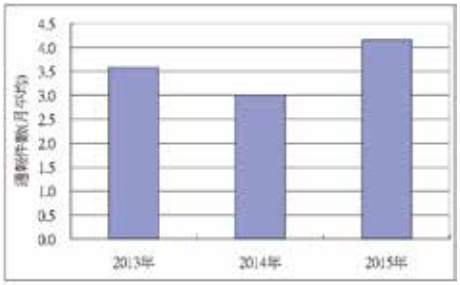

圖 2. 不同年度核醫造影異常通報件數比較

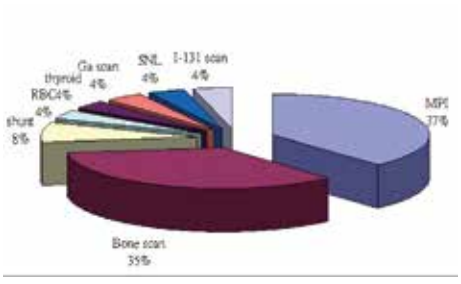

圖 3. 核醫造影異常通報項目分佈

PC018

運用 ISO 15189 打造優質核醫造影檢查服務—SNQ 參賽經驗分享

廖建國[1] 廖志恆[2] 許幼青[1] 張素雲[1] 莊紫翎[1] 王昱豐[1,3]

[1] 佛教大林慈濟醫院核子醫學科
[2] 全國認證基金會
[3] 慈濟大學醫學系

背景介紹：

國家生技醫療產業策進會 (生策會) 每年舉辦 SNQ 國家品質標章認證，期望做爲孕育品質力量的搖籃，致力打造傲人醫療及幸福台灣。2014 年本科以「運用創新與用心—打造優質核醫造影檢查服務」申請參賽並獲獎 (圖 1)。本文目的即爲整理參賽之過程及心得，提出經驗分享。


SNQ國家品質標章證書
CERTIFICATE OF SYMBOL OF NATIONAL QUALITY
運用創新與用心-打造優質核醫造影檢查服務
參加 2014 SNQ國家品質標章 醫療院所類/醫院醫事服務組 評鑑活動，
經大會評審委員會評選，決議通過認證，特此證明。
有效期限：中華民國104年12月31日止
This is to certify that Using a Creative and Considerate Scheme for Offering our Excellent Imaging Services of [redacted] has been awarded The Symbol of National Quality in the Medical Service Section, Hospital Category by Institute for Biotechnology and Medicine Industry.
Date of Validity: Until Dec. 31st, 2015

圖 1. SNQ 國家品質標章獲獎

選定主題：

本科近年來依據全國認證基金會 (TAF) 頒布之「醫學檢驗室認證規範 - 品質與能力要求」(ISO 15189)、「醫學領域之核子醫學影像檢查技術規範」及「醫學領域之核子醫學影像檢查對應 ISO 15189 使用指引」，建立造

影作業之品質管理系統，其目的即爲打造優質核醫造影檢查服務，因此選定此一主題參加醫療院所類醫院醫事服務組競賽。

撰寫計畫：

根據生策會之審核流程 (圖 2)，初審階段爲申請計畫書審查，複審階段則爲簡報審查。因此撰寫申請計畫書爲參賽中最重要的步驟，其內容包括營運資料 (院所簡介、營運現況、未來規劃、社會公益) 及申請項目說明 (專科簡介、結構面、過程面、結果面) 等二大部份。其中申請項目說明爲主要闡述專科服務品質的部份，內容如下：(1) 專科簡介包括中、英文簡介各 300 字及機構與專科照片；(2) 結構面包括服務目標與定位、人力結構：質與量、儀器設備：質與量及安全性、環境與空間規劃：光線、空氣、動線、寬敞度、安全性等；(3) 過程面包括特色及創新性、標準化、執行率、團隊合作、品管機制、資源整合；(4) 結果面包括安全性、服務質量、滿意度、正負面效果：(例如：正確率與不良事件發生率等)、社會評價、研究成果及應用 (包括學術論文發表) 等。

圖 2. SNQ 國家品質標章審核流程

參賽心得：

申請 SNQ 國家品質標章認證，其實只是將平日運用 ISO 15189 改善造影品質的成果及優點整理出來，透過 SNQ 評審團隊的認證，獲得第三者的肯定，這就如同參與全國認證基金會 (TAF) 的認證或其他品質系統的驗證。在準備的過程中，可以針對各項內容或要求，進行檢視與檢討改善，因此無論申請何種認證，都是提升作業品質的一種方式或工具，尤其對於企圖追求卓越品質的團隊，可以考慮透過第三者公證單位的評審，證明所提供的服務符合國家或國際品質的標準。

結論：

依據本科的經驗，運用 ISO 15189 可以打造優質的核醫造影檢查服務，對於提升造影作業之管理及技術品質頗有助益。各醫院可依據各別的需求，適時導入 ISO 15189 提升造影品質，未來有需要時也可以透過認證獲得肯定。

PC019

運用顧客回饋意見及 PDCA 改善報告傳送之正確性－個案報告

廖建國[1] 張素雲[1] 薛予婕[1] 林淑靜[1] 莊紫翎[1] 王昱豐[1,2]

[1] 佛教大林慈濟醫院核子醫學科
[2] 慈濟大學醫學系

背景介紹：

放射免疫分析完成後，數據經由儀器端之介面電腦傳送至醫院醫療資訊系統 (HIS) 之程序，爲醫檢師例行重要的工作之一。一般而言，報告經由電腦間的傳送，發生錯誤的機率非常低，除非電腦系統發生問題。本文目的即爲整理本科改善報告傳送錯誤之策略及結果，提出個案報告。

個案報告：

2015 年 6 月本院腸胃內科醫師來電反映，某位病人之 HBeAg 報告內容爲空白，經負責醫檢師查證後，迅速修正報告，並提報不符合事項。此不符合事項，經檢討後由品質主管運用 PDCA 改善循環工具擬訂改善計畫，並進行追蹤檢討。其中改善策略爲加強報告審查作業 (由項目負責人每週檢視報告) 及建立抽查機制 (由品質主管每月隨機抽查報告)，經追蹤三個月後，已無類似異常發生 (表 1)，因此將改善措施納入「資訊系統管理作業程序」。依照 ISO 15189 5.10.3 (g) 之規範要求，「意圖從實驗室外部資訊系統 (例如，電腦系統、傳眞機、電子郵件、網站、個人網際裝置) 直接接受資訊，實驗室應就檢驗結果、與其有關的資訊與備註 (如電子式與由電腦輸出副本有關時) 之重製的正確性加以查證。」雖然儀器端介面電腦之性能，已於儀器安裝時完成測試及查證，實際作業時，也很少發生報告傳送錯誤問題，但發生問題時仍應檢討其根本原因，並加以改善。此案例經品質主管利用院內檢驗管理系統，系統性的查證，發現過去也曾有部份錯誤，因此針對問題進行檢討改善。另外，電腦傳送異常之問題，雖然發生頻率甚低，每次發現問題時，也皆立即向資訊室反映，但是仍無法完全避免類似問題發生，因此在改善策略的訂定上，目前仍須依靠實驗室同仁的協助，藉由控制手段，提早發現問題，並進行補救，以降低報告錯誤對於病人安全的影響。

交辦來源：顧客回饋意見	負責單位:放射免疫分析實驗室
改善事項：報告傳送錯誤	
P 計畫(PLAN)： **現況分析：** 1、放射免疫分析後之數據，須經由儀器端之介面電腦傳送至醫療資訊系統(HIS)，傳送前醫檢師須先審查報告後，再執行傳送動作。 2、此次異常為 2015/06/03 臨床醫師反映 HBeAg 發出之報告，其欄位內無數值。 3、報告內無數值之可能原因為 (1)尚未發報告 (2)因電腦系統問題導致傳送失敗	
確認問題： 經查此次為已發出之確認報告，因此發生原因為電腦系統之問題，造成傳送失敗。	
預期目標： 預防再發生類似異常	
擬定改善措施： 一、加強報告審查作業，由項目負責人每週檢視報告。 二、建立抽查機制，由品質主管每月隨機抽查報告。	
D 執行(Do)： 一、由項目負責人每週檢視發出之報告是否正確，以確認傳送後之數據與 HIS 是否一致。 二、由品質主管每月隨機抽查報告，以加強報告傳送後的確認，並追蹤檢討改善情形。	
C 效果確認(Check)： 一、 隨機抽查各檢查項目(皆含 HBeAg)，7-9 月份分別抽查計 12、14 及 10 項，正確率均為 100%。 二、 連續追蹤三個月，未再發生類似異常。	
A 行動〈標準化/殘留問題〉(Action)： 一、將報告抽查機制納入「資訊系統管理作業程序」，以加強報告傳送異常之發現，維持資訊系統的正常運作。 二、電腦傳送異常之問題，雖於每次發現時，皆立即向資訊室反映，但仍無法完全避免電腦系統異常之發生，因此目前必須藉由控制手段，提早發現問題，並進行補救，以降低報告傳送錯誤所造成的影響。	

表 1. PDCA 循環改善計畫表

結論：

本案例針對報告傳送錯誤之問題，擬訂加強報告審查作業 (每週檢視) 及建立抽查機制 (每月抽查) 之策略，初步追蹤之改善成效良好。運用顧客回饋意見及 PDCA 循環工具，改善作業系統中的問題，的確有助於提升醫療品質。

PC020

高血鈣症導致詭異的骨骼掃描影像

許幼青[1] 莊紫翎[1] 廖建國[1] 陳薇璇[1] 王昱豐[1,2]

[1] 佛教大林慈濟醫院核子醫學科
[2] 慈濟大學醫學系

背景介紹：

高血鈣症是常見之代謝急症，其臨床症狀常與血鈣之高低程度有關，主要發生的原因分別是原發性副甲狀腺功能過高或者是惡性腫瘤相關因素，特別是鱗狀細胞癌 (例如頭頸部腫瘤、食道癌、肺癌等)，約 20-30% 的癌症患者在其疾病發生過程中會出現高鈣血症的情形，高鈣血症的嚴重度，以血中鈣濃度爲準，將高鈣血症的嚴重度分爲：1、輕度：血中鈣濃度爲 2.6 - 2.9 mmole /L (10.5-11.9 mg/dL)，2、中度：血中鈣濃度爲 3.0 - 3.4 mmole /L (12.0-13.9 mg/dL)，3、重度：血中鈣濃度爲 3.5 mmole/L (14.0 mg/dL) 以上。我們報告的這一位患者，因左側頰鱗狀上皮細胞癌來執行全身骨骼掃描，意外發現高血鈣症。

病例報告：

一位 48 歲中年男性，患者本身有左側頰鱗狀上皮細胞癌之病史，開刀後並進行放射治療療療程結束，104 年於本院執行全身骨骼掃描及 SPECT/CT，影像結果呈現分別於心臟、兩側肺葉以及胃部皆有攝取較多活性，故高度懷疑有三種可能性，第一種：急性心肌梗塞，第二種：副甲狀腺機能亢進，第三種：高血鈣症等因素所造成之詭異的骨骼掃描影像，建議抽血檢驗檢查關於副甲狀腺功能、血鈣及心臟等部分。檢驗檢查之結果 PTH-I：2.54 pg/mL、Ca：4.36 mmol/L、BUN：94 mg/dl、CRE：2.76 mg/dl，符合高血鈣症。

結論：

患者臨床症狀出現厭食、倦怠、全身軟弱以及噁心嘔吐，往往找不出任何原因，但在執行全身骨骼掃描中，常會有意外的發現，就如高血鈣症導致詭異的骨骼掃描影像。全身骨骼掃描可以幫助我們進一步執行抽血檢驗，可讓此患者得知是因爲血鈣過高引發其他詭異的骨骼掃描影像，可幫助臨床醫師發現患者出現的臨床症狀是因爲高血鈣症所導致，故降高鈣血症的處置，才會延緩病患的存活期，且高鈣血症才不易復發。

PC021

全身 Ga-67 掃描意外偵測肌肉膿瘍

許幼青[1] 莊紫翎[1] 廖建國[1] 陳薇璇[1] 王昱豐[1,2]

[1] 佛教大林慈濟醫院核子醫學科
[2] 慈濟大學醫學系

背景介紹：

鎵離子的特性與鐵離子相似，故進入人體內的運輸、攝取、儲存、代謝與鐵離子相似，且與血液中的攜鐵蛋白結合而停留於細胞內。鎵 -67 會在發炎感染處聚積，在臨床上可協助尋找感染或其它發炎性病灶，例如診斷骨髓炎、膿瘍、軟組織感染或有不明原因發燒等症狀。

病例報告：

一位 74 歲男性，本身有高血壓糖尿病病史，因爲高燒不止則進行血液培養，報告結果顯示爲金黃色葡萄球菌，醫師安排無打顯影劑之全身電腦斷層檢查，看有無任何感染或膿瘍，報告結果爲右側腰大肌有膿瘍的情形，進一步抽吸，內容物似血腫，培養顯示無金黃色葡萄球菌。會診感染科醫師建議安排全身 Ga-67 炎症掃描，看何處有感染或膿瘍，報告結果顯示爲左側下咽喉、頸部、胸壁、鎖骨及胸骨等處有活性攝取的情形，對照電腦斷層影像，發現有被疏漏膿瘍的可能性，故再次安排抽吸培養左側胸大肌，結果顯示金黃色葡萄球菌。

結論：

如本個案因全身電腦斷層檢查無打顯影劑之故，影像判斷有困難，而隨著時代的進步，珈瑪攝影機的解像力跟著提升，若再搭配 SPECT/CT 掃描則影像分析的效果會出乎意料之外，全身 Ga-67 掃描對於炎症評估的敏感度及特異性都較以前增加。

PC022

SPECT/CT 顯示膀胱遮蔽之尾骨病灶

張秀瑛[1] 莊紫翎[1] 許幼青[1] 廖建國[1] 王昱豐[1,2]

[1] 佛教大林慈濟醫院核子醫學科
[2] 慈濟大學醫學系

背景介紹：

全身骨骼掃描所施打的藥物爲 Tc-99m MDP，其代謝路徑乃由膀胱所代謝出體外，故檢查流程中有一重要環節則是造影前準備流程：檢查前需請患者排空膀胱，以減少膀胱尿液量，及減少骨盆內骨骼構造被尿液遮蔽，以提升影像品質。然而全身骨骼掃描爲平面式的影像，勢難以從平面影像中偵測出被膀胱尿液遮蔽的病灶，問題病灶可能會有所疏漏，此時若搭配執行單光子電腦斷層 SPECT/CT 檢查，可將轉換成 3D 立體影像，便可發現平面疏忽的可能臨床重要之病灶點。

病例報告：

一位58歲男性，因喝酒引發肝細胞癌，本身有高血壓及良性前列腺肥大的情形，有背痛超過6個月的情形，並接受手術及一連串的化學治療及放射治療，之後開始接受全身骨骼掃描及電腦斷層做日後的追蹤。102 年於本院執行骨骼掃描中，平面影像中發現：右側第 10 根肋骨外側方、第五腰椎之左側椎弓根處以及右邊髂骨有活性攝取，執行單光子電腦斷層 SPECT/CT 檢查時，意外發現左側薦椎及尾椎有活性攝取。薦椎及尾骨是最容易被膀胱擋住的骨頭，對於有症狀或前列腺的患者，若多執行側位像或許會有意外的發現。

結論：

全身骨骼掃描造影前準備流程非常重要，因其代謝路徑是從膀胱代謝出體外，所以往往於常規的平面影像上無法詳細區分膀胱附近之骨骼是否有病灶，但若針對有症狀或前列腺的患者，增加側位像則可避免前位像和後位像所疏漏的病灶，且對臨床醫師的後續的治療有很大的幫助。

PC023

鋼琴黑鍵般特殊形態的壓迫性骨折

陳薇璇[1] 許幼青[1] 張秀瑛[1] 莊紫翎[1] 王昱豐[1,2]

[1] 佛教大林慈濟醫院核子醫學科
[2] 慈濟大學醫學系

背景介紹：

全身骨骼掃描是核子醫學科常見的檢查之一，具有高敏感性，當病灶早期血流增加或成骨細胞活動增強時，可以藉由全身骨骼掃描清楚看到病灶，如癌症骨轉移、原發性骨腫瘤、骨折、代謝性骨病變。而外傷的病患要區分爲骨鬆性骨折或病理性骨折，有一定的難度，此時可藉全身骨骼掃描來做鑑別診斷。病理性骨折有可能是癌細胞轉移，或者是骨髓瘤等原因，而當骨骼產生蝕骨樣病變，造成骨骼疼痛，一般人容易誤以爲是外力導致，常常延誤治療的時機。

病例報告：

一位 65 歲女性，曾子宮外孕、沾黏性腸阻塞、子宮肌瘤切除。今年 4 月份因跌倒送醫，經 X 光檢查後，發現在 L3、L4 有壓迫性骨折，給予止痛治療後，仍持續背痛導致行動困難，於是臨床醫師安排磁振造影及全身骨骼掃描。經磁振造影檢查結果發現在 T10、T12、L2 到 L5 有急性的壓迫性骨折，而全身骨骼掃描則表現出第 6 根肋骨有活性攝取，且在 T10、T12、L2 到 L5 呈現特殊的橫線狀活性攝取，而被判斷有病理性骨折之可能，建議進一步檢查是否爲癌細胞轉移。病患於 6 月接受 T10、T12、L2 的椎體成形術，骨髓穿刺之病理報告證實爲漿細胞骨髓瘤 (plasma cell myeloma)。

結論：

壓迫性骨折一般來說都是由外力或者是骨鬆等原因所造成，但因全身骨骼掃描的影像中其型態特殊，而有不一樣的結果。骨鬆造成的壓迫性骨折，常會看到脊椎呈連續性之橫線狀的活性攝取；若是脊椎呈間隔性之橫線狀的活性攝取，則要考慮病理性的骨折的可能性。漿細胞骨髓瘤是一種惡性的腫瘤，會產生蝕骨樣病變，導致骨骼疼痛，常會被誤診爲背痛、骨質疏鬆等，搭配全身骨骼掃描來篩檢，往往會有意想不到的發現。

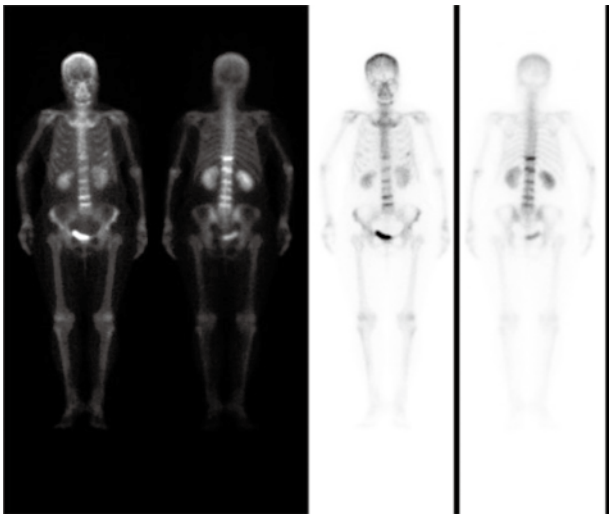

圖一：全身骨骼掃描表現出第 6 根肋骨有活性攝取，且在 T10、T12、L2 到 L5 呈現特殊的橫線狀活性攝取。

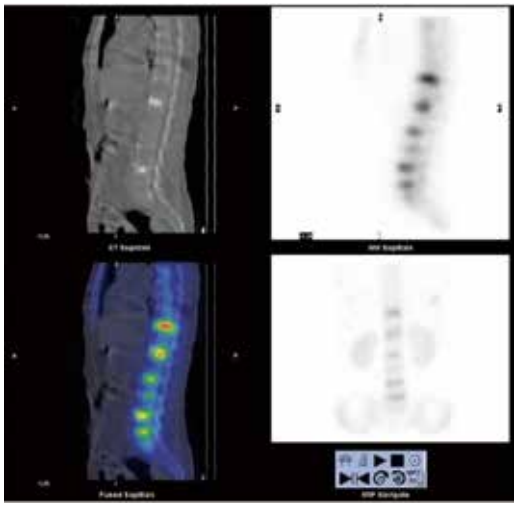

圖二：整合式單光子射出電腦斷層顯示在 T10、T12、L2 到 L5 呈現特殊的橫線狀活性攝取。

PC024

使用不同稀釋液之 CA 19-9 檢驗值比較及探討

張素雲[1] 廖建國[1] 薛伃婕[1] 林淑靜[1] 王昱豐[1,2]

[1] 佛教大林慈濟醫院核子醫學科
[2] 慈濟大學醫學系

目的

CA 19-9 例行檢驗作業中，有少數案例在稀釋過後，回乘稀釋倍數所得之檢驗值，比標準品最高濃度來的低，有明顯偏低之現象，本研究目的即爲收集日常作業中，檢驗值大於標準品最高濃度之檢體，嘗試以生理食鹽水進行稀釋，以比較不同稀釋液之檢測值，並探討使用生理食鹽水之適當性。

方法

從 2015 年 1 月至 2015 年 8 月，共搜集 10 支血清檢體。使用 Cisbio Bioassays ELSA-CA19.9 KIT (IRMA)，標準品線性範圍爲 0~265 U/ml，參考值 < 37 U/ml，當檢驗值大於最高濃度 265 U/ml 時，分別使用試劑套裝組所提供的稀釋液 (DILUENT) 和 0.9% 生理食鹽水稀釋後再行檢測。稀釋方法爲 20 µl 血清檢體加 180 µl 稀釋液，作 10 倍和 100 倍稀釋。另將相同的這 10 支檢體，委託外檢單位使用 CLIA 方法檢測 (線性範圍爲 0~2000 U/ml；參考值＜ 37 U/ml)，以比較不同稀釋液之 CA 19-9 檢驗值，並與其他方法學進行比較。

結果

檢驗值大於標準品最高濃度之檢體，用不同稀釋液分別爲 DILUENT (試劑組套) 和生理食鹽水稀釋 10 支檢體，並和使用 CLIA 法所測得之檢驗值比較，其結果爲稀釋 10 倍時，10 支檢體用 DILUENT 稀釋有 5 支檢體即有數值，生理食鹽水有 4 支有數值 (表 1)。若以 DILUENT 和生理食鹽水數值，分別和 CLIA 法數值做比較，則 DILUENT 和 CLIA 法有 6 支數值較接近，生理食鹽水和 CLIA 法數值有 4 支數值較接近，而使用生理食鹽水稀釋之數值都比 DILUENT 稀釋後數值高 (圖 1)。由於試劑組套所提供之 DILUENT 爲馬血清，與人類血清較爲接近，在免疫檢驗抗原抗體結合方法時可能會受干擾 (例如：嗜異性抗體、自體免疫抗體、補體、HAMA (human anti-mouse antibody)、藥物等)。因此當發生少數可能受干擾的個案時，可以考慮使用生理食鹽水稀釋再進行複驗比對，但生理食鹽水並不適合全面取代試劑組套提供的稀釋液。

結論

初步研究結果顯示，使用試劑組套內稀釋液之檢驗結果和 CLIA 數值之相關性較生理食鹽水來的佳，因此例行作業仍應使用組套內提供之稀釋液，而針對少部份個案，稀釋測定後所得之檢驗值比原倍偏低時，可以考慮使用生理食鹽水稀釋再進行複驗比對。

表 1. 使用不同稀釋液之 CA 19-9 檢測值比較

Sample No.	Diluent		NaCl	
	10x	100x	10x	100x
1	186	199	330.7	589
2	1710.3	1559	>	4116
3	816.1	409	970.9	1706
4	>	2180	2313.2	3843
5	2489	1313	>	3048
6	1848.4	1301	1774.6	2233
7	>	4422	>	6620
8	>	5847	>	10122
9	>	3448	>	4450
10	>	5077	>	7186

>：大於標準品最高濃度

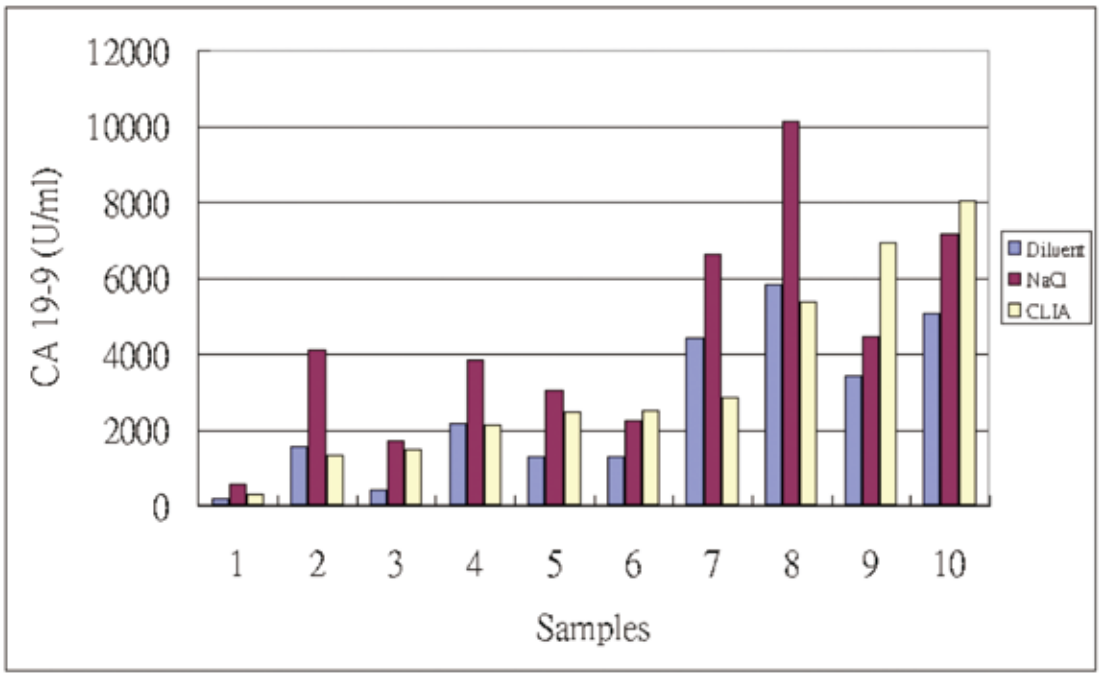

圖 1. 稀釋 100 倍檢體之 IRMA 檢驗值與 CLIA 結果比較 (Diluent 稀釋後檢驗值與 CLIA 之相關性 (r = 0.79) 較 NaCl 佳 (r = 0.67))

PC025

洗腎病人血液透析前後 BUN 及 PTH 之濃度變化及清除率比較

薛伃婕[1] 廖建國[1] 張素雲[1] 王昱豐[1,2]

[1] 佛教大林慈濟醫院核子醫學科
[2] 慈濟大學醫學系

背景：

監控洗腎成效雖是以血液中 BUN 爲主，但因洗腎病人腎功能損壞後，血中鈣磷不平衡，進一步刺激副甲狀腺機能亢進，增加分泌副甲狀腺素 (PTH)，使血液中 PTH 濃度上升，引起相關併發症，所以病人也需定期監控 PTH 濃度的變化。本研究目的爲初步分析血液透析前後 PTH 及 BUN 之濃度變化，並探討其各別的清除率。

方法：

蒐集 6 位病患，每位病人於進行血液透析前、後，使用 EDTA 管以及生化管，各採集一次血液測 PTH 及 BUN 濃度，總計各採集 12 支檢體。PTH 之檢驗方法爲使用 Cisbio Bioassays 試劑 (ELSA-PTH KIT)，而 BUN 之檢驗方法爲使用西門子 Dimension 全自動生化分析儀，之後比較各病人 PTH 以及 BUN 濃度於血液透析前、後的數據結果及計算其清除率。兩者清除率計算公式爲 (透析前濃度 - 透析後濃度) ／透析前濃度 x 100%。

結果：

6 位病人於進行血液透析後，PTH 濃度皆較血液透析前明顯降低，清除率介於 31.47% ～ 71.44% 間，平均清除率爲 51.45% (表 1)。

表 1. 洗腎病人血液透析前後 PTH 檢驗值及清除率

編號	血液透析前 PTH 濃度	血液透析後 PTH 濃度	清除率 %
1	246.6	153.44	37.78
2	615.56	421.83	31.47
3	253.75	134.75	46.90
4	779.37	255.99	67.15
5	370.53	245.91	33.63
6	128.2	36.62	71.44

濃度單位：pg/ml

而血液透析後 BUN 濃度亦較血液透析前大幅降低，清除率介於 85.48% ～ 71.6% 間，平均清除率爲 78.54%。

表 2. 洗腎病人血液透析前後 BUN 檢驗值及清除率

編號	血液透析前 BUN 濃度	血液透析後 BUN 濃度	差異度 %
1	50	13	74
2	62	9	85.48
3	92	21	77.17
4	81	23	71.60
5	85	19	77.65
6	38	7	81.58

濃度單位：mg/ml

由結果發現，透析過後 BUN 的清除率比 PTH 好，其主要原因應爲 BUN 分子較 PTH 小，通過透析膜的程度較PTH好。此外，血液透析時使用的透析膜的通透性、病人本身的生理功能狀況等，也可能影響洗腎的效率。由於 BUN 清除率較高，因此監控洗腎成效一般皆以 BUN 爲主，雖 PTH 不是主要用來評估透析成效的因子，但定期監控病人 PTH 濃度且加以治療，可預防因副甲狀腺亢進所引起的併發症。

結論：

由血液透析前後 PTH 及 BUN 之濃度變化，顯示透析過後 BUN 的清除率比 PTH 好，洗腎病人定期監控此兩項檢驗值均有其臨床意義。許多放射免疫分析實驗室均例行提供 PTH 的檢驗，實驗室定期提供精準的檢驗報告，有助於洗腎病人預防因副甲狀腺亢進所引起的併發症。

PC026

由乳癌確診病人 CA15-3 及 CEA 檢驗結果探討腫瘤標記的角色

林淑靜[1] 廖建國[1] 張素雲[1] 薛伃婕[1] 王昱豐[1,2]

[1] 佛教大林慈濟醫院核子醫學科
[2] 慈濟大學醫學系

背景：

乳癌是目前台灣女性癌症的第一名，早期發現、早期診斷及治療對乳癌患者的存活率具有重要的意義。本研究目的為分析乳癌陽性個案利用放射免疫分析方法檢測 CA 15-3 及 CEA 之結果，以探討兩項腫瘤標記在乳癌診療上所扮演的角色。

方法：

收集本院從 2013 年 1 月至 2014 年 12 月，透過乳房攝影檢查後結果為高度疑似為惡性腫瘤及可疑異常需考慮組織生檢 (疑陽個案 Birads 4,5) 共 88 例，其中經病理學 / 細胞學確診為乳癌之個案共 19 例 (IDC 13 例，DCIS 5 例，mucinous carcinoma 1 例)，良性乳房疾病共 18 例，未回院複診共 7 例，至外院複診 41 例，年齡 45-69 (平均 55) 歲。使用 Cisbio Bioassays 公司生產的 CA 15-3 及 CEA 放射免疫試劑測量血清中濃度，並分析單項檢測 CA15-3、CEA 及聯合檢測 CA15-3 及 CEA 之陽性件數及其敏感度。本院 CA15-3 血清參考值為小於 30 U/ml，CEA 血清參考值為小於 7 ng/ml，結果以高於正常參考值判定為陽性。

結果：

檢測結果發現 19 例乳癌確診個案中，僅有 1 例 CA 15-3 及 CEA 兩項檢測結果均為陽性，而其餘 18 例結果均為陰性，顯示無論單項或兩項聯合檢測結果其敏感度皆為 5.56% (表 1)。曾有相關文獻指出，以 CA 15-3 檢測乳癌之敏感度為 5-70%，而 CEA 之敏感度則為 9-39%。本研究結果顯示，兩項檢驗之敏感度與文獻發表之低值相近。臨床上，乳癌的診斷不能只根據腫瘤標記來判定，檢查乳癌仍應配合其他檢查，如乳房 X 光攝影、超音波、細胞診斷、病理切片和醫師的臨床檢查等，才能提高癌症診斷的正確率。縱然在癌症的篩檢上，CA 15-3 及 CEA 之敏感度均不高，僅能做為診斷的輔助工具，但其和癌症發展的程度及腫瘤是否轉移有關，因此在乳癌治療的追蹤上，卻是很好的工具。

表 1. 乳癌確診病人之乳癌型態及檢查結果

No.	乳癌型態	乳房攝影	CA 15-3	CEA
1	Ductal carcinoma in sisu (DCIS)	+	12.77(-)	3.25(-)
2	Ductal carcinoma in sisu (DCIS)	+	6.79(-)	1.24(-)
3	Ductal carcinoma in sisu (DCIS)	+	24.77(-)	1.99(-)
4	Ductal carcinoma in sisu (DCIS)	+	216.21(+)	33.37(+)
5	Ductal carcinoma in sisu (DCIS)	+	23.79(-)	0.37(-)
6	Invasive ductal carcinoma (IDC)	+	5.3(-)	1.15(-)
7	Invasive ductal carcinoma (IDC)	+	11.22(-)	2.4(-)
8	Invasive ductal carcinoma (IDC)	+	8.9(-)	<0.05(-)
9	Invasive ductal carcinoma (IDC)	+	19.4(-)	0.89(-)
10	Invasive ductal carcinoma (IDC)	+	5.9(-)	1.58(-)
11	Invasive ductal carcinoma (IDC)	+	5.23(-)	0.88(-)
12	Invasive ductal carcinoma (IDC)	+	12.92(-)	0.91(-)
13	Invasive ductal carcinoma (IDC)	+	17.63(-)	3.65(-)
14	Invasive ductal carcinoma (IDC)	+	16.94(-)	1.03(-)
15	Invasive ductal carcinoma (IDC)	+	23.9(-)	3.16(-)
16	Invasive ductal carcinoma (IDC)	+	10.91(-)	0.78(-)
17	Invasive ductal carcinoma (IDC)	+	0.92(-)	1.56(-)
18	Invasive ductal carcinoma (IDC)	+	7.78(-)	0.7(-)
19	Mucinous ca.	+	18.87(-)	1.36(-)

結論：

研究結果顯示，CA 15-3 及 CEA 對於檢測乳癌之敏感度 (5.56%) 並不高。因此，進行乳癌篩檢時，仍應搭配其他檢查 (如乳房 X 光攝影、超音波等) 較為理想。雖然 CA 15-3 及 CEA 只能做為乳癌的輔助檢查，但運用在乳癌治療的追蹤上，有助於及早發現轉移或復發。

PC027

全身骨骼掃描病人導尿之專業照護－個案報告

蘇淨儀[1] 廖建國[1] 張秀瑛[1] 莊紫翎[1] 林余珊[1] 王昱豐[1,2]

[1] 佛教大林慈濟醫院核子醫學科
[2] 慈濟大學醫學系

背景介紹

核子醫學科之全身骨骼掃描，可評估骨頭是否有轉移，更可協助癌症分期及治療追蹤。患者檢查前需排空膀胱，因尿液過多易遮蓋膀胱後面器官，如：骨盆或尾椎，進而影響醫師判讀，故檢查前務必請患者排尿，才能得到更正確的影像。本案例提出介入導尿之專業照護經驗，期能提供核醫護理師之參考。

個案報告

一位 77 歲男性，有 60 年的抽菸史，103 年 05 月體重減輕八公斤，伴隨咳嗽及咳痰，檢查發現右下肺葉腫瘤。持續門診追蹤治療。104 年 3 月抱怨背部酸脹疼痛，醫師安排全身骨骼掃描。檢查過程中，發現膀胱過漲，經詢問，病人主訴尿量不多且排尿困難，觸診發現膀胱有漲滿感。先進行非侵入性之指導性誘尿方式，如：廁所內聽流水聲、手握冰塊、按摩下腹部等措施，但患者仍舊無法排尿，故依醫囑建議病人進行單次導尿。經說明用意及副作用取得病人同意後，進行單次導尿，因尿液含有放射性藥物，執行人員需穿鉛衣後再穿隔離衣，為患者執行無菌之單導技術。置入導尿管時有受阻現象，疑似前列腺肥大，個案回應不知情。導出尿液 1,400 cc，顏色混濁深茶色且有氣味，由於導尿量過多，過程中持續關切是否出現身體不適並監控患者意識及生命徵象，避免膀胱內壓力下降太多致休克或膀胱出血等情形。

結論

肺癌患者，有三到五成的機率會骨頭轉移，需定期追蹤全身骨骼掃描。此例行性追蹤，意外發現個案長期有下腹脹、排尿困難而未就醫，導尿完畢後即協助患者至泌尿科門診就醫，經醫生評估後予以置放長期導尿管，防止泌尿道系統感染。此次骨頭掃描過程中，不僅提供常規檢查，也協助個案減輕脹尿的不適感，提供專業的醫療及護理協助。

PC028

正子造影個案管理追蹤流程及初步成效之探討

林余珊[1] 廖建國[1] 莊紫翎[1] 蘇淨儀[1] 王昱豐[1,2]

[1] 佛教大林慈濟醫院核子醫學科
[2] 慈濟大學醫學系

背景：

近十年來，『癌症』是衛生福利部努力改善國人健康的目標。因此，國人對於健康的重視也日益增加，可發現近年來，健康檢查的比率有逐漸增加的趨勢。但也發現民眾在檢查結束後，卻忘記後續追蹤的重要性，因此我們藉由個案管理的模式，希望提高民眾對於追蹤就醫的重視，並提供相關健康知識，以提升醫療品質。

方法：

對象爲正子造影自費健康檢查的民眾，待核醫科醫師判斷影像並完成報告後，對於報告正常的民眾，告知報告內有中英文報告，並詢問是否需要回診聽報告，如果民眾時間無法配合回診，等書面報告寄出後一週內，詢問是否需要回診聽報告，如不需要則結案；如需要，回診聽取報告後結案。而針對報告有異常的民眾爲收案個案，請核醫科醫師告知報告異常的部位，並同時在個案管理系統建檔，依病人的情況照會相關專科醫師的門診，後續以醫療系統及電訪關懷並追蹤是否至(院內外)專科門診就醫，如有就醫並於結案，如無就醫情況，定期每 3~6 個月追蹤關懷其情況(圖 1)。除了瞭解個案後續就醫的情況，及瞭解策略的成效性，並探討電訪個案的健康觀念。

圖 1. 正子造影健檢個案追蹤流程

結果：

本研究由 2015 年 01 月至 07 月，針對自費健康檢查的個案，進行檢查後電訪關懷，自費健檢個案共 21 位(已排除他院轉檢個案 1 位及已確診癌症的病患共 4 位，1 位個案因爲外國人不適合此機制)，未電訪追蹤介入前，個案追蹤就醫率爲 38% (8 位)，而介入個管後提升爲 90% (19 位)(圖 2)。在追蹤關懷的電訪過程中，可知未聽報告而有異常的民眾 (4 位)，後續有在鄰近的醫院就醫治療或再進一步檢查確診。由此顯示個案管理的模式，可提升異常個案的追蹤就醫率，有助於健檢的整體滿意度及達到健康檢查完整性之目的。

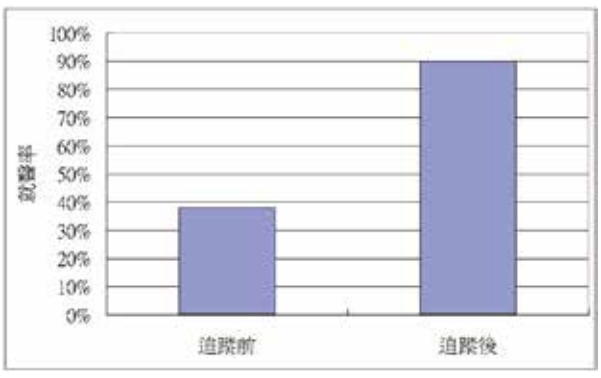

圖 2. 個案追蹤前後就醫率比較

結論：

正子造影作業導入個案管理的模式，從民眾一開始健康檢查到檢查結束，以及後續專科門診追蹤，給於連續性的醫療健康照護及電訪關懷，不但能提升異常個案之就醫率，也可提供受檢者相關健康知識，並提醒定期健康檢查的重要性，有助於提升醫療品質。

PC029

Different Interpretation of the Same Appearance of Three-Phase Bone Scan in A Case of Kienbock's Disease

Tzyy-Ling Chuang[1], Yuh-Feng Wang[1,2]

[1]Department of Nuclear Medicine, Buddhist Dalin Tzu Chi Hospital, Chia Yi, Taiwan;
[2]School of Medicine, Tzu Chi University, Hualien, Taiwan.

Introduction: We present a case of Kienbock's disease which showed the same appearance in three-phase bone scan while diagnosis and post-surgery bone graft viable evaluation.

Case report: A 28-year-old male had diabetes mellitus and glucose-6-phosphate dehydrogenase deficiency under insulin control. He had right wrist pain with limited range of motion for about one years. No previous trauma history was told. Three-phase bone scan showed all three phases positive at right wrist. MRI showed compatible with Kienbock's malacia of lunate. He received surgery procedure of curettage and vascular bone graft of right 3-4th intercompartmental artery fasciocutaneous flap with pedicled radius bone. Pathology of right lunate showed necrosis. One and half year later, X-ray showed good alignment. Three-phase bone scan was arrange for evaluation for vascularized bone graft, and showed right wrist uptake in all three phases which was suggestive for viable bone graft.

Discussion: Kienbock's disease is a rare disorder of the wrist described osteomalacia or avascular necrosis of the lunate. This is classically attributed to arterial disruption, but may also occur if venous congestion with elevated interosseous pressure. Revascularization techniques, including bone graft, often held for a period of weeks or months, but their use at later stages is controversial. The interesting point of our case is that we use three-phase bone scan in the pre- and post-surgical stage. Although they had the same image appearance, but had different meanings. So three-phase bone scan is a useful tool, as it had different utility in different scenario, especially when correlated with the history and clinical examination findings.

PC030

Bilateral Primary Adrenal Lymphoma Mimicking Functioning Kidneys in the F-18 FDG PET/CT Imaging of an End-stage Renal Disease Patient

Yi-Ling Chang[1], Pan-Fu Kao[1,2], Ming-Hung Tsai[2,3], Jui-Hung Weng[1,2]

[1]*Department of Nuclear Medicine, Chung Shan Medical University Hospital, Taichung, Taiwan;*
[2]*School of Medicine, Chung Shan Medical University, Taichung, Taiwan;*
[3]*Department of Hematology and Oncology, Chung Shan Medical University Hospital, Taichung, Taiwan.*

Abstract

A 51-year-old male patient has underlying disease of end-stage renal disease and suffered from intermittent fever, abdominal pain, and diarrhea for two months. A physical examination revealed massive ascites with multiple lymphadenopathy in the neck and inguinal regions. Laboratory tests revealed elevated serum lactate dehydrogenase, elevated β2-microglobulin, anemia and adrenal insufficiency. Neck lymph node biopsy revealed diffuse large B-cell lymphoma. He was referred for F-18 FDG PET/CT scan for pretreatment staging. The imaging revealed disseminated nodal disease pattern with dominant bilateral upper back FDG accumulation, which was initially recognized as functioning kidneys. The PET/CT fusion imaging helped to differentiate nonfunctioning kidneys from FDG avid bilateral adrenal lesions, as well as malignancy with adrenal metastases from primary adrenal lymphoma.

Keywords: Primary adrenal lymphoma, end-stage renal disease, F-18 FDG PET/CT

PC031

Incidental Finding of Multiple Ovary Cysts on the Tc-99m-labeled Red Blood Cells Subcutaneous Radionuclide Venography and Clinical Application of SPECT/CT Imaging

Yi-Ling Chang[1], Jui-Hung Weng[1,2], Chih-Ting Liu[3], Hsiu-Lan Chu[3], I-hsin Tsai[3]

[1]Department of Nuclear Medicine, Chung Shan Medical University Hospital, Taichung, Taiwan;
[2]School of Medicine, Chung Shan Medical University, Taichung, Taiwan;
[3]Department of Nuclear Medicine, Kaohsiung Medical University Hospital, Kaohsiung, Taiwan.

Abstract

A 39-year-old female patient complained of right lower leg pain, erythema and edema for 2 weeks. Cellulitis was impressed and symptoms were persistent after full course of antibiotics treatment. Thus, Tc-99m-labeled red blood cells subcutaneous radionuclide venography was arranged for clinical suspicion of deep vein thrombosis. Planar imaging revealed swelling right leg with patent deep venous flow and collateral superficial great saphenous vein. In addition to nonvisualized iliac vein and inferior vena cava, multiple hypodense lesions and collateral venous drainage in the abdomen were also noted. SPECT/CT imaging was arranged for further detection of lesion and imaging revealed multiple ovary cysts and effacement of the inferior vena cava. In conclusion, if disturbed iliac vein or abnormal collateral venous drainage in the abdomen is noted on the Tc-99m labeled red blood cells subcutaneous radionuclide venography, additional SPECT/CT imaging may perform for further information and differential diagnosis of swelling in the lower extremities; not only in detecting deep vein thrombosis.

Keywords: deep vein thrombosis, Tc-99m-labeled red blood cells subcutaneous radionuclide venography, SPECT/CT, ovary cyst

PC032

Metabolic Parameters of F-18 FDG in Evaluating Metastatic Status in Nasopharyngeal Carcinoma Patients

Chia-Chi Chang[1], Pei-Jung Li[1], Fong-Ru Lin[1], Meng-Fang Hsieh[1], Pei-Yao Lin[2]

[1]Department of Nuclear Medicine, Changhua Christian Hospital, Changhua, Taiwan;
[2]Department of Nuclear Medicine, National Taiwan University Hospital, Taipei, Taiwan.

Aim: Nasopharyngeal carcinoma (NPC) is a common malignancy in southern Asia with different staging stratification from other cancers. About 20% of metastatic free (M0) NPC patients, however turned to distant failure (M1) in 3 years after completion of treatment resulting in patient mortality (Kam et al, 2004). We thus analyzed the relationship between metabolic parameters of F-18 FDG PET in NPC patients with and without metastases (i.e. M0 and M1).

Materials: Eighty patients in all stages including 36 in stage IV were studied. They were devided into M0 vs. M1 (n = 69 vs. 11 in all stages; and 25 vs. 11 in stage IV). F-18 FDG PET was performed using an integrated PET/CT (Gemini GXL). The FDG metabolic parameters including SUVmax and SUVmean, primary and total tumor volume and glycolysis (i.e. PTV, PLG, TTV and TLG) were calculated using PMOD software. A threshold of 42% of the SUVmax was applied to delineate the PTV or TTV. The PLG or TLG was calculated as mean SUV multiplied PTV or MTV. Metastases were considered by histology or various images with a clinical concordance.

Results: Significant differences in PTV, PLG, TTV and TLG were found between M0 and M1 in patients covering all stages. However, only TTV and TLG revealed significant difference in the stage IV subgroup (Mo vs. M1: 26 ± 14 vs. 88 ± 54 and 213 ± 160 vs. 615 ± 160; $p < 0.01$, each). The SUVmax and SUVmean of primary tumors showed no statistical significance between M0 and M1 in either the all stage group or the stage IV subgroup.

Conclusion: TTV and TLG may play a role in evaluating metastatic status of patients with NPC, either in all stages or in stage IV subgroup.

PC033

The Effect of Diuretics Injection Timing on Interpretation of Urinary Tract System in F-18 FDG PET/CT

Shih-Ya Ma[1,2], Hueisch-Jy Ding[3]

[1]*Department of Nuclear Medicine, Yuan's General Hospital, Kaohsiung ,Taiwan;*
[2]*Department of Information Engineering, I-Shou University, Kaohsiung, Taiwan;*
[3]*Department of Medical Imaging and Radiological Sciences, I-Shou University, Kaohsiung, Taiwan.*

Introduction: Although F-18 FDG PET/CT scan has been proven useful in the detection of many tumors, it has a pitfall in detection of urinary tract tumor because of F-18 FDG accumulation in urinary tract due to excretion in urine. This prospective study was to investigate the effect of diuretics injection timing on interpretation of urinary tract system in F-18 FDG PET/CT.

Methods: Between June 2005 and June 2011, total 186 cases who received F-18 FDG PET/CT scans in our department with well hydration, normal renal function and euglycemia were included. All cases were further divided in to four groups based on the injection timing of diuretics (20 mg of furosemide). Group 1 did not receive furosemide and served as controls. Group 2 received furosemide immediately after injection of F-18 FDG. Group 3 received furosemide 20 min after injection of F-18 FDG. Group 4 received furosemide after first whole-body scan completed and 30 min before second pelvic delayed scan. A 4-point influence interpretation scale of F-18 FDG PET/CT was evaluated visually by experienced PET reader and based on bladder activities. Maximum standardized uptake values (SUVmax) of renal pelvis, ureter, bladder, liver and thigh were also collected.

Results: Image interpretation was significantly more influenced by bladder radioactivies in the Group 1-2 (score 3.3 ± 0.8) than the Group 3-4 (scores 1.5 ± 0.7) ($P < 0.001$). Comparing to the control group (Group I), all furosemide groups showed lower bladder SUVmax (especially in Group 3 and 4, $P < 0.001$), lower renal pelvic SUVmax ($P < 0.001$), lower ureteral SUVmax ($P = 0.001$).

Conclusions: Intravenous injection of diuretics can lower F-18 FDG activities in genitourinary tract, well tolerate by patients and avoid invasive bladder catheterization. The lowest bladder activities and best image quality can be easily achieved in Group 4, but it will prolong the whole examination time. However, Group 3 is adequate to improve image quality and will shorten examination time.

PC034

Radiation Safety Assessment to Caregivers of the Patients Treated with Iodine-131 for Thyroid Carcinoma

LY Chen[1], Kuo-Wei Lee[1], W. S Huang[2], Yu-Yi Huang[3], KH Ling[4], Ting-Chun Lin[3]

[1]*Institute of NuclearEnergy Research;*
[2]*Changhua Christian Hospital;*
[3]*Koo Foundation Sun Yat-Sen Cancer Center;*
[4]*Mackay Memorial Hospital Taipei Branch.*

Introduction: The release of out-patients after treatment with I-131 for thyroid carcinoma may cause the risk of radiation to public and family members. At present there are no national regulation in Taiwan to restrict the release of out-patients. This study assess the radiation safety to caregivers of the patients treated with I-131 for thyroid carcinoma.

Methods: The study population comprised the family caregivers and the patients were treated with I-131 for thyroid carcinoma from three hospitals which the protocol and procedures were approved by the appropriate institutional review board (IRB).The dose rates at 1 meter from the patients would be measured by survey meter when they left hospitals. Dosimetry data to caregivers were obtained by two thermoluminescent dosimeter badges in front of the chest for at least 1 week and were adjusted to give an estimate of values which might have been expected if the dosimeters had been worn indefinitely.

Results: When the patients treated with I-131 left the hospitals, the dose rates at 1 meter away from the patients ranged from 20 to 50 μSv/h. And the exposure to all the caregivers were well less than 1mSv that is the limit recommendation from ICRP for public.

Conclusions: At present there are no national regulation in Taiwan to the release of out-patients after treatment with I-131. This study has provided useful information on radiation safety and exposure to caregivers of patients treated with I-131. On the condition that the radiation dose rates at 1 meter for the patients are below 50 μSv/h, the release of out-patients has no distinct radiation risk.

PC035

Detection of Sentinel Lymph Node(s) in Breast Carcinoma: Using Combined Injection Techniques

Yi-Hsun Chen, Dom-Gene Tu

Department of Nuclear Medicine, Ditmanson Medical Foundation Chia-Yi Christian Hospital.

Introduction: The clinical application of breast lymphoscintigraphy has become widespread with using this technique as an alternative to total axillary nodal dissection in the evaluation of axillary node involvement. While sentinel node (SLN) scintigraphy is a standard procedure before breast surgery at many centers, there is still no consensus on how to perform the examination being concerned with different tracers, injection techniques and time schedules.

Methods: The retrospective study included 34 patients (median age 52.82 ± 9.57 years, range 34~79 years) with early stage breast cancer from May 2012 to May 2014 at Chia-Yi christian hospital. The subjects underwent ^{99m}Tc-phytate lymphoscintigraphy for localization of SLN. In each case, lymphoscintigraphy is conducted with surgical resection of breast cancer on the same day, using the following procedure. A total volume of 0.2-0.5 mCi /0.2-0.5 mL of ^{99m}Tc-phytate will be injected at periareolar and intradermal fractionated. After radiotracer injection, static images using γ-camera (Siemens E-cam) equipped with low-energy high-resolution collimator are performed; then, series images are taken with 5~10 min interval. Total imaging time needs about 2-3hours.

Results: Visualisation rate of the 34 patients are showed in the table.

Table. SLN visualized vs. non-visualized

Injection method	No. Visualized (%)	No. Non-visualized (%)
Intradermal (ID)	84.85%	15.15%
Periareolar (PA)	82.76%	17.24%
ID + PA	89.29%	10.71%

Conclusions: There is no obvious difference between the two methods in lymphoscintigraphy in our study. However, the detection rate for sentinel nodes is increased by using combined both methods. In the future work, we need more samples to verify the results.

PC036

Negative Gallium-67 Citrate Inflammatory Scan in Pathological Proved Acute Vertebral Osteomyelitis: A Case Report

Hsi-Huei Lu[1], Pei-Shan Wu[1], Nan-Tsing Chiu[1], Bi-Fang Lee[1], Wei-Jen Yao[1], Hung-Wen Tsai[2]

[1]Department of Nuclear Medicine, National Cheng Kung University Hospital, Tainan, Taiwan;
[2]Department of Pathology, National Cheng Kung University Hospital, Tainan, Taiwan.

Introduction: Osteomyelitis (OM) denotes an inflammatory process localized in the bone that lengthy regimen of antibiotics and aggressive surgical debridement are often required. The established role of radiopharmaceutical studies in diagnosing early and late stages of OM is well recognized. We present a case of negative gallium-67 citrate (^{67}Ga) scan with SPECT/CT, who had final pathological diagnosis of acute vertebral OM.

Case report: A 49-year-old man presented with acute onset low back pain with bilateral lower limbs weakness since a traffic accident 50 days ago, accompanied with fluctuating consciousness, leukocytosis, elevated ESR, and elevated CRP. Empirical antibiotics were started under the impression of OM, and ^{99m}Tc-methylene diphosphonate (^{99m}Tc-MDP) bone scan and ^{67}Ga scan were arranged for localization. Bone scan showed increased radioactivity in the L5-S1 vertebral bodies, whereas ^{67}Ga scan showed no abnormal radioactivity. Lumbar spine MRI favored an infectious spondylodiscitis and OM at L5-S1, and pathological specimen later proved acute OM and discitis in L5-S1.

Discussion: Early diagnosis of vertebral OM is important in order to prevent permanent neurologic impairment. ^{67}Ga scan is an excellent modality due to its high sensitivity, especially in diagnosis of vertebral OM and in monitoring the therapeutic response. Adjunctive SPECT/CT further enhances sensitivity and also improves spatial resolution. A negative ^{67}Ga scan is usually sufficient to exclude OM; however, rare false negatives are occasionally reported in the literature without definitely known etiology. Decreased ^{67}Ga uptake in patients with precipitated antibiotics use or leukocytopenia has been suggested. On the other hand, MR imaging is able to detect presence of vertebral pathology including infection, but cannot reliably discriminate subtle infection from degenerative change. We recommend that patients with high clinical suspicion and risk factors of vertebral OM should be evaluated with multiple modalities.

PC037

安全針具對放射性藥物進入體內之影響

游宜芳　郭俊良　張鈺弘 *

新竹馬偕紀念醫院核子醫學科

背景介紹：

針扎是醫護人員常見之工作傷害，所以醫療法修正自中華民國 101 年起，五年內醫療院所應按比例逐步完成全面提供安全針具。但無針式安全針具構造不同，臨床工作偶爾會看到大量放射性追蹤劑滯留在病人注射處的情況。因此本研究目的爲利用放射性藥物評估並定量使用非安全與安全針具是否對藥物滯留量造成影響。

方法：

本實驗模擬內含放射性藥物的注射針筒利用一種針式注射用輸液延長管和兩種不同型式之無針式注射用輸液延長管注入病人體內，實驗方法比照靜脈注射流程，分別評估放射性藥物殘留於不同種類之輸液延長管和注入病人體內含量。放射性藥物活度度量使用 GE Infinia Hawkeye SPECT，設定固定大小之 ROI 範圍，收集一分鐘計數來度量 (cpm)。每次之實驗活度度量記錄如下：(a) 度量 3 c.c. 注射針筒抽 1.5 c.c. 放射性藥物活度 (即全針活度)，(b) 度量將放射性藥物注射後之空針活度，(c) 度量將放射性藥物注射後之輸液延長管活度，(d) 度量使用 3 c.c. 生理食鹽水 (NS) 將殘留放射性藥物完全推出後，再次度量輸液延長管活度。

結果：

輸液延長管種類	藥物滯留於管內 百分比 (%)	用 NS 沖洗後滯留於管內 百分比 (%)	注射入病人體內劑量 百分比 (%)
	(c)/[(a)-(b)]	(d)/[(a)-(b)]	[(a)-(b)-(d)]/(a)
針式注射用 (T 型管)	1.26 ± 0.25	1.23 ± 0.27	92.74 ± 1.80
無針式注射用 (T 型管)	15.77 ± 0.21	1.59 ± 0.42	92.64 ± 1.72
無針式注射用	29.96 ± 2.77	3.71 ± 2.43	88.04 ± 2.95

每種輸液延長管各做 20 次。

結論：

當只單純將放射性藥物注入病人體內會發現使用無針式注射用輸液延長管藥物會滯留約 29.96%，比針式高許多。反之，不論利用何種型式之輸液延長管，當生理食鹽水將放射性藥物沖入病人體內後，88.04% 以上的藥物可進入。此外，兩種無針式注射用輸液延長管與針式注射用輸液延長管來做比較，發現無針式 T 型管與針式 T 型管差異爲 0.1%，而無針式與針式 T 型管差異則爲 5.1%。故爲確保病人可接受較正確的劑量以獲得良好的影像品質，以及保護醫護同仁減少針扎的傷害，建議臨床上可使用無針式 T 型注射用輸液延長管，但務必使用生理食鹽水沖洗。

PC038

提升員工對游離輻射防護的認知率

郭俊良[1] 游宜芳[1] 何建宗[2] 林雅惠[2] 張鈺弘[1]*

[1] 新竹馬偕紀念醫院核子醫學科
[2] 新竹馬偕紀念醫院職業安全衛生室

背景介紹：

依游離輻射防護法規定，設施經營者爲防止游離輻射危害，維護民眾健康與安全，輻射作業必須合理抑低其輻射劑量，更於今年職業安全衛生法第三十條第八點新增「雇主不得使妊娠中女性勞工從事有害輻射散布場所之工作」。本單位一直注重之輻射防護安全不只針對游離輻射工作單位與輻射作業人員，而更可利用品管的手法讓全院員工對游離輻射防護的認知有所提升，讓同仁們可更安心、放心於工作崗位上照顧病人。

方法：

利用經醫師與輻射防護委員會等專家進行過信效度評估所設計之問卷，於品管圈活動前後分別給院內會接受到游離輻射的人員進行問卷調查。調查同仁對輻射的認知與恐懼做要因分析統計，然後利用特性要因之解析得到四種改善對策，分別爲加強人員教育訓練、製作宣導影片和海報與制定核子醫學科檢查之輻射防護標準作業流程。最後由認知率來做監測基準，並由認知率的提升來印證不安率是否下降。

結果：

項　目	改善前認知率 (N = 283)	改善後認知率 (N = 291)
游離輻射檢查之劑量	15.19%	79.04%
法規規定之接受游離輻射劑量限度	15.90%	77.66%
世界天然背景輻射劑量	16.25%	80.76%
院內輻射防護委員會之功能	25.09%	83.16%
游離輻射與非游離輻射	26.50%	80.41%
如何降低游離輻射之曝露	39.58%	84.88%
輻射防護方法與偵測設備	39.93%	87.63%
院內放射性廢棄物處置流程	42.40%	86.94%
核子醫學檢查病人之衛教	42.76%	86.25%
單位內是否有輻射	59.72%	87.97%
對游離輻射認知率平均值	32.33%	83.47%
對游離輻射不安率平均值	36.99%	20.27%

結論：

由此品管圈活動，發現改善後認知率由 32.33% 增加到 83.47%，不安率由 36.99% 降低 20.27%。故未來將持續推動全院的輻射防護教育訓練課程，以提高院內同仁對輻射的認知和防護的技巧，讓同仁對接受游離輻射檢查的病人保持負責任態度，而不會因病人有做游離輻射檢查，導致員工有不安的情形，造成意外事故的發生。

PC039

F-18 FDG 正子掃描在偵測肺癌縱膈腔淋巴結轉移的效能

李佩蓉　林奉儒　張佳琪　謝孟芳　張柏齡

彰化基督教醫院

中文摘要

【目的】

肺癌是台灣死亡率最高的癌症，正確的分期有助於選擇適合的治療方式，減少不必要的侵入性治療，或增加治癒的機會，本次研究在評估正子掃描在偵測肺癌縱膈腔淋巴結轉移的效能。

【方法】

以 2012 年至 2013 年間進行過正子掃描且有病理報告的肺癌患者來分析，以病理報告爲標準，將正子影像分爲五級，一至三級爲陰性，四與五級爲陽性，對照病理報告中紀錄的淋巴群來分析正子掃描的正確性。

【結果】

病人共計 138 名，男性 91 名，女性 47 名，平均年齡爲 66.68 歲，有病理報告的淋巴位置共有 467 處，其中轉移有 49 處，未轉移有 418 處，正子掃描正確找出轉移的有 25 處，未能找出轉移的有 24 處，正確判斷沒有轉移的有 369 處，未能正確判斷沒有轉移的有 49 處，敏感性爲 51%，特異性爲 88.2%，陽性預測值爲 34%，陰性預測值 94%，正確率爲 84%。正子掃描在 Squamous cell carcinoma 肺癌淋巴轉移的敏感度與陽性預測值均優於 Adenocarcinoma 肺癌。

【結論】

這次研究的結果與其他條件相似的研究相近，正子掃描對於肺癌縱膈腔淋胞轉移的敏感性並不高，但是特異性卻相當不錯，當電腦斷層無法確定淋巴分期時，加做正子掃描排除淋巴轉移時，病人更適合進行治癒性的手術。

PC40

Effects of T4 Withdrawal and rhTSH Injection Peparations on Radiation Exposure of Thyroid Cancer Patients Receiving I-131 Treatment

Meng-Fang Hsieh[1], Pei -Jung Li[1], Fong-Ru Lin[1], Pei-Yao Lin[2], Chia-Chi Chang[1]

[1]*Department of Nuclear Medicine, Changhua Christian Hospital, Changhua, Taiwan;*
[2]*Department of Nuclear Medicine, National Taiwan University Hospital, Taipei, Taiwan.*

Purpose: To realize radiation effects of different preparative protocols on thyroid cancer patients receiving I-131 treatment.

Materials and methods: Twenty-eight differentiated thyroid cancer patients (9 men, 19 women; mean age: 44 yr) who prepared for I-131 treatment were divided into 2 groups (Gp). Gp 1 was prepared with T4 withdrawal (n = 22) while Gp 2 was prepared with standard rhTSH injection (n = 6). Both groups received a comparable I-131 dosage (averaged 115 vs. 121 mCi). Radiation exposure was measured at immediately, day 3 and 7 after I-131 administration using a radio-detector (SEI Inspector + EXP; Unit: K CPM). Data expressed as mean ± SD.

Results: A comparable radiation exposure was measured from patients immediately after I-131 administration between the 2 groups (74.59 ± 22.02 vs. 74.88 ± 19.47) as measured at 1 meter distance. However, the exposure was significantly decreased in Gp 2 at day 3 (11.62 ± 6.69 vs. 5.62 ± 3.41; $p < 0.01$; or 51.6% decrease) compared to that of Gp. 2. The trend sustained till day 7 after I-131 administration (0.39 ± 0.29 vs. 0.26 ± 0.23; $p < 0.05$; or 33.3% decrease).

Conclusions: Although comparable radiation exposure was found in patients prepared by both T4 withdrawal and rhTSH injection groups immediately after I-131 treatment, preparation with rhTSH injection group showed significantly reduced radiation exposure at day 3 and 7 after I-131 treatment.

PC041

Comparison of the Applicability between Planar and Tomographic Pulmonary V/Q scintigraphy with Utilizing New Diagnostic Criteria for Perfusion SPECT/CT

Yu-Hung Chen[1], Shu-Hsin Liu[1,4]

[1]*Department of Nuclear Medicine, Buddhist Tzu-Chi General Hospital, Hualien, Taiwan;*
[2]*Department of Medical Imaging and Radiological Sciences, Tzu Chi College of Technology, Hualien, Taiwan.*

Introduction: Planar V/Q lung scintigraphy has many shortcomings when interprets with PIOPED criteria. The high rate of inconclusive results and probabilistic reporting format made it become less preferred imaging test. However, with the emergence of SPECT, many of the flaws in using planar V/Q lung imaging have been overcome. We here compare the applicability between planar and SPECT V/Q scan with using new diagnostic criteria for perfusion SPECT/CT.

Materials & Methods: We retrospectively reviewed patients referred for V/Q scintigraphy from Sep. 2013 to June 2015. Subjects were included if perfusion SPECT/CT was performed. For planar V/Q scan, modified PIOPED II was used to determine the probability of pulmonary embolism. The interpretation of planar scan was conducted by 2 independent nuclear medicine physicians. For tomographic imaging, we use binary reporting approach with at least one major segmental equivalent mismatched perfusion defect as positive for pulmonary embolism; otherwise, the study is negative (modified from the study by Le Roux et al.). We will record the inconclusive rate and inter-observer variability in planar studies. Also, the comparison between planar V/Q scan and perfusion SPECT will be analysed.

Results: There were totally 38 patients referred for planar V/Q scan with perfusion SPECT/CT performed. In planar image studies, 12 (31.6%) patients were interpreted as intermediate by interpreter A, whereas 2 (5.3%) were interpreted to be intermediate by interpreter B. Twenty-two (57.9%) patients' planar scan interpretation results were concordant between 2 interpreter. On the other hand, discordant results were noticed in 16 (42.1%) patients. Among the 16 discordant results, 4 (10.5%) were highly discordant, namely, the imaging was interpreted as high probability by one of the 2 physicians and low/very low/normal by another. When interpreted with perfusion SPECT/CT, 14 (36.8%) subjects were positive for pulmonary embolism. If we use perfusion SPECT/CT as reference standard, 21 (55.3%) and 29 (76.3%) cases were correctly stratified by the two interpreters (correct if positive scan was interpreted as high probability or negative scan was interpreted as low/very low/normal scan). On the contrary, 5 (13.2%) and 7 (18.4%) were incorrectly interpreted. Most of the incorrect interpretations were due to pulmonary parenchymal diseases or pleural fluid collection. Among those patients classified as intermediate probability, the positive rate was 33.3% (4 out of 12) and 50% (1 out of 2) for interpreter A and B respectively.

	Planar image (n)			SPECT/CT as reference standard		
Interpreter	High	Intermediate	Low-normal	Discordance	Correct	Incorrect
A	11	12	15	16 (42.1%)	21 (55.3%)	5 (13.2%)
B	16	2	16		29 (76.3%)	7 (18.4%)

Conclusions: The rate of intermediate results and inter-observer variability in planar V/Q scan is innegligibly high. In addition, when compared with tomographic imaging, the rate of correct interpretation is still unfavourable. Many of the incorrect interpretations were due to pulmonary parenchymal abnormality or pleural fluids, which were easy to be identified from transmission CT. Thus, pulmonary perfusion SPECT/CT should always be performed in patients referred for pulmonary V/Q examination.

References:

1. Roach PJ, Schembri GP, Bailey DL. V/Q scanning using SPECT and SPECT/CT. J Nucl Med. 2013 Sep;54(9):1588-96.
2. Le Roux PY, Robin P, Delluc A, et al. V/Q SPECT Interpretation for Pulmonary Embolism Diagnosis: Which Criteria to Use? J Nucl Med. 2013 Jul;54(7):1077-81.

PC042

Bone SPECT in Evaluation of Patients with Lower Back Pain

Dung-Ling Yu[1], Hsin-Wen Huang[2]

[1]*Department of Nuclear Medicine;*
[2]*Department of Radiology. Mennonite Christian Hospital, Hualien, Taiwan.*

Objectives: The purpose of this study is to evaluate the role of bone SPECT in patients with lower back pain (LBP).

Methods: There were 41 patients (age range: 47-75 y/o, mean age: 65.3 y/o, M:F = 25:16) with LBP collected in this study. Bone SPECT and CT/MR on lumbar spines were performed on all of patients. Bone SPECT was performed within 1 month of CT/MR. The results of bone SPECT were graded as negative and positive, and the results of CT/MR were graded by radiologist as negative and positive.

Results: 15 (36.6%) out of 41 patients were positive on bone SPECT, and 17 (41.5%) out of 41 were positive on CT/MR. Totally, 20 (48.8%) out of 41 patients had positive on either bone SPECT or CT/MR. There were 11 (26.8%) patients with positive both on SPECT and CT/MR, 11 (26.8%) patients with positive only on CT/MR, and 6 (14.6%) patients with positive only on SPECT.

Conclusions: Although CT/MR have higher positive rate than bone SPECT in patients with LBP, SPECT have another 14.6% positive findings not detected by CT/MR. Our study suggests that bone SPECT has a complementary role with CT/MR in evaluation of patients with LBP.

PC043

PET-CT in Detection of Primary Site in Patients with Neck Lymph Node Metastasis from Unknown Primary Origin

Dung-Ling Yu[1], Wen-Sheng Hsu[2], Kuo-Tong Liaw[3]

[1]*Department of Nuclear Medicine;*
[2]*Department of Oral Surgery;*
[3]*Department of Head and Neck Surgery. Mennonite Christian Hospital, Hualien, Taiwan.*

Objectives: The study is to evaluate role of PET-CT in detecting primary site in patients with neck lymph nodes (LN) metastases from unknown primary origin (UPO).

Methods: We retrospectively collected 19 patients (age range: 47-75 y/o, mean age: 63.1 y/o, M:F = 15:4) with neck LN metastases from UPO. All of patients had negative results in conventional diagnostic studies to detect primary site. All of patients underwent PET-CT to detect the primary site within 2 weeks after conventional diagnostic studies. Biopsy was done while the primary site detected by PET-CT.

Results: Eight out of 19 (42%) patients had abnormal findings suggesting primary site, and 11 out of 19 patients had no abnormal uptake. Biopsy was done on 8 patients with possible primary site. The pathological results showed positive in 4 patients, with 2 in tonsillar area and 2 in nasopharyngeal roof, and inconclusive in 4 patients.

Conclusions: In total, PET-CT may detect primary site in 21% (4/19) patients with neck LN metastases from UPO. PET-CT is an useful diagnostic tool for defection of primary site of UPO presenting with neck LN metastases.

PC044

探討核醫放射藥品對骨質密度測定的影響

宋慶琳[1] 陳昱宏[1] 莊祿堂[1] 林育宣[1] 劉淑馨[1,2]

[1] 花蓮慈濟醫院核子醫學科
[2] 慈濟科技大學醫學影像暨放射科學系

目的

癌症的治療易造成骨質快速流失，增加骨折發生的機會，故臨床上常有骨頭掃描的病人會回來做骨質密度測量，根據 ISCD 建議在雙能量吸收儀 (DXA) 量測 Bone mineral density (BMD) 前不要注射放射性藥物，若有 Tc-99m procedures 則延後 48-72 小時。然而，許多研究仍呈現不同的結果，因此本研究便利用假體的試驗來探討 Tc-99m 對骨質密度檢查結果是否有影響。

材料與方法

本研究使用骨質密度儀機型爲 Hologic QDR4500W，使用的假體爲 Hologic Anthropometric spine phantom，並在 phantom 上放置長寬高約爲 16*14*7 cm 的塑膠盒 (如圖)。本試驗分實驗組與對照組，實驗組在塑膠盒內置入 5 mCi/ 5 mL 的 Tc-99m 及 95 c.c. 的水，對照組爲 100 mL 的水，各掃描十次，紀錄其 BMD 並以 Student's t-test 分析比較各組平均值的差異性。

結果

在此實驗中得到的結果發現實驗組 (塑膠盒內裝有 Tc-99m) 其測得的 BMD 平均值爲 0.9931，標準差爲 0.00166，對照組 (100 c.c. 的水) 其 BMD 平均值爲 0.9937，標準差爲 0.00271，兩者量測的 BMD 平均值並無顯著之差異 ($p = 0.56$)。

組別	N	BMD 平均值	標準差	p value
實驗組	10	0.9931	0.00166	0.56
對照組	10	0.9937	0.00271	

結論

此實驗結果初步得知放射性藥品並不會對 BMD 量測值造成顯著的影響，因此推測若病人先注射 Tc-99m methylene diphosphonate 再施行骨質密度檢查其結果並無顯著的影響。然而，本實驗爲小樣本的假體實驗，未來仍需更大型的人體試驗來應證。

PC045

Applicability of the Appropriate Use Criteria for Myocardial Perfusion SPECT: Experience in Single Center from Eastern Taiwan

Yu-Hung Chen[1], Mei-Ling Chen[2], Shu-Hsin Liu[1,3]

[1]*Department of Nuclear Medicine, Buddhist Tzu-Chi General Hospital, Hualien, Taiwan;*
[2]*Division of Cardiology, Department of Internal Medicine, Buddhist Tzu Chi General Hospital and Tzu Chi University, Hualien, Taiwan;*
[3]*Department of Medical Imaging and Radiological Sciences, Tzu Chi College of Technology, Hualien, Taiwan.*

Introduction: The prognostic value of stress myocardial perfusion SPECT (MPS) is well established, and its use is incremental to clinical, exercise electrocardiography and coronary angiographic information. This has led to a great expansion in use and subsequent expenditure. To aid in the optimal use of MPS, Appropriate Use Criteria (AUC) has been developed by American College of Cardiology. However, the impact and applicability are yet to be thoroughly investigated.

Materials & Methods: A retrospective review of 279 patients' MPS visits was conducted from Jan. 2015 to Mar. 2015 (patients referred for health exam and referred from other hospitals were excluded). Subjects were stratified according to 2009 AUC for MPS into appropriate, uncertain and inappropriate groups. For AUC stratification, patient's referring indications, past medical histories, lipid profiles in 3 months of MPI for calculation of Framingham risk, history of revascularization, previous stress tests results will be reviewed. The Framingham risk calculation was based on D'Agostino RB Sr et al.'s work published in 2008, which included diabetes as one of the risk factor. In addition to above mentioned data, the MPS reports and follow-up coronary angiographic (CAG) data, if available, will be recorded as well. We will analyze the appropriateness of MPS ordering according to AUC in our center. Furthermore, the percentage of MPS abnormality and CAG significant stenosis (stenosis ≥ 70% or FFR < 0.8) will be calculated in each AUC groups as well.

Results: Of the 279 patients evaluated, 75 patients were unable to be analyzed by AUC due to insufficient data (lack of lipid profile in 3 months of MPS). Among the 204 eligible subjects, 175 (85.8%) were stritified as appropriate, 4 (2.0%) were uncertain and 25 (12.3%) were inappropriate. For pre-operative evaluation (n = 19), 11 out of 19 (57.9%) were classified as inappropriate. There were 94 out of 175 (53.7%) MPS results reported to be abnormal in appropriate group, on the contrary, only 25% and 8.0% MPS results reported to be abnormal in uncertain and inappropriate groups. There were finally 70 patients received CAG (65 in appropriate group, 1 in uncertain group and 4 in inappropriate group). Among the 70 CAGs, 38 showed significant stenosis and were both in appropriate group and MPS positive. Five patients in uncertain and inappropriate group received CAG, no significant stenosis was detected, even if 2 of them were MPS positive.

AUC group	N (%)	MPS positivity	CAG significant stenosis (n = 70)
Appropriate	175 (85.8%)	94/175 (53.7%)	38/65 (58.5%)
Uncertain	4 (2.0%)	1/4 (25%)	0/1 (0%)
Inappropriate	25 (12.3%)	2/25 (8.0%)	0/4 (0%)

Conclusions: The percentage of appropriate use in our center is high as compared with the literature reported. Nevertheless, there was substantially inappropriate use in pre-operative evaluation, which might be resulted from unfamiliar to AUC in surgical specialties and the different risk factors used in pre-operative evaluation. In addition, we have noticed that the percentage of abnormal MPS report is significantly lower in uncertain and inappropriate groups. Also the CAG results showed no significant stenosis in those two groups, even if the MPS result is positive. This might indicated that AUC can select candidates for MPS and avoid unnecessary expenditures.

References:

1. Doukky R, Hayes K, Frogge N, et al. Impact of appropriate use on the prognostic value of single-photon emission computed tomography myocardial perfusion imaging. Circulation. 2013 Oct 8;128(15):1634-43.
2. Hendel RC, Berman DS, Di Carli MF, et al. CCF/ASNC/ACR/AHA/ASE/SCCT/SCMR/SNM 2009 Appropriate Use Criteria for Cardiac Radionuclide Imaging: A Report of the American College of Cardiology Foundation Appropriate Use Criteria Task Force, the American Society of Nuclear Cardiology, the American College of Radiology, the American Heart Association, the American Society of Echocardiography, the Society of Cardiovascular Computed Tomography, the Society for Cardiovascular Magnetic Resonance, and the Society of Nuclear Medicine. J Am Coll Cardiol. 2009 Jun 9;53(23):2201-29.
3. D'Agostino RB Sr, Vasan RS, Pencina MJ, et al. General cardiovascular risk profile for use in primary care: the Framingham Heart Study. Circulation. 2008 Feb 12;117(6):743-53.
4. Mahajan A, Bal S, Hahn H. Myocardial perfusion imaging determination using an appropriate use smartphone application. J Nucl Cardiol. 2015 Feb;22(1):66-71.

PC046

運用 HFMEA 手法及跨部門合作方式改善委外報告人工輸入錯誤發生率

呂佳靜　方雅潔　余景陽　何佩芸　陳冠羽　林慶齡　鄭嘉惠　林庭宇

國泰綜合醫新陳代謝內分泌科放射免疫室

前言

Healthcare Failure Mode & Effect Analysis (醫療失效模式與效應分析)，是一種風險分析工具，旨在分析系統範圍內潛在的失效模式，按照嚴重程度加以分類，並確定失效對於該系統的影響。本實驗室在藉由此方法進行風險評估並提升服務效益時發現，包含本實驗室之大多數醫學實驗室，在進行委外檢驗項目時，工作清單及報告因外部實驗室電腦系統無法與本身相通，檢驗醫令及數據報告均仰賴人工輸入，不僅費工耗時，且易產生「檢驗前 (preanalytic)」及「檢驗後 (postanalytic)」誤差，包含誤植檢驗項目或報告數據，嚴重者甚至造成誤診。本篇則呈現本實驗室進行風險評估後並聯合各部門進行跨部門合作的改善結果。

方法

Healthcare Failure Mode & Effect Analysis (醫療失效模式與效應分析)，首先流程分析出六項主流程與展開 16 項次流程 (見圖一)。再經由計算危害指數與決策數得知 , 需採行改善預防措施的失效原因有 7 項 (見圖二)，危害指數計算方式與定義詳見表一。

針對以上失效原因進一步提出「排除、控制或接受」的改善手段，本實驗室採取自動化的方式將缺失予以徹底排除，預計改善措施包含傳輸工作清單予委外單位 (實驗室→委外單位)、委外單位將報告傳輸至實驗室 (委外單位→實驗室)，以及資訊單位及委託連線公司設計程式將以上功能自動化。

結果

目前本實驗室已完成部份連線功能，可整批將檢驗指令及檢驗報告藉由 LIS 系統匯出形成電子檔案，再透過實驗室間傳輸後匯入各自的 LIS 系統，取代原本所有項目數據均需仰賴人工的輸入方式，避免人工輸入可能導致之失誤產生。預期危害指數中的嚴重程度不變，但發生頻率將大幅下降，危害指數從原本總分 72 分降為 44 分，降幅為 38.9%。

討論

經由以上結果可知，醫學實驗室在委外檢驗工作上，在透過 HFMEA 後均可能發現與本實驗室類似的風險，在排除方式上亦可如結果所述，藉由資訊系統將醫令 / 數據進行檔案封包並進行匯入 / 出，避免人工輸入的錯誤，然多數實驗室一旦面臨資訊傳輸時必然會因資安疑慮，無法於委託及受委託實驗室系統間直接進行數據及醫令拋轉，導致自動化程度不足，能否有進一步提升則須仰賴資訊人員的開發；此外各實驗室的資訊化程度不一，委託與受委託實驗室間的合作亦需互相配合。目前預計將類似的系統概念推展至其他有相同需求的實驗室，全面提升工作品質效率。

參考文獻

田霓、張慈容、蕭瓊子、施木青、盧章智、劉淳儀、吳錫金、張照勤 (民 100)。運用醫療失效模式與效應分析建立臨床檢驗不符合事件評估機制，醫療品質雜誌，5(4), P42-50。

胡寶雪、胡曉珍、黃惠如、趙慧玲、雷宜芳 (民 103)。運用失效模式與效應分析改善手術室病理檢體採集送檢流程及退件率，護理雜誌，61(2), P50-59。

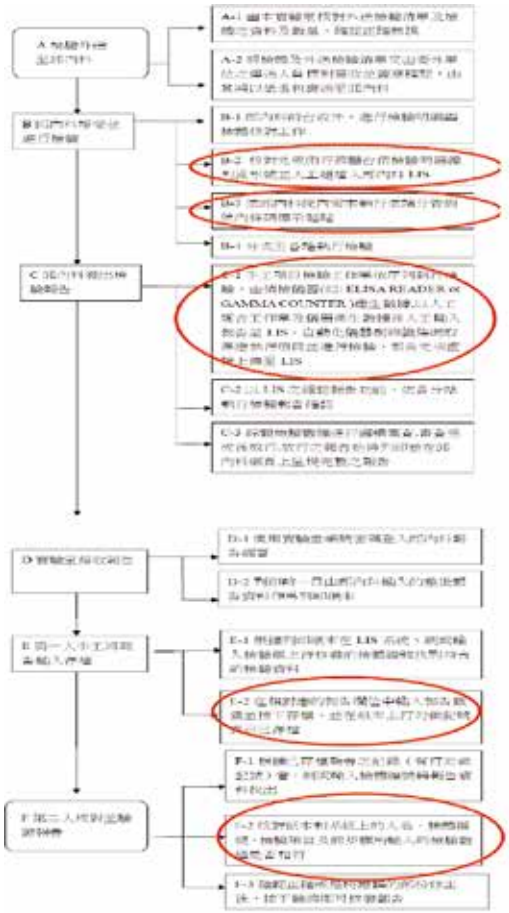

圖一

圖二

嚴重：報告錯誤（病人已受到醫療上處置）
重度：報告更改（由他人發現報告異常、檢體錯置/人為輸入錯誤，但病人還未受到醫療上處置）
中度：報告延誤（品管異常、測驗）
輕度：隨機誤差（內部主動發現報告錯誤且立即修改）

	嚴重 4	重度 3	中度 2	輕度 1
經常 4	16	12	8	4
偶爾 3	12	9	6	3
不常 2	8	6	4	2
很少 1	4	3	2	1

經常：每週發生 1 次或以上
偶爾：每月發生 1 ~ 3 次
不常：每季發生 1 ~ 3 次
很少：每年發生 3 次以下

表一

PC047

甲狀腺癌碘 -131 治療住院病人外釋後輻安生與健康衛教與評估

張桂蘭　朱秀蘭　張晉銓　陳毓雯　張玉芬

高雄醫學大學核子醫學科

摘要

目的

核醫對於甲狀腺癌治療在醫療以外科手術切除，殘餘的甲狀腺則施以碘 -131 治療，不論是停藥及施打 rhTSH 及住院病房的輻安管制技術皆已成熟。患者亦能從醫師及網路獲取輻防知識，但是高醫近幾年順利運作結果發現，因患者疾病本身症狀爲焦慮的特性，及一般家屬對輻射的觀念是負面的，所以出院後在正常衛教下，仍對於飲食及生活接觸上常有過度實行的情形；例如：不敢回家住 (住飯店)、不敢抱小孩、不敢吃各種食物，…等。針對這些情形，因此設計各項問卷題目，以了解並導正患者之心裡對攝取食物限制及出院後對輻射的恐懼，協助患者早日正常生活。

研究方法

設計出各式題目之問卷，出院後 9 日回診時填問卷紀錄，出院後問卷題目包括：1. 飲食紀錄，吃了甚麼？不敢吃甚麼？都不敢吃？ 2. 居住地點 3. 每天日和家人相處時間 4. 是否上班 5. 運動多久 6. 單獨睡覺，幾日？及輻射防護病房原碘治療急性症狀不同題目之問卷表，及服藥後不舒服情形項。

一個月後照護甲狀腺癌手術治療之個管師進行電話查訪，詢問生活及健康查訪，輻防人員協同給予正面回答解釋與問候。

結果與討論

由於 I-131 在注入病人體內 24 小時約有 76% 的活性會隨排泄物排出，依據輻防人會測量出病患 1 米處，70 uSV/h 量測之劑量率爲外釋標準，統計出 64% 患者在 1 米處劑量率均在 20 uSV/h 以下，遠低於法規限值 (110 uSV/h)，32% 在 20-50 u SV/h 之間；4% 在 50-70 之間；對於外釋後滯留在身上之相對劑量，加以說明出院後與家人相處之輻防安全準則及生活正確態度。統計出比較嚴重的問題是出院一兩個月後，仍有腫痛，心悸，及正常生活過度憂鬱等問題，教導患者輻安知識及諮詢內分泌科醫師討論症狀。並且醫院對甲狀腺癌開刀後碘 -131 治療前後安排個管師從連絡患者，安排住院，及心理輔導，至一系列安衛教，協助陪伴患者在治療路途中，可以用更輕鬆的心情面對。

PC048

FDG PET and Perfusion SPECT Findings in A Suspected Case of Rasmussen Encephalitis

Kuan-Yin Ko[1], Mei-Fang Cheng[1], Ruoh-Fang Yen[1]

[1]*Department of Nuclear Medicine, National Taiwan University Hospital.*

Introduction: Rasmussen encephalitis is a chronic, progressive inflammation of the brain of unknown origin that typically develops during childhood, characterized by intractable focal seizure and progressive neurological impairment associated with a progressive unilateral hemispheric atrophy. We reported one case that clinical and imaging data were infavour of Rasmussen encephalitis.

Case summary: A 3-year-old boy was admitted for a seizure consisting of right upper extremity twitching and deviation of the eyes to the right side. His medical history was unremarkable and developmental milestones had been normal. Findings of routine laboratory work-up, including cerebrospinal fluid (CSF) examination were normal. Electroencephalography (EEG) performed showed focal epileptiform discharges over left fronto-temporal area. The child's clinical condition deteriorated over the next few days. Antiepileptic medication was given initially with no obvious clinical response. Intravenous gamma globulin and prednisolone were added. Brain magnetic resonance (MRI) indicated no gross structural abnormality. Proton MR spectroscopy revealed decreased the ratios of NAA/choline and NAA/creatine, implying neural damage. The inter-ictal brain single photon emission computed tomography (SPECT) (Tc^{99m}-ECD) showed a left hemisphere decreased cerebral blood flow. Brain FDG positron emission tomography (PET) pointed to a large hypometabolic area at left frontal and left temporal lobes and a suspiciously active inflammatory process at left occipital to posterior parietal lobe. Rassmusen's encephalitis presented as epilepsia partialis continua was suspected. Combine meeting with medical specialties for further intervention such as hemispherectomy or vagus nerve stimulation will be held.

Conclusion: Brain SPECT and PET in Rasmussen encephalitis have revealed a pattern of diminished cerebral perfusion and metabolism corresponding to affected regions. They increased the diagnostic confidence in those cases which the MR imaging findings were subtle or bilateral and might help localize and guide brain biopsy.

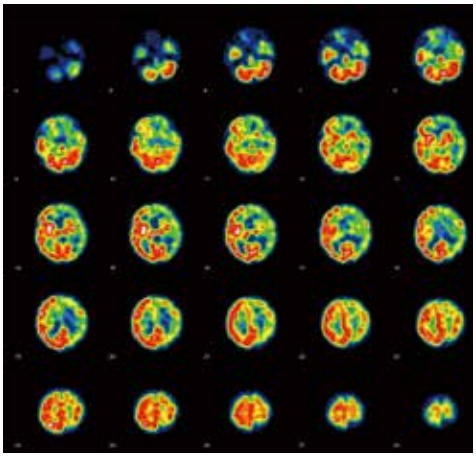

Figure 1. Inter-ictal brain SPECT (transaxial slices) showed a left hemisphere decreased cerebral blood flow.

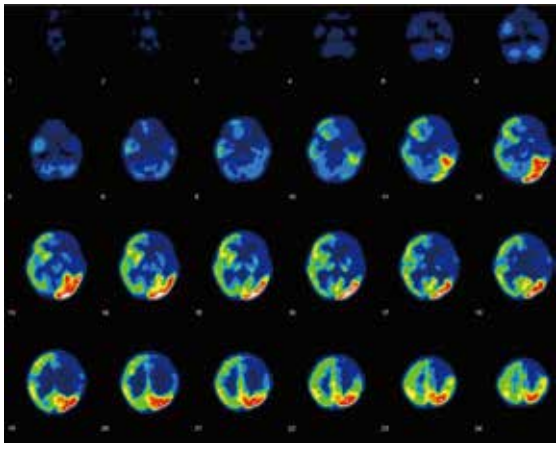

Figure 2. FDG PET images were obtained two days after SPECT, showing a large hypometabolic area at left frontal and left temporal lobes. Besides, an active inflammatory process at left occipital to posterior parietal lobe was suspected.

PC049

A novel Analysis of Dynamic ^{18}F-FDG PET/CT Standardized Uptake Values for Characterizing Solitary Pulmonary Lesions in A Region with Endemic Granulomatous Diseases

Yu-Erh Huang[1], Yu-Jie Huang[2], Mary Ko[3], Chien-Chin Hsu[4], Chih-Feng Chen[5]

Department of [1]Nuclear Medicine, [3]Pediatrics, [5]Radiology, Chiayi Chang Gung Memorial Hospital.
Department of [2]Radiation Oncology, [4]Nuclear Medicine, Kaohsiung Chang Gung Memorial Hospital.

Background: Granulomatous diseases (GDs) can be metabolically active and indistinguishable from lung cancer on ^{18}F-FDG PET imaging. Evaluation of solitary pulmonary lesions remains a diagnostic challenge in regions with endemic GDs.

Purpose: To measure the SUVs of solitary pulmonary lesions on dynamic ^{18}F-FDG PET/CT imaging and to compare the efficacy of the results with that of retention index (RI) in identifying malignant pulmonary lesions.

Material and Methods: A total of 49 patients had solitary pulmonary nodules or masses with histopathological diagnoses and triple-phase ^{18}F-FDG PET/CT imaging. For initial dynamic phase acquired for 50 minutes immediately after ^{18}F-FDG injection, time-SUV (TS) curves were generated. The slope of the TS curve was calculated and defined as SUV_{slp}. For early and delayed static phases acquired 1 and 3 hours respectively after ^{18}F-FDG injection, the SUV_{1h}, SUV_{3h} and RI were calculated.

Results: There were 37 malignant and 12 benign pulmonary tumors (MT and BT, respectively). Over half (7/12) of BT was GD. The SUV_{slp} value was significantly different between MT and BT while the RI value was not. SUV_{slp} is better than RI in terms of specificity and accuracy for MT. The value of SUV_{slp} was significantly higher in MT than in GD (0.072 $\pm$ 0.048 and 0.030 $\pm$ 0.017, respectively; $P = 0.02$), while the RI values of the two were both high (18.6% $\pm$ 19.5% and 19.6% $\pm$ 11.2%, respectively; P = not significant).

Conclusion: SUV_{slp} is better than RI at characterizing solitary pulmonary nodules and masses in regions with endemic GDs.

PC050

Subcutaneous Panniculitis-like T-cell Lymphoma Presenting as Sailor Collar Pattern: A Case Report

Yu-Ling Hsu[1], Dom-Gene Tu[1]

[1]*Department of Nuclear Medicine, Ditmanson Medical Foundation Chia-Yi Christian Hospital.*

Abstract

A 27-year-old male had intermittent fever for two months, accompanied with chillness, cough, and sorethroat. Body weight loss, post nuchal pain, and painful swelling over left axillary and supra-clavicular regions were also noted. Because of above symptoms and signs, biopsy over axillary region was performed, revealing subcutaneous panniculitis-like T-cell lymphoma. PET/CT scan for staging revealed sailor collar pattern over the patient's neck and upper trunk; also hepatomegaly and splenomegaly. The patient was then put on chemotherapy for further treatment.

Keywords: subcutaneous panniculitis-like T-cell lymphoma; sailor collar pattern

PC051

使用全手動方式計算心血池造影右心室搏出率之評估

吳忠順[1] 俞長青[1] 詹宏彬[1] 胡璿[1] 蘇詩琪[1] 彭南靖[1,2]

[1] 高雄榮民總醫院核醫部
[2] 陽明大學醫學院

背景介紹：

臨床常使用心血池造影 (Multigated Blood Pool Analysis, MUGA) 評估心室搏出率 (ejection fraction, EF)，此項檢查爲非侵入性且對於左心室 EF 準確性高，而右心室 EF 則因以原廠 iso-contour 程式分析時，可能受到周圍鄰近的血管組織干擾以及電腦軟體於圈選感興趣區 (ROI) 後，ROI 無法隨著右心室的收縮變化作有效的圈選等因素，使計算值受到嚴重低估，而與目視觀察受檢者收縮狀況有相當差距。本研究使用全手動方式 (manual) 計算右心室 EF，探討此種方式與使用 iso-contour 之差異。

方法：

本研究對象爲本部 104 年 7 月到 8 月間執行 MUGA 造影之受檢者，使用儀器爲 Siemens Symbia S，使用藥物爲 Tc99m-RBC 20 mCi。影像分析時先以原廠 iso-contour 程式繪製右心室及其背景 ROI，繪製時參照振幅圖及相位圖以避開其他組織的干擾，manual 方式則分別找出右心室最大舒張及收縮的影像後，參照 iso-contour 之描繪分別繪製右心室舒張末期、舒張末期背景值及收縮末期之 ROI。將背景值 ROI 內總計數以舒張末期之總畫素 (pixel size) 與背景值總畫素作等比率修正後，將右心室舒張末期 (EDC)、舒張末期背景值 (Bg) 及收縮末期 (ESC) 之總計數 (total counts)，輸入 excel 代入程式 EF =【(EDC counts- ESC counts)/ (EDC counts- Bg counts)】x 100% 計算。

結果：

本研究共收集 122 位受檢者，平均年齡爲 62.0 歲 (range：20-90 歲)，男性 76 位 (62.3%)，女性 46 位 (37.7%)，左心室 EF 平均值爲 58.2，右心室 EF 以 iso-contour 和 manual 方式計算的平均值分別爲 32.4 和 42.0。以左、右心室 EF 分別大於 50 及 40 爲正常，在左心室 EF 正常之 94 位受檢者中，以 iso-contour 和以 manual 方式計算之右心室 EF 正常者分別爲 29 位 (30.9%) 和 71 位 (75.5%)。若進一步比較左心室 EF 正常之族群中曾執行心臟超音波肺動脈收縮壓 (PASP) 檢查之受檢者，以 PASP 小於 40 mmHg 爲正常值界限，其中有 80.6% 之受檢者 PASP 爲正常。

結論：

本研究發現以 iso-contour 計算之右心室 EF 正常率明顯偏低 (只佔左心室 EF 正常者 30.9%)，而以 manual 方式計算右心室 EF，所得結果除更能符合以目視結果評估受檢者收縮狀況之期待，也與 PASP 檢查正常之比率相近，分析右心室 EF 時先以 iso-contour 方式，再輔以 manual 方式應可獲得更佳的效果。

PC052

A Case with Systemic Calcinosis (Subcutaneous and Cardiac Calcinosis) Characterized by Tc-99m MDP Bone Scintigraphy and Thallium Myocardial Perfusion Imaging

Ming-Che Chang[1,3], Ying-Ming Ciou[2], Ying-Hsuan Li[1], Kuang-Tao Yang[1]

[1]*Department of Nuclear Medicine, Changhua Christian Hospital;*
[2]*Department of Allergy Immunology and Rheumatology, Changhua Christian Hospital;*
[3]*Department of Medical Imaging and Radiological Sciences, Central Taiwan University of Science and Technology.*

Abstract

A Tc-99m MDP bone scan showed diffuse myocardial uptake in addition to linear subcutaneous uptake of isotope in the proximal thighs and pretibial regions, left hip and bilateral ischial regions in a 38-year-old woman who reported swelling, erythema and subcutaneous hard nodules at the left foot and dyspnea on exertion for months, undergoing peritoneal dialysis. Laboratory values revealed serum hypocalcemia, hyperphosphatemia, normal iPTH, elevated troponin-I level and elevated CPK-MB mass. Abdomen CT showed calcified subcutaneous deposits at bilateral hips but not notably abnormal myocardial calcification. Myocardial perfusion imaging using thallium-201 revealed reduction of myocardial radioactivity with global hypokinesis in the left ventricle. Atherosclerotic change was found on her left heart cathelation. Myocardial calcinosis was impressed.

PC053

Combined PET / CT Scan with Color Doppler Resistance Index of Ultrasound for the Assessment of Incidental Breast Cancer – A Case Report

Shu-mei Lu, Yu-Ling Hsu, Dom-Gene Tu

Department of Nuclear Medicine, Ditmanson Medical Foundation Chia-Yi Christian Hospital, Chia-yi, Taiwan.

Introduction: Positron emission tomography (PET), with or without integrated computed tomography (CT), is based on the principle of using ^{18}F-fluorodeoxyglucose (FDG) to evalutate glucose metabolism in inflammation and most malignant tumors. Its use in patients with breast cancer has been broadly investigated, shown to be useful in staging, re-staging, and treatment response monitoring, in primary and recurrent diseases.

Case report: A 55-year-old female with past history of right tonsil lymphoma (Diffuse large B cell lymphoma), stage III, has acceptedchemotherapy and splenectomy, also received PET-CT scan for re-staging plan .She was fasted except water for 6 hours before PET-CT scan; received intravenous injection of 8 mCi FDG; performed the scan from skull to thigh. The imaging revealed a hypermetabolic tumor in the outer upper quadrant of left breast around 1.5 cm (SUVmax: 2.7).

Later, she did the ultrasound for breasts, which we tried to find the correlation between different imaing modalities, to assess intratumoral blood flow by color Doppler ultrasonography. The lowest resistance index (RI) was recorded. The results showed a solid mass (1.33 x 1.15 x 1.11 cm) at 2 o'clock in left breast. Color Doppler resistance index (RI) was 0.941, highly suspected malignancy.

The patient then received left breast partial mastectomy, and the histopathological result has proved to be invasive ductal carcinoma.

Discussion: The analysis of vascular resistance index combined with findings on gray-scale sonographic images can be of great assistance in the assessment of nodular breast lesions greater than 1 cm, with high sensitivity and specificity. The results demonstrate that an RI ≥ 0.69 (0.7) in a nodule > 1 cm suggesting a higher risk for malignancy.[1,2] As we know, ^{18}F-FDG PET/CT has relatively high uptake in malignant tumors as well. In combination of these two imaing modalities, the reported case shows compatible findings between ^{18}F-FDG PET/CT and Color Doppler ultrasonography, suggesting the efficacy of Color Doppler ultrasonography alone, or with combination of PET/CT scan, can be a good diagnostic tool for evaluating breast tumors.

PC054

降低正子造影糖尿病受檢者腸道 FDG 攝取對判讀之影響

江泰林 [1] 陳遠光 [1,2]

[1] 新光吳火獅紀念醫院正子中心
[2] 新光吳火獅紀念醫院核子醫學科

背景介紹：

FDG PET 對於大腸癌有極高的敏感度，單一顆界限分明病灶又加上 FDG 攝取，可能懷疑爲惡性，整條均勻的 FDG 攝取，多半非惡性病變，糖尿病口服用藥主要減少腸道吸收葡萄糖機制降低血糖值，但有可能造成腸道內 FDG 廣泛性聚積，干擾病灶的偵測。

方法：

對於糖尿病用藥受檢者，未打 FDG 前就先喝緩瀉劑，使腸道提早受到緩瀉劑作用，降低腸道 FDG 聚積的干擾。收集受檢者有糖尿病口服用藥 74 人，分成有喝和沒喝緩瀉劑兩組，由醫師和放射師依影像 (升結腸段、橫結腸、降結腸、乙狀結腸區) 是否廣泛性吸收共同評分，影像品質優者 10 分（全腸道無 FDG 聚積）、良者 7 分（兩腸段輕微 FDG 聚積）、劣者 4 分（兩腸段 FDG 聚積）、差者 1 分（全腸道爲 FDG 聚積）。

結果：

有喝緩瀉劑 31 人受檢者裡一共有 15 位受檢者有 29 腸段 FDG 堆積，產生 FDG 堆積干擾影像發生率爲 48.3%；沒喝緩瀉劑 43 人受檢者一共裡有 30 位受檢者有 56 腸段 FDG 堆積，產生 FDG 堆積干擾影像發生率爲 69.7%。經統計影像品質評分結果有喝緩濟劑這組平均分數爲 7.6 ± 2.1；沒喝緩濟劑平均分數爲 5.9 ± 2.3，採用 student's t 檢定方式計算 P value 值，比較兩組之差異性，所得結果 P 值爲 0.0012，由數據 P 值得知有明顯差異，其影像品質有明顯改善。

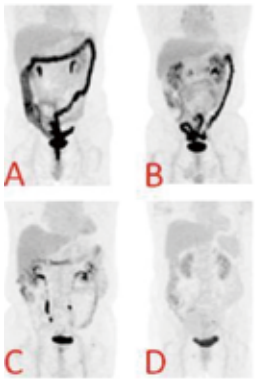

圖 1. 影像品質評分：A 爲 1 分、B 爲 4 分、C 爲 7 分、D 爲 10 分。

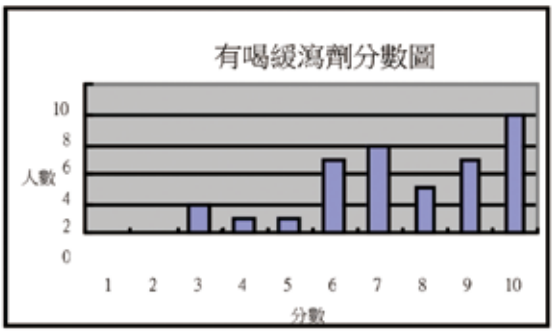

圖 2. 有喝緩瀉劑分數分佈圖，大多數人落於 6 到 10 分。

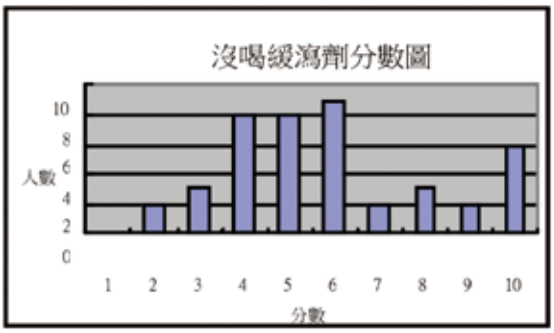

圖 3. 沒喝緩瀉劑分數分佈圖，大多數人落於 4 到 6 分。

結論：

對於糖尿病用藥之受檢者，施打 FDG 前喝下緩瀉劑加上對比劑是預防性的作法，使腸道提早受到緩瀉劑作用，來降低糖尿病受檢者腸道 FDG 堆積，可以改善腸道 FDG 聚積的影像品質，好的 FDG PET 影像可以協助醫師對病灶診斷與判讀的信心。

PC055

Aneurysmal Bone Cyst in Bone Scintigraphy: A Case Report

Ya-Cing Hsu, Ya-Chin Tsai, Dom-Gene Tu

Department of Nuclear Medicine, Ditmanson Medical Foundation Chia-Yi Christian Hospital.

Case report: A 16-year-old girl was referred for bone survey in our department. She felt bone pain at right arm for 2 weeks without swelling and trauma history. X-ray showed osteolytic lesions over right humerus. Bone scintigraphy was performed 3 hours after 20 mCi ^{99m}Tc-MDP injection, revealing no definite abnormal bone uptake. Following MRI demonstrated long segmental bone marrow lesion involving metaphysis and diaphysis. Curettage and biopsy were performed, and the pathologic report revealed aneurysmal bone cyst. Later, she received further curettage and bone grafting, and kept follow up in our orthopedic OPD.

Discussion: Aneurysmal bone cysts usually occur in the metaphysis of the long bones in the first two decades of life. They consist of cavernous blood-filled spaces. It has been reported that there is increased uptake in a ring-like pattern around the periphery of aneurysmal bone cyst in bone scintigraphy. However, the bone scintigraphy of our case showed no definite abnormal uptake. Bone scintigraphy is not specific for aneurysmal bone cyst, but the appearance of it might reflect the pathophysiologic change. Conventional treatment for aneurysmal bone cyst has been directed at the surgical removal of the entire lesion, or as much as possible. If no coexisting lesion is identified, lesions are usually treated with curettage and bone grafting, with more aggressive treatment reserved for recurrent lesions.

PC056

Tc-99m MDP Scintigraphy and F-18 FDG-PET Manifestations of Dermatomyositis in a Patient With Non-Small Cell Lung Cancer

Yi-Hsien Chou, Jei-Yie Huang, Ruoh-Fang Yen

Department of Nuclear Medicine, National Taiwan University Hospital and National Taiwan University College of Medicine, Taipei, Taiwan.

ABSTRACT

Dermatomyositis (DM) is an idiopathic inflammatory myopathy, associated with increased risk of malignant disease. Adenocarcinomas of the cervix, lung, ovaries, pancreas, bladder, and stomach account for approximately 70 percent of the cancers associated with inflammatory myopathies.

The initial presentation of our patient was arthralgia plus myalgia over proximal extremities and progressive weakness over both lower limbs. Followed by enlarging pruritic erythematous rash on forehead and bilateral eyelids, hoarseness with sore throat, and dyspnea, which eventually brought him to our hospital. Dermatomyositis was confirmed by skin biopsy and electromyography. Investigations for malignancy showed a LUL nodule in CXR and CT-guided biopsy revealed adenocarcinoma.

FDG-PET and bone scan were arranged for primary staging. In addition to hot areas at LUL nodule, left upper para-tracheal, para-aortic and left hilar nodes, FDG-PET displayed symmetrically increased tracer activity at muscle of bilateral proximal extremities. Bone scintigraphy with Tc-99m MDP also showed increased tracer uptake in muscle of bilateral proximal extremities, which is consistent with FDG-PET.

This case report demonstrates the rare condition of consistent findings in bone scan and FDG-PET of paraneoplastic dermatomyositis.

PC057

Incidental Finding of Solitary Plasmacytoma with Multiple Myeloma in Thallium-201 Myocardial Perfusion Scintigraphy

Hung-Pin Chan[1], Shyh-Jer Lin[2], Yu-Li Chiu[1], Chang-Ching Yu[1,3], Nan-Jing Peng[1,4]

[1]Department of Nuclear Medicine, Kaohsiung Veterans General Hospital, Kaohsiung City, Taiwan;
[2]Division of Hematology-Oncology, Department of Internal Medicine, Kaohsiung Veterans General Hospital, Kaohsiung City, Taiwan;
[3]Department of Information Engineering, I-Shou University, Taiwan;
[4]National Yang-Ming University, School of Medicine, Taipei, Taiwan.

Abstract:

Few studies have presented solitary plasmacytoma in thallium-201 myocardial perfusion scintigraphy (Tl-201 MPS). We describe here a 69-year-old man who was referred for Tl-201 MPS due to ongoing complaints of chest tightness and intermittent chest pain. Thallium-201 myocardial perfusion imaging revealed myocardial ischemia in RCA territory. A careful review of the cinematic raw data revealed focal hot uptake over the upper chest. The single-photon emission computed tomography/computed tomography (SPECT/CT) showed bony invasion over the sternal manubrium and biopsy showed plasmacytoma. Local radiotherapy was arranged for this patient. After 6 months follow-up, he complained general bone pain and was diagnosed multiple myeloma. SPECT/CT could provide a function-and-structure fused image for clinical use and a guide for therapeutic management. This case demonstrates the added value of Tl-201 MPS in finding unusual solitary plasmacytomas and monitoring post-stenting myocardial perfusion.

PC058

正子掃描在甲狀腺癌且碘 131 治療不佳病人之應用

張添信[1] 陳慶元[1]

[1] 台中慈濟醫院

背景介紹：

甲狀腺癌近幾年來，有逐漸趨升的現象，尤其今年更擠入國人癌症前十位，本院碘 131 治療病房啓用迄今 2-3 年，發現一些特殊族群，甲狀腺分化良好但放射性碘 131 治療不佳，且甲狀腺球蛋白 (Tg) 有上升趨勢，這一組群利用正子掃描 (PET/CT) 有很好的靈敏度在碘 131 治療不佳且分化良好 (RRDTC) 族群。

方法：

將治療過碘 131 同位素的病人，且甲狀腺球蛋白 (Tg) 數值上升，但碘 131 全身掃描 (I-131 cancer work up) 呈現陰性的病人進行比較，符合條件的病人總共 23 位，比較甲狀腺腺球蛋白 (Tg) 與正子掃描靈敏度 (sensitivity) 的關係。

備註：Tg 值需在 TSH 數值在 30 mU/L 才有意義。

結果：

利用 PET/CT 發現甲狀腺腫瘤在 Tg 在 10 μg/L 以下的靈敏度爲 25%，在 10-20 μg/L 區間爲 40%，在 50 μg/L 含以上爲 70%。

結論：

PET/CT 掃描能提供有效的診斷資訊在甲狀腺癌病人，尤其是在檢測高 Tg 值但碘 -131 全身掃描陰性病人尤其顯著，但須注意病人檢測 Tg 時，應加測甲狀腺球蛋白抗體 (Antibody Tg、ATA)，以免造成 Tg 值僞性偏高或偏低。正子掃描發現此特定族群高 Tg 但碘未吸收造影 (TENIS syndrome)，當甲狀腺癌細胞吸收 FDG 越高，甲狀腺細胞碘吸收能力越低。

關鍵字：甲狀腺癌、正子掃描。

PC059

Splenosis as A Supra-renal Incidentoloma: A diagnostic Trouble Solved by Heat-Damaged Erythrocyte SPECT/CT Scan

Jui-Hung Weng[1], Jhih-Wei Chen[3], Pan-Fu Kao[1,2]

[1]*Department of Nuclear Medicine, Chung Shan Medical University Hospital, Taichung, Taiwan;*
[2]*School of Medicine, Chung Shan Medical University, Taichung, Taiwan (ROC);*
[3]*Department of Medical Imaging, Chung Shan Medical University Hospital, Taichung, Taiwan.*

Abstract: Supra-renal incidentaloma is a diagnostic problem. We presented a case of 46 year-old man with a left supra-renal incidentaloma. The definite diagnosis of splenosiswas not made by FDG PET/CT or MRI until the use of heat-damaged erythrocyte SPECT/CT scan.

Heat-damaged erythrocyte scan not only avoided risky biopsy attempts or laparotomy but also detected more lesions than MRI. The role of heat-damaged erythrocyte scanin incidental lesions in those with a history of splenic trauma or splenectomy, and lesion localization by SPECT/CT, were both emphasized.

Legend

FIGURE 1. A 46-year-old gentleman visited urology outpatient department with the chief complaint of left renal colic. Except urolithiasis, a mass in left supra-renal region was incidentally identified by sonography. Serum potassium, aldosterone, plasma renin activity, CEA, CA19-9 and urine vanillyl mandelic acid were all within normal limit.

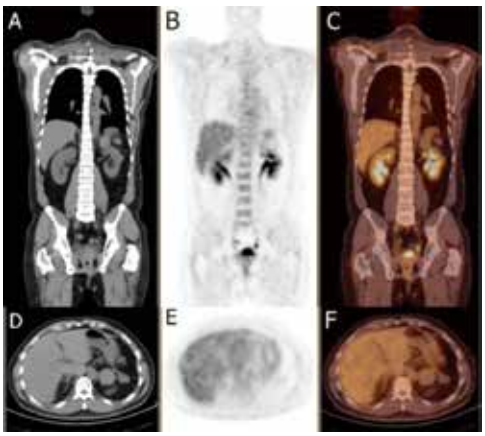

Figure 1

FDG PET/CT scan was performed, which disclosed a mild hypermetabolic mass (SUVmax: both 2.3 on 1 hour and 2.5 hours post injection images) about 3.6 cm in greatest dimension in left supra-renal region(A/B/C: coronal view of CT/FDG PET/fusion; D/E/F: transverse view). Although malignancy was unlikely, nature of the mass was not determined by FDG PET/CT. The following MRI suggested possible differential diagnoses including splenosis and lipid-poor adrenal adenoma.

Tracing back his medical history, splenectomy after a traffic accident in about 20 years ago was told. Thus, under the suspicion of splenosis for the left supra-renal mass, he underwent a nuclear heat-damaged erythrocyte scan with SPECT/CT.

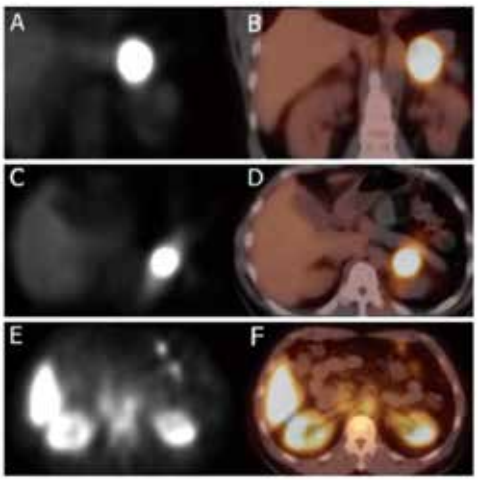

Figure 2

FIGURE 2. Heat-damaged erythrocyte scan showed a mass uptaking radiotracer in left supra-renal region (A/B: coronal view of SPECT/fusion; C/D: transverse view of SPECT/fusion) corresponding to the clinically

known incidentaloma by SPECT/CT correlation. In addition, at least two tiny radioactive foci in mesentery of LUQ of abdomen (E/F: transverse view of SPECT/fusion) suggestive of splenic implants were identified. Becauseof no more clinical symptom after conservativetreatment for renal colic, only close observation and follow up were suggested.

Intra-abdominal incidentaloma is an increasingly encountered clinical problem. [1]A high degree of certainty of diagnosis is critical for management decision. In this case, hormonally active tumor or malignant lesion was excluded by history and biochemical tests. However, FDG PET/CT and MRI of abdomen did not characterize the left supra-renal mass, not to speak of the abdominal implants. At least, by means of nuclear heat-damaged RBC scan, which not only confirmed the diagnosis but detected intra-abdominal implants, further invasive biopsy or laparotomy was avoided.

Splenosis represents the heterotopic autotransplantationof functional splenic tissue following splenic trauma or surgery. [2] It was reported to hadoccurred in up to 67% of patients who have suffered from a splenic rupture. [3]In this case, the splenic implants did not cause symptom and wereidentifiedincidentally, as had been reported before.[4] Same as cases had been reported in the literature, to confirm the diagnosis of splenosiswas a trouble for him even without a prior history of malignancy. Although any neoplasm should be excluded first, splenosis should be considered whenever a differentialdiagnosis of any tumor-like lesion disclosed on abdominalimaging in a patient with a splenic injury in the past.[5]

Although infrequentlyused in current clinical practice[6], ^{99m}Tc-labeled heat-damaged erythrocyte scintigraphy is widely accepted as the criterion standard test fordetecting splenic tissueand is superior to ^{99m}Tc sulfur colloid. [7,8]Any indeterminate soft tissue lesion in those with a history of prior splenectomy or splenic injury may warrant a heat-damaged erythrocyte scan, especially with SPECT/CT, which may likely help in the (differential) diagnosis and management decision.

REFERENCES

1. Berland LL, Silverman SG, RM Gore, et al. Managing Incidental Findings on Abdominal CT: White Paper of the ACR Incidental findings Committee. *J Am CollRadiol*. 2010;7:754-773.
2. Cotlar AM, Cerise EJ. Splenosis: the autotransplantation of splenic tissue following injury to the spleen. Report of two cases and reviewof the literature. *Ann Surg* 1959; 149:402-414.
3. Gupta K, Ahluwalia A, Jain T, et al. Abdominal splenosis mimicking peritoneal deposits-A case Report. *Pan African Medical Journal*. 2014;17:269.
4. YusteJR,Buades J, Guillen EF, et al. Posttraumatic Intrathoracic Splenosis: From Clinical Suspicion to Noninvasive Diagnosis. *The American Journal of Medicine*. 2014;127:e3-e4.
5. Ksiądzyna D.A case report of Abdominal Splenosis – a Practical Mini-Review for a Gastroenterologist. *J Gastrointestin Liver Dis*. 2011;20:321-324.
6. MacDonald A, Steven Burrell S. Infrequently Performed Studies in Nuclear Medicine: Part 1. *J Nucl Med Technol*. 2008; 36:132-143.
7. Gunes I, Yilmazlar T, Sarikaya T, Akbunar T, Irgil C. Scintigraphic detection of splenosis: superiority of tomographic selective spleen scintigraphy. *Clin Radiol*. 1994;49:115-117.
8. Hagman TF, Winer-Muram HT, Meyer CA, et al. Intrathoracic splenosis: superiority of technetium Tc-99m heat-damaged RBC imaging. *Chest*. 2001;120.

PC060

Application of Whole Body FDG-PET for Cancer Screening in A Cohort of Hospital Employees

Nan-Jing Peng[1,2], Gin Hu[1], Yu-Li Chiu[1]

[1]*Department of Nuclear Medicine, Kaohsiung Veterans General Hospital, Kaohsiung, Taiwan;*
[2]*National Yang-Ming University, School of Medicine, Taipei, Taiwan.*

Introduction: Whole body FDG-PET has been used to screen underlying malignancy in asymptomatic examinees and subjects with already known cancer for decades. We had a chance to survey a cohort of hospital employees using PET/CT and reported the preliminary results.

Methods: A total of 116 hospital employees above 55 year-old were informed to receive whole body FDG-PET in our hospital. Ninety-seven of them completed PET/CT from Feb. 2014 to Aug. 2014 in our PET center. The final confirmation of cancer was based on pathologic report and follow-up more than one-year.

Results: Among the 97 examinees, 92 were asymptomatic and 5 had already known cancers before. Five of the 92 asymptomatic examinees (5.5%) were found FDG-avid lesions, and another a FDG-devoid lesion. Five of them received surgical manipulation and the rest aspiration cytology of thyroid. Three of the 92 asymptomatic examinees (3.3%) were proven malignancy and 3 (3.3%) were benignancy. All of the proven malignant lesions were papillary thyroid cancers, and the benign lesions were meningioma, Castleman disease and thyroid nodule, respectively. About the 5 examinees with already known cancers, no definite significant lesion was found. After follow-up for more than one year, no definite abnormality was noted in the 91 examinees, including the 86 PET/CT negative asymptomatic examinees and the 5 examinees with already known cancers.

Category (n)	Cancer found by PET/CT	Cancer not found by PET/CT	Benign tumors	Total tumors
Asymptomatic (92)	3 (3.3%)	0 (0%)	3 (3.3%)	6 (6.6%)
Already known cancers (5)	0 (0%)	0 (0%)	0 (0%)	0 (0%)

Conclusions: PET/CT is a powerful tool for cancer screening. It bears the potential for combination of the merits of PET and CT, and beneficial for asymptomatic examinees and subjects with already known cancers.

PC061

Synchronous Mantle Cell Lymph Lymphoma and Hepatocellular Carcinoma: A Case Report

Ming-Tsung Wu[1], Wan-Yu Lin[1,2,3], Shih-Chuan Tsai[1,2]

[1]*Department of Nuclear Medicine, Taichung Veterans General Hospital, Taiwan;*
[2]*Department of Medical Imaging and Radiological Sciences, Central Taiwan University of Science and Technology, Taichung, Taiwan;*
[3]*School of Medicine, China Medical University, Taichung, Taiwan.*

Introduction: Mantle cell lymphoma (MCL) is one of the mature B cell non-Hodgkin lymphomas. Its behavior is most often that of an aggressive disease. Extranodal involvement may be observed in the bone marrow, the spleen, and the gastrointestinal system. Herein, we report a case of Mantle cell lymphoma with HCC that may be misdiagnosed as lymphoma with liver involvement, which may affect treatment options for this patient.

Case Report: This 78-year-old male was admitted to our hospital because of dyspnea on exertion and cough for one month, and body weight loss 5 Kg in two months. X-Ray film of the chest showed abnormal lung mass and chest CT showed mass lesion over right hilum about 8 cm in size. Lung cancer was suspected but pathological examination of the bronchoscopic biopsy confirmed Mantle cell lymphoma, classic type. Besides, a hypovascular liver mass were also noted on CT image. Liver function tests were with normal range but AFP (89.31 ng/ml) elevated. The viral marker was negtive for HBsAg, anti-HBs, anti-HBc (IgG), and Anti-HCV. Following three-phase abdominal CT revealed a 4-cm low-density mass at S7 without obvious arterial enhancement. PET/CT finding were compatible with lymohoma involving the right mediastinum, right supraclavicular region, the right pleural regions, the skeleton (C3, left humerus, right 7th rib), and the liver (one focal lesion at S7, SUV: 6.9). Secondary hepatic involvement with lymphoma was impressed; however, liver biopsy examination confirmed hepatocellular carcinoma, moderately differentiated. The patient had treated with first TACE for HCC and chemotherapy for mantle cell lymphoma. Follow-up CT scan and PET/CT scan will be performed 4 weeks after the final cycle.

Discussion: Coexistence of mantle cell lymphoma and hepatocellular carcinoma is extremely rare. Our patient was diagnosed with mantle cell lymphoma by bronchoscopic biopsy and multiple extranodal involvements in the mediastinum, right supraclavicular region, right pleural regions, bone and liver by the PET/CT. The focal FDG-avid lesion at the liver with hypovascular density but without obvious enhancement in the arterial phase on CT image is not a typical image for HCC. It may be misdiagnosed as mantel lymphoma with liver involvement and then be treated with chemotherapy for lymphoma. It is remarkable that even with considerable clinical information in this case it was difficult to distinguish HCC from secondary lymphoma involvement. Although a PET/CT would probably have yielded the diagnosis, a liver biopsy would have provide the definite diagnosis.

In conclusion, nuclear clinicians should consider during differential diagnosis that a focal liver mass observed in the PET/CT of patients diagnosed as mantle lymphoma could be associated with synchronous hepatocellular carcinoma.

PC062

南部某醫院放射免疫分析實驗室醫檢師接受輻射劑量研究

張淑芬[1] 李將瑄[1] 張朝鈞[1] 曾宜玲[1] 顏吉龍[1] 卓世傑[1]

[1] *奇美醫療財團法人奇美醫院核子醫學科 RIA*

背景介紹：

放射免疫分析實驗室之醫檢師每日皆須操作微量放射性物質，以進行檢驗工作。因此放射免疫分析實驗室之醫檢師，理應有接受輻射劑量。但南部某醫院放射免疫分析實驗室醫檢師，用以記錄輻射劑量之配章，卻均爲無接受輻射劑量之顯示（背景劑量）。本研究即利用輻射劑量筆，實際測量放射免疫分析實驗室之醫檢師所接受之輻射劑量可能爲多少？

方法：

本研究使用 POLIMASTER 輻射劑量筆，分別測量放射免疫分析實驗室不同醫檢師每日作業時之輻射劑量。每一位醫檢師配戴輻射劑量筆 1 日，並由醫檢師於作業前記錄劑量筆數值後，配戴於左上衣口袋，作業完畢後，記錄劑量筆數值及作業活度。共收集到含背景值之接受輻射劑量值及作業活度紀錄各 7 筆。

結果：

醫檢師每日接受之輻射劑量由高到低，依序爲 3 uSv 一筆，2 uSv 一筆，1 uSv 四筆，0 uSv 一筆（資料整理如下表）。對應之醫檢師每日作業活度則分別爲，867、938、335、60、555、228、595KBq。醫檢師接受之輻射劑量與作業活度，並未呈現完全之正相關情形（資料整理如下圖）。若以接受輻射劑量最大值之 3 uSv 與每月 22 個工作日計算，則南部某醫院放射免疫分析實驗室醫檢師可能接受含背景值之輻射劑量最大爲 66 uSv/月。

結論：

根據本文測量結果顯示，南部某醫院放射免疫分析實驗室醫檢師可能接受含背景值之輻射劑量最大爲 66 uSv ／月，仍遠低於每月約 1600 uSv 之法規劑量值。而醫檢師接受之輻射劑量與作業活度，雖未呈現完全之正相關情形，但操作較高活度之放射性物質，確實呈現接受較高輻射劑量之情形。不過由於本研究之樣本數太少，可能尚無統計上的意義。且若考慮約 0.06 至 0.15 uSv/h 之輻射環境背景值，則醫檢師作業所接受之輻射劑量，應該非常微小。

醫檢師	接受劑量	作業內容	作業活度
A	0.000 mSv	CEA	≈ 595 kbq
B	0.001 mSv	TR-Ab	≈ 60 kbq
C	0.001 mSv	Cortisol	≈ 228 kbq
D	0.001 mSv	T3、SAb	≈ 335 kbq
E	0.001 mSv	HBsAg	≈ 555 kbq
F	0.002 mSv	TSH、PTH-i	≈ 938 kbq
G	0.003 mSv	AFP、Tg	≈ 867 kbq

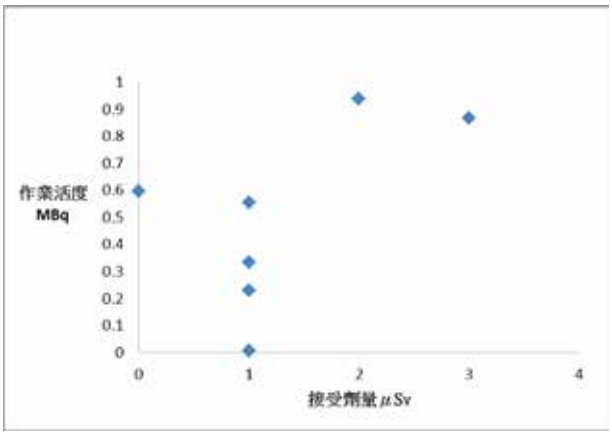

PC063

放射免疫分析實驗室應用社群網路軟體於作業管理之通訊內容研究 －以 Line 爲例

廖淑娟[1] 李將瑄[1] 蘇雅雯[1] 賴怡芳[1] 段淑薰[1] 卓世傑[1]

[1] 奇美醫療財團法人奇美醫院核子醫學科 RIA

背景介紹：

社群網路軟體所傳遞的資訊具有簡易、即時、可儲存、一對多、圖文並用、便宜等優點。因此使原本僅用於私人間通訊聯絡的社群網路軟體，現在正快速的運用於組織間之作業管理。事實上，許多放射免疫分析實驗室亦已將社群網路軟體應用於非正式之作業管理。但對於社群網路軟體傳遞訊息之內容，卻較少有實際之研究與資料。本文即嘗試分析兩組不同參與架構社群網路軟體 -Line 運用之訊息傳遞特性，以做爲後續研究與精進之參考。

方法：

本研究先將 Line 群組之通訊內容分爲三類，即，(1) 指示性質。(2) 討論性質。(3) 其他性質。再就兩組不同參與架構之 Line 群組，其通訊內容分別統計分析。兩組 Line 群組分別爲，(1) 院際組 - 各醫院放射免疫分析實驗室醫技主管參與之群組，共 11 人。(2) 同仁組 - 本科放射免疫分析實驗室同仁組成之群組，共 8 人。院際組之統計起訖時間爲 103 年 11 月 14 日至 104 年 8 月 20 日，約 9 個月。同仁組之統計起訖時間爲 104 年 6 月 12 日至 8 月 20 日，約 2 個月。

結果：

(1) 含圖、文之總筆數，院際組爲 213 筆，平均每月 23.6 筆。同仁組爲 861 筆，平均每月 430.5 筆。(2) 內容部分，院際組指示性質爲 4 個議題，18 筆，佔總筆數 8.5%，討論性質爲 9 個議題，135 筆，佔總筆數 63.3%，娛樂性質則爲 14 個議題，60 筆，佔總筆數 28.2%。而同仁組，指示性質爲 4 個議題，26 筆，佔總筆數 3%，在討論性質爲 9 個議題，283 筆，佔總筆數 32.9%，在娛樂性質爲 12 個議題，552 筆，佔總筆數 64.1%。(3) 通訊之貼圖、文字比例，院際組爲 24% 及 76%，同仁組則爲，43.4% 與 56.6%。相關數據整理如下表。

結論：

(1) 就訊息傳遞數量而言，同仁組以每月平均 430.5 筆，遠大於院際組之 23.6 筆，顯示同仁間之互動較院際頻繁。(2) 就訊息傳遞品質而論，院際組似乎較好，其指示與討論性質各佔總筆數的 8.5% 及 63.3%，娛樂性質僅佔 28.2%。而同仁組之指示與討論性質則各佔總筆數的 3% 及 32.9%，娛樂性質卻高達 64.1%。(3) 以訊息傳遞效率來說，院際組似乎較高。例如，指示性質院際組與同仁組皆爲 4 個議題，但院際組爲 18 筆，同仁組卻需 24 筆，其他討論與娛樂性質也有相同的情形。(4) 容易簡化訊息傳遞內容的貼圖使用，院際組與同仁組分別爲 24% 及 56.6%。但因同仁組娛樂性質之比例高達 64.1%，是否導致貼圖使用較高，則尚待觀察。

Line 通訊內容彙整表

	院際組（103.11.14 至 104.8.20）			同仁組（104.6.12 至 104.8.20）		
總筆數		213			861	
貼圖比例		24.0%			56.6%	
性質名稱	指示	討論	娛樂	指示	討論	娛樂
議題數	4	9	14	4	9	12
性質筆數	18	135	60	26	283	552
性質比例	8.5%	63.3%	28.2%	3%	32.9%	64.1%

資料來源：本文整理

PC064

^{99m}Tc-MAA 肝肺症候群：病例報告

朱家慧[1] 陳品萱[1] 陳沛穎[1] 林虔睦[1,2] 楊哲銘[1,2,3]

[1] 衛生福利部雙和醫院核子醫學科
[2] 臺北醫學大學醫學系放射線學科
[3] 臺北醫學大學醫務管理學系暨研究所

研究目的 (Purpose)

^{99m}Tc-macroaggregated albumin (^{99m}Tc-MAA) 常用於核醫肺灌注掃描，主要評估肺血管是否栓塞。但此病例乃利用 ^{99m}Tc-MAA 照影全身來診斷是否爲肝肺症候群 Hepatopulmonary syndrome (HPS)。

材料與方法 (Materials and Methods)

此病例報告之受檢者爲 60 歲男性，有肝硬化及呼吸困難，懷疑是否爲 HPS。此檢查不需禁食，請受檢者仰躺配合吸氣靜脈注射 5 mCi ^{99m}Tc-MAA，待 15 至 20 分鐘後掃描全身及腦部靜態影像。圈選肺部、腦部及背景之 ROI，此三 ROI 同一大小，將所得 counts 數比較及計算 SI 值 (SI = Brain count/ Lung count)。

結果 (Results)

正常受檢者之腦部活性應很低，此受檢者影像可看出在腦部有 ^{99m}Tc-MAA 聚積，肺部 ROI total count 爲 514445、腦部 34846、背景 56，SI 值爲 0.07。

討論 (Disscussion)

^{99m}Tc-MAA 可用於診斷 HPS 原因有二：一是由於肝功能失償導致血管擴張物質代謝變慢，造成肺泡及支氣管微血管不正常擴大；二是肺動、靜脈分流。但是其限制包含解離 Tc 的量，會影響判讀。

結論 (Conclusion)

^{99m}Tc-MAA 除了可以評估肺栓塞之外，還可利用影像鑑別診斷 HPS。但必須注意解離 Tc 的量，會影響判讀，使用腦肺 SI 值則可以降低此一影響。

PC065

全身骨骼掃描使用距離感測器於影像品質的影響

黃俊憲[1] 陳沛穎[1] 林虔睦[1,2] 楊哲銘[1,2,3]

[1] 衛生福利部雙和醫院核子醫學科
[2] 臺北醫學大學醫學系放射線學科
[3] 臺北醫學大學醫務管理學系暨研究所

背景介紹：

執行全身骨骼掃描 (Whole Body Bone Scan) 時，在無使用距離感測器 (Sensor) 情況下，對身型曲線較明顯的受檢者而言，頭和膝蓋以下較遠離偵檢器 (Detector)；有使用距離感測器，會根據受檢者的身型曲線變化自動調整偵檢器的遠近。本研究評估有使用距離感測器和無使用距離感測器對全身骨骼掃描影像品質的影響。

方法：

檢查以本科常規方式進行，受檢者靜脈注射 20 mCi ^{99m}Tc-MDP，待 3 至 5 小時進行全身骨骼掃描。收集 10 位受檢者，其中男性 8 位，女性 2 位，平均年齡爲 66.2 歲，這 10 位受檢者影像由同一位放射師處理、分析，再交由本科兩位核醫專科醫師判讀，將影像品質分爲三種：明顯差異 (影像差異足以影響診斷結果)、輕微差異 (雖有差異，但差異不足以影響診斷結果) 和沒有差異 (兩組影像幾乎相似)，再將其作比較分析。

結果：

經醫師判讀後，10 位受檢者有 9 位被歸類爲沒有差異，只有 1 位有輕微差異，差異部分在上顎 (頭部)，醫師認爲無使用距離感測器在上顎的影像解析度較好。而另一位醫師判讀結果，10 位受檢者影像全被歸類爲有輕微差異，主要差異位於頭部、肋骨和骨盆腔，有使用距離感測器影像品質較佳者爲 2 位 (20%)；無使用距離感測器影像品質較佳者爲 8 位 (80%)。

討論：

本研究結果顯示無使用距離感測器的影像品質較佳，其原因可能是使用距離感測器相對於無使用距離感測器，偵檢器和受檢者間的距離較大所致。

結論：

此一機型距離感測器的使用對於全身骨骼掃描影像品質無明顯增加，診斷結果也無顯著影響，本科據此一結果將停用距離感測器於全身骨骼掃描。

PC066

LV Dyssynchrony is Predictive of Ventricular Arrhythmia in Ischemic Cardiomyopathy After Cardiac Resynchronization Therapy

Guang-Uei Hung[1], Jing-Rong Huang[2], Ji Chen[3]

[1]*Department of Nuclear Medicine, Chang-Bing Show Chwan Memorial Hospital, Changhua, Taiwan;*
[2]*Department of Cardiology, Taichung Veterans General Hospital, Taichung, Taiwan;*
[3]*Department of Radiology and Imaging Sciences, Emory University School of Medicine, Atlanta, GA, USA.*

Background: For patients with coronary artery disease, larger scar burdens are associated with higher risk of ventricular arrhythmia. Left ventricular (LV) dyssynchrony is associated with increased risk of sudden cardiac death in patients with heart failure. The purpose of this study was to assess the values of LV dyssynchrony and myocardial scar assessed by myocardial perfusion SPECT (MPS) in predicting the development of ventricular arrhythmia in ischemic cardiomyopathy.

Materials and Methods: Twenty patients (14 males, mean age: 64 ± 12) with irreversible ischemic cardiomyopathy received cardiac resynchronization therapy (CRT) for at least 12 months were enrolled for MPS. LV dyssynchrony (phase SD and bandwidth) and scar (% of total areas) parameters were generated by Emory Cardiac Toolbox. Ventricular tachycardia (VT) and ventricular fibrillation (VF) recorded in the CRT device during follow-up were used as the reference standard of diagnosing ventricular arrhythmia. ROC curve analysis was used for generating the optimal cut-off values of LV dyssynchrony and scar parameters for predicting VT/VF.

Results: Ten (50%) of the 20 patients developed VT/VF during the follow-up (15.3 ± 12.7 months). ROC curve analysis revealed the areas under the curves were 0.86, 0.86 and 0.81 for phase SD, bandwidth and scar, respectively ($p < 0.0001$, $p < 0.0001$ and $p < 0.005$, respectively) for predicting the development of VT/VF. The optimal cut-off values were 55°, 183° and 23% for phase SD, bandwidth and scar, respectively. The sensitivity, specificity, positive predictive value and negative predictive value of 80%, 100%, 100% and 83%, respectively, for both phase SD and bandwidth; and were 80%, 70%, 72% and 78%, respectively, for scar.

Conclusion: LV dyssynchrony by phase analysis of MPS is a powerful predictor of ventricular arrhythmia in ischemic cardiomyopathy after CRT. Further implantation of ICD device for preventing sudden cardiac death may be considered for those patients with phase SD > 55° or bandwidth > 183°.

PC067

比較分析受檢者喝水量對全身骨骼影像造成的差異性

張春梅[1] 李昕迪[1] 俞長青[1,2] 蘇詩琪[1]

[1] 高雄榮民總醫院核子醫學部
[2] 慈惠醫事科學校

背景介紹：

受檢者注射 Tc-99m MDP 藥物，約 2.5~4 小時後進行全身骨骼造影檢查，受檢者採用仰臥姿勢。本研究評估受檢者喝水量是否影響骨骼與肌肉之比值。本研究使用手動方式 (manual) 圈選大腿骨骼及大腿內側肌肉平均計數，探討受檢者對喝水量大於 500 cc 與少於 500 cc 影像品質之差異。

方法：

研究對象爲本部 103 年 11 月間執行全身骨骼造影造影之受檢者，使用儀器爲 Philips BrightView，注射藥物爲 Tc99m-MDP 20 mCi，受檢者注射藥物時無提醒喝水量。檢查完成後紀錄受查者喝水量，將其分成大於 500 cc 與少於 500 cc 二組。依受檢者身體輪廓圈選全身前面像右大腿骨骼平均計數，背景 ROI 取其右大腿內側肌肉之平均計數作統計比較。分析資料時排除非 Philips BrightView 收集、造影姿勢不良、藥物或尿液污染、躁動、忘記自己有無喝水超過 500 cc 及無法溝通者。

結果：

本研究收集 237 位受檢者，共 91 位受檢者進行分析。平均年齡爲 61.8 歲 (範圍：19-99 歲)，男性 45 位 (49.5%)，女性 46 位 (50.5%)。大於 500 cc 與少於 500 cc 分別有 36 位與 55 位。本研究發現以全受檢者喝水量多與其骨骼與肌肉比值無顯著統計關係。然而經由多變數分析得到，女性相對於男性骨骼與肌肉比值顯著較高 (女性：2.30、男性：2.03，P-value：0.031)。再細究骨骼與肌肉個別的計數，發現骨骼的攝取會隨著年齡上升 (相關係數： 0.452，P-value：4.184e-06)，女性也相對於男性較多 (女性：13.6、男性：12.2，P-value：0.05)；而肌肉的攝取則只和年齡有正相關 (相關係數：0.477，P-value：1.069e-06)。不論是骨骼與肌肉比值或是骨骼與肌肉個別的計數，喝水大於 500 cc 與少於 500 cc 皆無關。

結論：

取全身骨骼掃描之延遲影像，使用電腦軟體程式 Esoft，圈選大腿骨骼與大腿肌肉，取二者平均計數之比值，分析受檢者喝水量多寡造成的差異性，本研究證明若將喝水量以 500 cc 爲分界，兩組有相近的骨骼與肌肉的對比度。然而透過其他資料的收集，我們得知較大的年齡傾向有較高的對比度。

PC068

I-131 MIBG 神經母細胞瘤治療：病例討論

李佩蓉　楊朝瑋　王連嚴　楊光道　李明哲

彰化基督教醫院

背景介紹：

神經母細胞瘤是源自脊索神經分支的癌症，爲孩童第三常見腫瘤。復發後的腫瘤多產生抗藥性，對化療與放療反應不佳。

材料與方法：

13 歲孩童診斷爲第四期神經母細胞瘤，於化療及放射治療成效不佳，安排了注射 1 mCi I-131 MIBG，影像發現多處有藥物吸收。進而安排由靜脈注射 I-131 MIBG 150 mCi，注射後一星期做全身 I-131 掃描及抽血檢查確認無骨髓抑制情況。

結果：

發現腹膜後腔有殘餘的癌症細胞，有轉移至肝臟、骨盆淋巴結、骨盆腔的腹膜及右邊的睪丸。骨轉移發生在 T4、T12、L5、骶骨和尾骨，以及兩側的髖骨、關節窩和股骨，藥物吸收良好。

結論：

I-131 MIBG 具有高特異性碘標記，可與腎上腺素受體結合，達到治療效果，且具細胞毒性的放射性元素，可將神經母細胞殺死，對化療與放療反應不佳的病人，它提高療效，降低副作用。

關鍵字：神經母細胞瘤、I-131 MIBG

PC069

新、舊型正子電腦斷層造影儀臨床造影所需時間之比較與探討

林渝馨[1] 陳威宇[1] 盧晞卉[1] 邱南津[1]

[1]國立成功大學醫學院附設醫院核子醫學部

背景介紹：

PET/CT 於近年來已成爲癌症評估上不可或缺的利器，本院爲提升南部民眾之福址，於今年初特別引進大中華區第一台西門子 Biograph mCT flow 正子電腦斷層造影儀，其具有 Continuous Bed Motion (CBM) 不間斷多速率掃描模式。經臨床應用後，於此提出新機西門子 Biograph mCT flow 和舊機西門子 Biograph 6 在實際臨床運用上，造影時間之差異分析。

材料與方法：

本實驗比較之兩造影工具分別爲：1. 西門子 Biograph mCT flow 正子電腦斷層造影儀，本機配備 40 切電腦斷層，晶體爲 LSO，由 4 環 (rings) 共 48 區 (blocks) 所組成，總晶體數爲 32448 個，最小切割爲 4 mm × 4 mm × 20 mm。造影端所搭配之作業版本爲 Syngo VG51A，執行 Continuous Bed Motion (CBM) 不間斷多速率掃描模式。2. 西門子 Biograph 6 HI-REZ 正子電腦斷層造影儀，本機配備 6 切電腦斷層，晶體爲 LSO，由 3 環 (rings) 共 36 區 (blocks) 所組成，總晶體數爲 24336 個，最小切割爲 4 mm × 4 mm × 20 mm。造影端所搭配之作業版本爲 Syngo VB20B，執行 Step and Shoot 步進式單一速率掃描模式。

本實驗以回溯的方式，收集 2015 年一月份 (新機型 mCT flow，n = 44) 與 2014 年一月份 (舊機型 Biograph 6，n = 36) 自費接受正子斷層掃描的病人，病人皆接受 370 MBq (10 mCi) 的氟 -18 去氧葡萄糖，根據病歷記載初始開始影像掃描與結束影像掃描的時間， 統計造影所需時間之差異， 其中造影範圍皆爲頭頂至大腿上半部。

結果：

兩種造影儀掃描所需時間統計後，舊機 Biograph 6 (n = 36) 平均所需時間爲 27.28 ± 3.20 分鐘；新機 mCT flow (n = 44) 平均所需時間爲 19.11 ± 2.43 分鐘，平均相差時間爲 8.164 ± 0.6304 分鐘 ($p < 0.0001$)，顯示二者具顯著差異。

討論：

1. 舊機 Biograph 6 之晶體共 3 個環，one bed 總長度 16.2 公分，而新機 mCT flow 之晶體共 4 個環，one bed 總長度約 22.1 公分，故其 mCT flow 掃描時間可有效減少。
2. 新機 mCT flow 之重組技術增加了 Time of flight (TOF) 與 Point spread function (PSF) 之功能，可增加偵測效率，以達到準確且快速之造影。
3. 新機 mCT flow 提供多速率掃描功能 (最多四段)，可針對不同部位設定不同掃描速度，如下肢，以往舊機 Biograph 6 一律使用 one bed 3 分鐘之條件進行掃描，而新機 mCT flow 因可多速率掃描，下肢可用 one bed 1 分鐘之條件進行掃描。
4. 舊機 Biograph 6 之掃描爲 Step and Shoot (SS) 之模式，除增加檢查床在 bed 間移動之時間，並且各相鄰床間影像必須要有重疊以維持影像均勻度，Biograph mCT flow 提供 Continuous Bed Motion (CBM) 之功能則可省去這些時間，故可有效減少掃描時間。
5. 舊機 Biograph 6 之 CT 爲 6 切，新機 mCT flow 之 CT 爲 40 切，故新機 mCT flow 在 CT 掃描時也爲減少造影時間有所貢獻。

結論：

以本院的觀察結果而言，新機 Biograph mCT flow 於臨床應用上確實能節省造影所需 1/3 至 1/4 之時間，對於經濟效益和病人便利性皆有幫助。

PC070

藉由常規額外準備核醫藥物以降低前哨淋巴結閃爍造影未顯影的失敗率

黃慧娥　洪佑昇　吳志順

奇美醫療財團法人柳營奇美醫院

背景介紹：

對於早期乳癌，前哨淋巴結切片 (sentinel lymph node biopsy) 目前已成爲是否要實施腋下淋巴結廓清術 (axillary lymph node dissection) 的標準作法，因此核醫淋巴閃爍造影扮演著更重要的角色。文獻上核醫前哨淋巴結定位所花費的時間約 30 至 60 分鐘，我們自己的經驗是顯影迅速，八成以上 10 分鐘內可以偵測到，但偶爾仍遇到長時間才顯影或未顯影的狀況。依據教科書可能原因包括腫瘤轉移阻塞或壓迫淋巴路徑，或是淋巴結太小放射活性太低偵測不到，或是原因不明。我們的目的是希望藉由多一次注射放射線同位素，以提升偵測前哨淋巴結的成功率。

方法：

核醫前哨淋巴結檢查有多種注射方式，我們選擇的原則如下：(一) 摸的到的腫瘤，於腫瘤上方皮內注射。(二) 摸不到的腫瘤，如有做超音波定位，於定位處皮內注射。(三) 摸不到的腫瘤，如沒有做超音波定位，於乳暈旁注射。(四) 先前接受切除性切片者，於手術傷口兩側分別注射。我們所曾經遭遇到失敗的病人有上述第二和第四兩類病人。依據教科書，如果病人淋巴結未顯影，標準作法包括熱敷、按摩、和手臂活動。如經上述規範仍未顯影者，且照影時間超過一小時有延遲開刀房作業之疑慮時，此類病人我們的做法是額外注射一支放射藥物，注射的位置選擇在乳暈旁， 選擇乳暈旁注射的理由是根據解剖學教科書，大多數的淋巴迴流路徑會經過乳暈周圍。

結果：

我們所遭遇到首次注射後前哨淋巴結未顯影的病人，再額外注射一支放射藥物，所有的病人皆偵測的到淋巴結顯影，成功率百分之百。

結論：

執行核醫前哨淋巴結定位檢查，如能常規預備額外的放射藥物，可以降低失敗的風險，減少未顯影時等待的焦慮，避免病人開刀範圍擴大。

PC071

使用安全針具注射核醫放射性藥物之效益評估

蘇詩琪[1] 吳忠順[1] 張春梅[1] 郭建瑋[1] 彭南靖[1,2]

[1] 高雄榮民總醫院核子醫學部
[2] 國立陽明大學醫學系

背景介紹：

依據本國修正醫療法第 56 條規定：「醫療機構對於所屬醫事人員執行直接接觸病人體液或血液之醫療處置時，應自中華民國 101 年起，五年內按比例逐步完成全面提供安全針具」，以有效地降低針扎事件的發生，維護醫事人員工作安全與健康。安全針具的執行對於核醫工作人員注射放射性藥物至受檢者體內，是一項極麻煩的技術，若使用不適當之安全針具，恐將導致放射性藥物外漏，使工作人員、受檢者及核醫儀器受放射性污染的危害，造成不必要的輻射暴露；或因放射性藥物劑量注射不足及留置針藥物殘留，造成影像品質下降。本研究針對本院可請領之兩款無針式注射用連接頭及延長管 (connect) 之安全針具做試驗，探討適合本部使用的安全針具種類及使用注意事項。

方法：

爲探討 Y 頭 connect 及單頭 connect 兩款安全針具，注射放射性藥物後沖洗生理食鹽水的兩個不同位置與生理食鹽水用量，對注射放射性藥物的便利性及影像品質的影響。分成四個試驗，四個受檢者注射 Tc-99m MDP 20 mCi 前先量測其總計數值 (結果 A)，工作人員在注射放射性藥物後給予 5 c.c 生理食鹽水沖洗安全針具，接著收集受檢者安全針具留置處 1 分鐘影像並計算其計數值及殘留量 (結果 B)，再給予 5 c.c 生理食鹽水 (共 10 c.c) 沖洗後收集 1 分鐘影像並計算其計數值及殘留量 (結果 C)，最後給予 5 c.c 生理食鹽水 (共 15 c.c) 沖洗後收集 1 分鐘影像並計算其計數值及殘留量 (結果 D)。

結果：

試驗	注射放射性藥物處	注射生理食鹽水處	總計數值 (結果A)	5c.c N.S (結果B)	10c.c N.S (結果C)	15c.c N.S (結果D)
(1)Y頭connect			3990 Kcts	525Kcts 殘留13.15%	332 Kcts 殘留8.32%	218 Kcts 殘留5.46%
(2)Y頭connect			4134 Kcts	41 Kcts 殘留0.99%	28 Kcts 殘留0.68%	25 Kcts 殘留0.60%
(3)單頭connect			4182 Kcts	10 Kcts 殘留0.24%	7.5 Kcts 殘留0.18%	7.5 Kcts 殘留0.18%
(4)單頭connect			4422 Kcts	16 Kcts 殘留0.36%	11 Kcts 殘留0.25%	11 Kcts 殘留0.25%

結論：

試驗 (1) 使用 Y 頭 connect，延用傳統 connect 注射方式於兩處分別注射放射性藥物及生理食鹽水，最後造成放射性殘留量最多，易影響影像品質；試驗 (2)(3)(4) 結果顯示，注射放射性藥物後至少應沖洗生理食鹽水 10 c.c 以上，才可有效沖洗殘留安全針具管壁上之活性；試驗 (3)(4) 結果顯示殘留量皆小於 0.5%，此款單頭 connect 安全針具最適合本部注射放射性藥物。

PC072

Comparison of Territoric Myocardial Perfusion and Defect Extension in Different Severity of Coronary Artery Stenosis in Multidetector CT Angiography

Pei-Shan Wu[1], Hsi-Huei Lu[1], Yi-Shan Tsai[2]

[1]*Department of Nuclear Medicine;*
[2]*Department of Radiology, National Cheng Kung University Hospital, Tainan, Taiwan.*

Introduction: Myocardial perfusion imaging (MPI) plays an important role in the assessment of cardiovascular event risk among patients with coronary artery disease (CAD). Improved sub-millimeter spatial resolution and faster acquisition times for cardiac images have resulted in increased use of multidetector computed tomography scans in the evaluation of CAD. The purpose of this study was to compare territoric perfusion and defect extension of MPI in different severity of three main coronary artery stenoses in multidetector CT angiography (MDCTA).

Methods: Sixty patients with suspected or known coronary artery disease were studied. MPI and MDCTA were performed within 3 months. For evaluation of stenosis of three main coronary arteries (LAD, RCA, and LCX) in MDCTA, lesions less than 50% luminal narrowing were scored as 0 (Score 0), lesions ≧ 50% and < 70% luminal narrowing were scored as 1 (Score 1), and lesions ≧ 70% luminal narrowing were scored as 2 (Score 2). Score 1 and 2 were defined as abnormal in MDCTA. Territoric perfusion and defect extension in stress and rest phases of MPI were compared in the three Score groups.

Results: There were 112 Score 0, 32 Score 1, and 36 Score 2 coronary arteries in MDCTA. MPI detected 17 moderate to severe perfusion defects, and 25 mild perfusion defects. Using MPI as reference standard, the sensitivity, specificity, accuracy, positive and negative predictive values for MDCTA to detect perfusion defects were 57.1%, 68.1%, 65.6%, 35.3% and 83.9%, respectively. Stress territoric perfusion of Score 2 group (73.5 ± 11.1%) was significantly lower than Score 0 (79.7 ± 7.1%, $p = 0.009$) and Score 1 groups (80.3 ± 8.3%, $p = 0.017$). Stress territoric defect extension of Score 2 group (12.3 ± 19.3%) was higher than Score 0 (4.5 ± 9.1%) and Score 1 groups (4.6 ± 7.8%) but without statistically significance.

Conclusion: When luminal narrowing more than 70% in main coronary arteries in MDCTA, stress territoric perfusion was significantly lower and stress territoric defect extension was relatively higher in MPI. The high negative predictive value of coronary artery stenosis in MDCTA may be helpful to exclude CAD. MPI remains mandatory for evaluating the functional relevance of coronary artery lesions.

PC073

Subacute Thyroiditis Presenting as Fever of Unknown Origin Detected by FDG PET/CT Scan: Report of a Case

Chia-Hao Chang[1], Yu-Sheng Hung[1], Chiang-Hsuan Lee[2]

[1]Division of Nuclear Medicine, Department of Medical Imaging, Chi Mei Medical Center, Liouying;
[2]Division of Nuclear Medicine, Department of Medical Imaging, Chi Mei Medical Center.

Introduction: Fever of unknown origin (FUO) remains a challenging issue in clinical medicine. Identification of the etiology of FUO is important and crucial in guiding further diagnostic and subsequent management. With PET/CT becoming widely available, FDG PET/CT scan becomes an optional approach in the detection of etiology of FUO. Here we report a case of subacute thyroiditis which is presenting as FUO clinically and detected on FDG PET/CT scan.

Case Report: A 47 years old female has the past history of right breast fibroadenoma and hepatic hemangioma. She suffers from fever off and on for about 3 weeks. Mild swelling of right neck is noted on physical examination. The laboratory examinations show elevated white counts, CRP, and ESR. There are negative findings in influenza rapid diagnostic test, acid-fast stain, blood culture, urine culture, sputum culture, and immunological complex. The thyroid profiles show T3/T4 are within normal limit, but supressed TSH (0.03 uIU/mL) and elevated thyroglobulin (370 ng/mL). Neck ultrasound shows hypoechoic nodules at both thyroid glands. Fine needle aspiration cytology of thyroid nodules is done but it is nondiagnostic cytology. The diagnostic CT scan, abdominal and cardiac sonography are negative findings. Because the etiology of FUO can not be diagnosed accurately, further evaluation with FDG PET/CT scan is arranged. PET/CT scan shows FDG avid lesions at right thyroid and lower portion of left thyroid and suggests high probability of active inflammation. In addition, there are no FDG avid lesions in whole body elsewhere. The consecutive Tc-99m thyroid scan shows suppressed thyroid uptake and I-131 thyroid uptake at 24 hours is 0.4%. In combination with clinical information and all examinations, subacute thyroiditis is diagnosed.

Discussion: FDG PET/CT scan is very sensitive in identifying anatomic locations of infection, inflammation and malignancy. Although FDG PET/CT scan is a powerful assessment tool for malignancy currently, it is still not a routine procedure for FUO due to the high-cost. However, the advantage of PET/CT in practice certainly can provide a prompt diagnosis and appropriate management. Besides, it can reduce application of many invasive or unnecessary diagnostic techniques for detecting the main disease underlying FUO etiology. Therefore, FDG PET/CT scan is suitable for FUO. In conclusion, FDG PET/CT scan has a valuable place in the evaluation of FUO.

PC074

比較兩種影像分析參數在 Tc-99m-TRODAT-1 單光子放射電腦斷層造影的半定量影像分析

吳麗君[1] 張雅蓮[1] 張家豪[1] 李將瑄[2]

[1] 奇美醫療財團法人柳營奇美醫院核子醫學科
[2] 奇美醫療財團法人奇美醫院核子醫學科

背景介紹：

Tc-99m-TRODAT-1 單光子放射電腦斷層造影是臨床上可用來評估巴金森氏病嚴重度、療效、或協助類似巴金森氏病的運動障礙疾病即次發性巴金森氏病患鑑別診斷。利用半定量分析方法在影像上用手動圈選尾核 (caudate nucleus)，殼核 (putamen) 和紋狀體 (striatum) 的 ROI 去進行計算可幫助醫師診斷。但本院核子醫學科並無購置扇形準直儀亦無電腦斷層影像，只能以低能量高解析度準直儀 (Low energy high resolution collimator) 去進行造影，而在原始分析條件下獲得之影像在圈選尾核及殼核時，沒有明顯的輪廓去區分兩者的界線，圈選 ROI 是件困難的事，本文做了 107 個案例用兩種影像分析參數去討論其相關性。

方法：

自 2014 年 9 月 24 至 2015 年 9 月 14 日收集 107 位病人，影像處理爲濾波式逆投射法 (filtered backprojection)。影像分析法一參數以巴特沃斯濾波器 (order: 10，cutoff: 0.3)，張氏衰減校正係數爲 0.15。影像分析法二參數以高斯濾波器 (FWHM: 6 mm)，張氏衰減校正係數爲 0.15。將兩組的資料以 t 檢定的成對樣本統計 (Paired Samples Statistics) 去了解相關性。

結果：

在影像分析法一所得到的影像，其紋狀體的輪廓是模糊的，不易分辨尾核及殼核的界線；而在影像分析法二所得到的影像，影像的雜訊比高，可清楚分辨尾核及殼核的界線，可幫助 ROI 的圈選。兩組不同條件影像統計結果所得到 P 值 (< 0.001) 爲非常顯著的差異。

結論：

用影像分析條件二可清楚分辨尾核及殼核的界線，以利 ROI 的圈選。其缺點爲當紋狀體攝取放射藥物較少時，其影像會有雜訊太多，但不會影響尾核及殼核的界線。其用不同條件分析的影像，所得到的結合率差異性是非常顯著，所以在判讀上必須參考原始的影像及臨床表徵。

PC075

Two Cases of Pulmonary Scleroing Hemangioma Presenting Different Findings on FDG PET/CT Scan

Yu-Sheng Hung[1], Yu-Wen Wang[2], Chiang-Hsuan Lee[3], Chih-Shun Wu[1]

[1]Division of Nuclear Medicine, Department of Medical Imaging, Chi Mei Medical Center, Liouying;
[2]Department of Radiation Oncology, Chi Mei Medical Center, Liouying;
[3]Division of Nuclear Medicine, Department of Medical Imaging, Chi Mei Medical Center.

Introduction: Pulmonary sclerosing hemangioma (PSH) is a relatively rare and benign neoplasm and often presenting as a solitary pulmonary nodule. Though FDG PET/CT scan has a role in indeterminate pulmonary nodule, the experience using PET/CT scans in PSH is limited. We herein present two cases of this kind of tumor with low and moderate FDG uptake on PET/CT scan.

Case 1: A 73 years old female complains cough with sputum for long time. The chest film shows a nodular shadow at left lower lobe. Chest CT reveals a solitary, well-defined, mildly lobulated, and homogeneous well-enhanced nodule, about 13 x 12 mm in size. The nodule shows mild FDG uptake (SUVmax: 1.4) on PET/CT scan. The postoperative diagnosis is PSH. Six years later, a nodular shadow is noted at the similar location on follow-up chest film. PET/CT scan reveals a well-defined and mildly lobulated nodule, about 15 x 8 mm in size, with mild FDG uptake (SUVmax: 2.1). CT-guided biopsy is done and the pathology is suggestive of recurrence of PSH.

Case 2: A 50 years old female suffers from left shoulder pain and a pulmonary nodule is noted at right middle lobe incidentally. Chest CT reveals a solitary, well-defined, round, and heterogeneous enhanced nodule, about 27 x 25 cm in size. The nodule shows moderate FDG uptake (WUVmax: 4.8) on PET/CT scan. The postoperative diagnosis is PSH. She remains free of disease clinically and radiographically for 6 years follow-up.

Discussion: In the reported articles, the clinical, radiological and PET characteristics of PSH are not specific enough for preoperative diagnosis. The imaging features of PSH on PET scan can demonstrate low or moderate FDG avidity, and accumulation of FDG presumably related to the degree of malignant potential and the tumor size. Therefore, PET/CT scan may be useful for the lesion which is predominately benign but potentially malignancy. When a pulmonary lesion with low FDG uptake and benign nature is highly suspected, observation is reasonable. However, a lesion with moderate or high FDG uptake, pathologic proof or resection should be considered, though the possibility of false-positive result caused by PSH can not be excluded.

PC076

The Comparison of One-site Injection and Two-site Injections in Sentinel Lymph Node Imaging for Breast Cancer

Dung-Ling Yu[1], Ching-Shyang Chen[2], Shang-Chih Lai[2]

[1]*Department of Nuclear Medicine;*
[2]*Department of General Surgery, Menonnite Christian Hospital, Hualien, Taiwan.*

Introduction: The purpose of this study is to compare the visualization of sentinel lymph node (SLN) between one-site injection and two-site injections in the patients with breast cancer.

Methods: In this study, we collected 33 patients with breast cancer receiving SLN study in patients with breast cancer. Among 33 patients, 17 patients (group A) were injected subdermally one site at peri-areolar area with 0.5 mCi of Tc-99m phytate, and 16 patients(group B) were injected subdermally two sites at peri-areolar and peri-tumor areas with 0.5 mCi of Tc-99m phytate. SLN imaging was performed at 30 mins, 1 hr, 2 hr and 3 hr after injection. The visualization of SLN and the time of visualization of SLN were used for comparison between group A and group B.

Results: 16 (94.1%) out of 17 patients showed visualization of SLN in group A, and 15 (93.8%) out of 16 patients showed visualization of SLN in group B. There was no statistical significance in the visualization of SLN between group A and B. SLN visualized within 1hr in 7 patients out of 16 patients in group A and 10 out of 15 patients in group B ($p < 0.01$).

Time of Imaging	Patient with SLN Visualized	
	Group A (n = 16)	Group B (n = 15)
30 min	2	4
1 hr	5	6
2 hr	8	5
3 hr	1	0

Conclusions: In conclusion, although there is no difference in the visualization of SLN between patients with one site injection and two site injections, there is early visualization of SLN in patients with two site injections. The study suggests that two site injections may shorten the time of study, and is recommended clinically.

PC077

接受放射性碘 -131 治療病人外釋時之輻射曝露率分佈

王文祥　陳輝墉　陳妍文

義大醫療財團法人義大醫院核子醫學科

背景介紹：

放射性碘 -131 治療在分化型甲狀腺癌【乳突癌 (papillary carcinoma)、濾泡癌 (follicular carcinoma)】，已經有超過 40 年以上的歷史，其原理就是藉由甲狀腺刺激素 (TSH) 之刺激強化該類惡性腫瘤原本保有之攝取碘的能力，再施以口服放射性碘 -131，這些具有放射性的碘會經由血液循環至甲狀腺腫瘤而留存在細胞中，放射性碘 -131 的 β 射線提供殺傷細胞的能量而達到治療的目的；另放射性碘 -131 的 γ 射線提供核醫造影檢查，其能量爲 364 kev，因此對於輻射安全問題較爲病人及其家屬所關心。

方法：

一般接受放射性碘 -131 治療所給予的活度較高 (從 31 mCi-200 mCi 視病況而定) 因此大劑量放射性碘 -131 治療病患需住院隔離（3~4 天）；由於放射性碘 -131 在病人體內 24 小時其間約有 76% 的放射性活度會隨尿液、唾液、汗等排出體外，因此住院其間鼓勵病人多喝水，每天至少 2,000 毫升以上（腎功能正常），待合乎標準值才可外釋。

結果：

針對 176 位病人（其中男性 43 人、女性 133 人；年齡 24~82 歲，平均 51.3 歲）接受放射性碘 -131 治療外釋時（放射性碘 -131 治療劑量 80 mCi-200 mCi），由輻射防護人員持輻射偵檢儀距病人 1 公尺處測量輻射曝露率，其輻射曝露率分佈如表：

放射性碘 -131 治療劑量	80 mCi	100 mCi	120 mCi	150 mCi	180 mCi	200 mCi
人數	9	62	40	49	1	15
最高曝露率 mR/hr	1.9	2.1	3.5	2.1	1.5	3.5
最低曝露率 mR/hr	0.11	0.03	0.05	0.03	1.5	0.06
平均曝露率 mR/hr	0.80	0.51	0.54	0.47	1.5	0.71

結論：

雖然目前國內對於接受放射性碘 -131 治療病人外釋時之輻射曝露率未有標準可遵循，但考量對周圍環境輻射曝露應合理抑低，建議遵循行政院原子能委員會八十一年修訂之“核子醫學防護措施指引”中之 I-131 治療病人在活度 ＜ 50 mCi，1 公尺處曝露率＜ 11 mR/hr，並經適當衛教指導下可以外釋出院。

PC078

Tc-99m MDP Bone SPECT/CT in the Evaluation of Right Tibia Osteoid Hyperplasia: A Case Report

Yu-Chien Shiau[1], Ya-Huang Chen[1], Chao-Chun Huang[1], Chia-Wen Lai[1], Po-Wei Li[1], Yen-Wen Wu[1], Su-Jane Shen[2], Shan-Ying Wang[1]

[1]Division of Nuclear Medicine, Far Eastern Memorial Hospital, New Taipei, Taiwan;
[2]Department of Nuclear Medicine, St. Martin de Porres Hospital, Chia-yi, Taiwan.

Introduction: Tc-99m MDP bone SPECT/CT is a useful diagnostic tool for various bone disease, including benign bone tumor, malignant bone tumor, stress fracture, osteomyelitis, etc. Since there were very rare reports concerning the application of bone SPECT/CT in the evaluation of osteoid hyperplasia. In this case report, we present a case of right tibia osteoid hyperplasia evaluated by Tc-99m MDP bone SPECT/CT.

Case Report: The 40-years-old woman denied systemic disease before her visit to our hospital. She suffered a palpable mass noted at right lower leg for years. She has been followed up in other hospital. However the tumor size enlarged recently, and she also complained about pain while walking. X-ray showed right middle fibular mass with periosteum reaction. MRI showed right middle-distal fibular lesion. DDx including old-age osteofibrous dysplasia (ossifying fibroma), adamantinoma, subperiosteum-arising vascular neoplasm (hemangioma, hemangioendothelioma, hemangiopericytoma, glomangioma, etc). Tc-99m MDP bone SPECT/CT showed a faint irregular hot spot in right middle fibular cortical bone, suspecting bone tumor, and more likely a benign bone tumor because of lower tracer uptake intensity. SPECT/CT offered spatial resolution to elucidate the location of the tumor in right tibia. After the above evaluations, surgery was indicated, and she was admitted for tumor excision. Pathology showed the tumor to be osteoid hyperplasia/osteoma. CD34, CD31 and ERG highlight hypervascular granulation tissue in an angiomatosis-like. The patient was followed-up in OPD.

Conclusions: Although the clinical application of Tc-99m MDP bone SPECT/CT used for the evaluation of osteoid hyperplasia is relatively rarely reported, we elucidated in this case that Tc-99m MDP bone SPECT/CT is useful for evaluation of osteoid hyperplasia or osteoma, helping more accurate localization, differential diagnoses, and to determine proper operation and treatment. In the future we hope to gather more cases for more detailed statistical analysis.

PC079

Rectal Cancer with Sacrum Metastasis Compared Among F-18 FDG PET/CT, Tc-99m MDP Bone SPECT/CT, CT and MRI: A Case Report

Yu-Chien Shiau[1], Ya-Huang Chen[1], Chao-Chun Huang[1], Chia-Wen Lai[1], Po-Wei Li[1], Yen-Wen Wu[1], Su-Jane Shen[2], Shan-Ying Wang[1]

[1]Division of Nuclear Medicine, Far Eastern Memorial Hospital, New Taipei, Taiwan;
[2]Department of Nuclear Medicine, St. Martin de Porres Hospital, Chia-yi, Taiwan.

Introduction: F-18 FDG PET/CT, Tc-99m MDP Bone SPECT/CT, CT and MRI are reported to be good clinical modalities in the evaluation of bone metastasis from various kinds of cancers. The sensitivity, specificity, and accuracy were frequently discussed. We present a case of rectal cancer with sacrum metastasis, evaluated by F-18 FDG PET/CT, Tc-99m MDP Bone SPECT/CT, CT and MRI. The image findings are compared and correlated.

Case report: The 51 years old female suffered from anal bleeding after defecation for two days. She came to our OPD and colonoscopy revealed a friable polypoid tumor noted at the 5 cm above the anal verge as fungating mass. Lab data showed AFP 5.56 ng/mL, CEA 1.9 ng/mL, CA-199 44.90 U/mL, and CA-125 10.06 U/mL. Under the impression of rectal cancer, she was admitted for further evaluation and treatment. LGI ultrasound showed an ulcerative mass encompassing 1/3 circumference of lumen was noted at rectum around 10 cm above anal verge. EUS with miniprobe (UM-DP-12-25R) showed hypoechoic lesion with whole layer involvement to serosa (max. thickness = 0.9 cm) with larying destruction. Under the impression of T3 rectal cancer, laparoscopy and lower anterior resection were done and followed by CCRT. Pathology showed pT2N2b adenocarcinoma. After 4-year follow-up, she complained about bilateral leg numbness and claudication for months. CT showed suspect tumor thrombus at IVC. F-18 FDG PET/CT showed suspicious metastasis around or in right paraaortic IVC bifurcation, and bone metastasis in sacrum. Tc-99m MDP bone SPECT/CT showed bone metastasis at upper sacrum. MRI showed multiple enhanced mass at sacrum, iliac bone and L5 vertebral body, compatible with bony metastasis. The tumor extended to right pre-vertebral space of L5 and S1. Tumor invaded into IVC at L5 level. Radio-oncologist and oncologist were consulted for further treatment. Chemotherapy and target therapy are considered first. MBD and OPD follow-up were arranged.

Conclusions: F-18 FDG PET/CT, Tc-99m MDP Bone SPECT/CT, CT and MRI are good clinical modalities in the evaluation of cancer with bone metastasis. In this case, we elucidated that F-18 FDG PET/CT and Tc-99m MDP Bone SPECT/CT are good clinical tools for accurate clinical staging and more proper treatment planning. In the future we hope to gather more cases for more detailed statistical analysis.

PC080

The Proposed Physiology-based FDG PET/CT Criteria in Advanced Head and Neck Cancer After Chemoradiotherapy: Validation with Histology and Comparison with the Hopkins Criteria

Shu-Hua Huang[1], Yen-Hsiang Chang[1], Bor-Tau Hung[1], Pei-Wen Wang[1], Hui-Ching Chuang[2], Chih-Yen Chien[2]

[1]Department of Nuclear Medicine, Kaohsiung Chang Gung Memorial Hospital and Chang Gung University College of Medicine, Kaohsiung, Taiwan;
[2]Department of Otolaryngology, Kaohsiung Chang Gung Memorial Hospital and Chang Gung University College of Medicine, Kaohsiung, Taiwan.

Abstract

Purpose: Distinguishing benign complications after concurrent chemoradiotherapy (CCRT) from a local residual tumor in advanced head and neck squamous cell carcinoma (HNSCC) remains a clinical challenge. In this study, we propose new criteria when considering physiological uptake patterns on FDG PET/CT in patients with advanced HNSCC after CCRT.

Materials and Methods: We retrospectively reviewed FDG PET/CT images of 61 patients with advanced HNSCC, which were taken within 16 weeks following CCRT. Both our criteria and the Hopkins criteria were jointly rated according to the uptake patterns of primary site. The histology of the primary site within a 1 month of the PET/CT study was used as the gold standard for sensitivity, specificity, positive predictive value and negative predictive value.

Results: PET/CT was arranged at a median interval of 10.5 weeks (range 4-16 weeks) after CCRT, and the pathologic residual rate was 55.7% at the primary site. The sensitivity, specificity, positive predictive value, negative predictive value, and accuracy of identifying residual disease were 91.2%, 51.9%, 70.5%, 82.4%, and 73.8%, respectively, by the Hopkins criteria, and 88.2%, 92.6%, 93.8%, 86.2%, and 90.2%, respectively, by our rating criteria. Our visual rating criteria corrected 11 of 13 (84.6%) false-positive results from the Hopkins criteria, while two more false-negative cases identified with our criteria were proven to be small residual tumors.

Conclusions: By incorporating physiological changes following CCRT, our visual rating criteria improved the accuracy of the currently used FDG PET/CT visual rating system, especially the number of false-positive cases with advanced HNSCC after CCRT.

PC081

Added Values for the Detection of Bone Metastases in Whole Body Bone Scans with A Computer-aided Detection Scheme: Irregular Flux Viewer (IFV)

Chang-Ching Yu[1,3], Nan-Jing Peng[1,4], Chung-Shun Wu[1], Hueisch-Jy Ding[2], Hung-Pin Chan[1]

[1]*Department of Nuclear Medicine, Kaohsiung Veterans General Hospital, Taiwan;*
[2]*Department of Medicine Imaging and Radiological Science, I-Shou University, Taiwan;*
[3]*Department of Information Engineering, I-Shou University, Taiwan;*
[4]*National Yang-Ming University, School of Medicine, Taipei, Taiwan.*

Aim: Tc-99m WBBS shows a high sensitivity but relatively low specificity due to bone variation. However, the differences between patients and physicians' experience, the poor image quality have limited the accuracy of image interpretation. So it is meaningful to develop computer aided diagnosis (CAD) system for WBBS, especially for the quantities' analysis of tumor and patients.

Methods: Most articles describe a computer-aided automatic detection for bone lesion, including quantitative clinical tools for elevating bone metastasis. The gradient vector flow detecting model and used to a quantitative scheme to detect possible abnormalities. Based on previous articles, we developed the Irregular flux viewer (IFV) system and hope to predict possible bone lesions in planar WBBS. To study the feature of irregular flux about the blood flow, this study design an easy algorithm for the software to view the irregular flux hot points and then gave the possibility of hot points that the tumors would be located. We presented a 54 year-old female who has endometrial cancer with organ metastases. WBBS showed no obviously abnormal tracer uptake over the T-spine region in WBBS, but magnetic resonance imaging (MRI) revealed T7-T9 metastases. IFV was used for WBBS of this patient.

Results: IVF not only evaluates the irregular flux in the bone marrow from planar WBBS imaging by computer-aided detection system, but also provides an algorithm to indicate the distribution of hot points. We supposed that the hot points probably represent the possible tumor location and occurrence. After analysis, we found new metastatic lesions in the T7-T9 region. The predicted lesion was similar to the MRI data.

Conclusion: IFV increases the accuracy of detection of bony metastasis and thus improves physician diagnosis. So our CAD scheme achieved a high level of detection accuracy, and would have a great potential in assisting physicians to detect metastasis in bone scintigraphy. However, it needs more studies and cases enrolled for examination of this system.

PC082

Incidental Thyroid Nodule Noted on MAA Scan Before Y-90 SIRT

Sin-Di Lee[1], Chin Hu[1], Nan-Jing Peng[1,2]

[1]*Department of Nuclear Medicine, Kaohsiung Veterans General Hospital, Taiwan;*
[2]*National Yang-Ming University, School of Medicine, Taipei, Taiwan.*

Abstract

We report a case of 61-year-old man who had recurrent hepatocelluar carcinoma (HCC) admitted for series evaluation before Yttrium-90 (Y-90) selective internal radiotherapy (SIRT). Intraarterial hepatic technetium-99m (Tc-99m) macroaggregated albumin (MAA) scan before Y-90 SIRT revealed an incidental low-density thyroid nodule with hot uptake surrounded by normal thyroid tissue with faint uptake and accompanied with mild uptake in gastric mucosa. Tc-99m pertechnetate scan revealed corresponding hot uptake in the thyroid nodule with only faint uptake of normal thyroid tissue, favored hyperfunctioning nodule. After Y-90 microsphere SIRT, bremstrallung imaging revealed no Y-90 microsphere deposition to thyroid.

The differential diagnosis of focal thyroid uptake in intraarterial hepatic Tc-99m MAA scan including uptake of free Tc-99m pertechnetate hyperfunctioned thyroid nodule and abnormal vascularity of thyroid. With Tc-99m pertechnetate scan, diagnosis of hyperfunctioned thyroid nodule can be established with more confidence.

PC083

Incidentally Finding of Colovesical Fistula Noted by Tc-99m MDP Bone Scan

Sin-Di Lee[1], Chin Hu[1], Chang-Chung Lin[1], Nan-Jing Peng[1,2]

[1]Department of Nuclear Medicine, Kaohsiung Veterans General Hospital, Taiwan;
[2]National Yang-Ming University, School of Medicine, Taipei, Taiwan.

Abstract

We report a case of 88-year-old man with rectal cancer post diverting T-loop colostomy and CCRT under hospice care. He received bone scan due to general pain. The scan revealed suspicious bony metastasis over right scapula; besides, irregular bowel uptake is noted as well. SPECT/CT revealed uptake in lumen of colon and tumor direct invasion to urinary bladder.

Colovesical fistula is the presence of a communication between colon and urinary bladder. It might complicated with recurrent urinary tract infection. SPECT/CT is able to revealed the tumor direct invasion and defect of fat pad, which indicated the route of the fistula and is the hint for surgical intervention. Even though the patient was under hospice care, the finding leaded to a better management of quality of life.

PC084

The Incremental Value of Tl-201 Dipyridamole SPECT Myocardial Perfusion Imaging in Patients with Normal Wall Motion on Non-stress Echocardiography

Jih-Fang Hsieh[1], Chiang-Hsuan Lee[1,2], Chih-Shun Wu[2]

Department of Radiology, Section of Nuclear Medicine
[1]Chi Mei Medical Center, Yongkang Dist., Tainan, Taiwan;
[2]Chi Mei Foundation Hospital, Liuying Dist., Tainan, Taiwan.

Purpose: We aimed to compare the incremental value of SPECT myocardial perfusion imaging (SMPI) for the detection of coronary artery disease (CAD) in patients with chest pain who had a normal wall motion (WM) on non-stress echocardiography.

Methods: A single-institution, retrospective study was performed. SMPI was performed with 2 mCi thallium (Tl)-201 under a standard dipyridamole pharmacological stress protocol and compared with corresponding non-stress echocardiography which were correlated subsequent coronary angiography. We retrospectively reviewed the myocardial SPECT images of the 1135 continuous patients from Jan 2014 to Dec 2014. We selected patients to be included in this study those with positive Tl-201dipyridamole SMPI with normal wall motion on non-stress echocardiography and who subsequently underwent coronary angiogram (CAG). Sixty two patients meet the criteria for inclusion in this retrospective study.

Results: Visual interpretation of Tl-201dipyridamole SMPI revealed 85.4% (53 out of 62 patients) were positive for CAD defined as > 50% stenosis for a total of 69 coronary territory lesions in patients who underwent CAG within 2 months after SPECT imaging. There were 23.2% (16 out of 69 lesions) with stenosis > 50% and 76.8% (53 out of 69 lesions) with stenosis > 70%.

Conclusion: The addition of Tl-201 dipyridamole SMPI to non-stress echocardiography increased true-positive test results by 85% compared with WM criteria in non-stress echocardiography. Fifty three patients (85%) were diagnosed with obstructive CAD (23.2% with stenosis > 50% and 76.8% with stenosis > 70%.) thanks only to isolated SMPI abnormalities; the cardiac origin of their chest pain would have been mistakenly “ruled out” on the basis of the absence of WM abnormalities on non-stress echocardiography.

PC085

Tc-99m MDP SPECT in Differentiation of Benign Versus Malignant Bony Lesions in the Vertebrae During Lung Cancer Staging

Jih-Fang Hsieh[1], Chiang-Hsuan Lee[1,2], Chih-Shun Wu[2]

Department of Radiology, Section of Nuclear Medicine
[1]Chi Mei Medical Center, Yongkang Dist., Tainan, Taiwan;
[2]Chi Mei Foundation Hospital, Liuying Dist., Tainan, Taiwan.

Purpose: The purpose of this study was to find out whether the particular localization of an intraosseous lesion in a vertebra is an indicator of its etiology in a group of patients who had bone scintigraphy as part of the workup for cancer staging in lung cancer.

Methods: A single-institution, retrospective study was performed. Bone scintigraphy including planar whole-body scans as well as SPECT imaging of the vertebra was performed in 84 patients. The diagnoses of bony lesions in the vertebrae were made on the basis of the findings of magnetic resonance imaging, computed tomography or plain radiography. Four anatomical regions were differentiated within the vertebra: the vertebral body, the pedicle, the facet joints and the spinous process.

Results: Taking into account the number of examinations, yielded the following following probability intervals for the malignancy of intraosseous lesions in the vertebrae: vertebral body 48%, pedicle 92%, facet joints 1% and spinous process 2%. Conclusion: It was concluded that lesions affecting the pedicle are a strong indicator for malignancy, whereas involvement of the facet joints and spinous process are usually related to benign disease. Lesions affecting the vertebral body process do not show a clear tendency towards either malignancy or benignity.

PC086

執行正子電腦斷層造影 (PET/CT) 時給予固定輔具的重要性

陳妍文　陳輝墉　王文祥

義大醫療財團法人義大醫院核子醫學科

背景介紹：

CT 是人體組織密度分佈的解剖影像，在 PET/CT 掃描中提供影像衰減校正、解剖定位資訊與輔助影像診斷的功能，但 CT 影像也會帶來困擾，我們發現在執行 PET/CT 造影時，受檢者的移動會造成影像重組完後的截斷式假影。

方法：

首先排除儀器損壞造成的假影可能，分析其他可能造成假影因素後，發現造影時有二因素可能造成此截斷式假影，一爲受檢者在執行 CT 掃描時有移動的動作，二是受檢者在收取 PET 影像時的移動。因此在受檢者造影時，給予約束帶等輔具固定肢體。

結果：

針對這樣受檢者的移動所形成的假影原因，我們給予約束帶束縛腰部與枕頭固定在腳踝，經過多位受檢者的造影後，發現受檢者無肢體移動。

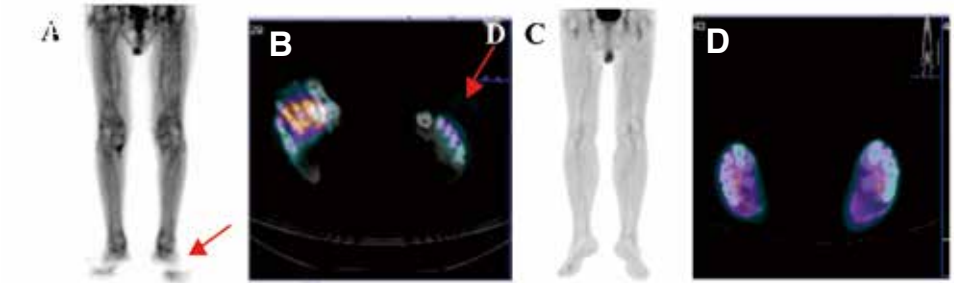

圖 (A) 爲 CT 衰減校正過後的 PET 影像；圖 (B) 爲 PET 和 CT 融合影像。可明顯看到在 PET 和 CT 融合影像上的錯位，研判爲受檢者在收取 PET 影像時，腳有移動，所以在 AC 過的 PET 影像 (圖 A) 有類似像截斷假影。圖 (C) 和 (D) 爲正常影像。

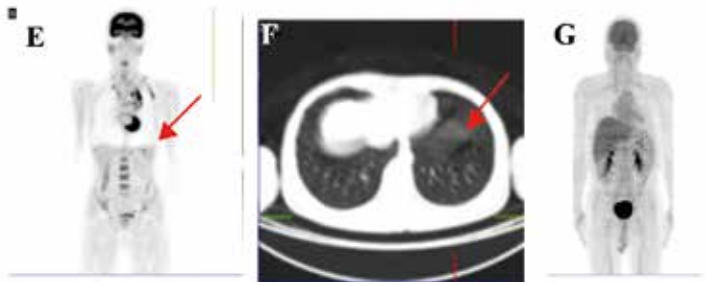

圖 (F) 爲 CT 影像，可明顯看到受檢者在 CT 掃描時有移動，爲病人咳嗽所至，所以在有衰減校正過的 PET 影像 (E) 上有截斷式的假影。圖 (G) 爲正常影像。

結論：

現今 PET/CT 醫學影像是提供各種癌症偵測與分期的重要利器，能清楚的顯示病灶的功能影像及正確位置，提供臨床醫師作爲治療的依據；因此在檢查過程應避免任何假影的發生。

PC087

使用 DOPS 與 Mini-CEX 訓練放射實習生之成果分析

曾旭吟　楊士頤　郭珮怡　李佩璇　莊雅晴　陳俊榮　李世昌　吳佩珊　李碧芳　邱南津　姚維仁

國立成功大學醫學院附設醫院核子醫學部放射免疫分析科

背景介紹：

常用的學習成效評量工具有 OSCE 臨床技能評估、Mini-CEX 迷你臨床演練評量、DOP) 臨床技術實作之觀察評估、MSF (360 度) 多元回饋及 CbD 案例討論，每一種評量的工具其目的不外乎讓學員或是實習生可以加深在學術與臨床上的相呼應，並且學習與病人的互動和案例上的延伸討論，更可以檢測在學習實做上的表現，使自己在好的表現可以維持，不好的表現可以加強訓練，補強不足的地方。其中，本部門使用 DOPS 與 Mini-CEX 兩項學習成效評量工具來評量放射實習生在臨床上的操作與病人的應對互動，並且雙向回饋，讓學生與老師教學相長。

方法：

以知識、技能和態度爲臨床能力的三大面向做評量，本部門使用 DOPS 與 Mini -CEX 兩項學習成效評量工具來評量放射實習生。Mini -CEX (Mini-clinical Evaluation Exercise) 注重與病人溝通時的表現技能，需要 20 至 30 分鐘時間觀察，藉由直接觀察的方式執行評量與教學。DOPS (Direct Observed Procedural Skills) 是對於臨床操作技術的評估，以確保醫療品質。

結果：

此次有使用 Mini-CEX 與 DOPS 評估項目有：Gallium scan、Tl-201 myocardium Stress and rest、CRFT (Comprehensive renal function test)、WBBS (Whole body bone scan)、PET 與 RIA，其中 RIA 只適用於評估 DOPS。由 DOPS 評估可發現在第 9 點影像傳輸與品保上的分數較爲其他評量內容分數低，Mini-CEX 評估在第 4 點臨床判斷的分數較爲其他評量內容分數低。

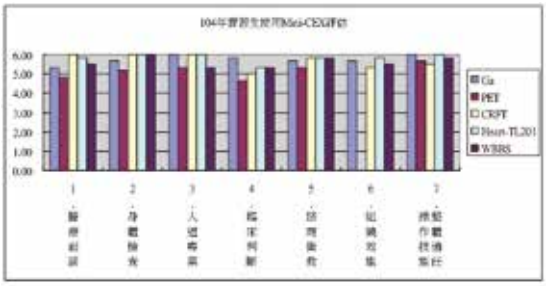

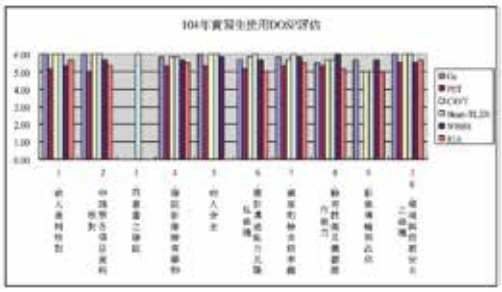

結論：

藉由 DOPS 與 Mini-CEX 這兩種評量評估實習生在實習時的學習成果，並且也可由分數的高低，讓老師們知道實習生在哪些項目或是哪些評量內容項目較爲不足或不熟悉，藉此在評量後可以針對實習生的不足作加強，使實習生更加熟悉臨床的技術，並且應用於教科書上的內容，發揮到念書與實作的內容融會貫通。不僅如此，除了補強實習生方面，還可以讓老師們對於下次教學內容做修正，使教學內容越來越完整，越來越豐富。

PC088

前瞻性探討台灣本土接受高劑量碘 131 住院治療甲狀腺癌病人體內輻射劑量衰減速率

鄭如金[1] 詹勝傑[1] 李冠瑩[1] 朱麗蓉[1] 王淑芳[1]

[1] 基隆長庚紀念醫院

背景介紹：

台灣每年有許多接受高劑量碘 131 治療的甲狀腺癌病人，但對於這些病人住院時體內放射線的衰減速率，並沒有本土性的相關研究，目前亦缺乏全國性統一外釋出院準則，因此我們設計了這個前瞻性研究，主旨在探討接受高劑量碘 131 治療甲狀腺癌病人住院時體內輻射劑量衰減情形。

研究方法：

收案的條件爲在基隆長庚醫院碘 131 病房住院治療之分化良好型甲狀腺癌病人，並能配合多時間點體內放射線偵測。我們在病房內設置輻射偵檢器 (Ludlum Model 375)，在住院吃碘 131 後的 1、5、16、21、27 及 40 小時 (分別爲 D1, D2, D3, D4, D5, D6)，病人立於偵檢器前一公尺處偵測體內輻射劑量，所得數值傳到病房中央 computer server 儲存。

研究結果：

從 2010 年 9 月到 2015 年 8 月，共收案 924 人次住院病人，621 位爲女性 (67.21%)，828 位爲 papillary cell carcinoma (89.61%)，68 位爲 follicular cell carcinoma (10.39%)。287 位 (31.06%) 住院原因爲接受甲狀腺癌摘除手術後做 ablation or adjuvant therapy (Group A)，637 位 (68.94%) 爲復發治療病患 (Group B)。72 位 (7.79%) 病人治療劑量小於 100 mCi (Group C)，686 位 (74.24%) 劑量爲 100 mCi (Group D)，166 位 (17.97%) 劑量爲 150~200 mCi (Group E)。

整體病患體內劑量半衰期平均爲 9.12 ± 4.10 hr，Group A 和 Group B 病患體內劑量平均半衰期分別爲爲 9.60 ± 4.09 hr 和 8.91 ± 4.09 hr (P = 0.148)，而 Group C, D, E 病患體內劑量平半衰期均分別爲 8.78 ± 4.18、9.03 ± 3.98 及 9.67 ± 4.53 (P < 0.0001)。

整體病患服藥後 24 hr 平均劑量爲 34.62 ± 15.79 μSv/hr，40 hr 平均劑量爲 15.96 ± 10.18 μSv/hr。病患體內輻射劑量下降到 100 μSv/hr 平均時間爲 14.12 ± 7.87 hr（range：4.44 ～ 53.97 hr），到 50 μSv/hr 平均時間爲 17.82 ± 5.72 hr（range：2.90 ～ 34.66 hr）。

Group A or B 病患下降到 100 μSv/hr 平均時間分別爲 15.27 ± 7.87 及 13.59 ± 7.82 (P < 0.003)；下降到 50 μSv/hr 平均時間分別爲 19.10 ± 5.43 及 17.82 ± 5.72 (P < 0.0001)。

Group C, D, E 病患下降到 100 μSv/hr 平均時間分別爲 8.11 ± 4.78、13.01 ± 7.42 及 20.53 ± 6.69 (P < 0.0001)；到達 50 μSv/hr 平均時間分別爲 12.16 ± 4.76、17.23 ± 4.85 及 22.7 ± 6.03 (P < 0.0001)。

結論：

若以本院外釋標準 50 μSv/hr 來看，所有住院滿 40hr 的本土甲狀腺癌病人皆可外釋。高劑量治療的病人其到達外釋標準所需時間明顯比低劑量來的長，治療劑量可做爲規劃病人住院時間的重要參考。

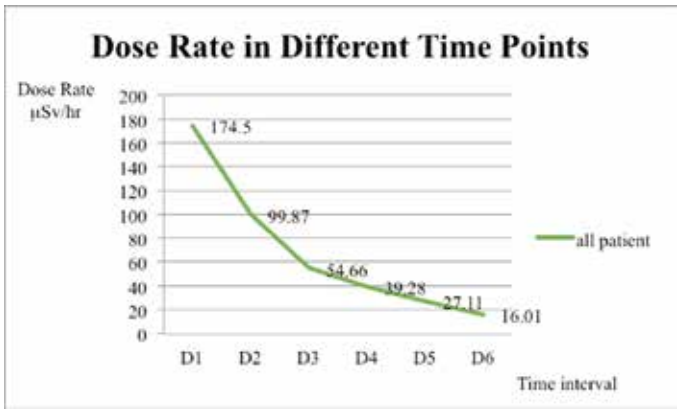

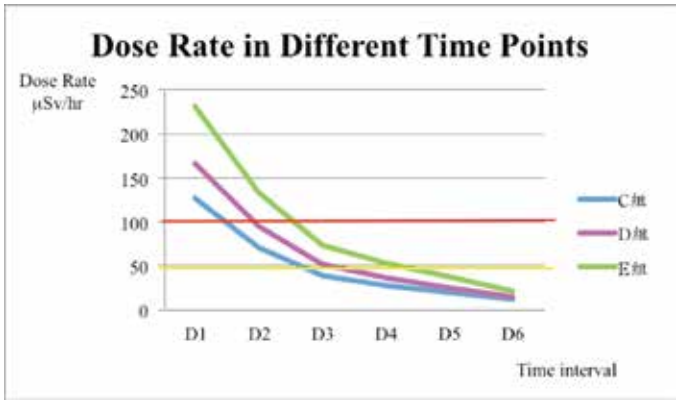

PC089

利用品管圈手法降低甲狀腺球蛋白報告逾時率

郭珮怡[1] 曾旭吟[1] 楊士頤[1] 李佩璇[1] 莊雅晴[1] 陳俊榮[1] 李世昌[1] 吳佩珊[1] 李碧芳[1] 邱南津[1] 姚維仁[1]

[1]國立成功大學醫學院附設醫院核子醫學部

背景介紹：

爲因應醫療上確立「以病患爲中心」的信念，落實安全就醫、全面品管作法，以服務病友的服務，提供正確有效率的檢驗報告爲臨床實驗室最重要的任務，除了考量檢驗結果正確性，檢驗報告的時效率也是重要課題之一。本次針對檢驗項目甲狀腺球蛋白進行報告逾時率分析，甲狀腺球蛋白 (Thyroglobulin，以下以 TG 表示) 是甲狀腺素製造過程中重要的媒介物，是已分化甲狀腺癌追蹤及預後判斷最重要之一個標記。

方法：

本科統計 102 年 7 月至 103 年 6 月間，改善前之 TG 報告逾時率爲 4.12%，利用 QCC 手法，發掘淺在問題並進行 PDCA 改善，依柏拉圖分析，找出影響報告延遲前 80% 的項目並擬定對策與執行：(1) 初次結果大於正常值，主因爲初次檢測病人，對策：增加檢驗次數。(2) 高於線性結果需稀釋，主因爲 hook effect (> 300 ng/ml)，對策：同時進行兩種稀釋倍數。(3) 組織液檢體，主因爲難以測定，對策：跟臨床醫生進行協調。(4) 重複檢測，主因爲人員專業度不足，對策：1. 進行人員教育訓練 2. 統整確認檢驗報告時應注意事項 3. 針對異常或特殊案例進行討論。

結果與討論：

改善中之 TG 報告逾時率爲 3.54%，持續追蹤至 103 年 12 月改善後 TG 報告逾時率爲 1.12%。針對臨界值附近的檢驗，和低於偵測極限附近的檢驗值，應增加檢驗次數 (原本一週執行兩次，變更爲一週執行三次)，雖然會增加成本，但對於臨床醫生及病人而言，有實質的意義。

結論：

本次改善活動成效良好，爲全科之品質改善，優點是報告逾時率的問題涵蓋全科室，改善過程中同仁腦力激盪，並將其他檢驗項目用同樣手法進行分析，降低全科全面報告逾時率，缺點是無法針對最需改善之處，人員之穩定性及判讀檢驗報告能力亦是往後持續改善的重要因素，唯有不斷的持續改進，是我們精進努力的目標。

PC090

A Case of Situs Inversus Detected on F18-FDG PET/CT during Health Examination

Shih-Fu Wang, Dom-Gene Tu, Yu-Ling Hsu

Department of Nuclear Medicine, Ditmanson Medical Foundation Chia-Yi Christian Hospital.

Case Report:

A 70-year-old man whose job is a farmer went to our hospital and asked for health check-up. He has no systemic diseases except hyperlipidemia. Occasional cough with sputum was noted. On the day of performing PET/CT scan, his serum glucose level was 100 mg/dl, and he was injected 299.7 MBq of 18F-FDG intravenously. The patient was imaged after one hour using a dedicated GEMINI GXL (PHILIPS) integrated PET/CT camera. The non-contrast CT scan was used for anatomical landmark and attenuation correction. As a result, his imaging depicted small lung nodules which were probably non-specific, and showed situs inversus incidentally.

The exact etiology of situs inversus is unknown, but an autosomal recessive mode of inheritance has been speculated. There may be a higher prevalence in certain ethnic groups. The overall incidence of this anomaly is of 1:5000 to 1:20,000, being slightly more common in males. Situs inversus may be complete (situs inversus totalis) or partial (situs inversus partialis), confined to either the thoracic or the abdominal viscera. This anomaly apparently does not influence normal life expectancy.

As a rare case of situs inversus detected on FDG PET/CT scan, the patient reminds us technicians to be aware of certain unexpected situations during daily practice.

PC091

RIA 實驗室風險因子的辨識

王安美[1] 吳明哲[1]

[1] 台北馬偕醫院核子醫學科

背景：

ISO 15189:2012 新版規範中其第 4.14.6 節「風險管理」載明「實驗室應針對影響病人安全的工作流程與檢驗結果之潛在失效的衝擊進行評估，並應調整流程以減少或消除已鑑別的風險，並將決定及採行措施予以文件化」，故將風險管理 (Risk Management) 納入評估與稽核、管理審查活動等。

醫學實驗室目前實施的日常品管 (Daily Control) 或能力試驗 (Proficiency test) 作業並不等同「病人安全」。因爲分析前階段 (Preanalytical phase) 與分析後階段 (Postanalytical phase) 的錯誤率 (Errors rate) 遠超過分析中階段 (Analytical phase)，因此醫學實驗室負責人應與所屬相關主管建立自己實驗室之風險因子的辨識。

方法：

風險分析 (Risk analysis)：爲系統利用現有的信息來識別危險 (Hazard identification) 並將其發生的可能性 (Probability) 與嚴重性 (Severity) 分類以進行風險評估 (Risk estimation)。收集與分析測試有關聯的資訊文件是很重要的，其中這些資訊應涵蓋實驗前中後分析。再依上述資訊辨識風險因子 (Risk factors)。

信息來源 (Sources of information)：例如監管 / 認證機構的要求、製造商的包裝說明書和操作手冊、製造商查證資料或性能規格、檢測人員的資格、培訓和能力、品管數據和操作步驟、能力試驗數據、品保文件包含矯正措施、先前失效的調查記錄、 出版文獻。以上說明可作爲風險因子之參考依據。

實驗室管理團隊則再依據上述信息資訊內容找出自己實驗室實驗中所可能發生之風險因子，進行風險分析，當然這些分析必須包括實驗前中後之分析。

1.1 風險分析 (Rsk analysis)：包含識別危險 (Hazard identification) 與風險評估 (Risk estimation)

1.1.1 識別危險 (Hazard identification)

1.1.1.1 檢體 (Specimens)：病人辨識與準備，樣本採集時間、採集量與容器，樣本標示樣本付託，樣本傳送條件，樣本接受和拒收，樣本儲存和穩定性，樣本處理，樣本干擾 (血脂、溶血、凝塊、泡沫等)，檢體離心的要求與轉速。

1.1.1.2 環境 (Environment)：溫度，濕度，汙塵，水質，電力故障 / 電源變化或電壓不穩 ，氣流 / 通風，光照強度 (有些須避光)，counter 的穩定性。

1.1.1.3 試劑 (Reagent)：運輸 / 接收，儲存條件要求，有效日期，泡製的時效，使用時要求，標準品的濃度變化，批號變化，平行比對，放射性碘的變質，品管的要求，污染變質。

1.1.1.4 檢測系統 (Test systems)：樣本分析 (Sample analysis)：採檢前病患的準備 (時間、空腹與否)，濃度線性區間，品管設定， 品管批號，病人辨識，檢體量，報告濃度範圍，臨

界值範圍，正常值濃度範圍，荒謬值的篩選。

1.1.1.4.1 儀器設備 (Instrument issue)：系統控制和功能故障 (機械 / 電子)，錯誤訊息，故障排除，運作干擾，溫度監測，清潔保養（counter 輻射污染），LIS 連線障。

1.1.1.4.2 操作人員 (Operators)：訓練，能力，適當的教育和經驗資歷，充足的人員，非認知錯誤 (疏忽或失誤) 與認知錯誤。

1.1.1.4.3 結果報告 (Result reporting)：不正確的結果，不正確的結果抄寫或轉錄，缺少關於報告解讀之參考。

結果：

實驗室可參酌上述說明，分別檢討實驗流程中辨識出可能造成實驗失效的因子，接著進行風險處理 (Risk treatment) 亦稱風險控制 (Risk control)。當潛在的不可接受風險被鑑定出，實驗室必須展現採用任何的方法、手段和實驗室品質政策和程序來降低危害 (Harm) 的可能性 (Probability) 使不可接受的風險轉降爲可接受的風險等級。

討論：

風險管理 (Risk Management) 是任務與承諾 (Mandate and Commitment)，實施風險管理前由實驗室管理階層先設計用於風險管理的架構 (Framework)。在實施過程中需要溝通與協談 (Communication and consultation)，營造共同參與風險管理的環境與氣氛。實施後要回顧監控此架構，並對此架構進行持續改進 (Continual improvement)，方能達到預期的效果和效率 (Effective and efficiency)。

放射免疫分析實驗室爲醫學實驗室的一員，基於「病人安全」的考量與潮流趨勢以及認證的要求，應該著手進行風險管理，以提升檢測報告解讀、品質的可信度。

PC92

全自動檢體分注儀 TECAN FREEDOM EVO 100 與 TECAN FREEDOM EVO 150 之檢驗性能比對

莊雅晴[1] 郭珮怡[1] 曾旭吟[1] 楊士頤[1] 李佩璇[1] 陳俊榮[1] 李世昌[1] 吳佩珊[1] 李碧芳[1] 邱南津[1] 姚維仁[1]

[1]國立成功大學醫學院附設醫院核子醫學部

背景介紹：

TECAN FREEDOM EVO 爲一高效能全自動檢體前處理系統，透過精密電腦軟體控制，利用八爪液體分注器，進行檢驗前檢體分注處理，取代傳統人工 pipette 作業，以提升檢驗時效與品質。爲符合臨床檢驗需求，實驗室面臨儀器設備汰舊換新，因應實驗室認證規範，針對新增儀器設備於使用前加以驗證其性能，以確保儀器設備分析結果之準確性。

方法：

1. 儀器設備：TECAN FREEDOM EVO 100 與 TECAN FREEDOM EVO 150。
2. 材料：病人檢體包含 (1) 六項定量項目 CA-153、TSH、LH、PSA、T4、Cs，共 75 支。(2) 兩項定性項目 HBs Ag、Anti-HAV，共 20 支。
3. 評估方法：(1) 六項不同檢體量需求的定量項目，挑選不同參考值區間的檢體，共 75 支，分別使用新舊 TEACN 操作，最終實驗結果先以圖形分佈，再利用統計分析軟體 EP Evaluator 8.0 計算相關係數 (R) 及迴歸方程式進行數據比對。本實驗室訂定相關係數 $R > 0.975$ 爲可接受。(2) 不同檢體量需求的定性量項目，共 20 支，分別使用新舊 TEACN 操作。本實驗室訂定結果一致率達 100% 爲可接受。

結果：

1. 六項定量項目使用 TECAN FREEDOM EVO 100 與 TECAN FREEDOM EVO 150 操作結果之相關性比對，R 值皆大於 0.975，符合本實驗室設定之允收範圍。
2. 兩項定性項目使用 TECAN FREEDOM EVO 100 與 TECAN FREEDOM EVO 150 操作結果之相關性比對，一致率皆達 100%，符合本實驗室設定之允收範圍。

結論：

依據實驗室認證規範，實驗室新增儀器設備啓用前應完成各項功能測試、人員教育訓練及性能比對之驗收程序，綜合上述統計分析結果，TECAN FREEDOM EVO 150 通過儀器設備性能比對測試，對於不同檢驗量需求之定性與定量項目皆符合本實驗室設之允收標準，確保新設備的啓用能提升檢驗效率及品質。

PC93

Solitary Right Pulmonary Hilar Lymph Node Metastasis of Recurrent Rectal Cancer on F-18 FDG PET/CT: A Case Report

Chao-Jung Chen[1], Tung-Bo Chao[2], Han-Gu, Chen[3]

Departments of [1]Nuclear Medicine, [2]Colorectal Surgery, and 3Pathology, Yuan's General Hospital, Kaohsiung, Taiwan.

Introduction: Recurrence in colorectal cancer (CRC) after surgical resection is very common. The most common recurrent sites are local recurrence, liver, lung, and peritoneum. Solitary recurrence such as in axillary lymph node, mediastinal lymph node, and thyroid has been reported but are rare. We present the case of a woman with rectal cancer that had a solitary recurrence in a right pulmonary hilar lymph node on F-18 fluorodeoxyglucose positron emission tomography/computed tomography (F-18 FDG PET/CT).

Case report: A 57-year-old female had radical protectomy for rectal adenocarcinoma (pT3N0M0) and adjuvant chemotherapy about 5 years ago. Regular follow-ups with abdominal computed tomography and chest X-ray were normal. However, recent serum carcinoembryonic antigen (CEA) level was remarkably elevated (13 ng/mL), and she was referred for F-18 FDG PET/CT to detect tumor recurrence. The 1-hour post injection F-18 FDG PET/CT image showed a single hot area of increased FDG uptake on the right pulmonary hilar lymph node without other involvement. The lymph node was enlarged with 2.0 cm in size and its maximal standardized uptake value (SUV) was 5.5 on the 1-hour post-injection image. Excision was done and the pathology showed a metastatic adenocarcinoma coming from colorectal origin.

Discussion: F-18 FDG PET/CT has been shown to be useful in detecting tumor recurrence in patients with CRC especially with unexplained rising serum CEA level. The right pulmonary hilar lymph node in our case showed solitary and intense FDG uptake. Its maximal SUV was 5.5 on the 1-hour post-injection image and higher than 4.49 which has been used as the cut-off value for determining malignancy in lung hilus. Furthermore, it is new as comparing with the previous F-18 FDG PET/CT. Therefore, metastasis from recurrent rectal cancer should be suspected. It is hypothesized that mediastinal involvement of recurrent CRC is usually a re-metastasis from a previously metastasized site, such as the lung or liver. Other routes are probably via the paraaortic lymphatic drainage or even skip metastasis. It has also been claimed that neoadjuvant chemoradiation followed by total rectal excision may alter tumor biology in ways that limit liver metastasis or favor lung metastasis. Therefore, we hypothesize that involvement of the pulmonary hilar lymph node in our case may be through a skip pathway. It may due to tumor biology alteration after surgery and systemic chemotherapy, supporting the hypothesis of seed and soil.

PC094

放射免疫分析之內部顧客滿意度調查分析

李佩璇[1] 曾旭吟[1] 楊士頤[1] 郭珮怡[1] 莊雅晴[1] 陳俊榮[1] 李世昌[1] 吳佩珊[1] 李碧芳[1] 邱南津[1] 姚維仁[1]

[1]國立成功大學醫學院附設醫院核子醫學部

前言：

滿意度調查乃醫療品質於結果面評估的一部份。實驗室於 96 年通過 TAF ISO15189 認證，依據 ISO15189 條文 4.7 諮詢服務及 4.8 抱怨處理要求，進行一年一度內部顧客滿意度調查，以作爲一種品質管理系統之監測，其目的在於能提供客戶有效之諮詢與抱怨服務，於必要時採取矯正措施，以確保並提升實驗室之服務品質滿足顧客之要求。

方法：

檢驗部門以提供正確有效之檢驗報告爲第一優先，因此本實驗室訂定一份以品質 (檢驗報告正確性)、速度 (報告等候時間)、設備 (檢驗項目是否充足、HIS 系統開立檢驗單)、態度 (服務態度) 等四大面向之滿意度調查問卷，對象爲全院醫師，發放 216 份書面滿意度調查問卷，期限爲 14 天。

結果：

合計發出問卷 216 份，回收 42 份，回收率爲 19.4%。醫師對實驗室品質 (5. 報告符合臨床診斷、8. 檢驗單內容、11. 生物參考區間符合臨床篩檢) 滿意度 89%、速度 (6. 報告時效) 滿意度 81%、設備 (1. 檢驗項目充足、7. 科部網頁資訊、9. HIS 系統開立檢驗單方便性與醫令名稱後備註核醫、10. 新開發檢驗項目) 滿意度 78%、態度 (3. 檢驗專業知識、4. 電話服務態度) 滿意度 87%。比較四面向，發現實驗室品質、速度與態度滿意度皆在 80% 以上，顯示全院醫師對這三面向項目是普遍認同滿意，而設備方面較不滿意項目爲「新開發檢驗項目」，是因爲宣導不周的關係，導致醫師不瞭解實驗室新開發之檢驗項目，針對這個問題我們會加強宣導。醫師在建議欄中提到建議事項爲 CA125 報告速度有點久。CA125 報告速度，實驗室進行檢討，增加施做次數加以改善並持續觀察。

結論：

藉由內部客戶滿意調查反映出的情況，可讓我們從不同層面探討出實驗室的優缺點，並加以改進實驗室所欠缺的部份，讓實驗室與客戶間的溝通達到平衡，藉以提升整體醫療照護與服務品質。

PC095

Factors Affecting Sentinel Lymph Node Mapping with ^{99m}Tc-phytate in Breast Cancer Patients

Chi-Ju Wu[1], Pei-Ing Lee[1], Ben-Long Yu[2], Yu-Yi Huang[1]

[1]Nuclear Medicine Department, Koo Foundation Sun Yat-Sen Cancer Center, Taiwan;
[2]Surgery Department, Koo Foundation Sun Yat-Sen Cancer Center, Taiwan Email: chijuwu@gmail.com.

Background: Sentinel lymph node dissection (SLND), rather than extensive nodal dissection, is accepted as the standard of axillary staging in early, clinically node-negative breast cancer. Accurate lymph node staging is essential for both prognosis and treatment. Successful SLN mapping with dual ^{9m}Tc-colloid and blue dye is greater than 90%. However, the use of ^{99m}Tc-phytate alone is not established yet. This study was to evaluate the potential factors associated with non-visualization of lymphatic mapping.

Material and Method: During 2013 January to 2015 June, 1525 breast cancer patients received pre-operatively SLN mapping with intradermal injection of ^{99m}Tc-phytate. After 2 hours of injection, 45° anterior oblique imaging was obtained. Visualization of accumulated radioactivity in suspected site are marked on the skin; while non-visualization of radioactivity in suspected site is reported as failed lymphatic mapping. This study was to compare the successful versus failure SLN mapping with several factors: age, tumor size, tumor location, previous examination, previous chemotherapy, and pathological nodal status.

Result: SLN mapping was successful in 1351patients (88.6%), and failed in 166 patients (10.9%). Univariate and multivariate analyses showed the significant factors affecting non-visualization of SLN are:elder age (> 50-year-old, OR: 2.3, 95% C.I. 1.6~3.2), previous excision (OR: 2.3, 1.5~3.4) and previous chemotherapy (OR: 4.0, 1.8~8.9).

Conclusion: The potential factors associated with non-visualization of SLN mapping pre-operatively are: elder age (> 50-year-old), previous excision and previous chemotherapy are associated with non-visualization of SLN mapping.

PC096

The Rural-urban Utility Difference of Bone Scan in Elders: A 7-year Retrospective Cohort Study from 2005 to 2010 in Taiwan

Hsuan-Ming Su[1,2], Fen-Hui Lin[2]

[1]*Department of Nuclear Medicine, Da-Chien General Hospital, Miao-li, Taiwan;*
[2]*Department of Information Management, National Sun Yat-Sen University, Kaohsiung, Taiwan.*

Introduction: Bone scan is the most common study in nuclear medicine. Medical resource abundance may change with area's urbanization level. We want to find out the urbanization relationship between bone scan elder examinees' residence and executive hospitals' location.

Methods: We used two 7-year datasets (2005 to 2010): Longitudinal Health Insurance Database (LHID) 2005 and Registration files, released by the National Health Research Institutes. Elders (age older than 65 years) who underwent bone scan in LHID were identified. The elders' registered areas were classified into 7 urbanization levels according to the report of Liu et al.. The bone scan executing hospitals' locations were also grouped as above. Level 1 to 4 was viewed as "urban," and level 5-7 was viewed as "rural." Chi-squared test was used for categorical variable. A value of $p \leq 0.05$ is considered statistically significant.

Results: We identified 10152 bone scans performed in elders. Of those bone scans, 99.9% were performed at urban hospitals. Of those performed at urban hospitals, only 14.1% were performed on patients from rural areas. 100% of urban elder examinees received bone scans at urban hospitals, but 0.77% of rural elder examinees underwent bone scans at rural hospitals.

Conclusions: There is a huge difference of bone scan utilization between elders whose registered areas are urban and whose are rural.

PC097

The Role of Renoscintigraphy in the Management of Page Kidney

Yu-Li Chiu[1], Chin Hu[1], Sin-Din Lee[1], Po-Yin Chen[1], Jen-Bin Wang[2]

[1]*Department of Nuclear Medicine and*
[2]*Section of Pediatric surgery, Department of Surgery, Kaohsiung Veterans General Hospital, Taiwan.*

Introduction: Page kidney is an uncommon condition that occurs secondary to microvascular ischemia and alternation of small-vessel hemodynamics due to external compression and activation of the rennin-angiotensin-aldosterone system, leading to hypertension. The choice of therapy for Page kidney depends on the clinical presentation of each case. We report one case of Page kidney and renoscintigraphy helps decision making of appropriate management.

Case Report: A 17-year-old man who received Fanton procedure for tricuspid and pulmonary atresia years ago suffered from intermittent severe left flank pain during catheterization procedure. Oliguira, elevation of blood pressure (up to 169/92 mmHg), aldosterone (912.9 pg/mL) and rennin (460.4 pg/mL) by subsequent laboratory analyses were also noted. Emergent CT showed left renal artery active bleeding with left renal parenchyma compression, suggesting Page kidney. Elective embolization of the lower pole segmental branch of left kidney with microcoils was performed on the same day. Then, this patient was treated hypertension with Amlodipine (Norvasc) 5 mg 1# BID, which didn't provide optimal blood pressure control. Besides, renoscintigraphy with 3 mCi Tc-99m diethylenetriamine pentaacetic acid (DTPA) revealed poor renal flow of left kidney with 6.53 ml/min of glomerular filtration rate (GFR). Therefore, open drainage of perirenal hematoma was done. After the operation, GFR improved mildly, left flank pain, and blood pressure returned to normal range at discharge.

Discussion: Page kidney was first described in animal experiments by Dr. Irvine Page in 1939. In the 1950s and 1960s the human counterpart became evident. Page kidney has been reported in all age groups, including pediatric, adolescent, and adult patients. There are multiple etiologies including trauma and nontrauma, such as iatrogenic intervention (including surgical complications such as following ureteral surgery, post-renal biopsy, lithotripsy, etc.), domestic violence, and parenchymal renal disease. Spontaneous bleeding has been reported in patients with warfarin therapy, pancreatitis and renal pathology (such as tumor, arteriovenous malformation, cyst rupture, glomerulonephritis, vasculitis or polyarteritis nodosa).

Multiple imaging modalities are available to diagnose Page kidney. Excretory urogram, computed tomography and ultrasound are commonly used. The gold standard for the diagnosis of Page kidney is selective renal arteriography to exclude renovascular lesions and renal-vein rennin assays to confirm hyperreninemia. Renoscintigraphy allows quantitative estimation of renal blood flow, parenchyma and excretion of "each" kidney. It is of value for evaluating renovascular hypertension with pharmacologic interventions and predicting renal function recovery after intervention.
There are no specific guidelines for the management of Page kidney in the literatures. Therefore, the aim of therapy is to preserve functioning renal tissue by correcting high blood pressure and relieving the external compression of the renal parenchyma. Close observation and appropriate medical therapy with antihytersentive agents are warranted for a reasonable period of time before surgical management because spontaneous resolution may occur. Multiple decompression procedures have been demonstrated, including nephrectomy, capsulectomy, capsulotomy, open or percutaneous drainage of hematoma, laparoscopic interventions, and angioembolization. Nevertheless, there is a trend toward less invasive procedures. In this case, renoscintigraphy played an important role in the determination of conservative or invasive treatment for Page kidney. It also allowed the clinical follow-up of renal function after intervention.

PC098

The Use of Dual-phase ^{18}F-FDG PET Imaging in Characterizing Adrenal Lesions

Kuo-Wei Ho[1], Yu-Erh Huang[1], Sheng-Lung Hsu[2], Ru-Shan Ke[1]

Department of [1]Nuclear Medicine, [2]Radiology, Chiayi Chang Gung Memorial Hospital.

Purpose: To evaluate the performance of dual-phase F-FDG PET imaging for characterization of adrenal lesions in oncology patients.

Materials and Methods: A retrospective review of data in 2140 patients who underwent dual-phase FDG PET/CT for oncological survey was completed, and 41 adrenal lesions were identified in 36 patients. The adrenal lesions were defined histologically (n = 2) or by imaging follow-up (n = 39). Dual-phase ^{18}F-FDG PET imaging was acquired at 1 and 3 hours after ^{18}F-FDG injection. The 1h SUV_{max}, 3h SUV_{max}, retention index (RI), 1h SUR (adrenal SUV_{max}/liver SUV_{avg}), 3h SUR, and ΔSUR (3h SUR minus 1h SUR) were calculated, and the differences between malignant and benign lesions were analyzed. Sensitivity, specificity, positive predictive value (PPV), negative predicted value (NPV), accuracy, and ROC analysis were also performed for these quantitative parameters.

Results: There were 15 malignant and 26 benign lesions. There were significant differences ($p < 0.01$) in 1h SUV_{max}, 3h SUV_{max}, 1h SUR, 3h SUR, and ΔSUR between benign and malignant lesions, while not in RI ($p = 0.051$). Based on ROC analysis, 1h SUV_{max} had the largest AUC. Applying a cut-off of 1h SUV_{max} ≧ 2.67, the sensitivity, specificity, PPV, NPV, and accuracy were 87%, 81%, 72%, 91%, and 83%, respectively; and when further applying a combined criteria of 1h SUV_{max} ≧ 2.67 and ΔSUR ≧ 0.2, the values were 73%, 96%, 92%, 86%, and 88%, respectively. Based on dual-phase analysis, the combination of 1h SUV_{max} and ΔSUR had high specificity and PPV.

Conclusion: ^{18}F-FDG PET with SUV analysis can accurately differentiate benign from malignant adrenal lesions. Further use of dual-phase ^{18}F-FDG PET images and applying a combined criteria of 1h SUV_{max} and ΔSUR led to high specificity and PPV for diagnosing malignant adrenal lesions.

PC099

反射性交感失養症－病例報告

張雅蓮　吳志順

.

奇美醫療財團法人柳營奇美醫院

前言

反射性交感失養症 (Reflex sympathetic dystrophy, RSD) 是四肢不明原因的腫、痛和血管收縮障礙，這種情況經常發生在創傷或手術後。RSD 經常發生在中風後偏癱病人的上肢，又稱爲複雜性局部疼痛症候群 (Complex regional pain syndrome, CRPS)。核子醫學中的骨骼三項掃描 (Three phase bone scan) 是鑑別診斷 RSD 的有效方法之一。我們報告一個典型的個案且發現 Blood pool 的放射性聚集的高低，可能和病人的紅腫程度有關。

案例報告

病人在 2015 年 8 月因腦中風導致右下肢無力、感覺遲鈍，合併右手 (不含手肘) 及右腳紅腫麻木，臨床懷疑可能爲 CRPS，故轉至本科作 Bone scan 以求證實。左下肢正常，無痛風，意識清楚、表達及吞嚥能力正常，但行動遲緩。

檢查方法爲靜脈注射 20 mCi 的 ^{99m}Tc-MDP，以 3 秒 / 張，收 60 張，作爲血流相，再接著照血池相，4 小時候照延遲相。

檢查前發現右手較右腳來的明顯紅腫，結果手部血池相之放射性聚集現象亦較右腳來的明顯，在延遲相時，手部關節處放射性活性聚集亦較腳部來的明顯。

結論

核醫的骨骼三相掃描是檢查 RSD 的利器，除了可證實 RSD 外，其影像上放射性活性聚集的高低可能亦可代表其臨床表徵，甚至疾病病程的演進與變化。

PC100

Os Trigonum Syndrome on the Three-phase Bone Scan with SPECT/CT: A Case Report

Jing-Uei Hou, Yi-Ching Lin, Shih-Chuan Tsai, Wan-Yu Lin

Department of Nuclear Medicine, Taichung Veterans General Hospital, Taiwan.

Introduction: Os trigonum is an accessory bone behind the talus, and it can be seen on the lateral foot radiograph. It is estimated to be present in 7~25% of adults, and could be asymptomatic. However, some people may develop a painful condition known as os trigonum syndrome. It is usually triggered by an injury, such as an ankle sprain. We present a case with os trigonum syndrome on the three-phase bone scan with SPECT/CT

Case report: A 38 years old male suffered from sprain of right ankle due to vehicle accident for one week. Progressive swelling and pain was developed. Thus, he came to our department of rehabilitation for help. The X-ray of right foot showed no abnormality. Then a three-phase bone scan with SPECT/CT was arranged. In the angiographic phase, there is hyperperfusion at the right foot. In the equilibrium blood pool images, there is hyperemia and focal activity at the right foot. In the delayed bone images and SPECT/CT images, there is intensively increased MDP uptake at the posterior aspect of the right talus. Diagnosis of os trigonum syndrome at the right foot was made. After treating with oral medication and transcutaneous electrical nerve stimulation, his condition improved.

Discussion: There are many problems can lead to posterior ankle pain, such as tendon or muscle problems, synovitis, and fracture. Os trigonum can be mistaken for a fracture if not carefully examined. Magnetic resonance imaging evaluation can demonstrate injury with inflammatory fluid surrounding the os trigonum clearly. However, bone scan may be useful for evaluating os trigonum syndrome, too. In our case, intensively increased MDP uptake at the posterior aspect of the right talus was noted in the delayed bone images. Moreover, when combined a three-phase bone scan, the condition of hyperperfusion and hyperemia is noted. And with SPECT/CT, we can have addition information of the exact location. In conclusion, combined three-phase bone scan and SPECT/CT is sensitive for detection of os trigonum syndrome, and can provide additional information.

PC101

A Pilot Study: Tc-99m-HL91 Imaging in Gold Nanoparticles and Localized Hyperthermia in a Hypoxia Tumor Model

Bi-Fang Lee[1], Hsin-Ell Wang[2], Nan-Tsing Chiu[1], Chien-Chung Hsia[3]

[1]*Department of Nuclear Medicine, National Cheng Kung University Hospital, College of Medicine, National Cheng Kung University, Tainan, Taiwan*
[2]*National Yang Ming University, Taipei, Taiwan*
[3]*Institute of Nuclear Energy Research, Lungtan of Taoyuan, Taiwan.*

Abstract

Gold nanoparticles (AuNPs) could be allowed for targeted molecular therapy of cancer. Hyperthermia ablation therapy could induce tumor growth delay. The present study was designed to evaluate the efficacy and safety of AuNPs and localized hyperthermia in a murine colon tumor model. To investigate the antitumor effects of AuNPs, mice bearing CT-26 were administered AuNPs. All mice injected with AuNPs were free of side effects. When tumor volumes reached 100 mm3, pretreatment images were acquired after injection of Tc-99m-HL91. When tumor volumes reached 500 mm3, they were divided into four groups, the control group (C group), AuNPs-only group (A group), localized hyperthermia group (H group) and the combined AuNPs and localized hyperthermia group (AH group). When tumor volumes reached 1000 mm3, histological examinations were performed. The treatment with combined AuNPs and localized hyperthermia significantly retarded the tumor growth and reduced the tumor volume lower than that of with AuNPs only, localized hyperthermia only, and controls. The accumulation of AuNPs was detected inside CT-26 culture cells *in vitro*. Moreover, the AuNPs were shown to be localized in the tumor cells *in vivo*. In conclusion, considering the potential advantages in terms of noticeable antitumor activity, the treatment with combined AuNPs and localized hyperthermia might be potentially useful in the clinical setting.

Keywords: murine tumor, gold nanoparticles, localized hyperthermia.

PC102

A Pilot Study: FDG-PET and Fibronectin Expression in Non-small Cell Lung Cancer

Bi-Fang Lee, Nan-Tsing Chiu

Department of Nuclear Medicine, National Cheng Kung University Hospital, College of Medicine, National Cheng Kung University, Tainan, Taiwan.

ABSTRACT

The high glucose metabolism of the lung cancer results in the high accumulation of FDG to make the lesions visualize. FDG-PET is good for the evaluation and assessment of the extension, malignancy, and clinical stage. Fibronectin (FN) is a biomarker of tumoral metastatic ability. It is a high-molecular-weight glycoprotein containing about 5% carbohydrate that binds to membrane spanning receptor proteins called integrins. The aim is to investigate whether FDG PET determines tumoral metastatic ability.

Forty-six patients had been studied in this retrospective study under the approval of IRB in NCKU hospital. The average age was 61.45 ± 21.88 years-old (range: 21-78). There were 20 females and 26 males. There were 34 adenocarcinoma, 5 squamous cell carcinoma, 1 large cell carcinoma, and 5 bronchoalveolar cancer. The stroma FN expression via IHC staining show the correlation with pathological stage. The patients with positive stroma FN expression have worse outcome. As for positive stroma FN group, SUV via FDG-PET-CT is higher than negative stroma FN group. [positive stroma FN group (n = 16): medium SUV = 7.8; negative stroma FN group (n = 19): medium SUV = 3; $p < 0.001$]
Stroma FN expression is correlated with uptake of FDG-PET in NSCLC lung cancer patients. The uptake of FDG-PET may have potential to predict stroma FN expression of tumor. FDG PET could demonstrate the tumoral metastatic ability.

Keywords: FDG, PET, fibronectin, non-small cell lung cancer

PC103

A Pilot Study: Tc-99m-HL91 in the Effect of Injectable in Situ forming Thermosensitive Implant in an Animal Tumor Model

Bi-Fang Lee, Nan-Tsing Chiu

Department of Nuclear Medicine, National Cheng Kung University Hospital, College of Medicine, National Cheng Kung University, Tainan, Taiwan.

ABSTRACT

Tc-99m HL91 (HL91) is a hypoxia imaging biomarker. Injectable in situ forming thermosensitive implant (IM) could be allowed for targeted molecular therapy of cancer. The aim of this study was to investigate the value of Tc-99m-HL91 imaging for IM therapy in a murine tumor model. As for Cryo-TEM image, IM was transferred to JEM1400 transmission electron microscope.The mice were implanted CT-26 colon tumors. When tumor volumes reached 300 mm3, pretreatment images were acquired after injection of HL91. The mice were divided into low and high hypoxic groups based on the tumor-to-non-tumor ratio of pretreatment HL91 images. When tumor volumes reached 500mm3, the mice were divided into two groups: implant and controls. When tumor volumes reached 1000 mm3, histological examinations and immunohistochemical staining were performed. IM was made of lipiodol, cholesterol, lecithin, dextrin, marcogol, hydroxystearate, vitamin E, cetyl alcohol, etc. Cryo-TEM image of lipid nanoparticles revealed the co-existence of tubular vesicles and vesicles of irregular shape. The animals demonstrated no toxic effects from the injection of IM. Histopathology sections from tumors injected with IM revealed necrosis of the tumor tissue. Treatment with IM delayed tumor growth and enhanced the survival of mice bearing high hypoxic CT26 tumors. Tumor hypoxia is associated with angiogenesis and tumor progression. Tumor hypoxia detected by Tc-99m-HL91 imaging suggests a poor prognosis. Our results indicate that Tc-99m-HL91 imaging allows identifying tumor hypoxia and predicting success of IM therapy for cancer. This study provides the first evidence that Tc-99m-HL91 can serve as an imaging biomarker for predicting the treatment responses of IM in a murine colon tumor model.

Keywords: Tc-99m-HL91, implant, colon tumorl

PC104

A Pilot Study: Tc-99m-HL91 Imaging in the Permanent Middle Cerebral Artery Occlusion of an Animal Model

Bi-Fang Lee, Nan-Tsing Chiu

Department of Nuclear Medicine, National Cheng Kung University Hospital, College of Medicine, National Cheng Kung University, Tainan, Taiwan.

ABSTRACT

Acute cerebral ischemia causes immediately injury, but the final pattern and severity of brain damage are determined by the cascades of molecular events which extend for days to weeks after acute cerebral ischemia. There were several promising neuroprotective compounds to reduce brain injury secondary to acute cerebral ischemia in recent years. Magnesium sulfate is a neuroprotective drug for HI brain injury. Tc-99m HL91 (HL91) is a hypoxia imaging biomarker that demonstrates the presence of tissue hypoxia, such as tumor hypoxia, ischemia cerebellum and ischemic myocardium. The aim of this study was to investigate the value of HL91 imaging to assess the neuroprotective compound in a rat model of permanent middle cerebral artery occlusion (MCAO). Sprague-Dawley rats were divided into 3 groups, one sham-control group, MCAO group, and the MCAO group using the neuroprotective compound (N-MCAO). In MCAO and N-MCAO group, rats underwent 90 min of focal ischemia with intraluminal suture occlusion of the middle cerebral artery. Then, N-MCAO group received the administration of magnesium sulfate. HL91 imagings were acquired at all three groups. Staining with Luxol fast blue demonstrated the presence of cerebral neuronal injury in the MACO and N-MCAO groups. N-MCAO groups had less caspase-3 expression than MCAO and sham-control groups. Increased caspase-3 expression 3 indicates progression of apoptosis. N-MCAO groups had less HL91 uptake than MCAO group, but more than sham-control group. HL91 is sensitive to be a promising agent for detecting cerebral hypoxia in a rat MCAO model. Furthermore, HL91 demonstrates the efficacy of magnesium sulfate as a neuroprotective drug for HI brain injury.

Keywords: Tc-99m-HL91, cerebral hypoxia, scintigraphy.

PC105

提升新進醫事放射師影像品質之合格率

楊士頤[1] 郭珮怡[1] 曾旭吟[1] 李佩璇[1] 莊雅晴[1] 陳俊榮[1]
李世昌[1] 吳佩珊[1] 李碧芳[1] 邱南津[1] 姚維仁[1]

[1]國立成功大學醫學院附設醫院核子醫學部

背景介紹：

影像學的正確診斷是擬定癌症治療計畫重要的一步，因此應用系統化的導入分析，提高影像報告品質十分重要。品管圈 (Quality Control Circle) 是同一個工作現場或工作相互關聯區域的人員自發性地進行品質管理活動所組成的小組。品管圈主要的目的是希望透過與問題相關的直接作業人員，組成小組進行改善活動，使員工在活動過程中學習到發掘問題的能力及改善問題的技巧，使品質管理系統不斷的提升，並達成所設定之品質目標。

本研究以 QCC 手法導入南部某教學醫院的核子醫學部，依照 QCC 分析骨骼掃描檢查之影像，找出影像不合格率之要因，並擬定對策與改善方案。

材料與方法：

本部由 3 位醫事放射師接受評估，透過排檢統計表及影像品質評核表，收集三個月骨骼掃描檢查影像≧ 1 項不良要因者，影像總數爲 630 案，不良影像爲 51 案。使用同一間攝影室之伽瑪攝影機，以減少不同廠牌之變異數。再由同一位評量者利用評核表評估 3 位醫事放射師，依據臨床上有可能影響影像品質項目進行勾選並分析“不通過”之重點要因。

結果與討論：

發覺淺在問題將不合格之項目進行統計，透過柏拉圖分析，找出影響影像品質前 80% 的項目：(1) 病患未解尿乾淨、(2) 影像灰階、(3) 汙染未排除。

改善前之影像品質不合格率爲 8.1%，針對柏拉圖前 80% 的項目，擬定對策：(1) 加強新進人員教育訓練、驗流程更詳細標準化、(2) 加強衛教、(3) 加照側位影像、(4) 污染衣物移除等方法逐步改善矯正，期望影像品質不合格率從 8.1% 改善降低爲 4.3%。

結論：

本次研究結果對病患而言，減少重檢機會。對同仁而言，提升醫學影像品質。對院方而言，提供病患完整的影像資訊，增加醫病間信賴度。目前改善執行結果良好，優點是影像品質的問題涵蓋全科室，改善過程中同仁腦力激盪，同心協力降低影像品質不合格率，找出問題及研擬對策，避免醫療疏失或減少醫療糾紛，進而保障病患安全並提高醫院的醫療品質。缺點是無法針對最需改善之處，人員之穩定性及影像判讀能力亦是往後持續改善的重要因素。

PC106

Application of Fluorine-18-deoxyglucose Positron Emission Tomography and Gallium Scan for Assessment in A Patient with Adult Onset Still's Disease

Jing-Uei Hou, Shih-Chuan Tsai, Wan-Yu Lin

Department of Nuclear Medicine, Taichung Veterans General Hospital, Taiwan.

Abstract: A 53-year-old woman suffered from pain over most of her entire body, especially the joints. Chest computed tomography (CT) revealed multiple lymphadenopathies over cervical, mediastinal, and axillary areas. A fluorine-18-deoxyglucose (FDG) positron emission tomography / computed tomography (PET/CT) revealed increased FDG uptake in many lymph nodes and the spleen. Lymphoma was suspected. However, the result of a biopsy showed no malignancy, and the gallium-67 citrate (Ga-67) scan showed no gallium-avid tumor throughout the whole body. Adult Onset Still's disease (AOSD) was diagnosed, and the patient responded well to steroid therapy. The follow-up PET/CT 6 months later showed complete remission of the FDG-avid lesions seen in the previous study. Our study suggests that FDG PET/CT combined with Ga-67 scan may be helpful in diagnosing patients with AOSD. In addition, the use of FDG PET/CT alone may be useful for the evaluation of disease distribution, disease activity, and therapeutic response.

Keywords: FDG PET/CT, Ga-67, Adult Onset Still's disease

Introduction: Adult Onset Still's disease (AOSD) is an inflammatory disorder of unknown cause. "Still's disease" was first described in children by George Still in 1896. In 1971, the term "Adult Onset Still's disease" was used to describe patients who had variable systemic features. Yamaguchi et al. have proposed that the classification of adult Still's disease requires the presence of 5 or more criteria, of which at least 2 are major criteria. Major criteria: 1. Temperature of > 39°C for > 1 week. 2. Leukocytosis > 10,000/mm3 with > 80% PMNs. 3. Typical rash. 4. Arthralgia > 2 weeks; Minor criteria: 1. Sore throat. 2. Lymph node enlargement. 3. Splenomegaly. 4. Liver dysfunction (high AST/ALT). 5. Negative antinuclear antibodies (ANA), rheumatoid factor (RF). Before the final diagnosis of AOSD is made, other malignancies and other rheumatic diseases should be ruled out.

Case Report: Our case was a 53-year-old woman. She suffered from pain over most of her entire body, especially the joints and the throat. In addition, skin rashes on the trunk without pruritus was noted. She had visited the Rheumatology, Neurology, and Orthopedic Outpatient Department several times. A chest CT was done which revealed multiple lymphadenopathies over cervical, mediastinal, and axillary areas. A PET/CT revealed increased FDG uptake in many lymph nodes including the bilateral neck, axillae, mediastinum, bilateral pulmonary hili, abdominal para-aortic region, iliac regions, and inguinal regions as well as the spleen (Fig. 1). Lymphoma was suspected first. However, a biopsy was done and no malignancy was found. Ga-67 scan was arranged, and no gallium-avid tumor was seen throughout the whole body (Figure 2). The laboratory data were negative for ANA, RF-IgM, and ENA, and ALT was high. The final diagnosis was AOSD. Methylprednisolone (Metisone) 4mg/day and non-steroidal anti-inflammatory drugs were prescribed initially. Six months later, the follow-up PET/CT showed complete remission of the FDG-avid lesions seen in the previous study (Fig. 1t).

Discussion: Adult Onset Still's disease (AOSD) is a chronic systemic inflammatory disorder. Other malignancies and

other rheumatic diseases should be ruled out first before the diagnosis is made. AOSD is characterized by spiking fever, leukocytosis, rash, and arthralgia. Some patients may also develop sore throat, lymphadenopathies, and hepatosplenomegaly. The therapeutic decision depends upon the severity of disease, and subsequent treatment decisions should be made in accordance with the clinical response. If the symptoms are mild, patients may respond to nonsteroidal anti-inflammatory drugs. If the symptoms are more severe, glucocorticoids or even pulse therapy should be considered.

In this study, we present the FDG PET/CT and Ga-67 scan findings of a patient who met the Yamaguchi classification criteria for AOSD. The FDG PET/CT scan was not very helpful in diagnosing AOSD in this case since lymphoma could not be ruled out. However, the FDG PET/CT scan results were useful for evaluating the distribution and severity of the disease. A negative Ga-67 scan could be beneficial as it would exclude lymphoma. After the diagnosis of AOSD was established, the patient received nonsteroidal anti-inflammatory drugs and glucocorticoids with a good response. Disease activity and therapeutic response were monitored by FDG PET/CT and the findings of a scan performed 6 months after treatment yielded were negative.

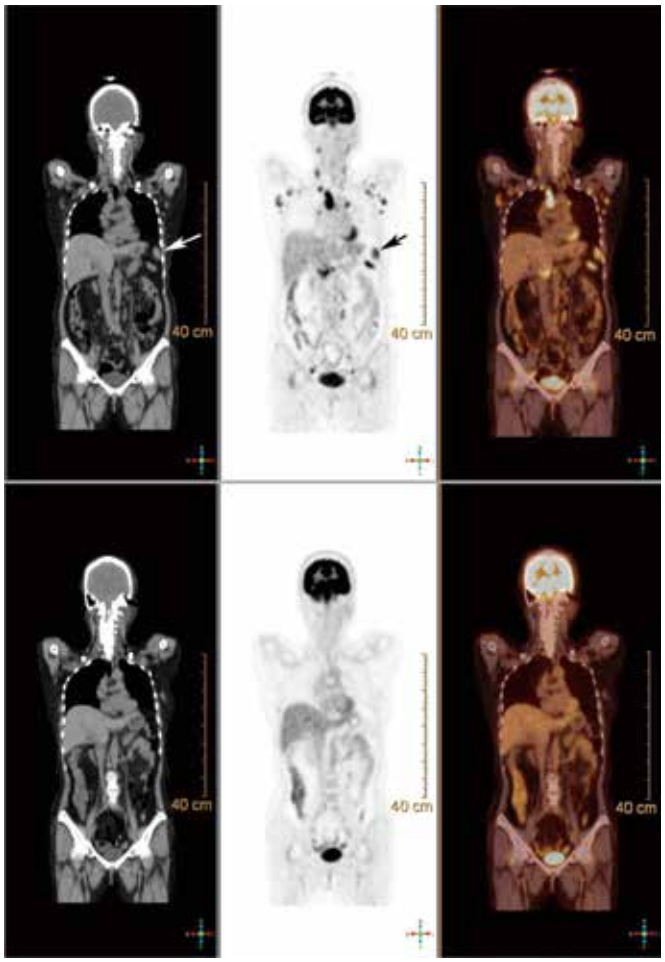

Figure 1.

In conclusion, there is no definitive diagnostic imaging study for patients with AOSD. Our study suggests that FDG PET/CT combined with Ga-67 scan may be helpful in diagnosing patients with AOSD. In addition, the use of FDG PET/CT alone may be useful for the evaluation of disease distribution, disease activity, and therapeutic response.

Legends: Figure 1. The F18-FDG PET/CT scan performed before treatment showed (upper row) increased FDG uptake at the bilateral neck, axillae, mediastinum, bilateral pulmonary hili, abdominal para-aortic, iliac regions, and inguinal regions, and also in the spleen (arrow). Lymphoma involving the aforementioned areas was considered first. However, a biopsy was done and no evidence of malignancy was found. Adult Onset Still's disease (AOSD) was diagnosed and the patient received medical treatment. Six months later, the follow-up F18-FDG PET/CT scan (lower row) showed complete remission of the FDG-avid lesions.

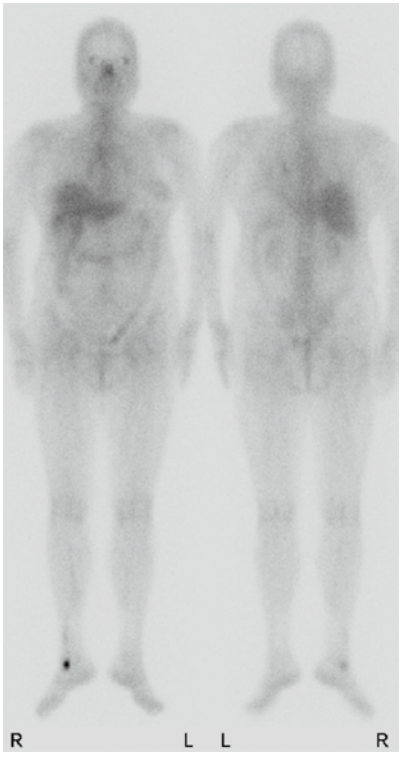

Figure 2.

Figure 2. A Ga-67 scan performed before treatment showed no gallium-avid tumor in the whole body scan.

PC107

左足部纖維瘤疑似爲黑色素癌 -- 案例報告

張雅蓮[1] 鄭筑予[2] 李將瑄[2]

[1] 奇美醫院柳營院區核醫科
[2] 奇美醫學中心永康總院核醫科

前言

FDG 正子檢查可使用黑色素癌的全身臨床分期，而足部纖維瘤造此案例僞陽性。回顧文獻，之前無案例，故提出報告。

案例報告

一位 60 歲女性病患，經內視鏡及切片診斷直腸黑色素癌，執行正子檢查做爲臨床分期。正子檢查除直腸及附近淋巴節有強烈 FDG 攝取病灶外，意外發現左足部有強烈 FDG 攝取病灶，疑似爲黑色素癌轉移。經手術切除，病理証實爲纖維瘤。

討論

FDG 正子檢查已廣泛使用黑色素癌的全身臨床分期，效果顯著。而在 FDG 正子檢查有許多有許多非惡性的攝取，常見爲發炎及良性病灶，此會造成誤判，而纖維瘤一般都不會攝取。此案例考量黑色素癌、位置、及強烈 FDG 攝取，術前判讀成黑色素癌轉移。惟手術切除，病理証實爲纖維瘤。所以足部纖維瘤可造成僞陽性，判讀黑色素癌轉移應列入鑑別診斷。

結論

足部纖維瘤可造成黑色素癌轉移的僞陽性，判讀時應列入鑑別診斷。

PC108

瀰漫性大型 B 細胞淋巴瘤於化療後雙側肺葉瀰漫性 FDG 攝取

鄭筑予[1] 李將瑄[1]

[1] 奇美醫療財團法人奇美柳營醫院核醫科

FDG 正子造影可以準確的評估淋巴癌對治療的整體療效以及是否有殘餘腫瘤。僞陽性結果可能是胸腺反應性增生、骨髓反應、發炎或感染。我們報告一位 60 歲男性的頸部右側淋巴結腫大，診斷爲瀰漫性大型 B 細胞淋巴瘤，於 2015/06/02 經全身正子造影掃描結果爲第 III 期，以 R-CHOP + Ibutinib/P 化療四個療程 (上一次爲 2015/08/17)。在 2015/09/02 爲評估淋巴癌化療療效，再度予以全身正子造影掃描檢查，經比較舊片，發現舊的病灶已經消失，即化療達到完全有效療效，但也發現新的雙側肺葉瀰漫性 FDG 攝取。回顧文獻，瀰漫性大型 B 細胞淋巴瘤於化療後雙側肺葉瀰漫性 FDG 攝取誠屬少見。故探討其原因，在抽血檢查、電腦斷層、正子造影等證據下，排除發炎感染以及殘存腫瘤的因素，認爲新的肺葉病灶應爲化療後之反應。

nanoScan® Family

Mediso
Medical Imaging Systems

Preclinical PET imaging systems

nanoScan® SPECT/MRI

nanoScan® PET/MRI

nanoScan® SPECT/CT

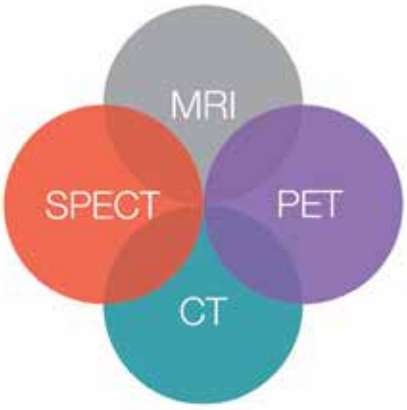

nanoScan® PET/MRI 3T

nanoScan® SPECT/CT/PET

nanoScan® PET/CT

First-class instruments to provide you with excellent image quality.

To know more about the latest information, please contact with...

TLSS

泰歷藥品儀器股份有限公司

TAIWAN LIFE SUPPORT SYSTEMS, INC.

0800-050-158

www.tlss.com.tw

大會組織表

主辦單位　行政院原子能委員會核能研究所、馬偕紀念醫院、中華民國核醫學學會

會　　長　吳明哲會長

指導委員（依姓氏筆畫順序，尊稱省略）

王安美、王信二、王昱豐、朱力行、李將瑄、杜高瑩、邱南津、林昆儒、吳明哲、姚維仁、洪光威、高潘福、高志浩、殷國維、林武智、林明賢、陳遠光、陳志成、陳慶元、陳輝墉、黃文盛、彭南靖、程紹智、辜啓泰、楊邦宏、廖炎智、鄭澄意、蔡世傳、樊裕明、諶鴻遠、鍾相彬、魏孝萍

論文評選組（依姓氏筆畫順序，尊稱省略）

召　集　人　王昱豐
執行秘書　廖建國
口頭論文基礎組　王信二、林武智、楊邦宏、鍾相彬
口頭論文臨床組　李將瑄、林昆儒、程紹智、顏若芳
壁報論文基礎組　王安美、吳志毅、魏孝萍、羅彩月
壁報論文臨床組　吳彥雯、程紹智、彭南靖、蔡世傳

籌備處（依姓氏筆畫順序，尊稱省略）

主　席　吳明哲
行政組　王安美、李貞儀、吳雨軒、陳玉蕙、歐陽慧、羅青雯
場務組　宋美慧、林穎稚、吳佩玲、吳佩姍、鄭雯文、張志源、張雯燕、管子葳、塗婉思
編輯組　王安美、杜高瑩、林谷鴻、張志源、吳汎琛、萬智杏

秘書處（依姓氏筆畫順序，尊稱省略尊稱省略）

秘書長　林立凡
執行秘書　侯正涵、姚珊汎、曾敬仁
秘　書　林孟倩、林讌如